

Table des matières

Message du Vice-Doyen de la Recherche
de la Faculté de Biologie et de Médecine.....

Programme.....

Abstracts :

THE Procédure Thérapeutiques

ODE Oncologie et Développement.....

NEU Neurosciences et Psyché

MCV Métabolisme et Cardiovasculaire.....

GEN Gènes et Environnement.....

EHU Environnement Humain

ENA Environnement Naturel.....

IMI Immunité et Infection

Index des Auteurs.....

Message du Vice-Doyen de la Recherche

Chers Collègues, Chers Amis,

Je vous souhaite la bienvenue à cette cinquième édition de la journée de recherche CHUV, qui touche cette année la thématique des *Neurosciences et Psyché*. Cette thématique intéresse les biologistes et médecins à de multiples niveaux. Elle est particulièrement intégrative, et s'inscrit bien dans la notion de domaines interdisciplinaires souhaitée par notre Faculté.

De façon presque réductrice, les *Neurosciences et Psyché* pourraient être définies comme la biologie de la communication. Mais loin d'être réductrice, la biologie de la communication est universelle. Partant de la transmission d'une stimulation électrique appliquée à un nerf et son effet sur la contraction d'un muscle situé à distance – à la fin du XIX^{ème} siècle – la communication est maintenant appréciée aux niveaux inter- et intra-moléculaires. Au niveau inter-moléculaire, dans le cadre des cascades de signalisations. Au niveau intra-moléculaire, lorsqu'un signal induit un changement de conformation voire de fonction de son récepteur, qui est perçu et interprété par le reste de l'environnement biochimique. Au-delà de la perception, la notion d'interprétation implique des systèmes de rétrocontrôles permettant d'ajuster la réponse à l'effet souhaité, déjà au niveau moléculaire.

Ce continuum "perception-interprétation-réaction" s'opère à tous les niveaux du vivant, depuis le génome viral capable de détecter les conditions cellulaires les plus appropriées pour sa réplication, au fonctionnement intégratif du cerveau et des sociétés d'individus, en passant par la communication inter-unicellulaires du monde des microbes. Dès lors on comprend l'ampleur du domaine. Du comportement intra-cellulaire au comportement social, la communication gère pratiquement toutes les étapes. Sa seule dépendance reste l'intégrité des structures physiques qui la sous-tendent, i.e. le système nerveux pour les organismes pluricellulaires. C'est dans ce sens que cette journée s'intéresse à certains aspect du fonctionnement, du dysfonctionnement et de la possible réparation du cerveau par les cellules souches, dans le cadre d'un programme scientifique dont je vous laisse découvrir la richesse.

Enfin, je n'aimerais pas omettre d'évoquer la conscience et la pensée abstraite. Produit Darwinien pour certains, élément fondateur pour d'autres, la *Psyché* est certainement l'aspect le plus fascinant associé à la complexité du cerveau. Bien qu'elle ne soit pas directement traitée dans les sessions plénières de cette journée, la *Psyché* appartient à l'un des axes stratégiques développés par l'ensemble de notre Université, en particulier par le programme Anthropos.

Je remercie tout particulièrement les membres du comité scientifique, qui ont établi le programme de très haute qualité auquel vous êtes conviés, alliant des invités de marque à des orateurs internes à la FBM, dans le cadre de la thématique à l'honneur.

Je vous souhaite d'emblée une excellente journée, et vous adresse mes meilleures salutations,

Philippe Moreillon
Vice-Doyen de la Recherche



CENTRE HOSPITALIER
UNIVERSITAIRE VAUDOIS

Unil
UNIL | Université de Lausanne
Faculté de biologie
et de médecine

Comité d'organisation 2006

Julien Bogousslavsky, Neurologie

Stephanie Clarke, Neuropsychologie

Patrice Guex, Psychiatrie de liaison

*Pierre Magistretti, Centre de Neuropsychiatrie
& Brain Mind Institute*

Philippe Moreillon, Décanat

Jean-Guy Villemure, Neurochirurgie

Administration de la Recherche :

Jovan Mirkovitch

Anne Tricot

Coraline Magnenat



CENTRE HOSPITALIER
UNIVERSITAIRE VAUDOIS

Unil
UNIL | Université de Lausanne
Faculté de biologie
et de médecine

CHUV RESEARCH DAY 2006
Thursday, February 2nd, 2006
"Neurosciences and Psyche"

- 08:30 Presentation of the 2006 Research Day - Professor Philippe Moreillon, Vice Dean for Research and Professor Pierre Magistretti
- 08:45 **Keynote speaker 1** **Professor Hans-Peter Hartung**
*Department of Neurology
Heinrich-Heine-University, Duesseldorf*
"Inflammatory CNS degeneration: implications for future therapy of multiple sclerosis"
- 09:30 **Coffee & Posters**
- 10:30 4 CHUV short talks
- 11:30 **Keynote speaker 2** **Dr. Ratan D. Bhardwaj**
*Department of Cell and Molecular Biology
Nobel Medical Institute, Stockholm*
"Neural stem cells: myths and reality"
- 12:15
Lunch, Coffee & Posters
- 14:00 **Keynote speaker 3** **Professor R G M Morris**
*Division of Neuroscience,
College of Medicine and Veterinary Medicine,
Edinburgh*
"The Synaptic Plasticity and Memory Hypothesis: New ideas, new findings"
- 14:45 4 CHUV short talks
- 15:45 **Coffee & Posters**
- 17:00 **Keynote speaker 4** **Professor Sophie Scott**
*University College London
Dpt of Psychology*
"Unpacking the neural basis of speech perception using functional imaging"
- 17:45 Poster Prizes Ceremony
- 18:00 **Apéritif & Buffet**



CENTRE HOSPITALIER
UNIVERSITAIRE VAUDOIS

Unil
UNIL | Université de Lausanne
Faculté de biologie
et de médecine

8 CHUV talks

Schedule	Names, departments	Titles
Morning		
10h30 - 10h45	Emmanuel Carrera Service de Neurologie	<i>"Detection of epileptic activity in acute stroke with continuous electroencephalogram"</i>
10h45 – 11h00	Alexandre Berney Service de Psychiatrie de liaison	<i>"Prospective study of long-term mood outcome following subthalamic Deep Brain Stimulation (STN-DBS) for Parkinson Disease (PD)"</i>
11h00 – 11h15	Isabelle Décosterd Service d'Anesthésiologie et Dpt de Biologie Cellulaire et Morphologie	<i>"The auxiliary beta2 subunit of voltage-gated sodium channel and hypersensitivity in a neuropathic pain model"</i>
11h15 – 11h30	Jean-René Cardinaux Centre de Neurosciences psychiatriques et SUPEA	<i>"Transducers of regulated CREB activity (TORCs) act as new calcium- and cAMP-sensitive coincidence detector in the central nervous system"</i>
Afternoon		
14h45 – 15h00	Ron Stoop Centre de Neurosciences psychiatriques	<i>"Neuropeptidergic modulation of brain stem projections from the central amygdale"</i>
15h00 – 15h15	Françoise Schenk Centre de Neurosciences psychiatriques et Département de Physiologie	<i>"Vieillissement: une adaptation optimale?"</i>
15h15 – 15h30	Leila Faiza Cammoun Laboratoire de traitement des signaux - EPFL	<i>"Schizophrenia connectivity investigation by Tractography of DTI"</i>
15h30 - 15h45	Micah Murray Service de Neuro psychologie	<i>"Rapid Brain Discrimination of Sounds of Objects "</i>

***THE
Procédures
Thérapeutiques***

Sequential steps in the diagnostic work-up of patients presenting with thoracic pain in primary care. The TOPIC study

¹FAVRAT B., ²Junod M., ²Herzig L., ³Burnand B., ²Verdon F.,

PMU et UMG¹, UMG², IUMSP³,

Introduction: Thoracic pain is frequently encountered in primary care, a symptom linked with different ailments which may necessitate immediate management. Our purpose was to investigate the successive steps in the diagnostic work-up of patients presenting with thoracic pain during the index encounter and to compare initial and 12-months follow-up diagnosis.

Methods: Among 24'620 consecutive primary care encounters, 58 physicians and one medical outpatient clinic included 672 patients presenting with thoracic pain (main or ancillary symptom). Physicians recorded a diagnostic description after initial appraisal (step1), completed history (step2), physical examination (step3), at the end of the index encounter (step4), following possible diagnostic tests, and after three months and one year. This diagnostic description was grouped in 5 clusters: chest wall, cardiovascular, psychogenic, respiration, digestion. The specific diagnosis retained at the end of the initial encounter was compared with the 12-month "correct diagnosis".

Results: A cluster diagnosis was reported in 70%, 82%, 92%, and 97% of encounters at step1-4, respectively (fig1). In 126 (19%) cases a change in the specific diagnosis was made after the index encounter (fig2). All patients who needed immediate treatment were appropriately managed. The major determinants of achieving a specific diagnosis at the end of the index medical encounter were: history taking (78%), physical examination (66%), a previously known patient (63%), initial appraisal (49%).

Conclusions: A diagnosis is rapidly obtained in patients presenting with thoracic pain in primary care and infrequently changed thereafter. Apparently no patient suffered from a delayed diagnosis. Knowing the patient, history taking and physical examination are major determinants to reaching a diagnosis.

Swiss survey of paediatric CT practice

¹VERDUN F., ²Gutierrez D., ³Lepori D., ³Gudinchet F.,

Inst. Radiophysique Appliquée/DUMSC¹, IRA/DUMSC², Radiologie/CHUV³,

Purpose: To investigate the variation of dose delivered in paediatric CT in order to establish a set of dose reference levels (DRL) that will be used to initiate an optimization process.

Material and Methods: This survey was organized under the auspices of the Swiss society of paediatric radiology. The 10 centres that perform the majority of the examinations were asked to fill-out a form containing the necessary information required to estimate patient dose (i.e. kV, mA, rotation time ...) for age groups: < 1 year; 1 – 5 years; 5 – 10 years and 10 – 15 years. The examinations considered were standard brain, face, neck, chest and abdomen. The centres were also asked to record the CTDIvol and DLP values indicated by the unit when examining actual patients.

Results: The survey involved 4 GE, 3 Philips, 2 Siemens and 1 Toshiba units. Per age class the range of doses varied by a factor of 5 to 10. For example, for children < 1 year, DLP varied: for brain from 66 to 414 mGy.cm; for chest from 12 to 198 mGy.cm and for abdomen from 29 to 258 mGy.cm. In spite of this large variation, the DRLs obtained during this study are compatible with recent available data (i.e. UK-NRPB W67 Report).

Conclusion: This survey allowed to establish a set of DRLs that will be used to propose standard sets of protocols and to follow the impact technology's progress on patient dose. This survey is now followed by the analysis of the range of image quality recorded.

Cost-effectiveness of risedronate therapy in postmenopausal women with varying risk of osteoporotic fractures: A Swiss Analysis

¹LAMY O., Lamy O., Krieg M., Wasserfallen J., Greiner R.,

*Médecine interne*¹,

Objective:

Osteoporosis and related fractures are a major source of illness and cost in Switzerland. The incidence of hospitalizations related to osteoporotic fractures increases sharply with age. This study assessed the economic impact of risedronate therapy in postmenopausal osteoporotic women with different risk profiles using computer modeling.

Methods:

A fracture-incidence based Markov model of osteoporosis with patients transition across states was used to estimate cost per any fracture averted, cost per hip fracture averted and cost per QALY gained. Model inputs were specific to Switzerland and included fracture and mortality rates, lengths of stay for acute and rehabilitation care and intervention cost including acquisition cost for 35mg of Actonel, office visits and monitoring of BMD. Health utilities and relative risk reductions were taken from published studies. Cost and outcomes were discounted at 3%.

A population of 1000 women with osteoporosis and one prevalent fracture was modeled with 5 years of risedronate therapy starting at 70 years. The analysis was repeated for populations with an additional history of maternal hip fracture, a history with any fracture since the age of 50 or both. Residual effect was modeled to be 2 years and a discontinuation rate of 50% was assumed.

Results:

In the base case population cost per QALY and per averted hip fracture were CHF 30'800 and CHF 44'921. In the presence of a maternal hip fracture, any fracture history or both, costs per QALY decreased to CHF 22'920, CHF 20'328 and 13'646 and cost per hip fracture averted decreased to CHF 33'840, CHF 29'178 and CHF 19'647. Cost per any fracture averted was CHF 22'007 in the base case analysis and CHF 15'623, CHF 14'140 and CHF 9'024 in the presence of additional risk factors.

Conclusions:

Risedronate is a cost-effective intervention in women with postmenopausal osteoporosis, absolute cost per unit of benefit gained varies according to the risk profile at baseline.

Psychiatric disorders: cause, coincidence and consequence of chest pain in primary care

¹FAVRAT B., ²Herzig L., ²Verdon F., ³Burnand B., ²Mühlemann N.,

PMU et UMG¹, UMG², IUSMP³ CHUV Lausanne

Introduction: Chest pain and psychiatric disorders are frequently encountered in primary care patients, but their relationship is poorly understood. We examined the role of psychiatric disorders in patients presenting with chest pain.

Method: 24'620 consecutive primary care encounters. 58 physicians and one medical outpatient clinic. **Inclusion:** 672 patients presenting with thoracic pain (main or ancillary symptom). Physicians decided if thoracic pain was caused by psychiatric disorders. They recorded the presence of psychiatric comorbidity and if pain generated anxiety. All diagnoses were confirmed by a 12 month follow-up.

Results: 77 (11%) cases of all thoracic pain were considered to be caused by a psychiatric disorder only (defined by the presence of an anxiety stimulus, anxiety symptoms and the absence of specific symptoms of other potential causes for thoracic pain). Psychiatric disorders included: anxiety disorder 32 (42%), acute anxiety 17 (22%), somatoform disorders 22 (29%), depression with anxiety 6 (7%).

In 241 (36%) cases chest pain coincided with psychiatric comorbidity and included: Anxiety disorder 82 (34%), acute anxiety 11 (4%), somatoform disorders 19 (8%), depression with anxiety 99 (41%) others 30 (13%). Such comorbidity occurred more frequently if chest pain was attributed to psychiatric disorders (64%) and less so when chest pain was due to a cardiac (23%) or respiratory cause (18%).

In addition, anxiety was considered to be a consequence of chest pain in 379 (56%) patients (described as a symptom at inclusion and independent from causes of chest pain).

Conclusion: Psychiatric disorders were considered to be the only source of chest pain in one of ten patients. Psychiatric comorbidity coincides with chest pain in a third of the patients. Chest pain engendered anxiety symptoms in more than half of the patients.

SYNDROME PARIETAL THORACIQUE - Revue de 300 patients consécutifs de l'étude TOPIC

¹FAVRAT B., ²Verdon F., ³Burnand B., ²Herzig L.,

PMU¹, UMG², IUMSP³, CHUV Lausanne

Objet : Les douleurs thoraciques d'origine « rhumatismales » ou syndrome pariétal thoracique (SPT) représentent un problème fréquent en médecine de premier recours et en médecine d'urgence mais sont mal étudiées. Nous décrivons ici leurs caractéristiques incluant la localisation de la douleur et les corrélations cliniques ainsi que le suivi à un an.

Méthode : 56 médecins praticiens ont examiné et suivi prospectivement 672 patients (p) ambulatoires inclus consécutivement pour des douleurs thoraciques. 300 d'entre eux diagnostiqués comme des SPT sont étudiés par un questionnaire détaillé à l'inclusion, à trois mois (moment du diagnostic) et, pour 97% d'entre eux, à 1 an.

Résultats : Un diagnostic de SPT est posé dans 1.3% de 24'000 consultations, pour moitié motif de consultation et pour moitié plainte d'accompagnement. Le SPT affecte toutes les classes d'âge avec un sexe ratio de 1. Il peut se présenter de différentes façons: la douleur est souvent intermittente, durant des heures ou des jours, légère ou modérée, bien localisée, déclenchée ou accentuée par une position ou un mouvement (50% des cas). La douleur peut aussi être durable durant quelques minutes, des heures ou des jours (35% des cas) mais aussi être intense, aiguë et angoissante (9% des cas) amenant souvent les p en urgence avec la crainte d'une affection cardiaque. La douleur est ressentie le plus souvent dans la région moyenne et haute de l'hémithorax gauche (figure 1) et elle peut irradier (29 p) notamment vers le bras gauche ou le cou (18 p).

Chez 210 p un seul point du thorax est douloureux. On peut identifier un syndrome précis chez 195 d'entre eux (tab I et figure 2). Chez 88 autres p la douleur s'étend sur une région plus étendue du thorax, en général gauche ou médiane-gauche, rarement droite ou bilatérale. Les caractéristiques de la douleur et la sensibilité locale à la palpation (parfois aussi aux épreuves de provocation) sont les clés du diagnostic. Cependant une sensibilité de paroi n'est pas notée chez 47 p. L'étiologie est le plus souvent indéterminée. Cependant le SPT -qui cause une inquiétude exprimée explicitement par 58% des p- peut être associée à un contexte de tension psychologique ou de détresse (13% des cas), à une toux ou une dyspnée (11%), à une fibromyalgie (3%), une thorcotomie antérieure (3%) ou à d'autres causes (8%). Le SPT peut coexister avec d'autres affections susceptibles de causer des douleurs thoraciques. Ainsi 15 des 92 p de plus de 60 ans souffrent d'insuffisance coronarienne.

Peu d'exams sont réalisés en urgence (27% des p) ou en différé. Un traitement (médicament, physiothérapie) n'a été proposé qu'à 31% des p et 23% seulement ont été revus uniquement pour le SPT. L'évolution à un an est favorable (une hospitalisation mais aucun décès liés au SPT). Les récurrences sont fréquentes: 109 p ont refait un épisode de SPT dans l'année et 121 p en avaient déjà présenté un avant l'épisode actuel.

Durant l'année de suivi, le diagnostic de SPT est abandonné chez 16 p en faveur d'autres diagnostics: oesophagite (7 p), anxiété / somatisation (4 p), angor pectoris (3 p) ou cancer bronchique / métastases pariétales (2 p) qui sont les principaux diagnostics différentiels des SPT

Conclusions : Le SPT est une cause majeure de douleur thoracique en médecin de premier recours. Cette affection est bénigne mais cause beaucoup d'anxiété. Elle peut être associée ou confondue avec des affections plus graves, notamment coronariennes et néoplasiques

Un questionnaire de prévention de la rechute schizophrénique : Zone Rouge Etude de faisabilité

¹ROTHEN S., ²Clerc A.M., ³Lakehal H.H., ¹Baumann R., ⁴Pasquier C., ¹Brahim J.,
¹Vianin P., ¹Pedroletti J., ⁵Leroy A.,

¹DUPA, ²Patiente, ³Membre du GRAAP, ⁴Usager, ⁵Vice-présidente de l'îlot

1. RESUME

Introduction : Des questionnaires de prévention de la rechute existent et ont généralement été élaborés par des professionnels en liens avec des laboratoires pharmaceutiques (Prelapse pour Lundbeck, PECC pour Janssen-Cilag). Leurs contenus sont directement inspirés, tant dans le but visé – évaluer les déficits, les symptômes - que dans la formulation – vocabulaire spécialisé - des textes de référence. Ce sont donc des outils techniques à l'usage exclusif du clinicien. Dans une perspective phénoménologique, intégrant les témoignages des usagers, des proches et des soignants et dans une problématique de santé communautaire, associant les acteurs du soin, il nous a semblé nécessaire qu'un outil, plus proche de l'utilisateur et utilisable par lui soit créé. De plus, cet outil se veut être un moyen de communication entre l'utilisateur et une personne de référence (soignant ou membre de famille)

But : Evaluer la qualité du questionnaire selon trois axes :

- le choix et la formulation des questions : les questions sont-elles compréhensibles, pertinentes et exhaustives ?
- la possibilité de mettre en évidence des signes idiosyncrasiques de rechute et
- de permettre le dialogue entre les différents partenaires

Methodologie : 20 binômes usager-soignant et 20 binômes usager-proche vont être créés. Sur une période de 6 mois, les usagers vont remplir le questionnaire à une fréquence libre, mais au minimum 6 fois. A chaque fois, le questionnaire sera ensuite discuté avec le partenaire (proche ou soignant). Le recrutement se fait à parts égales entre les associations d'usagers et de proches (GRAAP, L'Îlot) et les consultations ambulatoires (UPC, « E. Minkowski »).

Intérêt de ce questionnaire : ce questionnaire est à notre connaissance nouveau dans la mesure où il est un outil de l'utilisateur pour lui-même. De plus, il a été développé non pas uniquement par des professionnels, mais également par des usagers et des proches d'utilisateur.

Référent : *Stephane Rothen UREP, site de Cery, 1008 Prilly ; stephane.rothen@chuv.ch; tel : 021 643 66 49.*

Impact of a preformatted outpatient prescription form for anti-HIV drugs

¹VOIROL P., ²Devaud J., ²Voirol P., ³Cavassini M., ²Pannatier A.,

Service de Pharmacie¹, Service de Pharmacie², Services des Maladies Infectieuses³,

Background and objective

Prescription is a crucial step in the pharmacological treatment of patients. However, occurrence of errors in prescription is well documented. A preformatted form may improve the quality of prescription. A prescription form listing all the antiretroviral drugs available on the Swiss market with their dosage and package size was developed and used by the HIV outpatient clinic since February 2004.

The goal of the study was to evaluate the impact of this prescription form on the quality of prescription on a pharmaceutical point of view.

Design

Completeness of prescription was evaluated over a nine-month period in 2004 and compared to the traditional prescription forms over the same period in 2003. Results were compared using a 2-sided Fisher exact test.

Setting

Department of Pharmacy and HIV outpatient clinic of a large university hospital.

Main criteria of evaluation:

1) Presence of the formal (prescribers' name, affiliation, date, stamp and signature, patients' name and age) and medication related (name, dosage, pharmaceutical form, daily dose, frequency of administration, size of package, number of refill) data on the prescription form. 2) Ambiguous prescriptions on both types of prescription forms. 3) Occurrence of new types of errors generated by the preformatted form

Results

Seven hundred and ten preformatted prescription forms representing 1768 lines of prescription (2.5 drugs / form) and 643 traditional prescription forms representing 1491 lines (2.3 drugs / form) have been analysed. 63.2% of the preformatted prescriptions contained all the formal data vs 33.0% of the traditional ones ($p < 0.0005$). All the required medication related items were present in 98.5% of the lines of prescription on the preformatted forms vs 1.3% on traditional forms ($p < 0.0005$). Ambiguous prescriptions were more frequent with traditional forms than with the preformatted (2.2% vs 0.6%, $p = 0.015$). Confusion between lines on the preformatted form appears as a new kind of error (29 cases/1768 lines, 1.6%).

Conclusion

The preformatted prescription clearly improves the quality of prescription but may generate new kind of errors. The prescription form will therefore be adapted based on the conclusions of the study.

IMPACT OF MIGRATION ON HEALTHCARE RESOURCES CONSUMPTION IN AIDS PATIENTS

¹WASSERFALLEN J., ¹Hyjazi A., ²Cavassini M., ³Telenti A.,

*DIM*¹, *MIN*², *IMU*³,

Background : Countries with high immigration rates have presumably two coexisting populations : the native population, with early detection of seropositivity and timely initiation of antiviral therapy, and the migrant population, with late disease detection and sometimes delayed initiation of therapy. We wanted to assess whether healthcare resources consumption would be different in these two populations.

Material and methods : All patients followed-up in the Swiss HIV cohort study in our institution during the year 2000-2003 were considered. Hospital resource use was computed from the hospital information system and outpatient resource use, extracted from individual patient charts, was valued from official tariffs for the year 2002. Data were stratified by CD4 cell counts at enrolment, and repeated on the subgroup of patients with heterosexual infection.

Results : The two groups were made of 200 Europeans and 66 migrants. Migrants were statistically significantly younger (29 ± 8 years versus 37 ± 11 , $p<0.001$), less often of male gender (38% versus 70%, $p<0.001$), and predominantly infected via heterosexual contact (87% versus 52%, $p<0.01$). They had statistically significant lower mean CD4 level at enrolment (326 ± 235 versus 437 ± 305 , $p=0.002$) and more often below 200 CD4 cells/ml (35 versus 26%, $p=0.07$).

Resource consumption was similar in the 2 groups: the European group tended to be hospitalised more often, while the migrant group had significantly more outpatient visits and laboratory tests per year; however, total cost of care per year of follow-up was lower in the migrant group (CHF $3'332\pm 6'309$ versus $6'232\pm 18'456$, $p=0.037$). Healthcare resource use and costs were significantly higher in people with <200 CD4 cell counts in both groups.

When only patients infected by heterosexual contact were considered, the same differences in healthcare resource consumption were noted, but total cost of care was reduced and more homogeneous in both groups.

Conclusion : Migrant population infected predominantly by heterosexual contact had a lower CD4 cell counts, had more outpatient visits, but had lower costs of care than native population. Patients infected by other routes are responsible for a larger share of healthcare resource and costs, predominantly due to a trend towards higher rate of hospitalisation.

L'adoption de technologies prometteuses doit-elle être différée à cause du système de financement des hôpitaux ? L'exemple de la vaporisation laser de l'adénome prostatique

¹WASSERFALLEN J., ²Jichlinski P., ¹Pinget C.,

*DIM*¹, *URO*²,

Contexte : L'hyperplasie bénigne de la prostate peut être traitée par résection transurétrale (TURP) ou chirurgie radicale (CR). La TURP est associée à des complications hémorragiques et d'intoxication à l'eau, alors que la CR implique une plus longue durée de séjour à l'hôpital, et de fréquentes complications tant urinaires que sexuelles. La vaporisation laser (VL) amène la même destruction tissulaire que la TURP, tout en diminuant significativement la survenue de complications. Néanmoins, son impact financier sur le budget hospitalier est inconnu.

Méthode : L'efficacité et la sécurité de CR, TURP et VL ont été dérivées de la littérature. L'évaluation économique a été effectuée dans une perspective hospitalière, et a inclus l'acquisition du système et sa maintenance, les coûts de matériel à usage unique, et les coûts directement liés à la durée de séjour pour la TURP et la VL. Ces coûts qui ont été comparés avec le remboursement reçu dans le système APDRG.

Résultats : Les coûts et les prix ont été modélisés pour un nombre annuel de 120 patients. La VL diminuerait la durée de séjour de 2 jours, comparée à la TURP (médiane de 2 jours versus 4 jours). Toutefois, elle entraînerait un coût additionnel par patient de CHF 200 : coût additionnel total de CHF 1'926, compensé par une économie sur le matériel de la TURP (CHF 410), les transfusions sanguines (CHF 90), et la durée d'hospitalisation (CHF 1'226). Dans une perspective de payeur, les deux procédures sont classées comme APDRG 337, remboursé CHF 9'465, pour une durée de séjour standard de 3 à 9 jours. Toutefois, si la VL diminuait la durée de séjour à moins de 3 jours, le remboursement diminuerait de CHF 4'070, et entraînerait une perte de CHF 3'900 par patient traité par VL.

Conclusion : La VL améliore la qualité des soins aux patients et son devenir comparée avec la TURP, mais pourrait entraîner une perte financière pour l'hôpital. Si cette situation survient fréquemment, l'adoption de nouvelles technologies prometteuses par les hôpitaux pourrait devoir être différée pour des raisons économiques. Un système de financement délétère pour les soins aux patients et leur devenir devrait pouvoir être modifié rapidement pour éviter d'entraîner des effets secondaires indésirables.

The neuroprotective effect of induced hypothermia after global brain anoxia is dependent on the initial type and duration of circulatory arrest.

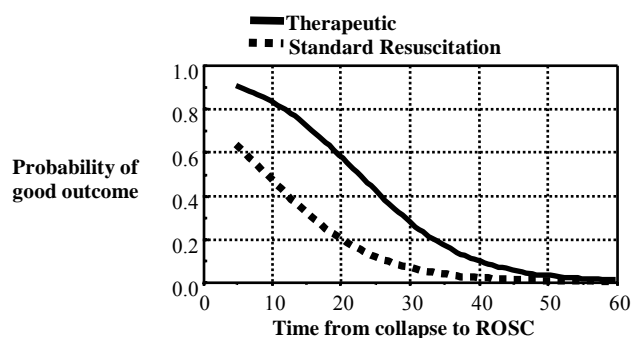
¹ODDO M., ²Marie-Denise S., ³François F., ⁴Vincent R., ²Lucas L.,

Soins Intensifs, CHUV, Lausanne¹, Soins Intensifs², Physiopathologie³, Urgences⁴,

Introduction: Induced hypothermia (IH) has been shown in two randomized controlled studies to improve neurological recovery after post-cardiac arrest (CA) coma. However, this treatment is still underused in clinical practice. To that respect, an important issue is to better identify pts who mostly benefit from IH.

Methods: We retrospectively analyzed 109 pts admitted to our ICU for persistent coma after out-of-hospital CA due to VF and non-VF rhythms (asystole and pulseless electrical activity). 54 consecutive pts were treated from June 1999 to May 2002 with standard critical care including normothermia (NT) and served as historical controls. 55 consecutive patients were treated from June 2002 to December 2004 with standard care plus mild hypothermia (to a central temperature of 33°C) for 24 hrs, via an external cooling technique (ice packs + cooling mattress). The outcome at hospital discharge was assessed using Glasgow-Pittsburgh Cerebral Performance (CPC) categories (good outcome = CPC 1 and 2, i.e. pts with sufficient neurological function to return home and live independently). The potential impact of IH was analyzed based on the type and duration of CA and the presence or absence of shock.

Results: In pts with CA due to VF, IH significantly improved neurological recovery (good outcome in 24/43 pts [55.8%] in the hypothermia group vs. 11/43 pts [25.6%] in the normothermia group, $p=0.004$). The frequency of discharge to long-term rehabilitation facilities (CPC 3) was also significantly lower (4.7% in the IH group vs. 18.6% in the NT group, $p=0.04$). In contrast, IH had no impact on the outcome after CA due to non-VF rhythms. When looking to hemodynamic status, the benefit of IH was maintained in patients with shock (good outcome in 5/17 pts in the IH group, vs. 0/14 pts in the NT group, $p=0.027$). The duration of CA (= time from collapse to return of spontaneous circulation, ROSC) was a strong independent predictor of outcome (OR for each additional 5 min: 0.53; 95% CI, 0.37-0.72, $p<0.001$). Indeed, IH was shown to be of particular benefit on the outcome of pts with relatively short duration of CA (<30 min, see **Figure 1**).



Conclusion: After prolonged cardiac arrest, induced hypothermia significantly reduced the rate of anoxo-ischemic encephalopathy in patients with ventricular fibrillation rhythms and with short duration of initial global ischemia, independently on their hemodynamic status.

AN ELECTRONIC PILL-CONTAINER (MEMS®) ADHERENCE INTERVENTION PROGRAM IN AN OUTPATIENT HYPERTENSION CLINIC IS EFFECTIVE IN LOWERING BLOOD PRESSURE

FIGUEIREDO H., Bugnon O., Burnier M., Favre M., Avenati T., Schneider M.P.

Pharmacie de la PMU, University Medical Outpatient Clinic-Lausanne Switzerland

INTRODUCTION

Therapy effectiveness in hypertension can be assessed through the measure of office blood pressure (OBP) and its correlation with the level of drug adherence.

AIMS

Correlation of patient adherence with OBP. Characterization of the long-term use of an electronic pill container (MEMS®) in an ambulatory hypertension clinic.

METHODS

Retrospective data (1998-2004) of patients having been prescribed the MEMS® for at least 2 months, because of uncontrolled OBP, were analysed. Clinical and pharmaceutical data were collected before, during and after the adherence monitoring period. Setting: University medical outpatient and hypertension clinics.

RESULTS

89 patients (62% men, median age: 53, median BMI: 30 kg/m², 70% Caucasian) were included. Most of the patients were taking 3 concomitant drugs. 88% of the patients took a renin-angiotensin system inhibitor, 73% a diuretic, 51% a Ca²⁺ channel blocker and 36% a β-blocker. Median follow-up with the MEMS® was 224 days (quartiles: 126-500). The MEMS® was used for more than 6 months in 53 patients (60%), 12 months in 32 patients (36%), 18 months in 22 patients (25%) and more than 24 months in 11 patients (12%). Global adherence was >90% in 37% of the patients.

Mean systolic OBP at the start and at the end of the monitoring period was 160 (SD=21, IC95: 155-165) and 145 (SD=21, IC95: 140-150) mmHg respectively (p<0.01). Mean diastolic OBP at the start and at the end of the monitoring period was 101 (SD=12, IC95: 98-103) and 91 (SD=12, IC95: 88-93) mmHg respectively (p<0.01).

CONCLUSIONS

Mean OBP decreased significantly during drug adherence monitoring. A correlation exists between adherence and OBP. A multivariable and cost-effective

ACCEPTANCE OF THE HEALTH HYPERTENSION PASSPORT, AN INTERACTIVE TOOL TO FACILITATE PATIENT INVOLVEMENT IN THE MANAGEMENT OF THEIR DISEASE

NIQUILLE A., Guignard E., Schneider M.P., Bugnon O.

Pharmacie Policlinique Médicale Universitaire, University Medical Outpatient Clinic, Lausanne Switzerland

Introduction

The Health Hypertension Passport (HHP) focuses on empowerment, and increase in patients health education, motivation and dialogue between care-partners. Beyond transmitting patient-oriented information on hypertension and risk factors, the HHP allows patient to record blood pressure, weight, physical activity and drug consumption data as well as questions/comments on health that should be passed on to the community pharmacist (CPh) or the general practitioner (GP).

Aims

To evaluate acceptance of the HHP by patients, CPhs and GPs.

Methods

CPhs and GPs were asked to distribute 5 to 20 HHPs and to inform patient about its use. Acceptance was evaluated by the rate of HHP distribution, quality and quantity of collected data and questionnaires at the end of the study.

Results

70% CPhs or GPs (28/40) agreed to participate. Only 114 HHPs were distributed (median=2/CPhs or GPs; quartiles: 0-5; range: 0-20) despite the high patients acceptance's rate (65%). The length of use was variable (median=54 days; quartiles: 47-74; range: 32-196). HHP was broadly well accepted and perceived as useful by most of the patients, CPhs and GPs. 58% of patients would like going on with their HHP and 59% of CPhs and GPs would like using it in daily practice.

Conclusion

The level of HHP acceptance was high but the HHP distribution rate by the CPhs and GPs was unfortunately poor. Therefore, CPhs and GPs' awareness of available and innovative tools in chronic disease management should be increased. Larger studies are needed to evaluate HHP clinical efficacy and acquire efficiency's recognition by health insurances.

Myasthenia Gravis (MG) in Lausanne: An analysis of factors responsible for unsatisfactory outcome

¹KUNTZER T., ²Dunand M., ³Borruat F., ²Botez S.,

Neurologie Bh07/306¹, neurologie chuv², neuro-ophtalmologie chuv³,

Objective: To study 41 patients with autoimmune MG in order to know the percentage and the reasons of unsatisfactory outcome.

Methods: Patients were initially diagnosed with MG, and referred lately to our Nerve-Muscle Unit. Outcome was rated according to the Myasthenia Gravis Foundation of America Postintervention Status. The Complete Stable remission, Pharmacologic Remission, Minimal Manifestations and Improved Status were considered as satisfactory outcome. Patients scoring Unchanged (U), Worse (W) or Exacerbated (E) during follow-up were all taken into account and the reasons leading to unsatisfactory responsiveness were analysed.

Results: Unsatisfactory outcome rate was 19.5% (8/41) with 4 patients scoring U, 3 W and 1 E at the last visit, but during the follow-up, 22 patients (54%) were U (3/22), W (8/22) or E (11/22). They were related to insufficient medication (36%), infectious diseases (23%) and no compliance (28%).

Conclusion: This study points out that more than 50% (22/41) of our MG patients had an unsatisfactory outcome during follow-up. Part (60%) of this unsatisfactory outcome could be prevented by tailoring adequate treatments during regular appointments by interested specialists in myology.

Detection of epileptic activity in acute stroke with continuous electroencephalogram

¹CARRERA E., ¹Michel P., ¹Despland P., ¹Maeder-Ingvar M., ²Ruffieux C.,
¹Debatisse D., ¹Ghika J., ¹Devuyst G., ¹Bogousslavsky J.,

*Neurologie*¹, *IUMSP*²,

Background and purpose : The role of continuous electroencephalogram (cEEG) in stroke unit is controversial. The purpose of this study is to determine the incidence and risk factors of electrical seizures and other electrical epileptic activity using cEEG in acute stroke patients. **Methods :** One hundred consecutive acute stroke patients admitted to our stroke unit underwent cEEG using 10 electrodes. After exclusion of 17 patients with EEG-modifying medications, 83 patients remained for analysis. In addition to electrical seizures, the following EEG patterns were recorded : repetitive focal sharp waves (RSHW), repetitive focal spikes (RSP) and periodic lateralized epileptic discharges (PLEDS). **Results** In the 83 patients who underwent cEEG without EEG-modifying medication, cEEG was recorded for a mean duration of 17:35 hours (range 1:12-37:10). Epileptic activity occurred in 14 (16.9%) patients : RSHW in 5, RSP in 6 and PLEDS in 3 patients. Electrical seizures occurred in 2 (2.4%) patients. On univariate Cox regression analysis, predictors for electrical epileptic activity were stroke severity (high NIHSS) (hazard ratio (HR) 1.13; p=0.001), cortical involvement (HR 4.81; p=0.040) and thrombolysis (HR 3.66; p=0.049). Age, sex, stroke type and cardiovascular risk factors were not predictor of electrical epileptic activity. On multivariate analysis, stroke severity was the only independent predictor (HR 1.11; p=0.009). **Discussion :** In acute stroke patients, electrical epileptic activity occurs more frequently than previously suspected. Because this activity may be associated with bad outcome or post stroke epilepsy, the usefulness of cEEG warrants further investigations especially in patients with severe strokes, cortical strokes and in those who benefit from thrombolysis.

Executive and procedural dysfunction of bipedal standing and gait in elderly patients. A prospective clinical-imaging study and a proposal for a new concept of cognitive deficits of bipedal gait.

¹GHIKA J., ¹Joray S., ²Meuli R., ¹Bogouslavsky J.,
NLG¹, RAD²,

Background: Highest level gait disorders (HLGD, Nutt et al. 1993), a combination of bipedal standing, rightening and locomotor dysfunction, are frequently found in association with small vessel disease, hydrocephalus, old age, or cortico-subcortical atrophy. Correlation of neurological and cognitive deficits with radioimaging in HLGD is poorly studied and present clinical definitions are unsatisfactory.

Methods: We analyzed clinically bipedal gait, postural reflexes and rightening reactions in 43 consecutive patients with HLGD including frontal gait disorder (FGD), frontal disequilibrium (FD), subcortical disequilibrium (SD) and isolated gait ignition failure (GIF). Neuroradiologists, unaware of clinical data, described CT and MRI scans. There were classified as: vascular lesions (VL) (i.e. leukoencephalopathy and/or lacunes and/or large strokes), hydrocephalus (Hy), cortico-subcortical atrophy (CSCA) or mixed patterns. **Results:** Pure VL were found in 11 patients (6 with some degree of CSCA); 10 had pure Hy; 13 had only CSCA ; 9 had mixed VL and Hy (5 with some degree of CSCA). When monosymptomatic, GIF (13 patients) was only found in pure CSCA, associated with a mild akinetic axial parkinsonism compatible with the diagnosis of pure akinesia; when associated with other patterns of HLGD, some degree of GIF was not specific of any neuroimaging pattern. SD was only found in the presence of basal ganglia and thalamic lacunes. FGD, the most frequent form of HLGD was not specific for any neuroimaging subgroup. FD was only found in patients with hydrocephalus, either alone or in mixed combination. In pure Hy (n=10), 6 patients presented with FGD and 4 with FD. Among patients with pure VL (n=11), 6 presented FGD and 5 SD. In 9 patients with mixed VL and Hy, FGD was found in 5, FD in 4, but SD or GIF were never observed. Almost all patients (95%) were cognitively impaired, 40% MCI and 55% with ICD-10 dementia, with prominent dysexecutive and memory dysfunction.

Discussion: None of the HLGD patterns was specific of any neuroradiological subgroups except for GIF with pure CSCA. SD was only found in the presence of lacunes in the basal ganglia/thalamus and FD in association with some degree of Hy. Cognitive impairment, with executive dysfunction at the forefront, was present in almost all patients. We suggest that HLGD is a continuum along progressive loss of executive control on recently acquired frontal bipedal standing, rightening reaction and gait pattern . According to recent knowledge, we propose to call GIF or freezing bipedal gait akinesia (probably due to loss of medial frontal function) and loss of context adapted bipedal gait progression (loss of anticipation, shifting directions or patterns, sequencing, inhibition of automatic patterns or archaic locomotor patterns, goal oriented strategy, probably due to loss of dorsolateral prefrontal control on gait) executive dysfunction of gait. Large sustentation base, small steps, stooped posture, decreased upgaze, loss of protective reflexes starting with antigravific retropulsion up to absent multidirectional antigravific protective reflexes and disequilibrium with inability to stand in bipedal posture could represent reemergence of archaic gait patterns when automatic procedural memory for bipedal gait is lost, when basal ganglia are involved, results in parkinsonian-like posture and gait with emergence of simian posture and gait. Re-emergence of disinhibited even more archaic patterns of locomotion and standing reflexes (climbing prehensive reflexes, jumping...) occur at end stages of frontal disequilibrium, paralleling cognitive executive dysfunction severity.

Electrocorticography (EcoG) and scalp EEG during intracranial vascular surgery: a new approach in neuromonitoring

¹Debatisse D., ¹Pralong E., ²Dehdashti A., ³Daniel R., ²Villemure J., ²Regli L.,

NCH, Neurophysiology¹, NCH², NCH, Christian Medical College, Vellore³,

Intraoperative monitoring has taken great strides in the last decade and has become a standard of care for many neurosurgical procedures. In intracranial vascular surgery, it is primarily aimed at detecting early ischemic changes and various neurophysiological approaches have been proposed to reduce intra- and postoperative morbidity. Somatosensory evoked potentials (SSEPs) present good sensitivity and specificity but are limited to aneurysms in the Sylvian artery territory. On the other hand, scalp EEG are useful for carotid surgery but are not sensitive enough for aneurismal surgery monitoring. This study presents our early results with a new methodology of intraoperative monitoring using simultaneous continuous scalp EEG and multilobar electrocorticographic (EcoG) recording during neurovascular procedures in 21 interventions. Excellent recordings were obtained in all cases. Data analysis showed that focal changes consistent with transitory cerebral ischemia were seen in a majority of cases (20/21) on the EcoG, but only in 4 out of 21 cases on the EEG. The most common abnormality detected on the EcoG were high frequency waves (beta3), which appeared just after vascular occlusion and were occasionally followed by slow waves or burst suppression pattern. In our hands, the EcoG was found to detected earlier and more changes than EEG.

Bilateral on-line EEG and EcoG during peri-insular hemispherotomy: Methodology and demonstration of dependent secondary epileptogenesis

¹Debatisse D., ¹Pralong E., ²Daniel R., ³Roulet E., ⁴Villemure J.,

NCH, Neurophysiology¹, Christian Medical College, Vellore², PED³, NCH⁴, f

Purpose:

The presence of epileptic spikes from the normal hemisphere is often encountered in patient's candidates for the surgical treatment of hemispheric epilepsy. This would seem at first a contraindication to surgery; however, the possibility of secondary epileptogenesis is to be taken into account when contemplating surgery in these circumstances. Such epileptic abnormalities could be dependent or independent from the primary foci located in the hemisphere to be operated. In the case of dependent foci, surgery could cure the epilepsy; on the other hand, persistent seizures could result if the foci were independent before surgery, though the seizure burden might be substantially reduced with surgery.

Methods:

We present the methodology of bilateral intra operative monitoring using scalp EEG (EEG) and Electrocorticography (EcoG), and the results obtained during peri-insular hemispherotomy in a child with pharmaco resistant epilepsy (infantile hemiplegis) who preoperatively presented bilateral electrographic epileptic abnormalities.

Results and conclusion:

Bilateral on-line EEG and EcoG monitoring during peri-insular hemispherotomy is feasible and confirmed the per-operative disappearance of the epileptic abnormalities present in the non-operated hemisphere. It confirmed the effect of hemispheric disconnection on contralateral dependent spikes, and their immediate cessation. To our knowledge, this methodology is for the first time applied, in human hemispheric epilepsy, to monitor secondary epileptogenesis with an online demonstration of the extinction of the contralateral foci.

Development of a panfungal real-time PCR

¹Hinrikson H., ¹Jaton K., ²Ciardo D., ³Altwegg M., ¹Bille J., ¹Hauser P.,

Institut de Microbiologie, CHUV¹, Department of Medical Microbiology, University of², Bio-Analytica AG, 6006 Lucerne³,

Objectives

To develop and evaluate a panfungal real-time PCR for early detection and presumptive identification of pathogenic fungi directly in clinical specimens.

Methods

Based on a comprehensive sequence alignment, we designed a panfungal PCR targeting the variable region 5 of the small-subunit (18S) ribosomal gene. The assay consisted of 4 forward primers, 8 reverse primers and 1 fluorescence-labeled probe to ensure efficient detection of ascomycetes, basidiomycetes and zygomycetes. The sensitivity was assessed by comparison to a quantitative *Aspergillus fumigatus*-specific PCR. The specificity was tested using reference DNAs of fungal, bacterial and human origins. A retrospective clinical evaluation was conducted using DNA extracts from clinical specimens of both patients with proven invasive fungal infections [N=15] and negative controls [N=18]. The identity of amplicons was determined by comparative sequence analysis.

Results

The analytical sensitivity of the panfungal PCR was found comparable to that of the *A. fumigatus*-specific approach, i.e. one target copy per reaction. However, in order to avoid false positive reactions due to minute fungal contaminations introduced occasionally while sampling or processing specimens, the diagnostic detection limit was considered 5 target copies per reaction. The specificity for fungal DNA was confirmed by amplification of all fungal reference DNAs investigated and by the absence of positive reactions with reference DNAs of bacterial and human origins. The clinical sensitivity and specificity were 87 and 100%, respectively, when considering a particular specimen as PCR positive if it exhibited at least 2 positive reactions per triplicate testing. False negative results were obtained with 2 specimens previously shown to contain only trace amounts of target DNA. Sequencing of the clinical amplicons allowed presumptive identification of yeasts (*Candida* [N=5], *Cryptococcus* [N=1]), molds (*Absidia* [N=1], *Aspergillus* [N=2], *Fusarium* [N=1]), *Rhizomucor* [N=2] and *Pneumocystis* [N=1] to at least the species group level. For instance, the usually more susceptible *Candida* species (e.g. *C. albicans*, *C. parapsilosis*, and *C. tropicalis*) were clearly distinguished from the usually less susceptible species such as *C. glabrata* and *C. krusei*.

Conclusion

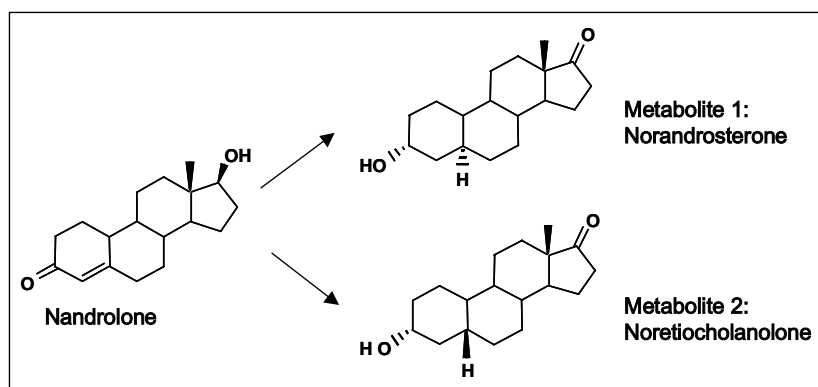
The present panfungal real-time PCR represents a promising tool for improved diagnosis and empirical treatment of invasive fungal infections thus warranting further clinical validation.

Concentrations of Nandrolone metabolites in urine after the therapeutic administration of an ophthalmic solution

AVOIS L., MANGIN P., SAUGY M.,

Laboratoire Suisse d'analyse du Dopage, IUML

Nandrolone, or 19-nortestosterone, is an anabolic steroid initially introduced for the treatment of anemia, osteoporosis and breast carcinoma. Nandrolone is available in several pharmaceutical formulations as 17 β -hydroxyester in an oily matrix or as a nandrolone salt (decanoate or sodium sulfate) in an aqueous solution. The pharmaceutical formulation most widely used is Deca-Durabolin®, but other products, as Keratyl® eye drops solution, are also currently administered.



Nandrolone is one of the most abused anabolic steroid in various sports and the presence of its metabolites in urine at low concentrations is always submitted to discussion, because of possible endogenous production or intake of contaminated nutritional supplements [1-3].

Analyses for nandrolone according to the World Anti-Doping Agency (WADA) protocol are based on the identification of the nandrolone two principal urinary metabolites, which in humans are glucuronides of 19-norandrosterone and 19-noretiocholanolone. For the first and main metabolite, a limit of 2 ng/ml has been set by the anti-doping code.

In this study, a therapeutic dose of a nandrolone sodium sulphate containing eye drops solution (Keratyl®) has been administered to several male volunteers during 3 days and urines have been collected during 3 weeks. Surprisingly, contrary to all expectations, the urinary concentrations measured in urines reached 450 ng/ml and 70 ng/ml for norandrosterone and noretiocholanolone, respectively. Concentration levels near 2 ng/ml were found 10 to 15 days after the last administration, depending on individual metabolism. Thus, inter-variability as well as intra-variability of nandrolone metabolism, regarding this particular administration mode, were also evaluated.

Recently, our laboratory has been involved in a nandrolone positive case which led to the investigation of the Keratyl® product. It appears that medical profession often considers these kind of pharmaceuticals as "trivial medication", is not aware that such products can lead to a positive case and consequently, do not warn athletes against using this medication.

Acknowledgements: Florian, Lambercier, Aurélien Desmarchelier, Sylvain Giraud

[1] Robinson N, Taroni F, Saugy M, Ayotte C, Mangin P, Dvorak J. Detection of nandrolone metabolites in urine after a football game in professional and amateur players: a Bayesian comparison. *Forensic Sci Int.*, **122** (2001) 130-5.

[2] Baume N, Avois L, Sottas PE, Dvorak J, Cauderay M, Magin P, Saugy M. Effects of high intensity exercises on ¹³C-nandrolone excretion in trained athletes. *Clin J Sport Med*, (2005) In Press.

[3] Baume N, Mahler N, Kamber M, Mangin P, Saugy M. Research of stimulants and anabolic steroids in dietary supplements. *Scandinavian Journal of Medicine & Science in Sports*, (2005) In Press.

AN AMBULATORY SYSTEM TO ASSESS 3D KNEE FUNCTIONS PRE AND POST OPERATIVELY FOR PATIENTS WITH ACL RUPTURE

¹JOLLES B., ²LUTHI F., ³AMINIAN K., ¹SIEGRIST O.,

Département de Chirurgie / Service OTR¹, SUVA², EPFL / LMAM³,

INTRODUCTION: Anterior Cruciate Ligament (ACL) injuries may lead to knee joint instability, which in turn may cause meniscal tears and cartilage lesions.

Although several studies have shown that injuries of the ACL affects performances of daily activities, the three dimensional (3D) gait patterns after ACL injury and/or surgery are not clearly understood.

The purpose of this study was twofold: firstly, to develop an ambulatory system based on gyroscopes which enables the evaluation of 3D knee kinematics. Secondly, to compare the function of ACL deficient and healthy knees, before and after surgery.

METHODS: Five young patients (31 ± 7 y.o.) with symptomatic and isolated ACL deficiency participated in this study. Patients were evaluated first after accident and complete knee function recovery and a second time, 13 months (range 12-15) after operation. Each evaluation consisted in laxity measurement using a KT-1000 arthrometer, the IKDC score, and a 30 m walk at comfortable pace monitored by an ambulatory datalogger (Physilog®) and two 3D gyroscopes (fig. 1).

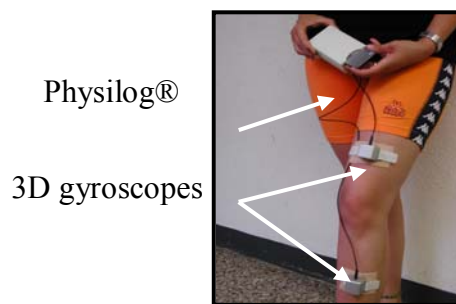
In order to assess the performance of the device, the repeatability was evaluated. Spatio-temporal parameters of gait as well as 3D kinematics were calculated. To diminish the effect of skin movement, the mean range of motion (ROM) around each axis were performed under more than 15 gait cycles. In addition, to remove the effect of acceleration and deceleration at the beginning and the end of the walk, only the steady part of the walk was considered.

RESULTS: The repeatability was less than one degree for flexion-extension and internal-external rotation, which was sufficient to show functional differences during the clinical evaluation.

After the accident and prior to the reconstruction, a ROM decrease was present in flexion-extension and internal-external rotation for the pathologic knee in comparison to the contralateral knee. A year after the surgery, four patients were evaluated as normal (A) and one almost normal (B), according to the IKDC. However, kinematics showed a decrease in flexion-extension and an increase in internal-external rotation.

DISCUSSION & CONCLUSIONS: In this investigation we proposed an ambulatory system for the estimation of 3D angles for knee joint using kinematic sensors. This system is a simple alternative to gait laboratory systems, with which it was possible to perform an analysis in a relatively long distance and extract the ROM. This technique allowed us to better compare the healthy and deficient knee functions, pre and post operatively. Although this study has been interpreted with caution given to the small number of subject, these results were very encouraging for future evaluation of patients with cruciate ligament injuries.

Fig. 1: To record 3D knee motion, an ambulatory system including a datalogger (Physilog®) and two kinematics sensors was



used.

ESTIMATION AND VISUALIZATION OF LOWER LIMBS ORIENTATION ANGLES USING BODY-FIXED SENSORS

¹JOLLES B., ²FUA P., ¹LEYVRAZ P., ³AMINIAN K.,

Département de Chirurgie / Service OTR¹, EPFL / CVIab², EPFL / LMAM³,

INTRODUCTION: In the quest for an alternative to optical motion analysis systems which are often used in the study of human movement, body-fixed sensors have been recently used. Body-fixed miniature sensors consisting of accelerometers and gyroscopes can be used to obtain joints and segments kinematic values, allowing to realize low-power, ambulatory recording systems carried by the subject for long-term measurements. This study presents a new method for accurate estimation of lower limb angles in sagittal plane which is based on a combination of accelerometers and gyroscopes. It presents also a new tool to visualize motion data with synthetic skeletons performing the same actions as the subjects.

METHODS: Lower limbs movements during gait were captured by 4 modules of sensors attached on both shanks and thighs. Each module consisted of a gyroscope and bi-axial accelerometers. The model of knee angle estimation was based on processing the outputs of a pair of virtual sensors placed at the knee center of rotation on the adjacent segments. Since both virtual accelerometers express the acceleration of the same point, they should have the same modulus, while their arguments' difference yields the knee joint angle. The model of shank orientation angle estimation was based on placing a virtual sensor on ankle aligned with the shank segment orientation. The method fuses the information of the angles obtained by gyroscope and accelerometers to cancel gyroscope drift. Since the acceleration on ankle is low during foot-flat and quiet standing periods, the information of accelerometers can be used as an inclinometer to correct the gyroscope drift. Finally, the thigh angle is obtained by just adding shank angle with knee angle.

Ten healthy subjects, aged between 44 and 70 years, participated in this experiment. The volunteers performed three 30s flat treadmill walking trials at speeds 2km/h, 3km/h and 4km/h, as well as a freely arbitrary flexion and extension of knee such as sitting, standing and swinging. For comparison and validity appreciation, a motion measurement system (Zebris, D) was used as the reference system.

RESULTS: The results of all tests were very close to those of the reference system and presented very small errors (mean<0.70°, standard deviation<2.0° for knee angle estimation, and mean<0.87°, standard deviation<94.0° for shank angle estimation) and excellent correlation coefficients (>0.994 for knee and >0.997 for shank). Figure 1 shows the calculation of knee flexion-extension angle of a subject during walking at 3km/h.

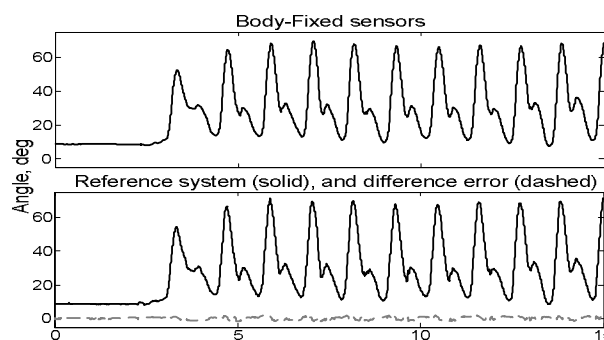


Fig. 1: Knee angle estimated using body-fixed sensors, and compared with reference system.

DISCUSSION & CONCLUSIONS: The proposed system offers a new accurate tool for lower limbs motion monitoring. The gait visualization tool provides a simple tool to monitor and display motion for long-term monitoring where camera based systems could not be used.

REFERENCES: ¹Aminian K, Trevisan C, Najafi B, Dejnabadi H, Frigo C, Pavan E, Telonio A, Cerati F, Marinoni EC, Robert Ph, Leyvraz PF. Evaluation of an ambulatory system for gait analysis in hip osteoarthritis and after total hip replacement. *Gait and Posture* 2004; 20:102-6.

ACKNOWLEDGEMENTS: This work was supported by a Swiss National Foundation Grant (FNRS 3200-064951).

TRANSIENT STRIATAL DELIVERY OF GDNF VIA ENCAPSULATED CELLS LEADS TO SUSTAINED BEHAVIORAL IMPROVEMENT IN A BILATERAL MODEL OF PARKINSON DISEASE

¹ETEMAD-SAJADI A., ¹Etemad-Sajadi A.,

Neurochirurgie¹, CHUV-Lausanne

Numerous studies have shown the neuroprotective and regenerative benefits of glial cell line-derived neurotrophic factor (GDNF) in animal models of PD. Brain delivery of GDNF can, however, be associated with limiting side-effects in both primates and PD patients, rendering the duration of delivery a critical factor. In the present study, the effects of transient versus sustained GDNF delivery by encapsulated cells were evaluated in a bilateral animal model, closely mimicking advanced PD. One week following bilateral striatal 6-hydroxydopamine injections in rats, capsules loaded with human fibroblasts genetically engineered to release GDNF were bilaterally implanted in the striatum. GDNF delivery resulted in a significant improvement of movement initiation and swimming performance in the lesioned animals, associated with striatal reinnervation of dopaminergic fibers. To test the sustainability of the behavioral improvement, GDNF-secreting capsules were withdrawn in a subgroup of animals, 7 weeks post-implantation. Strikingly, both the behavioral and morphological improvements were maintained until the sacrifice of the animals 6 weeks post-GDNF withdrawal. The sustained cellular and behavioral benefits after GDNF washout suggest the need for temporary delivery of the trophic factor in PD. Retrievable encapsulated cells represent an attractive delivery tool to achieve this purpose.

Colonic Movements in Healthy Subjects as Recorded by Magnet Tracking System

¹Hiroz P., ²Schlageter V., ²McManus J., ²Demierre M., ¹Givel J., ²Kucera P.,

Service de chirurgie viscérale¹, Institut de physiologie², CHUV Lausanne

Introduction: Current methods to investigate colonic transit rely mainly on radio markers and scintigraphy. A new non invasive and radiation free technique, the Magnet Tracking System (MTS), allowing continuous evaluation of gastrointestinal motility is now available. The purpose of this study is to investigate colonic propulsive activity and to compare the displacement of a magnetic pill and standard radio markers.

Methods: MTS is based on the continuous tracking of a small magnet progressing through the digestive tract. The coordinates of the magnet are calculated from signals recorded by an array of magnetic sensors located over the abdomen and displayed in real time. Twenty healthy volunteers with regular daily transit swallowed the magnet and a pill containing 10 radio markers. MTS recording was performed at waking, after ingestion of a standard 600 kcal breakfast and two hours later after a black coffee. Frequency, origin and amplitude of the movements were analyzed. Abdominal X-rays were taken to compare the positions of the radio markers and the magnet.

Results: Out of 150h of recording, 86 movements larger than 4cm were observed, among which 25 greater than 10cm and up to 30cm. Variable velocities, up to 1cm/s, were measured. Although recorded in every colonic segments, movements were more frequent in the left colon, and more often (82%) in aboral direction. On X-rays, the markers were widely spread. With respect to markers, the magnet was delayed in the proximal colon but advancing faster in the distal part. However, on average, the global transit time of the magnet and of the markers were the same.

Conclusion: The MTS allowed accurate 3 dimensional characterization of the dynamic of the movements. Large movements were recorded in all segments including the ascending colon. Standard X-rays showed that, in healthy volunteers, magnet and pellet displacements could be correlated. The MTS offers a new opportunity to study in detail colonic motility disorders.

Monitoring of Voriconazole Blood Levels in Adult Patients: 1-Year Experience at a University Hospital.

¹PASCUAL A., ¹Bolay S., ¹Marchetti O.,

Maladies Infectieuses¹, CHUV Lausanne

Background Voriconazole (VRC) is first choice therapy for aspergillosis and a new Rx option for candidiasis. Inter- and intra-individual variations of VRC blood levels related to non linear pharmacokinetics, polymorphism of cytochrome CYP2C19, drug interactions and hepatic dysfunction have been reported and may affect efficacy or tolerance. The aim of the study was to evaluate the clinical impact of monitoring of VRC blood levels.

Methods Retrospective analysis of 35 VRC Rx courses in 33 adult patients (Pts) during 2004. Standard definitions for diagnosis of mycosis, response to therapy, and serious adverse events (SAE) (NCI criteria). VRC blood levels were measured by HPLC.

Results Indications for VRC therapy (median dose: 4 mg/kg bid, duration: 50 d) were aspergillosis (58%), candidiasis (26%), and other mycosis (15%). VRC blood levels were measured in 19 of 35 (54%) Rx courses. Median # and intervals between VRC blood levels measurements: 4.5 (1-9) and 7 d (1-62). Among 8 Pts with VRC levels >5.5 mg/L, 4 presented with neurological SAE (hallucinations and encephalopathy, 2 each), which resolved after VRC dose reduction (1) or discontinuation (3). Median VRC troughs levels were not different in Pts with or without SAE (6.3 vs 7.0 mg/l). However, adjustment of VRC dosing limited median exposure to VRC levels > 5.5 mg/L in Pts without compared to Pts with neurological SAE (5 vs 12.5 d) (P=0.06). Cholestasis was observed in 26% of Rx courses: no correlation with VRC levels was found. No SAE occurred in the 16 Rx courses during which VRC blood levels were not measured.

Conclusions One-year experience of monitoring of VRC blood levels suggests that prolonged overdosing may be associated with neurological SAE. Monitoring may help to improve management in this subset of patients.

VRC trough levels (mg/L) and clinical course :

	< 0.2 (mg/L)	.2 – 5.5 (mg/ L)	> 5.5 (mg/L) (c)
Success	/2 (a,b)/9	/8	
SAE-/9	/82/8		

a) 1 Pt with rifampin-interaction: persistent fever resolved

b) 1 Pt received VRC 400 mg/d orally: relapse of aspergillosis responded to VRC dose increase (600 mg/d)

c) Median VRC dose 4 mg/kg bid (3.5-4.5). Tacrolimus-interaction in 1 pt

Treatment for pathological gambling: Influence of co-morbid substance abuse

¹WANKMUELLER N., ^{1,3}Simon O., ¹Aufrère L., ¹Rossier Y., ¹Asal S., ^{1,3}Klila H.,
¹Rihs-Middel M., ^{1,3}Besson J., ^{1,2}Martin-Sölch C.,

1 Center for pathological gambling, Department of Adult Psychiatry, University of Lausanne, Switzerland

2 Mood and Anxiety Disorder Programm, NIMH, NIH, Bethesda, USA

3 Center for drug dependence, University Department of Adult Psychiatry, University of Lausanne, Switzerland

1, 3 Division of Substance Abuse

Background and aims: It is still unclear how additional substance abuse, which is often associated with pathological gambling, influences the treatment of pathological gamblers. In this study, we investigated the role of co-morbid substance dependence on the treatment and the drop out rate of patients recruited in a Swiss outpatient clinic for pathological gambling.

Sample and methods: 128 patients were included, who all presented a primary diagnosis of pathological gambling (based on DSM IV, SOGGS and standardized clinical interview). We assessed tobacco, alcohol, heroin, cocaine, cannabis and medication abuse or dependence and compared their influence on the drop out rate and type of treatment (brief counseling, motivational interviewing or cognitive-behavioral therapies).

Preliminary findings: 51% of our patients are smokers, 19 % showed symptoms of alcohol abuse, 4% used cannabis, 1,6% were cocaine dependent, 1.6% were medication dependent and 0.8% were heroin dependent. The drop out rate seemed to be higher in patients smoking ($p < .05$), abusing or being dependent on illicit or prescription drugs (cannabis ($p < .005$), heroin ($p < .05$), cocaine ($p < .05$), prescription drugs ($p < .01$)). Most of the patients seeking only brief counseling had co-morbid substance dependence.

Implication for the field: Patients with symptoms of substance dependence are more likely to drop out or to attend a brief counseling instead of engaging in a therapy. Therefore, co-morbid substance dependence (although it appears to be a poor treatment predictor) should be considered at onset of treatment for pathological gamblers.

Implantation d'électrodes dans la paroi colique terminale porcine: étude de la tolérance et de la stabilité à un mois

¹GIÉ O., ¹Hiroz P., ²Schlageter V., ³Gardaz J., ¹Givel J., ²Kucera P.,

Service de chirurgie viscérale¹, Institut de physiologie², Service d'anesthésie³,

But :

L'objectif du projet multidisciplinaire Colostim est le développement d'un appareillage implantable pour la stimulation électrique du côlon pouvant favoriser la motilité intestinale en cas de constipation chronique. La tolérance de l'organisme porcin à l'implantation d'électrodes de stimulation (Medtronic, Model 6500 Unipolar Temporary Myocardial Pacing Lead), ainsi que la stabilité de ces derniers après fixation à la paroi du rectum ont été étudiées. Le choix de ce segment intestinal présente plusieurs avantages : étant fixé à la paroi abdominale postérieure, il s'agit d'une localisation idéale pour l'implantation d'électrodes reliées à un câbles et donc soumises à une tension constante ; le rectum est par ailleurs facilement accessible par voie transanale à une sonde de manométrie permettant de valider les stimulations.

Méthode :

Une laparotomie médiane a permis l'accès à la cavité abdominale de 6 porcs. Après exposition du rectum, 6 électrodes ont été implantées dans la paroi colique distale et fixées par deux points de suture intra pariétaux. Les câbles reliant les électrodes au stimulateur électrique extra corporel ont été tunnelisés et exteriorisés au niveau dorso-lombaire. Les animaux ont été sacrifiés après 4 semaines et les sites d'implantation des électrodes sur la paroi rectale analysés en détail, après prélèvement de tout le côlon distal.

Résultats :

Les électrodes ont été retrouvées au site d'implantation chez cinq porcs, fixées à la paroi intestinale par les deux points de sutures. Chez un animal, les six électrodes étaient détachées de la paroi colique.

Aucune réaction inflammatoire n'a pu être mise en évidence autour des câbles.

Conclusions :

Notre étude a démontré la stabilité des électrodes implantées dans la paroi colique et l'efficacité de la fixation utilisée. Aucune délocalisation n'a été mise en évidence à l'exception d'un cas, dont la désolidarisation est probablement à mettre en relation avec une traction excessive exercée sur les câbles de stimulation peu après l'implantation.

Il est de lors possible d'affirmer la faisabilité de l'implantation au long cours d'électrodes dans la paroi intestinale distale du porc.

ODE
Oncologie et
Développement

A RasGAP-derived cell permeable peptide potently enhances genotoxin-induced cytotoxicity in tumor cells.

¹MICHOD D., ¹Widmann C.,

*DBCM*¹,

Tumors are diverse and heterogeneous, but all share the ability to proliferate without control. Deregulated cell proliferation coupled with suppressed apoptotic sensitivity constitutes a minimal requirement upon which tumor evolution occurs. One of the most commonly used treatments is chemotherapy, which frequently uses chemical compounds that induce DNA damage, such as cisplatin, adriamycin or mitoxantrone. Anticancer agents are effective only when tumors cells are more readily killed than the surrounding normal tissue. If the efficacy of these agents is partly determined by their ability to induce apoptosis, then tumors cells must be more susceptible to apoptosis than the normal tissue from which they arose. We have recently demonstrated that RasGAP, a regulator of Ras and Rho GTP-binding proteins, is an unconventional caspase substrate because it can induce both anti- and pro-apoptotic signals, depending on the extent of its cleavage by caspases. At low levels of caspase activity, RasGAP is cleaved at position 455, generating an N-terminal fragment (fragment N) and a C-terminal fragment (fragment C). Fragment N appears to be a general blocker of apoptosis downstream of caspase activation. At higher levels of caspase activity, the ability of fragment N to counteract apoptosis is suppressed when it is cleaved at position 157. This latter cleavage event generates two fragments, N1 and N2, that in contrast to fragment N potently sensitizes HeLa cells toward cisplatin-induced apoptosis. In the present study we show that a cell permeable peptide derived from the N2 fragment of RasGAP specifically sensitizes cancer cells to three different genotoxins commonly used in chemotherapy.

Mammographic texture synthesis using genetic programming and clustered lumpy background

¹CASTELLA C., ²Kinkel K., ³Descombes F., ⁴Eckstein M., ⁵Sottas P., ⁶Verdun F.,
⁶Bochud F.,

Institut de Radiophysique Appliquée¹, Clinique des Grangettes, Chêne-Bougerie², Haute Ecole Cantonale Vaudoise de la Santé, Lausanne³, University of California, Santa Barbara⁴, Institut Universitaire de Radiophysique Appliquée⁵, Institut Universitaire de Radiophysique Appliquée⁶,

We investigate the digital synthesis of images mimicking real textures observed in mammograms. These images can be potentially used to study human and model observer in perception experiments. The advantages of the method are that the statistical properties of the generated images can be predicted and that it allows to produce unlimited number of images with such properties.

We used the previously developed clustered lumpy background (CLB) technique in conjunction with a genetic algorithm (GA) to synthesize the images. To maximize the realism of the synthetic textures, we combined a mathematical approach with psychophysics experiments involving radiologists judgments about the realism of the images. For the mathematical part, 36 statistical features were computed and averaged over 1000 regions of interest of real mammograms. The same features were measured for the synthetic textures and a Mahalanobis distance was used to quantify the similarity of the features between real and synthetic textures. The similarity (in terms of Mahalanobis distance) was used as GA fitness function for evolving the free CLB parameters. In addition, experienced radiologists were asked to qualify the realism of the typical structures that are expected to be found on real mammograms: glandular and fatty areas, fiber crossings.

Results show that the GA found CLB parameters generating synthetic images statistically close to real mammograms. Moreover, the psychophysics experiments confirm that all above-mentioned structures are well reproduced on the generated images. This means that we dispose of an arbitrary large database of textures mimicking mammograms with traceable statistical properties.

APO010 kills hematological tumor cells while having no effect on the repopulating function of hematopoietic progenitor cells

¹NAHIMANA A., ²Greaney P., ¹Lagopoulos L., ¹Aubry D., ²Dupuis M., ¹Duchosal M.,

*Hématologie*¹, *Apoxis*²,

Purging of malignant cells may improve the effectiveness of autologous stem cell transplantation (ASCT). Here we describe a new pro-apoptotic agent, APO010, which has a promising profile as a purging agent as it kills tumoral cells at concentrations which do not adversely affect the function of CD34+ hematopoietic progenitor cells.

A panel of hematological malignant cells and human hematopoietic CD34+ progenitor cells were assessed for their sensitivity to APO010-induced cell death as determined by annexin-V and 7-AAD/PI staining. In addition, the functional capacity of hematopoietic progenitor cells treated with APO010 was determined by colony forming unit (CFU) assays.

APO010, a recombinant variant of Fas ligand, efficiently induced cell death in cell lines and primary cells representing multiple myeloma (MM), acute myeloid leukaemia (AML) and lymphomas. Furthermore, hematopoietic progenitor cells were resistant to 200 ng/ml APO010, a concentration that resulted in the death of 60-100 % cancer cells. In addition, CFU assays revealed that hematopoietic progenitor cells treated with 200 ng/ml APO010 were able to differentiate into the expected hematological lineages.

The data indicate that APO010 can selectively kill hematological tumoral cells while having no effect on the repopulating function of hematopoietic progenitor cells. These results warrant the testing of APO010 as an ex-vivo purging agent in ASCT.

Mutant recombinant serpins as highly specific inhibitors of human kallikrein 14

¹Felber L., ¹Kündig C., ²Borgoño C., ³Chagas J., ⁴Tasinato A., ¹Jichlinski P., ¹Gygi C., ¹Leisinger H., ²Diamandis E., ¹Deperthes ., ⁵Cloutier S.,

*Unité de Recherche en Urologie, CHUV/Med Discovery CH-1066 Epalinges, Switzerland¹,
Department of Pathology and Laboratory Medicine, Mount Sinai Hospital, Toronto, Canada²,
Centro Interdisciplinar de Investigacao Bioquimica, Universidade de Mogi das Cruzes, Brazil³,
Unité de Recherche en Urologie, CHUV, CH-1066 Epalinges, Switzerland⁴, Unité de Recherche en
Urologie, CHUV/Med Discovery CH-1066⁵,*

The reactive center loop (RCL) of serpins plays an essential role in the inhibition mechanism acting as a substrate for their target proteases. Changes within the RCL sequence modulate the specificity and reactivity of the serpin molecule. Recently, we reported the construction of α 1-antichymotrypsin (ACT) variants with high specificity towards human kallikrein 2 (hK2) (Cloutier SM, Kündig C, Felber LM, Fattah OM, Chagas JR, Gygi CM, Jichlinski P, Leisinger HJ & Deperthes D (2004) Eur J Biochem 271, 607-613.) by changing amino acids surrounding the scissile bond of the RCL and obtained specific inhibitors towards hK2. Based on this approach, we developed highly specific recombinant inhibitors of human kallikrein 14 (hK14), a protease correlated with increased aggressiveness of prostate and breast cancers. In addition to the RCL permutation with hK14 phage display-selected substrates E8 (LQRAI) and G9 (TVDYA) (Felber LM, Borgoño CA, Cloutier SM, Kündig C, Kishi T, Chagas JR, Jichlinski P, Gygi CM, Leisinger HJ, Diamandis EP & Deperthes D (2005) Biol Chem 386, 291-298.), we studied the importance of the scaffold, serpins α 1-antitrypsin (AAT) or ACT, to confer inhibitory specificity. All four resulting serpin variants ACTE8, ACTG9, AATE8 and AATG9 showed hK14 inhibitory activity and were able to form covalent complex with hK14. ACT inhibitors formed more stable complexes with hK14 than AAT variants. Whereas E8 based inhibitors demonstrated a rather relaxed specificity reacting with various proteases with trypsin-like activity including several human kallikreins, the two serpins variants containing the G9 sequence showed a very high selectivity for hK14. Such specific inhibitors might prove useful to elucidate the biological role of hK14 and/or its implication in cancer.

Overexpression of the Chemokine Receptor CXCR4 in Neuroblastoma Reveals Increased Tumor Growth in Vitro and in Vivo.

^{1,2}MEIER R., ²Gross N., ²Auderset K., ²Flahaut M., ²Mühlethaler-Mottet A.,
²Balmas Bourloud K., ³Joseph J.,

*Paediatric Oncology Research Unit, Paediatrics¹, Pediatric Oncology Research, Pediatrics²,
Department of Pediatric Surgery, Pediatrics³,*

Neuroblastoma (NB) is a devastating childhood neoplasm in its higher stages, and a majority of patients present at diagnosis with advanced and metastatic disease. Chemokines and their receptors have been recently involved in the process of metastasis. In addition the particular SDF1a/CXCR4 axis may play a pivotal role in the control of cancer cells homing and therefore in the site-specific metastasis mechanism. The aim of this study was to evaluate the role of the particular chemokine receptor CXCR4 and its ligand SDF1-a in vitro as well as in vivo taking advantage of the recently developed orthotopic mouse model for human metastatic neuroblastoma.

Surface fluorescence analysis and semi-quantitative RT-PCR assays showed variable CXCR4 protein and mRNA expression levels in NB cell lines. Cells with no detectable CXCR4 (IGR-NB8-E6), with low constitutive (IGRN-91-E2) or high exogenous CXCR4 expression (IGR-NB8-C3,-A9, -B2) were generated and selected for further analyses. In vitro experiments revealed that CXCR4 expression was associated with an enhanced capacity of cells to migrate toward the SDF1a ligand. Moreover, enhanced growth and serum independent growth were observed in all CXCR4 overexpressing clones.

In vivo studies were performed by orthotopic engraftment (adrenals) of groups of nude mice with cell lines expressing different CXCR4 levels. Tumour intake was found similar in mice engrafted with CXCR4-negative IGR-NB8-E6 (75%) and CXCR4-overexpressing IGR-NB8-C3 (88%). In contrast, in vivo tumour growth was tremendously faster in the CXCR4 overexpressing group (mean volume was 1728 mm³ after 53 days) as compared to the group engrafted with CXCR4-negative cells (860 mm³ after 126 days), suggesting a role for the CXCR4 chemokine receptor in increased cell proliferation. PCR results of mice livers were found to be positive in some animals without significant difference (IGR-NB8-C3 (57%), IGR-NB8-E6 (33%)). Surprisingly, no metastases were found in the bone marrows of the animals.

In conclusion, constitutive over-expression of CXCR4 in NB cells was shown to mediate increased migration and growth in vitro. Whereas in vivo data revealed a pivotal growth promoting effect, suggesting that CXCR4 targets growth pathways rather than site specific metastasis.

Studying the Antiapoptotic Properties of Fragment N through 3D Structure Determination

¹FAVRE D., ²Walicki J., ²Widmann C.,

Département de biologie cellulaire et de morphologie¹, DBCM²,

Cleavage of RasGAP, a regulator of Ras signaling, at low levels of caspase 3 activity generates an antiapoptotic N-terminal fragment named "fragment N". At higher caspase activity, this fragment is further cut into fragments N1 and N2 and loses its protective effect. RasGAP could thus be viewed as an apoptostat in the sense that it can allow the cell to determine when caspases have been mildly activated to fulfill functions other than apoptosis or when caspases are strongly activated to mediate apoptosis.

The antiapoptotic function of fragment N is dependant on the activation of the Ras-PI3K-Akt pathway. Fragment N requires the presence of the parental RasGAP protein to mediate its protective function. However, the molecular mechanisms underlying the ability of the full-length RasGAP protein to allow fragment N to activate the Ras-PI3K-Akt pathway is not understood at the present time.

In order to better understand the mechanistic processes by which fragment N protects cells against apoptosis, we will determine the 3D structure of RasGAP and its fragments by crystallographic studies. Here, we present data about the purification of recombinant RasGAP, as well as fragment N2 and its SH3 domain.

Characterisation of CD4+Foxp3+ T cells in peripheral blood and normal or tumor-invaded lymph nodes in melanoma patients by six-color flow cytometry

¹JANDUS C., ¹Bioley G., ¹Cerottini J., ¹Speiser D., ¹Romero P.,

Division Onco-Immunologie, Institut Ludwig de Recherche sur le Cancer¹,

The results of many clinical trials of therapeutic vaccination of cancer patients indicate that despite specific CD8 T cell responses induced in a significant proportion of vaccinated patients, only 3-10% had measurable clinical benefit. In this context, CD4 T cells may be of relevance, and their dual role in anti-tumor immunity needs to be elucidated in more detail. Recent identification of the transcription factor Foxp3 as a key player in the development and function of natural regulatory T cells and the successive commercialisation of a monoclonal antibody specifically recognising the human Foxp3 protein have opened up new possibilities for the monitoring of this cell subset.

Using 6-color flow cytometry, the frequency, differentiation and activation state of CD4+Foxp3+ T cells were evaluated in peripheral blood (PB), in normal and tumor infiltrated lymph nodes (NLN/TILN) and at non-lymphoid tumour sites in melanoma patients.

Moreover, these were compared to the frequency of CD4+Foxp3+ T cells in healthy donor (HD) PB. CD4+Foxp3+ T cells were found to be over-represented in PB from patients compared to HD, with a mean 2-fold increase. While a similar frequency of CD4+Foxp3+ T cells in NLN and in PB could be observed, a significant increase (mean 3-fold) was seen in tumour infiltrating lymphocytes (TIL) and TILN. Additionally, while a significant proportion of PB and NLN derived CD4+Foxp3+ T cells displayed a naïve phenotype (CD45RA and CCR7 expression), the majority of TIL or TILN derived CD4+Foxp3+ T cells exhibited an antigen-experienced phenotype. Interestingly, while there were no significant differences in terms of activation phenotype in whole CD4+ T cell populations of TIL, TILN and PBMCs of a portion of the studied patients, gating on the CD4+Foxp3+ T cell subset showed that these cells were significantly activated in the tumour microenvironment. The presence and localisation of CD4+Foxp3+ T cells in lymphocyte infiltrated areas of tumour lesion sections from melanoma patients are also examined by immunohistochemistry. Further studies are now ongoing in an enlarged group of melanoma patients to confirm these preliminary results, and to assess the function, cytokine secretion pattern and the antigen-specificity of CD4+Foxp3+ T cells at the clonal level.

Results obtained in this study could open the way for the development of new cancer vaccination strategies, to elicit strong and long-lasting anti-tumor immune responses.

Redirecting viral immunity against tumors: anti-TAA Antibody-MHC/viral peptide conjugates induce growth inhibition of subcutaneous solid tumors by LCMV specific CTLs

¹CESSON V., Stirnemann K., Robert B., Corradin G., Luescher I., Mach J., Donda A.,

Département de biochimie- UNIL¹,

The immunotherapeutic strategy described here consists in the antibody mediated targeting of antigenic MHC/peptide complexes on tumor cells in order to sensitize them to T lymphocyte cytotoxicity. Structurally, Fab' fragments derived from a high affinity anti-TAA monoclonal antibody, are chemically coupled via a bismaleimide linker to in vitro refolded MHC/peptide complexes. We and others have demonstrated the ability of such conjugates to coat and induce tumor cells killing by peptide specific T cell clones in vitro. As a first in vivo model, using transgenic OT1 mice, we have established the proof of principle that syngeneic T cells could be redirected against subcutaneous tumors and induce tumor growth inhibition upon systemic treatment with anti-TAA-MHC/antigenic peptide conjugates (Donda et al, Cancer Immunity 3, 11, 2003).

Here we describe the first viral model, where natural anti-viral CTL responses, generated by LCMV virus infection can be redirected to and inhibit the growth of subcutaneous tumors. The stability of the antibody-MHC conjugate was improved by the covalent cross-linking of the LCMV immunodominant peptide gp33 in the MHC groove through coupling by photoreactive group activated by UV excitation. At the peak of LCMV response, systemic treatment with anti-CEA Fab-H-2Db/gp33 peptide conjugates redirected the H-2Db/gp33 restricted anti-viral CTL response to freshly grafted subcutaneous CEA-expressing colon carcinoma cells (MC38-CEA+). Mice were followed over one month and all treated mice remained free of tumors, whereas 6 controls mice grafted with the same carcinoma cells, treated with the anti-CEA fragment alone, had fast growing tumors. We are currently assessing the ability of such conjugate to inhibit the growth of existing and palpable tumors in LCMV infected mice.

These first results of tumor graft inhibition obtained a syngeneic tumor mouse model by exploiting anti-viral CTLs responses generated in immunocompetent mice are encouraging for the potential clinical application of this immunotherapeutic strategy.

Involvement of full-length RasGAP in the anti-apoptotic response induced by its cleavage fragments.

¹WALICKI J., ¹Yang J., ¹Widmann C.,

DBCM¹, CHUV Lausanne

We have recently identified RasGAP, a Ras-specific GTPase-activating protein, as a caspase substrate. RasGAP is cleaved at position 455 at low caspase activity generating an amino-terminal fragment (fragment-N) and a carboxy-terminal fragment (fragment-C). Surprisingly, fragment-N generates a potent survival signal that is at odds with the usual pro-apoptotic function of cleaved caspase substrates. Fragment N protects cells by activating the Ras-PI3K-Akt pathway. Here we have addressed the question as to whether fragment N could induce anti-apoptotic response independently of its parental RasGAP molecule. Our results show that expression of fragment N in mouse embryonic fibroblast lacking RasGAP did not result in Akt activation. Full-length RasGAP is therefore required for fragment N to induce a survival signal. It appears however that this requirement does not involve a direct interaction of RasGAP with its cleavage fragment as these two molecules didn't bind to each other in co-immunoprecipitation experiments. Our results indicate that fragment N modulates the function of its parental molecule to generate a protective signal in cells having mildly activated their caspases.

Histone deacetylase inhibitors strongly sensitise neuroblastoma cells to TRAIL induced apoptosis by caspases dependent changes in the ratio of pro- and anti-apoptotic proteins

^{1,2}MUHLETHALER-MOTTET A., ²Balmas Bourloud K., ²Flahaut M., ²Auderset K., ²Meier R., ³Joseph J., ⁴Beck Popovic M., ²Gross N.,

DMCP/Laboratoire d'Oncologie Pédiatrique¹, DMCP/Laboratoire d'Oncologie Pédiatrie², DMCP/Chirurgie pédiatrique³, DMCP/Onco-hématologie pédiatrique⁴,

Childhood neuroblastoma (NB) is a clinically and biologically heterogeneous neoplasm which behaviour can be explained by differential regulation of apoptosis. Tumour necrosis factor-related apoptosis-inducing ligand (TRAIL) selectively induces apoptosis in most tumour cells, but not in normal tissues. The non-invasive S-type caspase-8 positive NB cell lines are weakly sensitive to TRAIL, whereas the invasive N-type caspase-8 negative NB cell lines are resistant. Histone deacetylase inhibitors (HDACIs) are a new class of anti-cancer agent inducing apoptosis or cell cycle arrest in tumour cells with very low toxicity toward normal cells. HDACIs were recently shown to increase apoptosis induced by TRAIL in several tumour cells weakly sensitive to TRAIL.

We show that the HDAC inhibitors Sodium Butyrate (NaB), suberoylanilide hydroxamic acid (SAHA) and Trichostatin A (TSA) induced apoptosis in S-type and N-type NB cell lines. HDACIs induced cell death by activating the caspases cascade, Bid and the mitochondrial pathway. In addition, sub-toxic doses of HDACIs strongly sensitise the caspase-8 positive S-type NB cell lines to TRAIL induced apoptosis in a caspases dependent manner. Combined treatments increased the activation of caspases, Bid and BimEL, and the inactivation of the anti-apoptotic proteins XIAP, Bcl-x, RIP, Flip and survivin. It also enhanced the loss of Dym and the release of cytochrome c and AIF from the mitochondria into the cytosol. HDACIs trigger the mitochondrial pathway and sensitise NB cells to TRAIL by accelerating the kinetics of the apoptotic cascade and by increasing the ratio between pro and anti-apoptotic proteins.

HDACIs are therefore interesting new anti-tumour agents for targeting heterogeneous tumours such as neuroblastoma as these agents display a strong toxicity toward the most aggressive N-type NB cells and highly sensitise the S-type NB cells to TRAIL induced apoptosis.

Characterization of Teicoplanin-Susceptible and Teicoplanin-Resistant *Staphylococcus aureus* by Matrix Assisted Laser Desorption Ionisation Time of Flight Mass Spectrometry (MALDI-TOF MS) and Peptidoglycan Muropeptide Analysis.

¹MAJCHERCZYK P., McKenna T., Moreillon P., Vaudaux P.,

Microbiology Fundamental¹, UNIL Lausanne

Background & Purpose Teicoplanin (Tec) is a glycopeptide antibiotic that inhibits the polymerisation of peptidoglycan (PG) glycan chains, and hence the crosslinking of its muropeptides. Glycopeptide-resistant (r) *S. aureus* isolates emerge under therapy with Tec. Unexpectedly, Tec-r subpopulations also emerged in the tissue-cage fluid of rats infected with *S. aureus*, never exposed to this drug (J. Antimicrob. Chemother. 2001; 47:163-70). The present study used two different techniques to analyse perturbations of the cell wall present in such Tec-r subpopulations. One examined the ionisable components on the surface of intact bacterial cells by MALDI-TOF MS. This provides information on global modifications of cell surface components. The other analysed the PG muropeptide pattern after digestion of their glycan chains, a method generating structural information on the PG scaffold skeleton.

Methods The Tec-sensitive parent (isolate MRGR3) and its stable Tec-r variant recovered from tissue-cage fluids (isolate 14-4) were studied. MALDI-TOF MS was performed directly on colonies picked off agar plates, embedded in matrix and the ionisable cell surface components directly analysed. For muropeptide analysis walls were purified, stripped off their teichoic acids, their glycan chains digested with mutanolysin and separated by HPLC. Eluted muropeptides were detected by UV absorbance.

Results and Conclusions MALDI-TOF MS revealed fingerprints compatible with reference *S. aureus*. However, each isolate contained unique and very reproducible peaks that enabled them to be differentiated. For example an intense 825 Da peak was present in the Tec-r variant, but was practically absent from the Tec-sensitive parent. These results indicate that Tec-sensitive and Tec-r variants differed in some surface components that affected their ionisation. On the other hand both strains revealed indistinguishable muropeptide patterns that were compatible with published *S. aureus* PG. Thus, although surface alterations were present in the Tec-r variant, they were not related to an abnormal PG skeleton. The combination of these two techniques is an elegant new strategy to help determine the localization of wall alterations in different bacterial variants. The ionisable nature of the altered molecules and the fact that they are not associated with an altered PG scaffold should help target further investigations on other surface components such as teichoic acids or proteins.

Cancer immunotherapy using a bifunctional CD1d/ anti-tumor antibody fusion protein to redirect the NKT cell-mediated immune response to the tumor site

¹STIRNEMANN K., Cesson V., Corradin G., Mach J., Donda A.,

Institut de Biochimie, Université de Lausanne¹,

The aim of the present project is to exploit at the tumor site the ability of CD1d to activate NKT cells when presenting the high affinity glycolipid GalCer or analogs. The activation of NKT cells will then initiate within the tumor the rapid induction of other effector cells of the immune system such as NK cells. For this purpose, we have engineered a genetic fusion between mouse β 2-microglobulin, CD1d and the anti-tumor antibody single chain scFv 4D5, recognizing the HER-2/neu tumor antigen. The fusion protein is well produced in HEK 293 cells in a transient transfection system and is purified in a single step by His-Tag/Ni-NTA chromatography. The 76 kDa CD1d-4D5 protein is properly folded as shown by its ability to bind to HER-2 expressing tumor cells and its recognition by anti-CD1d antibodies. When loaded with GalCer, the CD1d fusion is able to activate mouse NKT hybridoma cells. This specific activation is shown by presentation assays with pulsed target cells expressing or not HER-2, as well as with plastic coated fusion protein. In both cases, NKT activation is revealed by IL-2 release and surface upregulation of CD25. The capacity of the fusion to activate mouse NKT cells is being investigated in similar presentation assays with detection of intracellular IFN- γ . In view of testing the anti-tumor activity of the CD1d-4D5 fusion *in vivo*, a murine lung metastasis model was developed. The B16 melanoma cell line was transfected with the human HER-2/neu antigen and the luciferase gene was introduced by retroviral infection in order to monitor the development of lung metastases by Bioluminescence Imaging. The anti-tumor effect of the fusion will then be tested *in vivo*, first by immediate treatment after tumor graft and, if effective, with delayed injections of the CD1d-4D5 protein.

A similar strategy was initially developed in our laboratory for MHC class I chemically coupled to an anti-tumor antibody fragment and loaded with a strong antigen of non tumor origin such as a viral peptide. The capacity of such conjugates to redirect to the tumor site specific anti-viral CTLs was demonstrated both *in vitro* and *in vivo*. The advantage of using CD1d is that, being a monomorphic antigen presenting molecule, it would allow the development of a single conjugate to treat a majority of patients, in contrast to the polymorphic MHC class I molecule. Additionally, this strategy will recruit to the tumor site cells from the innate immune system.

Implication of PAX5 in the activation of the human Telomerase Reverse Transcriptase gene (hTERT) in the lymphoid tissues and cell lines

¹BOUGEL S., ²Benhattar J.,

Institut de Pathologie¹, Pathologie² CHUV, Lausanne

Background :

About 85 % of cancers engage the activation of the telomerase enzyme. Telomerase maintains the length of chromosome ends, which normally shorten during cellular life. This leads to the immortalisation of the cell by preventing the apoptotic signal. The hTERT catalytic subunit of the telomerase is the limiting factor of telomerase activity. It has been previously demonstrated in the laboratory that the regulation of hTERT mainly rests on the binding of the CTCF (CCCTC-binding factor) repressor to the first two exons of hTERT. When CTCF is bound to the hTERT gene, no transcription is possible. However, hTERT expression is allowed as soon as the binding of CTCF is perturbed, which occurs when :

- the CTCF binding sites are methylated, as CTCF is a methylation-sensitive factor,
- a paralogue of CTCF, called BORIS (*Brother of the regulator of Imprinted Sites*) is expressed and takes the place of CTCF on the same binding sites.

Objectives :

To determine which mechanism of the hTERT regulation is involved in the lymphoid tissues and cells lines.

Methods :

The expression of hTERT, BORIS and PAX5 were analysed by RT-PCR and immunohistochemistry (IHC) in different kind of lymphoid tissues and cell lines. The methylation of the hTERT promoter was tested after bisulfite modification. The Genomatix software was used to analyse the potential binding sites present on the hTERT gene. The PAX5 binding to the hTERT gene was checked by electrophoretic mobility shift assays (EMSA) in Nalm6 lymphoid cell line. Transfection of a PAX5 expression vector was performed in the BJ hTERT-negative cell line. The CTCF binding to the hTERT gene was tested by chromatin immunoprecipitation (ChIP) experiments in Nalm6.

Results :

hTERT was expressed in B and T lymphomas but also in the germinal centres of normal lymph nodes. The hTERT promoter was not methylated in most of the lymphoid tissues and cell lines. The BORIS protein was not expressed in any of them. PAX5 protein was identified to bind just behind the potential CTCF binding site. PAX5 is a B-cell specific transcription factor. In most of the lymphoid tissues, we observed a co-expression of PAX5 and hTERT. PAX5 bound *in vitro* to the hTERT gene. Exogenous expression of PAX5 was able to activate the transcription of hTERT in BJ. By ChIP, CTCF was found to bind weakly to the hTERT gene in Nalm6.

Conclusion :

In a majority of lymphoid tissues and cell lines, hTERT expression is not regulated neither by methylation nor Boris protein. Up-regulation of PAX5 is necessary for activation of hTERT expression in a hTERT-negative cell line. In summary, in telomerase-positive B cells, PAX5 could activate hTERT by preventing the inhibitory effect of the CTCF repressor.

Beta-1,3-D-Glucan (BGL) Antigenemia in Neutropenic Cancer Patients (Pts) with Invasive Aspergillosis (IA) and Candidiasis (IC).

¹SENN L., ¹Robinson J., ²Schmidt S., ¹Knaup M., ³Asahi N., ³Satomura S., ³Matsuura S., ²Duvoisin B., ¹Calandra T., ¹Marchetti O.,

Maladies Infectieuses¹, Radiologie², Wako, Japan³,

β-1,3-D-Glucan (BGL) Antigenemia in Neutropenic Cancer Patients (Pts) with Invasive Aspergillosis (IA) and Candidiasis (IC).

L SENN*, JO ROBINSON, S SCHMIDT, M KNAUP, N ASAHI, S SATOMURA, S MATSUURA, B DUVOISIN, T CALANDRA, O MARCHETTI. CHUV, Lausanne, Switzerland; Wako, Osaka, Japan.

Background: IA and IC are associated with high morbidity and mortality in neutropenic cancer Pts. New diagnostic tests are needed for early diagnosis of invasive mycosis. BGL, a fungal cell wall antigen, can be detected in the systemic circulation of Pts with IA or IC. The aim of the study was to evaluate the utility of BGL monitoring in neutropenic cancer Pts at high risk of IA and IC.

Methods: Prospective study of consecutive episodes of neutropenia (median duration 22 d) in Pts with acute leukemia. IA and IC were defined according to EORTC-MSG criteria. Blood was collected 2x weekly before onset of fever and daily thereafter. BGL was measured by turbidimetric or colorimetric assays (Wako, Japan). Positive tests defined by 2 consecutive BGL values >6 and > 5 pg/ml, or >11 pg/ml for both tests (2 cut-off values).

Results: 23 episodes of invasive mycoses occurred during 130 neutropenic episodes: 12 IC (1 proven, 11 probable) and 11 IA (3 proven, 8 probable). 16 samples/episode (3-35) were analyzed over 35 days (17-122).

Cut-off (pg/ml)	BGL (turbidimetric)		BGL (colorimetric)	
	2x > 6	2x > 11	2x > 5	2x > 11
Sensitivity %	43	24	86	43
Specificity %	100	100	91	100
PPV %	100	100	72	100
NPV %	86	82	96	86
Likelihood ratio	43	24	9.6	43
Positive test	0.57	0.76	0.15	0.57
Negative test				

Colorimetric BGL with cut-off of 2 consecutive values > 5 provided the best performance for diagnosis of IA and IC. Median time (0 d) between fever onset (as first sign of IFI) and BGL positivity was significantly shorter than that between fever onset and conventional diagnosis of IFI (13 d) (p<0.0001).

Localization and function of hTERT variant proteins in human cell lines

¹YAN P., ²Benhattar J., ²Seelentag W., ²Bosman F.,

Institute of Pathology¹, Pathology²,

Telomerase is a ribonucleoprotein complex composed of a reverse transcriptase catalytic subunit (telomerase reverse transcriptase gene, hTERT) that copies the template region of its RNA subunit to the end of chromosomal telomeres. Telomerase activity (TA) has been found in almost all human cancer tissues, cancer cell lines, stem cells and proliferative cells. We found that hTERT protein localized diffusely in the nucleoplasm and more intensely in the nucleoli of cancer cells and proliferating normal cells. In the majority of tumors, hTERT protein expression was rather heterogeneous: some cells expressed hTERT whereas others did not and in addition staining intensity varied importantly. Furthermore, granular cytoplasmic staining was occasionally found in some subpopulations of tumor cells. We hypothesize that the variation in hTERT cellular localization might be due to hTERT splicing variants. At least six splicing variants of hTERT have been identified, including 4 deletion (á, â, áâ and ã) and 2 insertion sites. We are addressing this issue through transfection of full-length hTERT and of its splice variants in telomerase negative and positive cells. To this end EGFP was fused to hTERT-FL, hTERT-á, hTERT-â and hTERT-áâ. The different constructs were transfected into two telomerase-negative (GM847 and U2OS) and two telomerase-positive cell lines (HeLa and HT29). In telomerase negative cell lines, TA was only detected with the hTERT-FL, but not with the splicing variants. The GFP-hTERT-FL and GFP-hTERT-á fusion protein had a similar localization pattern, in which the protein diffusely localized in the nucleoplasm, especially close to nuclear membrane. The GFP-hTERT-â and GFP-hTERT-áâ fusion proteins formed aggregates in nucleus, and cytoplasmic expression was sporadically observed in some transfected cells. We then transfected different ratios of hTERT-FL and hTERT-á into HeLa cells and found that the TA was reduced with increasing amount of hTERT-á. In conclusion, nuclear protein expression was observed in transfected cells with hTERT-FL and three deletion variants, and cytoplasmic protein expression only with hTERT-â and hTERT-áâ. In view of these data, we propose that hTERT-á form an inactive telomerase heterodimer, suggesting that the á-deletion variant might be a negative regulator of TA. Our results provide new information regarding the function of hTERT splice variants in human tumors.

Molecular cytogenetic characterization of doxorubicin-resistant neuroblastoma cells: Acquired multi-drug resistance results from a large amplification of chromosome 7q21 region involving MDR1 and HFZ genes.

¹GROSS N., ¹Flahaut M., ¹Mühlethaler-Mottet A., ²Martinet D., ³Fattet S., ¹Balmas Bourlout K., ¹AUderset K., ⁴Meier R., ⁴Joseph J.,

Pediatric Oncology Research, DMCP¹, Medical Genetic Service², Laboratoire de Pathologie Moléculaire des Cancers, Institut Curie-Paris³, Pediatric Surgery, DMCP⁴,

Neuroblastoma is an extremely heterogeneous neural crest-derived embryonic childhood neoplasm representing the second most common solid tumour in children. Despite the most recent advances in combined therapy the overall survival of patients with high stage disease has not improved in the last decades. Treatment failure is in part attributed to the development of multi-drug resistance. To address the mechanisms involved in the development of multi-drug resistance, we have generated two doxorubicin-resistant neuroblastoma cell lines (IGRN-91R and LAN-1R). These cells were shown to overexpress the MDR1 gene product coding for the P-glycoprotein and were resistant to other MDR1- and non MDR1-substrate drugs. Indeed, the MDR1 inhibitor verapamil only partially restored sensitivity to drugs, confirming that P-glycoprotein-mediated drug efflux was not responsible for 100% resistance. High resolution and array-based comparative genomic hybridisation analyses revealed the presence of an amplicon of the 7q21 region as the unique genomic alteration common to both doxorubicin-resistant cell lines. Microarray analysis of the resistant versus sensitive cell lines only revealed a limited amount of differentially expressed genes. Most of the upregulated genes in resistant cell lines were found to be located to the 7q21 region. Two of these genes, MDR1 and HFZ were selected for further exploration of their role in the resistant and malignant behaviour of neuroblastoma.. This study represents the first molecular cytogenetic and genomic approach to identify genomic regions involved in the multi-drug resistant phenotype of neuroblastoma. These results could lead to the identification of relevant target genes for the identification of the mechanisms of acquired drug resistance and the development of new therapeutic issues to fight aggressive paediatric tumours such as neuroblastoma.

Effect of MegaFasLigand (MFL) on human peripheral blood leukocytes (PBL_e)

¹LAGOPOULOS L., ¹Nahimana A., ²Greaney P., ²Dupuis M., ¹Duchosal M.,

Hematologie, CHUV-Lausanne¹, Apoxis SA, Lausanne²,

Background: MFL is a novel pro-apoptotic recombinant molecule inducing apoptosis via the Fas pathway. MFL is a highly potent killing agent of hematological cancer cells but has no killing effect on hematopoietic progenitor cells (Greaney and al., *Leukemia Research*, In Press), making it an ideal candidate for purging in autologous hematopoietic stem cell (HSC) transplantation. The effect of MFL on immune cells, contributing to the majority of cells reinfused in the transplantation procedure, remains unknown.

Aim: To evaluate the toxicity of MFL on human primary immune cells.

Material and Methods: Three peripheral blood lymphocyte (PBL_e) preparations were collected, and cultured with MFL (1, 10 and 200 ng/ml) or medium alone. Parameters followed were viable cell count (using trypan blue exclusion dye), and cell surface Fas expression and apoptotic markers (annexin-V and 7AAD) which were analyzed by FACS. *In vivo* humoral recall functions were evaluated using PBL_e xenotransplanted into immunodeficient mice that were treated with MFL and subsequently immunized with a T cell dependent recall antigen (tetanus toxoid, TT).

Results: The sensitivity of immune cells to MFL is dependent on cell type and can be summarized as follows

- 1) Macrophages (CD14⁺) express high levels of Fas and were highly sensitive to MFL-induced cell death (100% death at 25 ng/ml MFL).
- 2) T cells were sensitive towards MFL. Cytotoxic T cells (CD3⁺CD8⁺: 62% annexin-V) were more sensitive than helper T cells (CD3⁺CD4⁺: 11% annexin-V) when treated with 200 ng/ml MFL. Memory T cells (CD3⁺CD45RA⁻/RO⁺: 47% annexin-V) and memory helper T cells (CD3⁺CD4⁺CD45RA⁻/RO⁺: 38% annexin-V) were more sensitive to 200 ng/ml MFL than naive T cells (CD3⁺CD45RA⁺/RO⁻: 9% annexin-V) and naive helper-T cells (CD3⁺CD4⁺CD45RA⁺/RO⁻: 5% annexin-V), respectively. This correlated with Fas expression being higher in memory compared to naive T cell populations.
- 3) NK cells (CD3⁺CD2⁻) exhibited intermediate sensitivity to MFL.
- 4) B cells express low levels of Fas and were almost completely resistant to MFL-induced cell death except for memory B cells (CD19⁺CD27⁺), which were moderately sensitive (12% increase in 7AAD when treated with 200 ng/ml MFL).

In vivo experiments using human PBL_e treated with MFL, then incubated with TT and subsequently transplanted into immunodeficient mice are currently ongoing and will be presented in detail. Initial results indicate that antigen-specific humoral recall responses can be elicited on PBL_e incubated with up to 10 ng/ml MFL.

Conclusions:

The sensitivity of immune cells to MFL was dependent on the immune cell type. Macrophages and memory T cells were most sensitive to MFL, whereas naive T cells, NK cells, and B cells were more resistant. In comparison, immune cells were more resistant than the majority of hematological cancer cells tested (Greaney and al., *Leukemia Research*, In Press). Together, these observations indicate that MFL may kill cancer cells while having minimal effect on immune cells, supporting the potential use of MFL as a purging agent in autologous HSC transplantation.

NEU
Neurosciences et Psyché

Distribution of GABA receptors in human auditory cortex: an immunohistochemical analysis

¹SACCO C., ²Tardif E., ³Probst A., ³Tolnay M., ⁴Fritschy J., ²Clarke S.,

Division Autonome de Neuropsychiatrie¹, Div. Autonome de Neuropsychologie², Inst. of Pathology, Univ. of B³, Inst. of Pharmacology and Tox⁴,

GABA, the primary inhibitory neurotransmitter, and its receptors play an important role in modulating neuronal activity in the central nervous system and are implicated in many neurological disorders. Human primary and non-primary auditory areas were investigated immunohistochemically using antibodies against GABAA and GABAB receptors. The supratemporal plane of 5 hemispheres in 3 normal brains (2 male, 1 female; average age 64+/-17 yr) were cut into 40 micrometer-thick sections and stained immunohistochemically for antibodies against the GABAA receptor subunits alpha1, alpha2, and beta2/3, the GABAB receptor subunits R1 and R2, and adjacent sections were Nissl-stained. Consistent staining patterns of all receptors were obtained within the cytoarchitectonic auditory areas TC, TB, and TA. GABAA receptor staining produced strong neuropil staining throughout all cortical levels as well as the visualization of fibers and neurons in layer VI. GABABR1 and GABABR2 immunoreactivity yielded neuronal labeling throughout all cortical layers with darkly stained pyramids in layer III. Our results demonstrate a strong presence of GABAA and GABAB in human auditory cortex, suggesting a crucial role of GABA in shaping auditory responses in the primary and non-primary auditory areas.

Cognitive impairment in early multiple sclerosis

¹SIMIONI S., ¹Annoni J., ¹Bruggimann L., ¹Souza Lima F., ³Ruffieux C.,
¹Bogouslavsky J., ¹Schluep M.,

Neurologie CHUV¹, Médecine Sociale et Préventive²,

Background and purpose: Cognitive deficits were estimated to occur in 30-70% of the patients suffering from multiple sclerosis (MS), even in its early phase. However, early MS was never clearly defined and this may have influenced previous results on cognitive functioning. We assessed cognition in a strictly defined sample of early MS patients (Expanded Disability Status Scale [EDSS] score ≤ 2.5 , disease duration < 6 years) with definite relapsing-remitting or possible MS. We studied the influence of fatigue and depression on cognition and the impact of cognitive deficits on handicap and quality of life (QoL).

Methods: 106 patients (32 males, mean age 34.4, mean disease duration 2.38 years, mean EDSS 1.73) were tested on long-term memory (Rey's Auditory Verbal Learning Test), executive functions (Behavioural Assessment of the Dysexecutive Syndrome) and attention (Trail Making Test). Fatigue was measured by the Fatigue Assessment Instrument, anxiety and depression using the Hospital Anxiety and Depression scale (HAD, cut-off ≥ 8 for both dimensions) and a psychiatric interview (QSP). The London Handicap Scale and the SEP-59 assessed handicap and QoL respectively. Parametric tests were used.

Results: 29 patients (27.4%) presented cognitive deficits and 8 showed more than 1 domain affected. Memory impairment was the most frequent (12.3%), followed by attentional (8.4%) and executive deficits (5.7%). On HAD, 46.8% of the patients had a significant score for anxiety and 18.1% for depression but only 8 patients reached the diagnostic criteria on the QSP. After exclusion of these 8 patients, the prevalence of cognitive deficits was still of 25.5%. On fatigue scale, 56% of the patients presented a significant score.

Cognitive deficits were correlated to marginal or significant depression scores on HAD (Pearson, $p=0.006$) but neither to anxiety nor to fatigue. Impaired patients showed a major effect on QoL (t-test, $p<0.000$) and handicap (t-test, $p<0.000$).

Discussion: We confirmed the occurrence of cognitive deficits in early MS. Such impairment was still present after exclusion of patients with clinical depression. Our results also suggest that the impairment is not severe (generally 1 domain affected) and involves mostly learning capacities. As expected, cognitive impairment was related to depressive scores, handicap and QoL. However, it appeared unrelated to anxiety and to fatigue, one of the most disabling MS symptoms often presented as influencing cognition.

Opioid receptors in skin – link between stress and skin disease?

¹BIGLIARDI P., ¹Panizzon R., ¹Bigliardi-Qi M.,

*Dermatologie*¹,

Opioid peptides and its receptors are highly conserved and crucial for survival in stress situations. Besides their well known role in antinociception, they control cell differentiation, proliferation and influence apoptosis in various tissues. We are first to discover their presence in skin and established their functions in modulation of chronic itch and wound healing.

Opioid receptor is a key player in induction of chronic itch. This could be confirmed using m-opiate receptor knockout mice experiments and clinical studies on patients with chronic itch. We have induced a dry skin dermatitis as a model for chronic itching on knockout and wild type mice. m-Opioid receptor knockout mice revealed significant less scratching behavior, less epidermal hypertrophy and different density and quality of epidermal nerve endings compared to the wild type mice. In addition, topically applied opioid receptor antagonists relieved significantly chronic pruritus in a double-blind, placebo-controlled, cross-over study in 40 patients with atopic dermatitis.

Several findings suggest that the d-opioid receptor and its endogenous ligands (enkephalins) are important in cell differentiation and proliferation. We proved the existence of a functional active d-opioid receptor in different skin cells using RT-PCR, western blot analysis and migration assays. In addition, d-opioid receptor knockout mice revealed a phenotype of thinner epidermis and higher expression of cell differentiation marker cytokeratin 10 (CK 10) compared to wild type mice. In a burn wound model d-opioid receptor knockout mice showed significant wound healing delay and a severe epidermal hypertrophy at the wound margin. This can be explained by a change of cell differentiation and migration due to the absence of a functional active d-opioid receptor.

In summary, these experiments proved that the skin and the nerve system interact with each other in a bi-directional way, i.e. nerve system release neuropeptides in stress situations affecting skin homeostasis and sensations and vice versa. Therefore, the opioid receptor system is an excellent model to study the connection between psychological stress and aggravation of different skin diseases.

The mammalian central nervous synaptic cleft contains a high density of periodically organized complexes

¹ZUBER B., ²Nikonenko I., ²Klauser P., ²Muller D., ¹Dubochet J.,

Laboratoire d'analyse ultrastructurale¹, Neuropharmacologie, Centre Médical Universitaire, Université de Genève²,

Cryo-electron microscopy of vitreous section (CEMOVIS) makes it possible to observe cells and tissues at high resolution in a close-to-native state. The specimen remains hydrated; chemical fixation and staining are fully avoided: there is minimal molecular aggregation and the density observed in the image corresponds to the density in the object. Accordingly, organotypic hippocampal rat slices were vitrified under high pressure and controlled cryoprotection conditions, cryosectioned at a final thickness of ca. 70 nm and observed below -170 °C in a transmission electron microscope. The general aspect of the tissue compares with previous electron microscopy observations. The detailed analysis of the synapse reveals that the density of material in the synaptic cleft is high, even higher than in the cytoplasm and that it is organized in 8.2 nm periodic trans-cleft complexes. Novel structures of presynaptic and postsynaptic elements are also described.

Rapid Brain Discrimination of Sounds of Objects

¹Murray M., ²Camen C., ³Gonzalez Andino S., ²Bovet P., ⁴Clarke S.,

Neuropsychology and Radiology, CHUV¹, Faculté de psychologie et des sciences de l'éducation, Geneva University², Neurology Department, Geneva University Hospital³, Neuropsychology, CHUV⁴,

Electrical neuroimaging in humans identified the speed and spatio-temporal brain mechanism whereby sounds of living and man-made objects are discriminated. Subjects performed an 'oddball' target detection task, selectively responding to sounds of either living or man-made objects on alternating blocks, which were controlled for in their spectrogram and harmonics-to-noise ratios between categories. Analyses were conducted on 64-channel auditory evoked potentials (AEPs) from non-target trials. Comparing responses to sounds of living versus man-made objects, these analyses tested for modulations in 1) local AEP waveforms, 2) global response strength, and 3) the topography of the electric field at the scalp. In addition, the local auto-regressive average (LAURA) distributed linear inverse solution was applied to periods of observed modulations. Just 70msec post-stimulus onset, a common network of brain regions within the auditory 'what' processing stream responded more strongly to sounds of man-made versus living objects, with differential activity within the right temporal and left inferior frontal cortices. Over the 155-257msec period, the duration of activity of a brain network including bilateral temporal and pre-motor cortices differed between categories of sounds. Responses to sounds of living objects peaked ~12ms later and the activity of the brain network active over this period was prolonged relative to that in response to sounds of man-made objects. The earliest task-related effects were observed at ~100ms post-stimulus onset, placing an upper limit on the speed of cortical auditory object discrimination. These results provide critical temporal constraints on human auditory object recognition and semantic discrimination processes.

Glial mechanisms of axonal growth protection by ammonia

¹BRAISSANT O., ²Henry H., ²Cagnon L., ³Honegger P., ²Bachmann C.,

Laboratoire de Chimie Clinique, CHUV¹, LCC, CHUV², IPHYSIOL, UNIL³,

Hyperammonemia affects CNS development and causes mental retardation. We showed in reaggregated primary cultures of embryonic rat telencephalon that ammonium (NH₄⁺) impairs axonal growth and decreases intracellular creatine (Cr), while Cr co-treatment protects axons in a glial dependent manner. To understand the link between NH₄⁺ toxicity and axonal growth inhibition, we analyzed the effects of NH₄⁺ on Cr in developing brain cells, and which intra- and extra-cellular signaling pathways are implicated.

Cr is synthesized by AGAT and GAMT and transported into cells by CT1. In our culture model, we analyzed the expression of AGAT, GAMT and CT1 in neurons, astrocytes and oligodendrocytes. We show that NH₄⁺ alters not only the glial expression of GAMT and CT1, but also the activity of AGAT, GAMT and CT1 as shown by intracellular measure of Cr and guanidinoacetate.

Intracellular signaling pathways were studied at the level of MAP kinases, which regulate axonal growth. We focused on activated (e.g. phosphorylated) states of Erk1/2, SAPK/JNK and P38 MAPKs. We show that NH₄⁺ decreases the phosphorylation of Erk1/2 and SAPK/JNK, while it increases phospho-P38. Cr co-treatment reactivates phospho-Erk1/2 under NH₄⁺ in the presence of glial cells only, suggesting that Erk1/2 might be implicated in the protection of axonal growth by Cr under NH₄⁺.

Extracellular signaling was studied by conditioning experiments. Mixed cell cultures including glia were exposed to Cr, and their medium was used to condition neuronal cultures exposed to NH₄⁺ (in which axons are not protected by Cr). This culture medium led to axonal growth protection in neuronal cultures against the effect of NH₄⁺.

Our work demonstrates that NH₄⁺ alters metabolism and transport of Cr in brain cells and suggests that soluble factors, released or controlled by glia, as well as MAPKs are involved in the protection of axonal growth by Cr.

Supported by the Swiss National Science Foundation.

MAPK signaling pathways in ammonium-induced impairment of axonal growth

¹BRAISSANT O., ²Cagnon L., ²Honegger P., ²Bachmann C., ²Braissant O.,

Laboratoire de Chimie Clinique, CHUV¹, LCC, CHUV²,

Hyperammonemia affects CNS development and causes mental retardation. We showed that NH₄⁺ exposure impairs axonal growth and alters expression and phosphorylation of Neurofilament-M. NH₄⁺ decreases brain cell intracellular creatine (Cr), while Cr co-treatment protects axons in a glial dependent manner (Braissant et al. 2002, J.Neurosci.). As MAP kinases regulate neurite outgrowth and neuronal differentiation, we investigated whether members of the MAP kinase family are implicated in NH₄⁺ toxicity for axons and in their protection by Cr. We focused on the activation of Erk1/2 usually associated with cell proliferation and differentiation, and on the activation of SAPK/JNK and P38 usually linked to cell stress. Phosphospecific antibodies recognizing the activated forms of Erk1/2, SAPK/JNK and P38 were used in western blotting and immunohistochemistry experiments. Using reaggregated primary cultures of embryonic rat telencephalon as experimental model, we show that phospho-Erk1/2 is preferentially expressed in neurons and that NH₄⁺ exposure decreases the activation of Erk1/2 by phosphorylation. Cr exposure seems to reactivate phospho-Erk1/2 expression in mixed cell cultures exposed to NH₄⁺. In control conditions and under Cr treatment, phospho-SAPK/JNK seems to be expressed in neurons as well as in glial cells, preferentially in the fiber rich-peripheral zone. NH₄⁺ exposure decreases phospho-SAPK/JNK mainly in neurons, and particularly in the fiber rich-peripheral zone of the cultures. Unlike Erk1/2 and SAPK, phospho-P38 expression is very low in control conditions, while it is increased under NH₄⁺, particularly in the peripheral zone of the 3D cultures where neuronal processes are altered by NH₄⁺ exposure. Cr treatment seems to repress NH₄⁺ activation of P38. Our data indicate that NH₄⁺ and Cr alter MAP kinase pathways in our model of hyperammonemia, and more particularly in the region of axonal and dendritic growth. Supported by the Swiss National Science Foundation.

Frequency-Dependent Correlation between EEG and BOLD Responses Determined Non-invasively throughout the Human Brain

¹MARTUZZI R., ²Murray M., ¹Meuli R., ³Thiran J., ¹Maeder P., ⁴Michel C.,
⁴Gonzalez Andino S., ⁴Grave de Peralta Menendez R.,

Service de Radiodiagnostic et Radiologie Interventionnelle, CHUV, Lausanne¹, Division Autonome de Neuropsychologie, CHUV, Lausanne², Signal Processing Laboratory, EPFL, Lausanne³, Functional Brain Mapping Laboratory, Department of Neurology, University Hospital, Geneva⁴,

To better understand relationships between electrophysiologic and hemodynamic signals, we examined EEG spectral power and blood oxygen level dependent (BOLD) responses in humans performing a passive visual task. 128-Channel EEG and whole-brain 3-Tesla fMRI were separately acquired. Identical stimulation paradigms were used with both imaging techniques. The visual stimulus (70° wedge checkerboard presented to the lower left visual quadrant) flickered at 8 reversals per second for durations of 12, 18, or 24sec each followed by 24s of rest. Each stimulus duration was repeated 20 (fMRI) or 30 (EEG) times. fMRI data were analyzed with SPM2 to obtain activation maps. After artifact rejection, single trials of EEG data (1sec pre-stimulus and 1sec post-stimulus onset) were submitted to the ELECTRA distributed linear inverse solution (Grave de Peralta Menendez et al., 2004 *Neuroimage* 21: 527). At each node of the inverse solution space, the power spectrum for each trial was computed. For each frequency separately (1-256Hz), power post-stimulus was non-parametrically contrasted with that pre-stimulus in order to obtain one statistical spatial map per frequency. These maps were compared with the fMRI results. This analysis revealed that the degree of correlation between these maps varied across EEG frequencies, with peaks observed at low frequencies (<8Hz), ~46Hz and, ~150Hz. These results suggest that there is a frequency-dependent relationship between BOLD and EEG signals within restricted brain regions, at least in case of a passive visual task. (Funding from SNSF grants 3200B0-100606 to RM; 3152A0-100745/1 to RGPM)

Glutathione deficit during development induces anomalies in the rat anterior cingulate GABAergic neurons: relevance to schizophrenia

¹CABUNGCAL J., ²Nicolas D., ²Kraftsik R., ¹Cuénod M., ³Do K., ²Hornung J.,

Center for Psychiatric Neuroscience, Department of Psychiatry¹, Département de Biologie Cellulaire et de Morphologie², 1Center for Psychiatric Neuroscience, Department of Psychiatry³,

A series of studies in schizophrenic patients report a decrease of glutathione (GSH) in prefrontal cortex (PFC) and cerebrospinal fluid, a decrease in mRNA levels for two GSH synthesizing enzymes and a deficit in parvalbumin (PV) expression in a subclass of GABA neurons in PFC. GSH is an important redox regulator, and its deficit could be responsible for cortical anomalies, particularly in regions rich in dopamine innervation. We tested in an animal model if redox imbalance (GSH deficit and excess extracellular dopamine) during postnatal development would affect PV-expressing neurons. Three populations of interneurons immunolabelled for calcium binding proteins were analyzed quantitatively in 16 day-old rat brain sections. Treated rats showed specific reduction in parvalbumin immunoreactivity in the anterior cingulate cortex, but not for calbindin and calretinin. These results provide experimental evidence for the critical role of redox regulation in cortical development and validate this animal model used in schizophrenia research.

Keywords: Animal model; Anterior cingulate cortex; γ -amino butyric acid; Glutathione; GBR 12909; Inhibitory interneurons; L-buthionine-(S,-R)-sulfoximine (BSO); Oxidative stress; Parvalbumin-immunoreactive; Schizophrenia

The auxiliary beta2 subunit of voltage-gated sodium channel and hypersensitivity in a neuropathic pain model

¹PERTIN M., ²JI R., ³BERTA T., ⁴POWELL A., ⁵GILLIARD N., ⁴TATE S., ⁶ISOM L., ⁷WOOLF C., ⁵SPAHN D., ³DECOSTERD i.,

Anesthesiology-DBCM¹, Department of Anesthesiology, Harvard Medical School, Boston, USA², Service d'Anesthesiologie CHUV et Département de Biologie Cellulaire et de Morphologie UNIL³, R&D Department, GlaxoSmithKline, Stevenage, UK⁴, Service d'Anesthesiologie CHUV⁶, Department of Pharmacology, University of Michigan, Ann Arbor, USA⁶, Department of Anesthesia and Critical Care, MGH & Harvard Medical School, Boston, USA⁷,

The auxiliary beta2 subunit of voltage-gated sodium channel and hypersensitivity in a neuropathic pain model

After peripheral nerve injury, abnormal excitability of injured and adjacent non-injured primary sensory neurons participates to development of pain symptoms. Voltage-gated sodium channels (VGSC) are responsible for action potential generation and change in their expression can contribute to mechanisms of neuropathic pain. In the present study we investigated whether β 2 subunit of VGCS is regulated in the spared nerve injury (SNI) model of neuropathic pain and assessed its function using sensory testing in mice lacking the β 2 subunit (KO- β 2).

The SNI model consists of the injury of tibial and common peroneal nerves, leaving the sural intact, allowing the distinction between injured and non-injured neurons for further analysis. Western blot and immunohistochemistry for β 2 subunit were performed on dorsal root ganglia (DRG) and nerves after SNI or sham surgery. Mechanical allodynia was recorded in SNI operated KO- β 2 mice and their wild-type controls in response to a series of calibrated monofilament applied on the sural skin nerve territory.

β 2 immunoreactivity (IR) was highly augmented after SNI: 27% of DRG neurons were β 2-IR positive, compared to 2% in controls. The same regulation was shown in peripheral nerves with accumulation of the subunit in the neuroma and confirmed by western blot. β 2 subunit is mainly regulated at the plasma membrane compared to cytoplasm, and although injured neurons showed the most marked upregulation, β 2 subunit expression was also increased in neighbouring non-injured neurons. Moreover, after SNI the KO- β 2 mice showed an attenuated response to mechanical stimuli compared to wild-type.

β 2 is over-expressed after peripheral nerve injury, in injured and in a less extend in non-injured neurons. It may contribute to nerve hyperexcitability by regulating the density of functional VGSC in the cell membrane and play a key role in the generation and maintenance of neuropathic pain.

Supported by SNSF and the P. Mercier Foundation

A PREFRONTAL CORTEX DEFECT OF GLUTAMATE RELEASE CAPACITY IN THE PHENCYCLIDINE (PCP) MODEL OF SCHIZOPHRENIA

¹BACCAGLIONI E., ²Brambilla L., ³Magara F., ⁴Ros J., ⁴Pellerin L., ³Magistretti P., ⁵Volterra A.,

UNIL - Centre de Neurosciences Psychiatriques¹, University of Milan, Italy², Centre de Neurosciences Psychiatriques³, DP, UNIL⁴, DBCM, UNIL - Centre de Neurosciences Psychiatriques⁵,

Subchronic administration of PCP, a psychotomimetic agent acting as an NMDAR channel blocker, produces in rodents a syndrome that models some aspect of schizophrenia. Our research investigates the consequences of PCP administration on glutamatergic functionality in rodents' prefrontal cortex (PFC).

Rats were treated once daily for 7 or 14 days with either PCP (5mg/kg) or saline. 24h after the last treatment, glutamatergic functionality is evaluated in terms of glutamate release capacity in acute PFC slices stimulated with high KCl (60mM). Slices from rats pre-exposed to PCP released less glutamate than slices from saline-treated animals. Such defect persisted 72h after the last treatment and was not observed in a different cortical area, the visual cortex. For 14 days treatments, the adaptive changes are extinguished 7 days after the last exposure to PCP. These findings were then reproduced in mice.

Furthermore, we tested the effect of antipsychotics (haloperidol and olanzapine) in PCP-treated animals. PCP treatment lasted 14 days, antipsychotics were administered in parallel starting from the 8th day (when the glutamate release defect is already established). Both antipsychotics reversed the PCP-induced defect, restoring a normal glutamate release capacity. The plastic modifications apparently occur at the level of glutamatergic terminals, because synaptosomes prepared from the PFC of PCP-treated animals showed defective glutamate release in comparison to control animals. In this preparation we are now studying the molecular target of PCP action, focusing our attention on a likely presynaptic NMDAR and the regulation of Ca⁺⁺ increases leading to neurotransmitter release. We are moreover interested in the effects of PCP treatment on PFC functionality, so to establish a possible link among the glutamatergic function, the performance in behavioural test involving this region and its metabolic activity during the test.

Therefore, the "PCP model" highlights functional anomalies that could underlie aspects of the psychopathology of schizophrenia (glutamatergic hypofunction).

Allostatic working memory processing in schizophrenia: Human and animal model coherence.

¹PREISSMANN D., ²Cocchi L., ³Do K., ⁴Vianin P., ⁵Schenk F.,

Département de Physiologie, Institut de Psychologie¹, Dep. Physiologie, Inst. Psychologie, Inst. Sciences du Sports et de l'Education Physique, Center of Psychiatric Neurosciences², Center of Psychiatric Neurosciences³, Dep. Universitaire Psychiatrie Adulte⁴, Dep. Physiologie, Inst. Psychologie, Center of Psychiatric Neurosciences⁵,

The most evident symptoms of schizophrenia are severe impairment of cognitive functions like attention, abstract reasoning and working memory. The latter has been defined as the ability to maintain and manipulate on-line a limited amount of information. Whereas several studies show that working memory processes are impaired in schizophrenia, the specificity of this deficit is still unclear.

Results obtained with a new paradigm, involving visuospatial, dynamic and static working memory processing, suggest that schizophrenic patients rely on a specific compensatory strategy. An animal model of schizophrenia with a transient deficit in glutathione during the development reveals similar substitutive processing, masking the impairment in working memory functions in specific test conditions only.

Taken together, these results show coherence between working memory deficits in schizophrenic patients and in animal models. More generally, it is possible to consider that the pathological state may be interpreted as a reduced homeostatic reserve. However, this may be balanced in specific situations by efficient allostatic strategies. Thus, the pathological condition would remain latent in several situations, due to such allostatic regulations. However, to maintain a performance based on highly specific strategies requires in turn specific conditions, limiting adaptive resources in humans and in animals. In summary, we suggest that the psychological and physical load to maintain this rigid allostatic state is very high in patients and animal subjects.

Time course of aquaporin expression after transient focal cerebral ischemia in mice

¹BADAUT J., ²de Castro Ribeiro M., ²Hirt L., ²Bogouslavsky J., ¹Regli L.,

*Neurochirurgie*¹, *Neurologie*²,

Cerebral oedema contributes to morbidity and mortality in stroke. Aquaporins (AQPs) 1, 4 and 9 have been identified as the three main water channels in the brain. To clarify their role in water movement, we have compared their expression patterns to brain swelling after transient focal brain ischemia.

There were two peaks of maximal hemispheric swelling at 1h and at 48h after ischemia, coinciding with two peaks of AQP4 expression. At 1h after occlusion, AQP4 expression was significantly increased on astrocyte endfeet in the core and in the border of the lesion. At 48h, AQP4 expression was increased in astrocytes in the border of the lesion over the whole cell. AQP9 showed a significant induction at 24h that increased gradually with time, without correlation with the swelling. The expression of AQP1 remained unchanged.

These results suggest that AQP4, but not AQP1 or AQP9, may play an important role in water movement associated with the pathophysiology of oedema after transient cerebral ischemia in the mouse.

Thiol-reactive protein labeling of brain proteins with infrared DY-680 and DY-782 maleimides.

¹RIEDERER B., ²Bonvallat S., ²Riederer B.,

Centre des Neurosciences Psychiatrique, CNP¹, CNP²,

A direct comparison of differentially labeled proteins separated in a single two-dimensional electrophoresis gel facilitates identification of potential marker proteins. Here we describe a procedure to label different sets of proteins with infrared maleimides and subsequent detection by one- and two-dimensional gel electrophoresis and analysis by an infrared imaging system for age-specific proteins. The procedure allows a detection of complex protein mixtures of less than 5 µg total amounts or 0.1 ng of individual proteins. Several applications, such as protein detection either by Coomassie blue- or silver-stains, or by Western blots or by protein identification via MALDI-TOF have been investigated. In conclusion, thiol-labeling with infrared dyes provide an additional tool for a detection of less abundant and cystein-containing proteins . In several diseases and during aging oxidation of proteins is changed, therefore we are currently elaborating this labeling procedure to identify and quantify oxidized and reduced cystein-containing proteins .

Changes in regional a-[11C]methyl-L-tryptophan trapping in patients with Major Depression treated with citalopram augmented with pindolol.

¹Berney A., ²Nishikawa M., ³Gobbi G., ³Debonnel G., ²Diksic M., ³Benkelfat C.,

Psychiatrie-CHUV¹, MNI-McGill², Psychiatrie-McGill³,

Objective and Methods: Positron emission tomography (PET) coupled with the use of a-[11C]-methyl-L-tryptophan (11C-aMtrp), is believed to provide an index of the brain regional rates of 5-HT synthesis, through the measure of 11C-aMtrp brain trapping constant K^* . The effects on 11C-aMtrp regional trapping of citalopram, augmented with the mixed 5-HT_{1A} and b-adrenoceptor antagonist pindolol, in patients treated for Major Depression was investigated using a 24 days, two-arm, randomized, double-blind study design. All patients received citalopram 20mg/day augmented with either pindolol 2.5 mg tid or placebo from day 11 to 24. HDRS-17 mood scores, as well as PET estimates of 11C-aMtrp trapping were obtained at baseline, and after 10 and 24 days of treatment, respectively. A voxel-wise approach (SPM99), as well as an a priori selected Volume-Of-Interest (VOI) based analysis were applied, focusing on the brain areas/5-HT pathways previously identified as the sites of regional differences in 11C-aMtrp trapping between unmedicated patients with MDE and controls: dorsolateral prefrontal cortex (DLPFC), Anterior Cingulate Cortex, Mesial Temporal Cortex, Thalamus, and Caudate Nucleus.

Results: Repeated Measure ANOVA on HDRS-17 scores revealed a significant decrease over time (mean \pm SD score at entry=23.3 \pm 3.9, at day 24=13.2 \pm 5.4, $F=35.27$; $df=2$; $p<0.0001$), with no significant treatment condition effect or time x treatment interaction. VOI's were submitted to Repeated Measure ANOVA, using hemisphere (R, L) and time (baseline, day-24), as repeated measures, revealing a Time x Treatment interaction in the DLPFC ($F=6.27$ (1,7); $p<0.05$), and a Time x hemisphere x Treatment interaction in the Caudate Nucleus ($F=13.06$ (1,7); $p<0.01$). Post-hoc comparisons (Newman-Keuls test) indicated that the addition of pindolol, relative to placebo, resulted in a significant increase in 11C-aMtrp trapping in these structures. SPM maps were obtained using proportional scaling to examine whether regional changes in 11C-aMtrp trapping correlated with clinical improvement: in the group as a whole, increases in trapping correlated with a reduction of HDRS-17 in the Cingulate Cortex (BAs 32 and 24), Precentral Gyrus (BA40), and the Medial Frontal Gyrus ($p<0.05$; corrected).

Conclusion: Pindolol augmentation as a therapeutic strategy in the pharmacotherapy of Major Depression, may rely upon the enhancement of aspects of 5-HT neurotransmission/5HT synthesis, in pathways believed to regulate mood.

Prospective study of long-term mood outcome following subthalamic Deep Brain Stimulation (STN-DBS) for Parkinson Disease (PD)

¹Berney A., ¹Saraga M., ²Wider C., ²Gronchi A., ³Burkhard P., ¹Guex P.,
²Bogouslavsky J., ²Ghika J., ⁴Pollo C., ⁴Villemure J., ²Vingerhoets F.,

Psychiatrie-CHUV¹, Neurologie-CHUV², Neurologie-HUG³, Neurochirurgie-CHUV⁴,

OBJECTIVES: Changes in mood, on occasions of clinical severity, were reported in PD patients who underwent STN-DBS (Berney et al. 2002, Mayberg et al. 2002, Anderson et al. 2003 for review). The aim of this study was to further characterize long-term mood outcome, in PD patients prospectively studied for at least 2 years after STN-DBS implantation.

METHOD: PD patients were systematically examined preoperatively (T0), at 10.2±2.9 months (T1) and 35.7±10.6 months (T2) following STN-DBS, using the Montgomery Asberg Depression Rating Scale (MADRS) and a brief structured psychiatric interview (MINI), in addition to the cognitive and motor assessments.

RESULTS: 30 PD patients (17M/13F, mean PD duration 15.1±4.8 years, mean age at implantation 64.7±7.9 years) were studied. Repeated measures analysis of variance (ANOVA) on MADRS scores showed a significant [Time x Gender] interaction; post-hoc analysis revealed that female patients significantly worsened their mood scores over time (mean MADRS T0: 10.1±4.2, T1: 15.4±9.4; T2: 13.9±8.5; p<0.05), whereas mood scores did not significantly change for male patients. Using DSM-IV diagnostic criteria's for Major Depression and a cut-off score of > 15 on the MADRS, 4/ 30 (13%) were depressed at baseline, 7/ 30 (23%) at T1 and 9/ 30 (30%) at T2. At final follow-up less than half (4/ 9) of the patients with Major Depression had an antidepressants at effective dosage.

CONCLUSIONS: This long-term follow-up study reveals a high rate of Major Depressive Episodes following STN-DBS, which may constitute an additional risk factor with disease progression for the development of co-morbid depression, especially in female patients.

References:

Berney A, Vingerhoets F, Perrin A et al. Effect on mood of subthalamic DBS for Parkinson's disease: a consecutive series of 24 patients. *Neurology* 2002;59:1427-1429.

Mayberg HS, Lozano AM. Penfield revisited? Understanding and modifying behavior by deep brain stimulation for PD. *Neurology* 2002;59:1298-1299.

Anderson KE, Mullins J. Behavioral changes associated with deep brain stimulation surgery for Parkinson's disease. *Curr.Neurol.Neurosci.Rep.* 2003;3:306-313.

Role of amino acid transport in the regulation of dendritic development by BDNF

^{1,2}MARTIN J., ¹Burkhalter J.,

*Physiologie*¹, *Physiologie, CNP Cery*²,

Brain development is accompanied by marked changes in neuronal metabolism. There is also increasing evidence that BDNF regulates neuronal development, in particular dendritic growth and branching of different types of neurons. Although these effects are well documented, little is known about the regulation of neuronal metabolism in particular the role of amino acid transport in the promotion of neuronal differentiation by BDNF. In the present study, we show that BDNF increases System A amino acid transport in cortical neurons by selective upregulation of the sodium-coupled neutral amino acid transporter (SNAT)1, a novel System A amino acid transporter isoform. Upregulation of SNAT1 expression is required for the enhancement of dendritic growth and branching of cortical neurons by BDNF. In addition, stimulation of System A activity in this way by BDNF is also necessary to increase levels of tissue-type plasminogen activator (tPA), a protease that we demonstrate to be essential for the effects of BDNF on cortical dendritic development. Together, these results indicate that SNAT1 and System A amino acid transport play a critical role in the regulation of dendritic morphology by BDNF, and suggest a role of these mechanisms in protein synthesis-dependent forms of synaptic plasticity.

Glutathione (GSH) deficit in schizophrenia: Dysfunction of NMDA receptors and alteration of NMDA-mediated responses.

¹STEULLET P., Lavoie S., Guidi R., Cuénod M., Do k.,

Departement de Psychiatrie, Centre de Neurosciences Psychiatriques¹,

Background. Synthesis of glutathione (GSH), an antioxidant, is compromised in schizophrenia. Patients show a GSH deficit in cerebrospinal fluid and prefrontal cortex, and a decrease in gene expression of the modulatory subunit of glutamate-cysteine ligase, the rate limiting enzyme of GSH synthesis. A polymorphism of this gene is also associated with the illness. Here, we studied the effects of GSH deficit on NMDA receptor function.

Methods. GSH deficit was induced in slices of rat hippocampus or in cultured cortical neurons by L-buthionine-(S,R)-sulfoximine (BSO). The effect of GSH deficit on NMDA receptor function was assessed by electrophysiological techniques in hippocampal slices and by intracellular calcium measurements upon NMDA stimulation in cultured neurons.

Results. In hippocampal slices, a GSH deficit caused decrease in NMDA receptor-mediated fEPSPs. Hypofunction of NMDA receptors under GSH deficit was due in part to oxidation of extracellular redox-sites on NMDA receptors. In GSH-depleted cultured neurons, but not in control neurons, dopamine depressed NMDA-mediated calcium responses. Blockade of D2 receptors with sulpiride or GSH replenishment with GSH-ethyl-ester abolished the effect of BSO treatment on dopamine modulation of NMDA responses. This suggests that GSH deficit also alters intracellular pathways leading to increase in efficacy of D2 receptor-mediated signalling and a decrease in NMDA responses. The mechanisms underlying such alteration of dopamine modulation of NMDA responses are under investigation.

Conclusions. A GSH deficit, like that observed in schizophrenics, affects NMDA receptor function. Thus, a GSH deficit could be one causal factor for the hypofunction of NMDA receptors in schizophrenia.

Impact of functional PET/SPECT brain imaging in multidimensional assessment of mild cognitive impairment: Preliminary Results

¹ALLAOUA M., ²JORAY S., ¹PRIOR J., ²GHIKA J., ²BOGOUSLAVSKY J.,
¹BISCHOF DELALOYE A.,

*Médecine Nucléaire*¹, *Neurologie*²,

Aim:

Mild cognitive impairment (MCI) is an important clinical entity considered to be an intermediate state between normal and pathologic aging. The exact sensitivity and specificity of neuropsychological tests, functional brain imaging and genetic approaches is still under evaluation. Our aim was to define the role of functional brain imaging with PET and SPECT when combined with neuropsychological investigations and genetic approach.

<----->

Methods:

We studied 13 patients with suspected MCI referred to our University Memory Clinics (8 men/5 women, mean age 68±7 years), who underwent extensive neuropsychological testing, morphological brain CT or MRI imaging and determination of ApoE genotype. Patients underwent functional brain imaging with F-18-FDG PET (n=6) or Tc-99m-ECD SPECT (n=7). Qualitative and semi-quantitative analysis has been applied for all patients (Hermes BRASS/ Xeleris NeuroGam).

<----->

Results:

In 6 patients qualitative and semi-quantitative functional neuroimaging demonstrated significant decrease of activity in the temporal (unilateral, n=4, bilateral, n=2), as well as in the hippocampal region (unilateral, n=3, bilateral, n=3), whereas the other 7 were normal. There was a significant association between decreased bilateral cortical and hippocampal activity with the learning performance on clinical testing.

<----->

Conclusions:

Both qualitative and semi-quantitative PET/SPECT brain imaging appears to be an excellent marker for MCI. When combined with neuropsychological test, it may improve the diagnosis of MCI and add new tools for the study of patients with mild cognitive impairment. Its exact role in discriminating normal from pathological aging remains to be determined.

<----->

<Literatur/References:>

1- Arnaiz E, Jelic V, Almkvist O, Wahlund LO, Winblad B, Valind S, Nordberg A. Impaired cerebral glucose metabolism and cognitive functioning predict deterioration in mild cognitive impairment. *Neuroreport*. 2001 26;12(4):851-855.

INFLUENCE OF CYP2B6 POLYMORPHISM ON THE STEADY-STATE PLASMA LEVELS OF THE ENANTIOMERS OF METHADONE

¹Crettol S., Déglon J., Besson J., Croquette-Krokkar M., Gothuey I., Hämning R., Monnat M., Hüttemann H., Brocard M., Cochard N., Brawand M., Baumann P., Eap C.,

Unité de Biochimie et Psychopharmacologie clinique, Centre de Neurosciences psychiatriques, Département de Psychiatrie¹,

Background: Previous in vivo or in vitro studies suggested that cytochrome P4503A4/5 (CYP3A4/5) and, to a smaller extent, CYP2D6 are the major cytochrome P450 isoforms involved in methadone metabolism. However, recent in vitro studies suggested a predominant role of CYP2B6, even over CYP3A4/5.

Method: 209 methadone maintenance treatment patients were genotyped for CYP2B6*4, *5, *6, *7 and *9 alleles. Steady state trough and peak (4 H after methadone intake) plasma concentrations, corrected by the dose and the weight of the patients, were measured.

Results: CYP2B6 strongly influences (S)-methadone trough ($p=0.01$) and peak ($p=0.03$) concentrations, with the CYP2B6*6 genotype having the highest influence. Trough (S)-methadone plasma levels were highest in subjects with the *6/*6 genotype (209 ng/ml per mg/kg), intermediate in heterozygous carriers of the allele *6 (*1/*6, 4/*6, *5/*6), and lowest in non-carriers (105 ng/ml per mg/kg; *1/*1, *1/*4, *1/*5, *4/*5, *5/*5), $p=0.0004$. On the other hand, a weaker influence of CYP2B6 was observed on (R)-methadone plasma levels (non significant at trough and a tendency toward significance at peak, $p=0.07$).

Conclusion: In vivo CYP2B6 contributes strongly to (S)-methadone and to a smaller extent to (R)-methadone metabolism. As (R)-methadone is the active enantiomer with regard to the opioid effects, the in-vivo importance of CYP2B6 genetic polymorphism remains to be determined.

LEARNING INDUCED CHANGES IN THE PROCESSING OF INTERAURAL TIME DIFFERENCE: AN ERP STUDY

¹SPIERER I., ²Tardif e., ³Murray m., ⁴Sperdin h., ⁵Clarke s.,

Medecine, Neuropsychologie¹, physiologie², neuropsychologie, radiologie³, psychologie⁴, neuropsychologie⁵,

The present study aims at determining to which extent central auditory structures underlying the processing of interaural time differences (ITD), an auditory lateralisation cue, could be modified by a short training session. Learning-induced neurophysiological changes have been assessed in 8 normal subjects by comparing pre- and post-training mismatch negativity (MMN), an negative AEP wave which indexes automatic detection of a change in a homogeneous auditory sequence. During EEG recording, stimuli were presented in an oddball fashion with a standard (S, $p = 0.875$) and a deviant (D, $p = 0.125$) white noise burst that differed in their ITD (S = 375 microsecond; D = 500 microsecond). The training session consisted in a 40 minutes long spatial discrimination task (two-alternative forced choice paradigm, subjects had to indicate whether the two elements of a pair of sounds (S-S or S-D) were at the same location or not).

Behavioural and neurophysiological changes were found after the training session. In the discrimination task, performance showed a significant increase. Pre-training AEPs did not show any differences between responses to S and D whereas post-training AEPs revealed a large MMN for the deviant stimuli. Increase in behavioural performance correlated significantly with MMN amplitude.

In conclusion, auditory-spatial discrimination training leads to rapid neurophysiological changes as reflected by the emergence of a MMN in the post-training recording suggesting fast cortical plasticity within neuron networks that underlie ITD processing.

Anticiper, décider, s'orienter à l'aide d'une représentation potentiellement dissociable: les capacités d'un animal modèle

¹SAUTTER C., ²SCHENK F.,

Département de physiologie¹, Département de physiologie, Institut de psychologie, Centre de neuroscience psychiatrique²,

Savoir où l'on est, d'où l'on vient ou simplement pouvoir reconnaître un lieu précis sont des problèmes que toutes les espèces mobiles doivent résoudre pour être au bon moment, au bon endroit. Or, les espèces les plus évoluées peuvent calculer des relations spatiales entre les éléments qui forment l'espace. Ils témoignent ainsi de la capacité d'utiliser un système de référence allocentré dit « carte cognitive » (Tolman 1948), une forme de mémoire « prospective » (O'Keefe et Nadel 1978), qui encore aujourd'hui reste source de controverses. Les propriétés d'une telle élaboration peuvent être mises à l'épreuve par l'utilisation de protocoles expérimentaux particuliers dont le paradigme du labyrinthe radial (Olton & Samuelson 1976). Il s'agit d'une structure dans laquelle le rat développe spontanément une stratégie qui lui permet de visiter toutes les branches une seule fois sans nécessairement reposer sur un algorithme simple. Dans ce travail, on a analysé comment des animaux qui avaient appris à patrouiller correctement dans un dispositif radial opalescent (donc sans vision de l'environnement) pouvaient répondre à la dissociation des référentiels disponibles dans leur espace de navigation: un repère lumineux, une pente et des traces olfactives. Les résultats indiquent trois types différents de réponse. Lorsque le labyrinthe, la lumière et la pente étaient dissociés de l'environnement de la chambre par une rotation de 90 degrés, les sujets étaient perturbés transitoirement, montrant ainsi que leur performance pouvait s'ajuster aux éléments contrôlés. Au contraire, la rotation de la lumière seule, dissociée ainsi du reste des informations, engendrait une perte drastique de l'efficacité suggérant une rupture du système d'orientation. La dissociation du référentiel olfactif a déclenché une perturbation retardée suggérant une hypothétique accumulation d'incertitude due à la perte de cohérence des informations olfactives qui devrait confirmer le bien-fondé des décisions de visite. L'ensemble de ces résultats suggèrent donc que les informations présentes n'étaient pas utilisées de manière univoque. En particulier, il semblerait que les stratégies des animaux découleraient à la fois de la signification des informations attendues et de l'analyse des données sensorielles. Ce mode de fonctionnement irait dans le sens d'une mémoire prospective, probablement par une adaptation des attentes au présent de la perception. Ce type de protocole nous semble particulièrement adapté à la détection de perturbation des processus de décision, une manifestation fréquemment observée en psychiatrie.

O'Keefe, J., & Nadel, L. (1978). *The hippocampus as a cognitive map*. Oxford: Oxford University Press

Olton, D.S., & Samuelson, R. (1976). Remembrance of Placed Passed: Spatial Memory in Rats. *Journal of Experimental Psychology : Animal Behaviour Processes* 2, 97-116

Tolman E. C. (1948). Cognitive maps in rats and men. *Psychological Review*, 55, 189-208

HARDWIRED AUDITORY ‘WHAT’ AND ‘WHERE’ PROCESSING IN HUMANS REVEALED BY ELECTRICAL NEUROIMAGING

¹DE SANTIS L., ²Meylan R., ³Tardif E., ³Clarke S., ⁴Murray M.,

Neuropsychologie, hôpital Nestlé¹, The Functional Electrical Neuroimaging Laboratory, Division Autonome de Neuropsychologie, CHUV, Lausanne², The Functional Electrical Neuroimaging Laboratory, Division Autonome de Neuropsychologie, CHUV, Lausanne; Institut de Physiologie, Université de Lausa³, The Functional Electrical Neuroimaging Laboratory, Division Autonome de Neuropsychologie, CHUV, Lausanne; Service Radiodiagnostique et Radiologie Inte⁴,

The auditory system includes two parallel functional pathways – one for treating the identity of sounds and the other for their spatial attributes (so-called what and where pathways). We examined the spatiotemporal mechanisms along auditory what and where pathways and whether these pathways are hardwired for differentially processing spatial and pitch information of physically identical stimuli. Electrical neuroimaging of auditory evoked potentials was applied to a passive ‘oddball’ paradigm comprised of two varieties of blocks of trials. On what blocks, band-pass filtered noises varied in pitch, independently of perceived location. On where blocks, the identical stimuli varied in perceived location independently of pitch. Beginning 100ms post-stimulus, the electric field topography at the scalp significantly differed between conditions, indicative of the automatic recruitment of distinct intracranial generators. A distributed linear inverse solution and statistical analysis thereof revealed activations within the superior temporal cortex and prefrontal cortex bilaterally that were common for both conditions, as well as regions within the right temporo-parietal cortices that were selective for the where condition. These findings support models of automatic parallel processing of auditory information, such that segregated processing of spatial and pitch features may be an organizing principle of auditory function. (SNSF grants 3200BO-105680/1 to MMM and 3100A0-103895/1 to SC)

The expansion of 350 CTG repeats in Myotonic Dystrophy transgenic mice does not induce disorder in peripheral motor and sensory systems

¹GANTELET E., ²Kraftsik R., ³Gourdon G., ⁴Kuntzer T., ⁴Barakat-Walter I.,

*Neurologie*¹, *Department de Biologie Cellulaire et de Morphologie*², *INSERM U383, Hôpital Necker, Paris*³, *Laboratoire de Recherche Neurologique, CHUV, Université de Lausanne*⁴,

Myotonic dystrophy (DM1) also known as Steinert disease is an inherited autosomal dominant disease. DM1 is mainly characterized by skeletal muscle degeneration, delayed muscle relaxation after voluntary contraction and muscular weakness. It was demonstrated that this complex disease results from the expansion of CTG trinucleotide repeats in the 3' untranslated region of the DM protein kinase (*DMPK*) gene on chromosome 19, which encodes a serine-threonine protein-kinase. The severity of the clinical symptoms of DM1 is correlated with the length of expansion of these CTG repeats.

Although several electrophysiological and histological studies have been carried out to verify the possible involvement of peripheral nerve abnormality with DM1, the results have not been univocal and the real incidence of this involvement is uncertain. Therefore, at present, the possible association between peripheral neuropathy and DM1 remains an open question. To investigate whether motor and sensory neuropathy can be associated with DM1, we used DM1 transgenic mice model (generated by G.Gourdon). These mice carry the human genomic DM1 region with 350 CTG repeat expansion which express the DM1 phenotype or with 20 CTG repeat expansion which does not express the DM1 phenotype and are used as control.

To detect the loss of neurons in the spinal cord or in dorsal root ganglia (DRG), as well as changes in sciatic nerves and neuromuscular junctions in DM1 (350 repeat) transgenic mice, several histological and morphometric techniques were used. The number of motor neurons in the anterior horns of the spinal cord and the number of sensory neurons in DRG at the lumbar level (L4-L6) was quantitated on serial semi-thin sections (1µm thick) by the physical disector method. Fifteen pairs of sections were used from each spinal cord segment and about 20 section pairs from each ganglion. The statistical analysis of the morphometric results clearly showed there is no loss in the number of the motor or sensory neurons in DM1 transgenic mice compared to control (20 CTG repeat) or wild type control mice. Possible changes in the structure and number of myelinated axons in sciatic nerves were studied by the StereoInvestigator and NeuroLucida programs. The results of these methods revealed that no significant difference can be found either in the number of myelinated axons or in the diameter of these axons between DM1 (350 CTG repeat) mice and (20 CTG repeat) or wild type control mice. Moreover, the stability of the neuromuscular junction was studied on serial longitudinal cryostat sections (20 µm thick) from gastrocnemius, soleus, tibialis and fibularis muscles. The muscle sections were labeled with either acetyl cholinesterase (AChE) histochemical staining or rhodamine-conjugated α bungarotoxine. The histological and morphometric analysis of neuromuscular junctions demonstrated that the shape, the distribution and the number of endplates are not affected in DM1 (350 CTG repeat) transgenic mice compared to controls.

In conclusion: our combined results strongly suggest that in the DM1 transgenic mouse model the expansion of 350 CTG repeats does not lead to motor and sensory neuropathy. Since the length of CTG repeat expansion correlates with the severity of the clinical symptoms, we will go on to study DM1 transgenic mice with longer (750) CTG repeats (FRNS 102175/12003, Novartis, 04A16, 2004 and SUVA, 2005).

Delayed sensorymotor development, motor impairments, and abnormal peripheral nerve structure in mice expressing a soluble, truncated form of SCG10.

¹GANTELET E., ²Bondallaz P., ³Magara F., ⁴Barakat-Walter I., ⁵Grenningloh G.,

Neurologie¹, Département de Biologie Cellulaire et Morphologie, Université de Lausanne², Centre de Psychiatrie Neurosciences³, Laboratoire de Recherche Neurologique, CHUV, Lausanne⁴, EPFL⁵,

SCG10 is a neuronal membrane-associated protein enriched in growth cones. As a potent microtubule destabilizing factor it is thought to regulate microtubule dynamics during axonal elongation. Towards a further analysis of the *in vivo* function of SCG10, we have used gene targeting to disrupt the mouse SCG10 gene. The mutant mice express a truncated form of SCG10 lacking the N-terminal subcellular targeting domain (encoded by exon 2), which is responsible for the transport of SCG10 to growth cones. Neurons isolated from mutant mice show a cytosolic distribution of SCG10 similar to the related protein stathmin. We followed the somatic and sensorymotor development of homozygous mutant mice and WT controls from postnatal day (PND) 2 to 22, by means of an elaboration of the test battery of Fox. The mutant mice were viable, albeit their number at weaning was considerably lower than expected by the Mendelian ratio, suggesting the SCG10 mutation reduces survival fitness in early life. Somatic growth appeared to be compromised in homozygous mutants, as body weight was significantly reduced starting from PND 8 to 22. Motor proficiency was reduced in mutant mice, showing reduced grip strength from PND 18 and a complete inability to perform the coat hanger test. However, the onset of some reflexes was not affected by the mutation. Grip strength was reduced independent from body weight, suggesting a genuine motor deficit, that worsens over time (test repeated at 3 and 6 months). Histological and morphometric analysis of sciatic nerve revealed a significant decrease in the number of myelinated axons in the mutant mice suggesting that the reduced skeletal muscle strength is caused by changes in peripheral nerve structure. These data suggest that functional SCG10 is necessary for effective axonal growth and maintenance (FRNS 3100A0-104258 (G.G) and 102175/12003 (I.B.W))

Interhemispheric integration at different spatial scales

¹FORNARI E., ¹Knyazeva M., ¹Meuli R., ¹Maeder P.,

*Radiodiagnostic et Radiologie Interventionnelle*¹,

Background. Natural images contain a wide spectrum of spatial information, ranging from extremely low to very high spatial frequencies (SF). To encode complex shapes/objects, local descriptions of the retinal image at multiple spatial scales must be integrated across space and pooled across SF components. Various SF are thought to impact differently to the integration processes. Here we summarize our EEG/fMRI studies in humans aimed at mapping neural assemblies involved in the Gestalt-based interhemispheric integration of the bilateral stimuli systematically varying in SF.

Methods. In separate EEG and fMRI experiments, 15 subjects viewed bilateral sinusoidal black-and-white gratings drifting with a temporal frequency of 2 Hz. The stimuli either obeyed Gestalt grouping rules (iso-oriented collinear gratings, IG) or violated them (orthogonally-oriented (OG1) and out-of-phase gratings (OG2)). In the EEG experiment we presented stimuli in the range of 0.25-8.0 c.p.d., the fMRI experiments were limited to 0.5-2.0 c.p.d. During EEG recording session, the stimulus order and exposure were randomized. The high surface sampled EEG (128 channels, EEG/ERP system EI. Geodesics Inc.) was submitted to spectral analysis with an emphasis on interhemispheric coherence (ICoh). During fMRI recording session, the stimulus conditions were alternated with background in a balanced-randomized order 5 times 15 s each. Functional MRI images were acquired with an EPI gradient echo T2* weighted sequence (FA 90, TE 66, pixel size 3.75 x 3.75mm, acquisition time 1.7s) with a TR = 3s. Preprocessing, single subject analysis and group statistics were conducted on SPM99.

Results. Stimulation with bilateral iso-oriented collinear gratings synchronized EEG signals interhemispherically in the beta band (20-31 Hz) band. Principal Component Analysis suggested that several independent sources produced narrow-band interhemispherically coherent signals within this band. The two of them (21-23 Hz, beta1 and 26-28 Hz, beta2 components) clearly differentiated the “good-Gestalt” stimulus from the “bad-Gestalt” stimulus. Sensor location and SF of the stimuli also modulated ICoh of these components. Therefore, the EEG data suggested distributed neural substrate for interhemispheric synchronization at different SF.

The fMRI experiments revealed areas associated with interhemispheric integration (IG > OG1/2) activated invariantly across SF (bilaterally in the collateral sulcus, Vp, V4) and areas where the activation was modulated by SF (lingual gyri ventrally and precuneal region of cingulate sulci medio-dorsally). Among the regions tuned for SF, ventral locations showed a decrease in activation with SF, while medio-dorsal locations revealed the opposite tendency.

Further, with regression analysis, we localized cortical territories in which interhemispheric synchronization measured with ICoh predicted BOLD signal. It appeared that the ICoh values of the beta1 and beta2 components related to separate anatomo-functional brain circuits. The beta1 ICoh values predicted activation in the collateral sulcus area mostly overlapping with the BOLD-defined ventral locations. The beta2 component correlated with BOLD bilaterally in the subregion of cingulated sulcus already shown with BOLD increase and within the large area of parieto-occipital and intraparietal sulci, which missed among integration-associated areas as revealed with just BOLD increase.

Conclusion. Combined EEG/fMRI approach revealed distributed neural substrate for interhemispheric integration at different spatial frequencies.

Working memory in schizophrenia: dynamic visuo-spatial information processing

¹DEPPEN P., ¹Chappuis C., ¹Do K., ³Vianin P.,

*Centre de neurosciences psychiatriques, Unité de recherche sur la schizophrénie (LUNEP)¹,
Département de psychiatrie, section Minkowski³,*

Working memory, commonly defined as the ability to hold mental representations on line transiently and to manipulate these representations, is known to be a core deficit in schizophrenia. The aim of the present study was to investigate the visuo-spatial component of the working memory in schizophrenia, and more precisely to what extent the dynamic visuo-spatial information processing is impaired in schizophrenia patients. For this purpose we used a computerized paradigm in which 29 patients with schizophrenia (DSM-IV, Diagnostic Interview for Genetic Studies) and 29 age and sex matched control subjects (DIGS) had to memorize a plane moving across the computer screen and to identify the observed trajectory among 9 plots proposed together. Each trajectory could be seen max. 3 times if needed.

The results showed no difference between schizophrenia patients and controls regarding the number of correct trajectory identified after the first presentation. However, when we determine the mean number of correct trajectories on the basis of 3 trials, we observed that schizophrenia patients are significantly less performant than controls (Mann-Whitney, $p = 0.002$). These findings suggest that, although schizophrenia patients are able to memorize some dynamic trajectories as well as controls, they do not profit from the repetition of the trajectory presentation.

These findings are congruent with the hypothesis that schizophrenia could induce an unbalance between local and global information processing: the patients may be able to focus on details of the trajectory which could allow them to find the right target (bottom-up processes), but may show difficulty to refer to previous experience in order to filter incoming information (top-down processes) and enhance their visuo-spatial working memory abilities.

Fluorescence imaging of mitochondrial Na⁺ dynamics in intact astrocytes

¹BERNARDINELLI Y., ²Chatton J.,

Departement de Physiologie¹, Departement de physiologie, Departement de Biologie Cellulaire et de Morphologie, Cellular Imaging Facility²,

Astrocytes have the unique property of experiencing large changes of intracellular Na⁺ following the activation of the Na⁺-coupled glutamate transport. The plasma membrane Na⁺/K⁺-ATPase is primarily responsible for intracellular Na⁺ regulation. The present study investigated whether cytosolic Na⁺ changes are transmitted to mitochondria, which could therefore contribute to the intracellular Na⁺ regulation. Mitochondrial Na⁺ changes were monitored using the Na⁺ sensitive fluorescent probe CoroNa Red in intact primary cortical astrocytes. Glutamate, as well as agents known to increase cytosolic Na⁺ in astrocytes all led to mitochondrial Na⁺ elevation. Simultaneous mitochondrial and cytosolic Na⁺ measurement using SBFI-AM revealed that Na⁺mit amplitude followed the Na⁺cyt profile for glutamate concentrations above ~5-10μM. However, lower glutamate concentrations that evoked minute cytosolic changes led to unexpectedly large Na⁺ responses. Blockers of potential entry pathways (K⁺, Ca²⁺, Na⁺ channels, Na⁺/Ca²⁺ antiporter, etc.) failed to inhibit mitochondrial Na⁺ responses. However, opening of mitochondrial KATP channels using diazoxide increased mitochondrial Na⁺. Inhibition of mitochondrial Na⁺/H⁺ antiporter using ethylisopropyl-amiloride caused a steady increase in mitochondrial Na⁺ indicating that Na⁺ extrusion from mitochondria is mediated by these exchangers. Thus, combined fluorescence imaging of mitochondrial and cytosolic Na⁺ in intact astrocytes revealed that mitochondria are equipped to efficiently sense cellular Na⁺ signals and to actively regulate their Na⁺ content.

Deficits of early information processing in adolescents with psychotic disorders revealed by visual backward masking

¹HOLZER L., ¹Jaugey L., ¹Halfon O., ²Herzog M.,

DP-CHUV/SUPEA¹, EPFL/Brain and Mind Institute²,

Background : schizophrenic patients show strong deficits over a broad range including "higher" cognitive and executive functions and "lower", basic sensory information processing. The latter deficits are of particular interest since deficits on these early stages might cause deficits on higher, cognitive levels. Using a new backward masking paradigm, shine-through, we could show that target processing is strongly impaired in adult schizophrenic patients whereas basic visual functions, such as figure-ground-segmentation and feature binding, are spared (Herzog et al., 2004; Brand et al., 2003). This masking technique seems to be very sensitive for patients diagnosed for negative symptoms.

Objectives : to evaluate whether the shine-through paradigm is also suitable to show visual information processing deficits in adolescents with psychotic disorders.

Method : we presented a vernier target that was followed by a grating mask. A vertical vernier consists of two bars that are slightly offset in the horizontal direction randomly either to the left or to the right. Observers have to indicate this offset direction. We determined the stimulus onset asynchrony (SOA) between the vernier and the grating onset for 34 adolescents (mean age = 15.7 years old,) : 12 with schizophrenia spectrum disorders according to DSM IV criteria, 7 adolescents at high risk of psychosis, and a comparable control group of 11 healthy adolescents and 3 adolescents with non psychotic disorders.

Results : our preliminary data show that adolescents with psychotic disorders need SOAs of 97.7 ms to reach a comparable performance level whereas adolescents at high risk for psychosis need SOAs of only 55.7 ms, and controls of 16.5 ms.

Conclusion : our results suggest that backward masking is a promising tool to detect vulnerability to schizophrenia spectrum disorders with early deficits possibly affecting later cognitive or executive functions.

Electrophysiological correlates of syntactic and semantic processing in the healthy and damaged brain

¹BURGAT L., ¹Murray M., ²Isel F., ³Clarke S., ¹Buttet Sovilla J.,

Division Autonome de Neuropsychologie, CHUV¹, Universität Hamburg², Institut de Physiologie³

Electrophysiological methods can be used to address the temporal aspects of auditory verbal comprehension. Lesion data have also contributed to understand language-related ERP components. In order to examine possible interactions between syntactic and semantic processing, event-related potentials (ERPs) were recorded during French sentence comprehension using a violation paradigm. The task consisted of judging the acceptability of correct and incorrect sentences. Incorrect sentences contained syntactic, semantic, or both kinds of violations. ERPs to correct sentences were compared with those containing violations. Participants were four healthy subjects and three patients suffering from aphasia. ERPs from healthy subjects showed the following. Syntactically anomalous sentences showed several phases of differential ERP responses [Early Anterior Negativity (~150ms), Reference Related Negativity (~300ms), and P600]. Semantic anomalies yielded only an N400 enhancement. Sentences with both violations resulted in the same ERP sequence as in the case of syntactic anomalies alone – there was no N400 modulation. That differential ERP effects were non-cumulative therefore supports the predominant role of syntactic processing in sentence processing. The absence of an additive effect in the time window 300-600 ms provides evidence that a syntactic violation can disturb some aspects of the semantic processing.

By contrast to these findings, patients with left frontal damage (including inferior and middle frontal gyri, and portions of the basal ganglia) showed intact N400 and P600 effects, but no LAN to grammatical anomalies. A patient with damage to left parietal and posterior temporal cortex demonstrated an intact LAN, but no measurable N400 or P600. This suggested that parieto-temporal regions are involved in the semantic processing measured by the N400 and that the left frontal cortex might support early syntactic processes, supporting independent syntactic and semantic processing.

These preliminary data confirm that timing of specific aspects of syntactic and semantic processing appears to be crucial for successful oral comprehension. Patients' explicit everyday oral comprehension skills may dissociate from those detected during on-line sentence processing. ERP correlates and their evolution over time in patients with different types of aphasia and different types of lesions will allow a better understanding of the underlying processing and the reorganization involved in recovery.

Modulation of astrocyte glucose metabolism by pro-inflammatory cytokines and beta-amyloid peptide: for better or for worse?

¹GAVILLET M., ¹Allaman I., ¹Marti M., ¹Magistretti P.,

LNDC, EPFL¹,

Local alterations of brain energy metabolism and oxidative stress are features of neurodegenerative disorders, notably of Alzheimer's disease (AD). Both amyloid peptide and inflammation mediators have been shown to play a significant role in AD pathogenesis. The aim of the present study was to investigate the effects of pro-inflammatory cytokines (TNF α and IL-1 β) and beta-amyloid (A β) on glucose metabolism in primary cultures of mouse cortical astrocytes.

We observed that the pro-inflammatory cytokines TNF α (0.25ng/ml) and IL-1 β (20ng/ml) as well as A β (A β ₂₅₋₃₅, 25 μ M) increase glucose utilization, as assessed by the [³H]-2-deoxyglucose uptake technique. Interestingly, when combined, they have synergistic effect on glucose utilization. Beta-amyloid (A β) also increases cellular glycogen content and lactate release, whereas pro-inflammatory cytokines have opposite effects. Effects on glucose oxidation to CO₂ through tricarboxylic acid cycle (TCA) or pentose phosphate pathway (PPP) show alternative pattern. Treatment with either TNF α or IL-1 β alone increases TCA activity at the expense of PPP whereas combined treatment with TNF α +IL-1 β massively increases both TCA and PPP, an effect also observed following A β treatment.

Taken together these results show that both pro-inflammatory cytokines and beta-amyloid peptide strongly modulate astrocyte glucose metabolism. In particular these substances increase metabolic pathway that are potentially ROS producing. Furthermore, they turn astrocyte glucose metabolism from "cooperative" to more "selfish" cells. Given the central role of astrocytes-neuron metabolic unit in brain energy metabolism this could have a major impact on neighbouring neurons.

Intracortical connectivity of layer VI pyramidal cells in the barrel cortex of mice.

¹PICHON F., ¹Welker E.,

*DBCM*¹,

The whisker-to-barrel pathway of rodents is formed by a series of somatotopic projections from the mystacial whisker follicles to the layer IV of the primary somatosensory cortex such that each follicle corresponds to a cluster of cortical neurons, called barrel. Barrels are present in layer IV but form part of a functional column that comprises the entire depth of the somatosensory cortex. Interestingly, the cortex of the barreless mouse strain is organized such a manner that thalamocortical afferents do not remodel their projections in layer IV and barrels fail to appear. Nevertheless, functionally, a columnar organization persists, indicating that functional columns are not only provided by thalamocortical projections and layer IV cells. Since in the visual cortex of cats, layer VI cells contribute to the response properties of layer IV neurons, we asked the question: do layer VI pyramidal cells contribute to the columnar organization in the primary somatosensory cortex of mice? To address this, we morphologically analyzed the distribution of intracortical axon collaterals of layer VI neurons after in-vivo juxtacellular injections of biocytin in the C2 barrel column. In normal mice, results show that we can split layer VI of the somatosensory cortex into two sub-layers: upper part contains pyramidal neurons projecting both in layers IV and VI, among them we found one cell projecting mainly in its barrel, whereas lower part contains pyramidal neurons projecting mainly in infragranular layers. Taking into account the fact that upper part of layer VI is directly innervated by thalamus, these results highlight an indirect excitatory pathway from thalamus to layer IV that could be involved in columnar organization of the primary somatosensory cortex of mice.

Visual and olfactory place-discrimination deficit in rats with low glutathione during development: an animal behaviour model with relevance to schizophrenia

¹CABUNGCAL J., ²Cuénod M., ²Do K., ²Schenk F.,

Department of Psychiatry and Center for Psychiatric Neuroscience¹, Department of Adult Psychiatry and Center for Psychiatric Neuroscience²,

Glutathione levels ([GSH]) is decreased in cerebro-spinal fluid and prefrontal cortex of schizophrenics (Do et al., 2000), consistent with the decreased fibroblast mRNA levels of two GSH synthesizing enzymes in patients (Tosic et al., 2004). Since GSH is an important endogenous anti-oxidant that protects cell from oxidative stress induced damage, its deficit could lead to synaptic loss resulting in abnormal neuronal connectivity. In our animal model, albino rats were treated from P5-P16 with L-buthionine-(S,-R)-sulfoximine (BSO), an inhibitor of GSH synthesis. This early treatment induces a transitory (P5-P18) decrease in brain GSH levels by 40-50% (Rougemont et al., 2002). Cognitive function was evaluated in adult rats using the homing board task (Schenk, 1989). The animals' capacity to perform place learning or place discrimination using visual and olfactory sensory modalities was assessed. We found in BSO-treated rats, impaired place discrimination when all proximal (not distal) visual and olfactory cues were removed. Place discrimination was highly precise in control (PBS) - and BSO-treated rats when only one olfactory cue was present (on trained escape location). While place discrimination improved in control rats, it became inaccurate in rats with early GSH (BSO) deficit, when five new different olfactory cues (one for each possible escape location) were used. Our data suggests that these deficits are not attributable to sensory impairments but rather to problems arising at the level of integration. The olfactory deficit observed in the proposed animal model is consistent with the reported olfactory identification and discrimination impairment in schizophrenia.

Caractéristiques neurologiques et cognitives de différentes souris transgéniques APP avec des plaques amyloïdes : comment un ensemble de déficits peut résulter d'une modification génétique spécifique.

¹GIULIANI F., ²CHALARD R., ²SCHENK F., ³LEUBA GFELLER G.,

Institut de psychologie¹, Institut de psychologie, Département de physiologie, Centre des neurosciences psychiatriques², Service Universitaire de Psychogériatrie, Centre des neurosciences psychiatriques³,

Des souris APP de différentes cohortes et de différents âges ont été suivies afin d'évaluer le développement d'un modèle de maladie d'Alzheimer sur les plans cognitifs et comportementaux. La démarche suivie combine des manipulations génétiques susceptibles d'induire la formation des dépôts beta-amyloïdes chez ces souris transgéniques avec des traitements anti-inflammatoires (anti TNF alpha IP chronique) ou une modulation génétique (KO ou surexpression).

Sujets : 197 souris mâles âgées entre 50j et 15 mois ont été distribuées dans 5 groupes, à savoir : 1) APP+/+/-+, 2) Control, 3) APP+/-x traitement anti-TNF, 4) APP+/-TNF-/-, 5) APP+/-TNF+/-x traitement anti-TNF. Ces souris ont été testées dans différentes tâches mais on ne présente ici que les résultats d'une phase d'apprentissage spatial en bassin de Morris (acquisition sur 5 jours et test de rétention). Le comportement stéréotypé ainsi que la vitesse de nage ont été évalués pendant le test de rétention. Une évaluation complémentaire a été fondée sur le répertoire des troubles du comportement des animaux. Enfin, une étude histologique a été effectuée sur les souris afin de déterminer le pourcentage de plaques beta-amyloïdes au niveau de l'hippocampe.

Nous avons enregistré des atteintes plus graves et plus précoces chez les animaux APP homozygotes. Ces derniers n'ont pas pu présenter un comportement adaptatif suffisant pour discriminer la zone de la plate-forme. Ils montrent une grande labilité émotionnelle, associée à de nombreux troubles comportementaux et de très importants dépôts amyloïdes dans l'hippocampe. Chez les animaux APP hétérozygotes, c'est seulement à l'âge de 15 mois qu'apparaît un déficit d'apprentissage. Néanmoins, on voit apparaître à 6 mois déjà une labilité émotionnelle qui ne devient pathologique qu'à partir de 15 mois.

L'administration d'un traitement anti-TNF aux APP hétérozygotes n'a pas permis d'améliorer leur performance mais atténue la labilité émotionnelle caractérisée par les comportements stéréotypés. Enfin, la quantité des dépôts de plaques est environ trois fois moins élevée chez ces hétérozygotes de 16 mois que chez les APP homozygotes de 8 mois.

Chez les animaux APP hétérozygotes sans le récepteur p55 du TNF-alpha (APP/TNF-/-), l'apprentissage de lieu est altéré dès l'âge de 6 mois, ce qui suggère que la disparition de ce récepteur n'a pas diminué le développement pathologique mais module l'évolution du comportement avec l'âge. Il semble donc que le blocage de l'expression de TNF chez des souris APP amplifie la réduction des capacités cognitives chez les jeunes adultes mais permette d'éviter l'apparition de comportements stéréotypés, ce qui expliquerait l'absence paradoxale de déclin cognitif lorsque ces animaux sont plus âgés. Enfin, le pourcentage de plaques amyloïdes a été trouvé deux fois plus élevés pour les KO TNF APP hétérozygotes de 15 mois que chez des APP hétérozygotes du même âge (APP+/-PBS).

Enfin, les animaux APP hétérozygotes surexprimant le TNF-alpha (APP/TNF+/+) ne survivent que si on leur administre un traitement anti-TNF chronique. Ces animaux ont un déficit d'apprentissage. Un traitement anti-inflammatoire prolongé n'améliore pas la capacité cognitive mais permet à la fois d'éviter l'apparition des troubles comportementaux et de réduire à des valeurs négligeables la concentration des plaques amyloïdes.

Grâce aux observations complémentaires des troubles du comportement, il a été possible de déceler des traces d'amélioration thérapeutique des traitements effectués. Toutefois cette amélioration ne semble pas spécifiquement cognitive, mais bien plutôt atténuer les troubles comportementaux qui contribuent pourtant lourdement au handicap des patients atteints de MA.

Cognitive and emotional deficits and self defeating behavior in conduct disordered adolescents

¹BOLOGNINI M., ²Stéphan P., ²Weinguni P., ²Suter M., ²Romailer M., ²Jubin A., ²Plancherel B., ²Halfon O.,

SUPEA Research Unit CH-Lausanne Switzerland¹, SUPEA²,

The main objective of the present project* is to examine differential patterns of neuropsychological functioning within a sample of delinquent and substance use adolescents. Biological theory and research suggest that neurological and cognitive dysfunction play a role in the outcome of conduct disorders (CD) and/or substance abuse (SUD). Therefore general cognitive abilities (IQ), executive cognitive functioning (ECF), constructive thinking (CT) and alexithymia will be taken into account.

The target population will include three different groups of adolescents aged 13-18 years: 50 adolescents with conduct disorders without substance use (CD), 50 adolescents with conduct disorders using substances (CD+SUD) and 50 adolescents using substances but without conduct disorders (SUD).

The main hypotheses of this research are that adolescents with CD will suffer from cognitive deficits at the level of ECF, CT, and alexithymia more than in their general cognitive function. As self-defeating behavior cannot be exclusively explained by cognitive deficits, we expect impulsivity and alexithymia to be explaining predictors. Finally, alexithymia and depression would be a risk factor for CD subjects to acquire SUD as well as a more important predicting factor than ECF for conduct disorder.

The investigation method chosen includes a face-to-face interview, computer-administered tests and self-reports.

Referring to the expected results, the present project aims to bring answers to the question of the relationship between emotions and cognition in behavioral disturbances. Many research projects have already investigated the impact of cognitive particularities on substance use and conduct disorders as well as alexithymia and impulsivity in these areas. However, to our knowledge, there is no study assessing the relationship between deficits in the emotion area (alexithymia) and cognition (ECF).

Prevention experts have argued that efforts to prevent violence and substance abuse should be combined because the risk factors for violence overlap those for substance abuse. Our clinician activity shows that when co-morbidity is present adolescents withdraw in repeated defeating behavior which are particularly dangerous for their development. Taking into account the relation between emotion and cognition in these pathologies is doubtless an issue to the present therapeutic impasse provoked by these behavioral disturbances.

* Research financed by the Swiss National Science Foundation, n° 3200B0-109827, 2005-2007.

Autophagic cell death and transient focal ischemia in neonatal rats

¹PUYAL j., ¹Vaslin A., ¹Waechter V., ¹Mottier V., ¹Clarke P.,

*DBCM*¹,

Autophagy, a mechanism whereby eukaryotic cells degrade parts of their own cytoplasm and organelles, is a normal physiological process active in homeostasis and atrophy. Although autophagy is a normal physiological process, autophagic cell death, or type II cell death, has been reported in neurons during normal development and in neurodegenerative pathologies Huntington's, Parkinson's and Alzheimer's diseases. The mechanisms leading to delayed cell death after hypoxic-ischemic injury are known to involve apoptosis and necrosis, but the role of autophagic cell death in the ischemic area is unclear. The aim of this study was to investigate if autophagic cell death occurs after hypoxic-ischemic injury in a transient focal ischemia model of neonatal rat. Twelve day-old Sprague-Dawley rat pups underwent permanent left middle cerebral artery occlusion (MCAO) in association with 1.5 h occlusion of the left common carotid artery. Evolution of the brain infarction was studied from 0 h to 14 days in cresyl violet-stained coronal sections. Autophagic cell death is being investigated using acid phosphatase histochemistry, immunocytochemistry and Western blots against several endocytic (EEA1, Rab5) and lysosomal (cathepsin D, LAMP1) markers and electron microscopy. The first results showed that many neurons were highly reactive to acid phosphatase histochemistry in the ischemic area from 5 h following MCAO. By using immunocytochemistry, we showed that neurons in the ischemic area were immunoreactive for EEA1 and LAMP1 from 5 h to 48 h post-ischemia. Electron microscopy revealed numerous large electron-dense membranous vacuoles or autophagosomes. In conclusion, our results suggest that neuronal death following cerebral ischemia involves an autophagic pathway.

Vieillesse : une adaptation optimale?

¹PREISSMANN D., ²Grandchamp N., ³Schenk F.,

*Département de Physiologie, Institut de Psychologie, Center of Psychiatric Neurosciences¹,
Dep. Physiologie, Center of Psychiatric Neurosciences², Dep. Physiologie, Inst. Psychologie, Center
of Psychiatric Neurosciences³,*

Le vieillissement est majoritairement considéré comme un déclin cognitif généralisé car la plupart des études comportementales humaines et animales mettent en évidence une diminution des capacités cognitives. Cependant, nous proposons de modifier cette perspective par une description du vieillissement qui éclaire les ajustements adaptatifs tout autant que les déclin.

Dans cette étude, nous avons cherché à savoir si des rats âgés subissaient passivement une diminution de capacités ou si les différences comportementales, observées par rapport à des adultes, seraient dues à des changements de stratégies résultant de tentatives d'adaptation. Ainsi des rats adultes (6-9 mois) ont été comparés à des rats sénescents (24 mois) dans 2 tâches spatiales différentes : le bassin de Morris et le labyrinthe radial à 8 bras.

Les expériences faites dans le bassin ont montré que dans nos conditions, les capacités de rétention à court et moyen terme (jusqu'à 3 jours) d'une position spatiale ne sont pas affectées par le vieillissement. Cependant, les rats âgés semblent souffrir d'un déficit spécifique lorsque de longs délais (15 jours) de rétention sont imposés. Ce déficit n'apparaît qu'à un âge avancé car des rats âgés de 15 mois sont encore en mesure de retenir cette information. Cependant à efficacité équivalente, les stratégies des rats âgés semblent différentes de celles des adultes. Plus que les adultes, les rats âgés étaient facilement détournés dans leur trajectoire par la présence d'un indice remarquable dans le bassin. Ainsi le vieillissement semble s'accompagner d'un changement dans le poids relatif accordé aux indices saillants.

Dans une procédure particulière du labyrinthe radial où seulement 4 bras sur 8 étaient appâtés (chaque bras portant en outre une marque olfactive spécifique), on n'enregistre pas une augmentation des erreurs totales chez les sujets les plus âgés. De manière prévisible, ceux-ci retournent plus souvent sur leurs traces (erreurs de mémoire de travail), mais ils sont plus performants que les adultes à sélectionner précocement les 4 bras renforcés. Cette efficacité ne semble pas dépendre de la modalité (visuelle et/ou olfactive) utilisée pour s'orienter.

Dans l'ensemble, ces résultats indiquent que le vieillissement ne serait pas uniquement synonyme de diminution des capacités cognitives mais plutôt d'une adaptation aux contraintes biologiques provoquées par le vieillissement. Cette adaptation permettrait notamment de maintenir une bonne performance dans certaines tâches par des stratégies différentes et un changement de priorité. Finalement, il nous semble que cet éclairage du vieillissement rend plus nette la limite entre le normal et le pathologique et permet d'éviter de « pathologiser » le vieillissement de manière systématique.

DYSREGULATION OF GLUTATHIONE METABOLISM: A RISK FACTOR FOR SCHIZOPHRENIA

¹GYSIN R., ²Tosic M., ²Deppen P., ²Cuénod M., ²Do K.,

Département Universitaire de Psychiatrie-CHUV/Centre de Neurosciences Psychiatriques¹, Centre for Research in Psychiatric Neuroscience, CHUV²,

Schizophrenia is a complex multi-factorial psychiatric brain disorder. It affects individuals at the centre of their personality and concerns about 1% of the world population. Both environmental and genetic factors are implicated in the vulnerability to develop this disease. Previous studies showed reduced levels of glutathione (GSH), the main non protein cellular redox regulator, both in cerebrospinal fluid and prefrontal cortex of schizophrenia patients (Do et al. 2000). In case-control association studies for candidate genes of GSH metabolism we found a strong association between schizophrenia and single nucleotide polymorphisms in the GSH key synthesizing enzyme glutamate-cysteine-ligase (GCL) modifier subunit (GCLM) gene (Tosic et al. submitted). In this study we investigated if these genetic anomalies led to functional consequences at the protein expression, as well as at the enzyme activity levels. Since GSH is ubiquitously present in cells, these parameters of the GCL regulation were determined in fibroblasts derived from skin biopsies. Moreover, in the GCLM knock-out mouse model it was observed that the lack of GCLM led to an increased sensitivity to oxidative stress (Yang et al., 2002). We thus compared between patients and controls the functional parameters at baseline, as well as under oxidative stress induced conditions by treating cells with tert-butylhydroquinone, a substance known to produce reactive oxygen species. In the presented study we observed that compared to controls schizophrenia patients had a reduced GCL activity under oxidative stress conditions, a reduced protein expression of GCLC under baseline, as well as under oxidative stress conditions, and an uncoupling of GCLM and GCLC protein expression in response to oxidative stress. Finally, in the group of patients we observed an inverse correlation between the levels of GSH increase under oxidative stress conditions and the severity of positive symptoms of the disease.

Replenishment of glutathione levels in neurons and astrocytes models of schizophrenia

LAVOIE S., Steullet P., Cuénod M., Do K.,

Centre de Neurosciences Psychiatriques Lausanne

In schizophrenia patients, a decrease in glutathione levels ([GSH]) in cerebrospinal fluid and prefrontal cortex was observed. A decrease in the expression of the gene coding for the modulatory subunit of g-glutamyl-cysteine ligase (GCL), the limiting enzyme of GSH synthesis, was also observed. In addition, a polymorphism of this gene is significantly associated with the illness. As a major cellular non-protein redox regulator, GSH plays an important role in protecting cells against oxidative stress and in redox modulation of the function of some proteins. In rat models with a GSH deficit, morphological and electrophysiological anomalies analogous to those of patients were observed, such as a decrease in spines number in prefrontal cortex and an alteration of NMDA receptor-mediated responses. We aim to find substances that could re-establish normal physiological [GSH] in cortical cells with compromised GSH synthesis and to study the underlying mechanisms.

In cultured neurons and astrocytes depleted in GSH with BSO (L-buthionine-(S,R)-sulfoximine), an inhibitor of GCL, a membrane permeable analog of GSH (GSH-ethyl-ester or GSHEE) succeeded in replenishing cellular [GSH]. GSHEE also abolished dopamine-induced depression of NMDA-dependent calcium response observed in BSO-treated neurons. Furthermore, g-glutamyl-cysteine-ethyl-ester (GCEE), a membrane permeable analog of the end product of GCL, increased [GSH] mostly in astrocytes. These results show that GSHEE and GCEE can re-establish normal [GSH] in brain cells by bypassing the first limiting step of GSH synthesis, which is mediated by GCL.

In a search for other substances that could boost GSH synthesis in non BSO-treated cells, curcumin was found to be the most efficient of the compounds tested. It increased [GSH] by about 50% and 100% in neurons and astrocytes, respectively. Low concentrations of quercetin (5 uM) and tert-butylhydroquinone (tBHQ; 10-20 uM) induced an increase in [GSH] of about 20% in neurons, while a high concentration (100 uM) decreased [GSH] and led to cell death. By contrast, in astrocytes, low concentrations of quercetin and tBHQ had no effect, while a high concentration increased [GSH] by more than 50%. These results indicate that neurons and astrocytes are not responding similarly to some of the tested substances, suggesting that the mechanisms regulating GSH synthesis and the susceptibility to oxidative stress might differ in the two cell types. The resistance of astrocytes to oxidative stress is presumably due in part to the ability of these cells to maintain high [GSH].

Stress response and patterns of Fos expression in the brain of 129X1 mice spontaneously exploring or withdrawing from a novel environment

¹MAGARA F., Steimer T., Marcon C., Magistretti P.,

Centre Neurosciences Psychiatriques¹,

In mice of the strain 129X1/SvJ, we observed a considerable individual variability in the coping attitude (exploration vs withdrawal) towards novel environments, with up to 50% of the mice refraining to move in response to changes of housing or testing environment. Provided that these coping attitudes were found to be consistent upon repeated testing, we inspected patterns of cerebral activation in explorer and non-explorer mice by means of FOS protein immunohistochemistry.

In addition, we investigated stress response in mice spontaneously entering the novel environment, as compared to those forced to enter, or left in visual contact with it.

Albeit preliminary, results indicate that

- 1) Withdrawn mice show reduced activation of hippocampal and frontal cortical fields, suggesting the involvement of these brain regions in motivational and exploratory drive
- 2) Elevation was higher for mice forced to enter, as well as for mice refusing to enter the novel environment, as compared to those spontaneously exploring it. This suggests that inhibited coping attitude is associated to a higher stress response.

Enhanced endocytosis in excitotoxic cell death

¹VASLIN A., ¹Puyal J., ¹Borsello T., ¹Clarke P.,

*DBCM*¹,

Endocytosis has been shown to be enhanced in some cases of neuronal death such as in NMDA-treated hippocampal slices or in kainate-treated retinal amacrine cells. This new phenomenon may be important for understanding the causation of cell death in excitotoxicity.

The enhanced endocytosis was shown in rats that received an icv injection of 4.4 kD FITC-dextran before a transient focal cerebral ischemia. They were sacrificed 24 h later, when there was strong neuronal endocytosis restricted to the ischemic zone only. We have therefore begun to analyze the underlying mechanisms in rat cortical neuronal cultures.

Enhanced endocytosis of FITC-dextran (4.4kD) was observed in NMDA-treated neurons, as measured by fluorescence spectrometry. This endocytosis increased with the dose of NMDA and the duration of NMDA treatment. In order to study specifically the endocytotic mechanism, we determined a combination of concentration and timing that enhances endocytosis but with minimal cell death. Moreover, we confirmed that the internalization of dextran was due to endocytosis by the fact that the dextran-labelling did not occur at 4°C. Use of commercially available inhibitors of different types of endocytosis revealed two components of dextran internalization. One occurred constitutively and was blocked by inhibitors of classical fluid-phase dynamin-independent endocytosis. The other component was induced by NMDA, insensitive to fluid-phase inhibitors, but sensitive to inhibitors of dynamin-mediated endocytosis such as sucrose and also to the JNK pathway inhibitor D-JNKI1, a powerful neuroprotectant.

The induced endocytosis may provide a means for delivering neuroprotective agents specifically into the cells that need them.

The frontal cortex may be the site of synaptic and cytoskeleton reorganization with aging and Alzheimer's disease

¹LEUBA G., ³Carnal B., ³Vernay A., ⁴Kraftsik R., ⁵Riederer B.,

*CNP & SUPAA, Département de Psychiatrie¹, SUPAA, Département de Psychiatrie, CHUV³,
Département de Biologie cellulaire et de Morphologie, UNIL⁴, Département de Biologie cellulaire et
de Morphologie, UNIL, & CNP, Département de Psychiatrie, CHUV⁵,*

In addition to memory and associative cognitive disorders, patients with Alzheimer's disease (AD) often show executive and attention deficits which may appear rather early - or in the course of the disease - and affect cognitive as well as daily living activities. As modifications of cytoskeletal proteins may affect synaptic and dendritic plasticity at a number of levels, we compared the variations in neuropile intensity of several synaptic and cytoskeletal markers in frontal area 9 of 4 AD and 4 control patients, and evaluated them also with regard to beta-amyloid deposits. All measurements were performed using the KS400 (Zeiss) image analysis system.

While the distribution of the presynaptic marker synaptophysin, linking to small synaptic vesicles, appeared unchanged in AD patients, that of alpha-synuclein, another presynaptic protein and component of Lewy bodies - was significantly increased, as well as that of MAP2, a cytoskeletal protein associated to the somato-dendritic part of neurons and to spines. GAP43, a growth-associated protein synthesized in neurons and primarily localized to axons, was on the contrary significantly decreased. These results may indicate an increased remodeling activity in dendrites and spines, as well as a decreased axonal activity and/or connectivity in AD frontal cortex. The latter point was further confirmed by a significant decrease in the staining of non-phosphorylated neurofilament protein with the SMI32 antibody, representing normal cells and dendrites. On the contrary, the SMI31 antibody, reacting with a pathologically phosphorylated epitope in axons, was increased in AD. Phosphorylated protein tau, as detected with the AD2 antibody, was increased as well. In 2 severe AD cases, SMI31 and AD2 stained also a number of neuronal cell bodies, not reactive in control samples, and correlating with neurofibrillary tangles labeled by the Gallyas silver impregnation. The amount of beta-amyloid deposits was significantly higher in AD than in controls, but without a strong correlation with the phosphorylated marker antibodies. A possible influence of beta-amyloid on the reorganization of dendritic and axonal connectivity has to be further studied.

Effects of Hypoxia-Ichemia on the c-Jun NH3-terminal kinase pathway (JNK) : studies in a neonatal rat model

¹TRUTTMANN A., ²Ginet V., ³Clarke P., ²Magnin G.,

Néonatalogie, DMCP¹, NAT/DMCP², IBCM/Unil Lausanne³,

Purpose: Perinatal cerebral asphyxia is a major cause of mortality and severe long term neurological disabilities in infants. C-Jun NH2-terminal kinase (JNK) pathway has been shown to mediate cell death following stroke, and a strong neuroprotection was obtained through its inhibition in several models of cerebral ischemia. The purpose of our studies was to investigate the expression and activation of JNK isoforms (JNK1, JNK2 and JNK3) in a hypoxic-ischemic (Vanucci-Rice model) animal model.

Methods: 7-day-old Sprague-Dawley rats underwent an unilateral common carotid artery ligation followed by 2 hours exposure to 8.5 % oxygen in a chamber. Cresyl violet staining was used to determine the extent of the brain lesion. Expression and activation of JNK isoforms were studied at different time points by immunohistochemistry, Western blotting and immunoprecipitation with antibodies against JNK1, JNK2/3 and P-JNK.

Results: 2 hours of hypoxia were necessary to obtain a consistent lesion size with low mortality. Brain damage was generally confined to the hemisphere ipsilateral to the ligation and affected the cerebral cortex, hippocampus, striatum and thalamus. Interestingly, JNK activation in cerebral cortex (phosphorylation, P-JNK) was decreased as early as 30 minutes after hypoxia corresponding mainly in a decrease of P-JNK1. Furthermore expression of JNK1 and the 54 kD form of JNK2/3 decreased after hypoxia whereas the 46 kD form of JNK2/3 slightly increased.

Conclusion: It appears to be essential to distinguish JNK isoforms to understand cell death response in hypoxia-ischemia. In fact JNK2 or 3 would be more involved in brain damage than JNK1 whose activation and expression decreased following hypoxia-ischemia. JNK pathway will be further investigated in striatum, hippocampus and thalamus to determine potential differences in regional JNK response to hypoxia-ischemia.

Transducers of regulated CREB activity (TORCs) act as new calcium- and cAMP-sensitive coincidence detector in the central nervous system.

¹Kovács K., ²Halfon O., ³Magistretti P., ¹Cardinaux J.,

Centre de Neurosciences Psychiatriques, Service Universitaire de Psychiatrie de l'Enfant et de l'Adolescent, Département de Psychiatrie - CHUV¹, Service Universitaire de Psychiatrie de l'Enfant et de l'Adolescent, Département de Psychiatrie - CHUV², Centre de Neurosciences Psychiatriques, Département de Psychiatrie - CHUV, Brain and Mind Institute, EPFL³,

One of the key features of memory processes is to link two different input signals by association and to preserve this coupling at the level of synaptic connections. In this study we report that TORCs function as coincidence detectors in neurons sensing calcium influx and simultaneous adenylate cyclase activation. TORCs are newly discovered CREB coactivators increasing transcription independently of CREB Ser133 phosphorylation. Recently it has been shown in pancreatic cells that TORC2 translocates to the nucleus in a dephosphorylation-dependent manner, Ca²⁺ activating the phosphatase calcineurin and cAMP inhibiting the kinase responsible for TORC2 phosphorylation.

Here we show that TORC1 and TORC2 are present in adult mouse brain, as well as in cultures of cortical, hippocampal and striatal neurons. TORC1 and TORC2 readily translocate to the nucleus of cortical neurons upon stimulation with KCl and forskolin (FSK). Functionally, this nuclear translocation results in the synergistic activation of a CRE-reporter gene transfected into mouse cortical neurons. Consistent with the involvement of TORCs, calcineurin inhibitors abolish this effect without affecting CREB Ser133 phosphorylation. Expression of a TORC dominant negative protein consisting of the first 147 amino acids of TORC1 fused to GFP drastically decreases the Ca²⁺- and cAMP-mediated enhancement of CREB-dependent transcription. Moreover, CREB mutants unable to interact with TORCs do not support the synergism between Ca²⁺ and cAMP pathways. To definitely prove the involvement of TORCs, we show that shRNAs precluding the expression of endogenous TORC1 and TORC2 completely abolish this synergism.

Taken together, these data constitute a compelling body of evidence that in neurons Ca²⁺ and cAMP synergistically activate CREB-mediated transcription by recruiting TORCs to the nucleus. In addition, we show that TORCs can function as dopamine and glutamate coincidence detectors, which is highly relevant for the drug addiction field. Finally, we show that BDNF, as a CREB target gene, is strongly induced by Ca²⁺ and cAMP in a TORC-dependent manner. In conclusion, our data highlight an important mechanism relevant to long-term gene expression regulation in the context of synaptic plasticity, memory and drug addiction.

This work is supported by Swiss National Research Foundation grant n° 3100A0-105773.

Segregation and heritability of inhibited and non-inhibited temperamental traits in the mouse strain 129X1/SvJ

¹MAGARA F., Petit J., Marcon C., Magistretti P.,

Centre Neurosciences Psychiatriques¹,

The mouse strain 129X1/SvJ have been widely studied because of its use as embryonic stem cell donor in gene targeting experiments. Mice of this strain have often been reported to show passive coping in a variety of behavioral paradigms. It has been proposed that their poor proficiency is caused by anxiety rather than to learning or motivational deficits (e.g.: Dockstadter et al., J Neurosci. 2001)

In a preliminary series of experiments performed on 90-days old male 129X1 mice, we observed that a number of animals refrained to move upon their first exposure to a novel testing environment (a Lât maze and/or a light/dark box). We exposed therefore the animals to a free exploration paradigm (Misslin & Ropartz, Behav Proc 1981), and observed that 16 out of 38 mice refrained at all to enter novel homecage compartments in the time-lapse of 10 minutes from door opening. Pre-session activity in the familiar compartments was not different between explorers and non-explorer animals, suggesting that failure to enter the novel compartments was not due to drowsiness or neglect. Interestingly, individual mice show very low habituation to the free exploratory task, as their exploratory or passive coping attitude is largely consistent upon multiple exposures. Breeding to each other animals selected for high or low exploratory drive resulted in the generation of two recombinant substrains characterized by a considerable difference in locomotor attitudes, especially evident on first exposure to virtually any arena. When tested on an elevated plus maze, a mild correlation between open arm entries and novel compartments entries could only be found for non-neophobic animals, whereas animals refraining to explore the novel cage compartments did not necessarily show agoraphobia on the plus maze.

Taken together, the results show that:

- 1) locomotion in a novel environment is a consistent trait in the behavioral profile of individual mice, a useful model of a the human inhibited temperamental trait.
- 2) neophobia/trait anxiety and agoraphobia/state anxiety, (as assessed on the elevated plus maze) are unrelated forms of anxiety, as also recognized by the most recent classification of human anxiety disorders. Work is ongoing to clarify the genetic and extragenetic components of the inheritability of trait anxiety.
- 3)in an inbred strain, is possible to produce sublimes characterized by different locomotor drive. This opens perspectives for the study of individuality at the behavioral level.

Troubles du comportement dans l'atrophie corticale postérieure

¹Brioschi A., ¹Joray S., ¹Carota A., ²Borruat F., ³Bogouslavsky J., ¹Ghika J.,

Consultation de la Mémoire, Service de Neurologie, CHUV¹, Hôpital Ophtalmique Jules-Gonin, Lausanne², Service de Neurologie, CHUV³,

Introduction : Décrite pour la première fois par Frank Benson en 1988, l'atrophie corticale postérieure (ACP) ou « syndrome de Benson » est une forme rare de démence dégénérative. L'ACP se distingue de la maladie d'Alzheimer (MA) par la présence précoce, et prépondérante au cours de l'évolution, d'un dysfonctionnement visuel, alors que les capacités mnésiques sont relativement préservées. Les manifestations cognitives de l'ACP sont bien caractérisées, avec notamment une alexie, une agnosie visuelle et une agnosie topographique. De plus, un syndrome de Balint (apraxie optique, ataxie optique, asimultagnosie), un syndrome de Gerstmann (acalculie, agraphie, confusion gauche-droite, agnosie digitale), des troubles praxiques, ainsi qu'une aphasie transcorticale sensorielle peuvent s'ajouter au tableau. Dans le cadre de la MA, les déficits cognitifs s'accompagnent d'importants changements comportementaux bien décrits. En revanche, des symptômes neuropsychiatriques ne sont généralement pas rapportés dans l'ACP.

Objectifs : Objectiver et décrire les troubles du comportement des patients avec ACP évalués à notre Consultation Mémoire ambulatoire.

Méthode : Onze patients, droitiers, qui présentent un diagnostic clinique d'ACP. Tous ont bénéficié d'une imagerie fonctionnelle au fluorine-18 FDG-PET qui confirme un hypométabolisme des régions cérébrales postérieures. Un examen neuropsychologique détaillé incluant des échelles globales (MMSE, Mattis DRS) a été pratiqué. Un questionnaire d'évaluation des troubles psychiatriques et comportementaux, le « Neuropsychiatric Inventory » (NPI), a été administré au conjoint. Le NPI évalue la sévérité et la fréquence de dix symptômes comportementaux rencontrés dans la démence.

Résultats : Les patients sont âgés en moyenne de 63.7 ± 6.9 ans, répartis en 6 hommes et 5 femmes. La sévérité de la démence est modérée (CDR=2) à sévère (CDR=3). Le tableau neuropsychologique met en évidence dans tous les cas des difficultés visuelles et praxiques sévères. La mémoire épisodique verbale est en général légèrement à modérément déficitaire. En revanche, le raisonnement, la mémoire sémantique, les fonctions exécutives et l'attention sont préservés ou faiblement altérés. Sur la base du NPI, tous les patients présentent des troubles du comportement. Le score total du NPI est élevé et montre une grande variabilité (moyenne 26.1 ± 27.1). L'anxiété, l'apathie, l'irritabilité et l'agitation sont fréquentes dans cette population. Par contre, les hallucinations, l'euphorie et la désinhibition apparaissent en faible proportion.

Conclusion : Les troubles neuropsychiatriques sont fréquents dans notre population d'ACP de stade modéré à sévère, puisqu'ils affectent tous les patients. Les troubles du comportement chez des patients présentant une ACP apparaissent toutefois moins importants que ceux rencontrés dans la MA. Ces résultats pourraient s'expliquer par une atteinte tardive des régions corticales limbiques.

Modulation of neurite outgrowth by serotonin 1A receptor in hippocampal neuron culture

¹ABAZA A., ¹BÜRGI R., ²HEN R., ¹HORNUNG J.,

Department of Cellular Biology and Morphology, University of Lausanne¹, Center for Neurobiology and Behavior, Columbia University²,

Early expression of serotonin (5-HT) during brain development suggests that 5-HT is a critical factor in modulating neuronal differentiation with potential consequences in adult brain functions. Mice lacking the 5-HT_{1A} receptor (5-HT_{1A}R) during the early postnatal development generate an anxiety-like behavior, associated with increased growth of hippocampal CA1 pyramidal neuron dendrites. Using dissociated hippocampal culture, we showed that neurons respond to 5-HT stimulation by increased neurite elongation and branching during their early phase of neuritic growth. The growth of the major process is stimulated via the activation of the 5-HT_{1A} receptor whereas the minor processes growth is stimulated by the activation of multiple 5-HT receptors. To test which are the other 5HT receptors responsible for the growth of the minor processes and to identify the way of transduction of the signal after 5HT_{1A} stimulation, we dissociated hippocampal neurons from embryonic day 16 wild type mice, cultured in defined medium supplemented or not with 5-HT_{1A}; 5-HT_{2A}, C; 5-HT₄ receptor agonist; adenylyl cyclase agonist; NMDA receptors antagonists. Cell morphology was visualized by cytoskeleton labelling. We study hippocampal neurons at stage III of differentiation, when the axonal process is morphologically distinguishable from dendrites. Stimulation of WT neurons with 5-HT_{2A},C receptor agonist stimulates the growth of the minor processes by increasing their length and branching whereas 5-HT₄ receptor agonist has not effect. Stimulation of WT neurons with NMDA receptors antagonist produced a similar effect than stimulation of the 5-HT_{1A} receptor. In addition increasing cAMP induced the developpement of the minor processes in hippocampal neurons.

Support: SFN 31-62113.00

Dopamine receptors modulate differentially the neurite outgrowth and the molecular organization of growth cones in cortical neuronal cultures

¹PETCHANIKOW C., ¹ZALILA H., ¹MONACHON C., ¹NICOLAS D., ¹HORNUNG J.,

*DBCM*¹,

Dopamine (DA) has been shown to modulate the growth of dissociated cortical neurons by activation of two classes of receptors (D1-like and D2-like). The aim of the present study is to define the specific contribution of the D1 or the D2 receptors in the regulation of neurite outgrowth as well as their specific contribution to the molecular organization of the growth cones in cultured cortical neurons. Cortical neurons of embryonic mice were cultured using defined medium. Cultures were chronically exposed to DA (5 μ M), or agonist/antagonists (10 μ M) for D1 (SKF-38392/SCH 23390) or D2 (quinpirole/raclopride) receptors for the whole duration of the experiment (48 hours). The morphology of the neurons was visualized by tubulin immunostaining and specific markers of growth cone organization (actin and tyrosinated tubulin) were visualized by immunofluorescence. Pictures were taken using light microscopy (cell morphology) and confocal microscopy (cytoskeletal proteins) and morphometric analysis done with Neurolucida software followed by quantitative analysis. As compared to control conditions, DA-treated cells showed an increase in the branching and a decrease in the length of their neurites as well as large and conspicuous lamellipodia and filopodia. Those characteristics were also observed in SKF-treated cells with an increase in length of filopodia. Quinpirole-treated cells showed an opposite morphology with a reduced branching and an increased length of the neurites associated with size-reduced growth cones. Our data show two opposite effects: an increase of the growth cone activity associated with an increase in branching and reduction in maximal length of the neurites (D1 receptor activation) and a reduction in branching and increased growth rate of the axon (D2 receptor activation). Although, little is known on the mechanism leading to such changes, this opposite effects could be linked to opposite action of both receptors on the level of cAMP or on the activity of the DARPP32 protein. Further analyses of the dynamic morphological changes of the neurites in response to dopamine receptor activation are warranted. Support: SNF 31-62113.00 to JPH.

Schizophrenia connectivity investigation by Tractography of DTI

¹CAMMOUN L., ²Deppen P., ³Bovet P., ²Cuénod M., ⁴Hagmann P., ²Do K.,
⁵Thiran J.,

EPFL¹, Center for Psychiatric Neuroscience, Department of Psychiatry, Lausanne University Hospital (CHUV)², Department of Psychiatry, Lausanne University Hospital (CHUV)³, Department of Radiology, University Hospital, Lausanne, Switzerland⁴, Signal Processing Institute, Swiss Federal Institute of Technology, Lausanne, Switzerland⁵,

Introduction

Multiple lines of evidence suggest that schizophrenia is associated with abnormalities in neural circuitry and impaired *structural connectivity*. Although largely investigated by imaging studies, very few results have been published on in-vivo image-based connectivity investigations, and those published report contradictory findings. In this project, we propose to conduct a group study to evaluate the differences in structural connectivity between schizophrenia patient and control subjects using Diffusion MRI. The proposed methodology is based on *Tractography* method, a technique allowing inferring the main neural fiber tracks from Diffusion MRI data. The main studied brain bundle is the thalamo-frontal one, proposed to be involved in schizophrenia.

Materials and methods

We investigated 9 schizophrenic patients as assessed by the DIGS (Diagnostic Interview for genetic studies, DSM IV criteria) and 9 healthy controls. We have got from each volunteer a DT-MRI dataset (3 T, b = 1000 s/mm²), and a high resolution anatomic T1.

In order to compare the thalamo-prefrontal connections between schizophrenic and control populations, for each subject, a whole brain tractography is first simulated by the random-walk algorithm [1], the frontal lobe and the thalamus are extracted to define the ROIs and the left and right thalamo-frontal bundles are therefore selected. The frontal lobe is currently defined by Talairach atlas and the thalamus is segmented using the coupled region based level sets method in DT_MRI [2].

In order to see an eventual correlation with the investigated connections, the cognitive functions, which are reported to depend on the integrity of prefrontal and thalamo-prefrontal circuits, were assessed, using a battery of neuropsychological tests: Tour de Hanoi, memory tests of verbal and non verbal learning, different working memory paradigms, Finger Tapping Test, Reaction time as well as Wechsler Intelligence Scale.

Results

In a pilot study (patients : n=9; controls: n=9), the methodology applied is feasible and give results in correct range. In the schizophrenic sample the left thalamo-frontal fibers number appeared to be statistically significantly bigger than the right one and this is not the case in the control samples. However, no significant change in the number of the thalamo-frontal fibers was observed.

Interestingly, an inverse correlation between the number of thalamo-frontal fibers and the performance in of Tour de Hanoi, a test of planification reported to be impaired in schizophrenia, was observed in the patients but not in control subjects (Pearson

correlation $r=0.75$, $p<0.05$): the least number of fibers corresponded to the worst performance of the test.

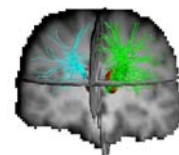
Conclusion:

This pilot study shows first the feasibility of investigating the schizophrenia connectivity by the mean of DTI. The assymetry in the thalamo-frontal bundle observed among the schizophrenic subjects and not among the controls is also coherent with previous works showing abnormalities especially in the left hemisphere. The observed inverse

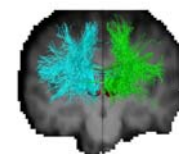
correlation between the number of fibers and an executive function is consistent with the proposed impaired connectivity in schizophrenia

References :

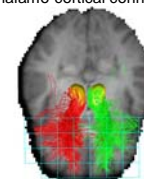
[1] Hagmann P, et all. Neuroimage. 19:545-54, 2003,[2] Jonason et all ISMRM 2005.



Example of Thalamo-cortical connections in schizophrenic patient



Example of Thalamo-cortical connections in control



Example of Thalamo-cortical connections in control Talairach boxes are in blue, and thalamus in yellow

Synaptic changes in the lateral amygdala as an underlying factor for the elevated rate of anxiety disorders in an animal model for patients with Temporal Lobe Epilepsy.

¹PICKENHAGEN A., ²Pralong E., ²Debatisse D., ²Villemure J., ¹Magistretti P., ¹Stoop R.,

Centre de Neurosciences Psychiatriques¹, Unit of Neurosurgery, CHUV²,

Epilepsy is a chronic disorder characterized by spontaneously recurrent seizures. Its most prevalent form, temporal lobe epilepsy (TLE), often originates in the hippocampus and/or amygdala and is frequently associated with profound fear and anxiety disorders. Recently, it has been shown that fear conditioned learning potentiates synaptic transmission in the lateral amygdala of rodents. Furthermore, we have found that hippocampal epileptic activity can also cause potentiation of synaptic transmission between CA3 pyramidal cells. From these findings we hypothesize that TLE causes fear and anxiety disorders through long-lasting changes in synaptic transmission in the lateral amygdala (LA). To test our hypothesis, we used a horizontal slice preparation of the rodent brain which includes the hippocampus and amygdala as well as preserved interconnections. Within this preparation we studied the spreading of epileptic bursts by means of c-fos expression as well as multiple extracellular and whole-cell patch-clamp recordings. We found spreading of epileptic activity between hippocampus, perirhinal cortex and lateral and basolateral amygdala with varying delay times in between burst-onsets. This suggests the existence of a number of different networks underlying the spreading of bursts. We also looked at the long term effects of this epileptic activity on cellular excitability and synaptic transmission in the LA, and found significant differences in the amplitudes of excitatory postsynaptic currents. Interestingly, the nature of these changes depended on the cell type from which the measurements were made. Thus, pyramidal cells with so-called "highly adapting spiking patterns" underwent a decrease in amplitude, while pyramidal cells with little adapting spiking patterns showed increases in amplitudes. We are now starting to compare these results with in vitro recordings from amygdala of human patients.

Neuropeptidergic modulation of brain stem projections from the central amygdala

¹VIVIANI D., ²Poisbeau P., ¹Stoop R.,

Centre de Neurosciences Psychiatriques¹, Université Louis Pasteur - Straasbourg²,

The emotional expression of anxiety and fear involves changes in a number of physiological parameters, among which heart rate, respiration, blood pressure and temperature.. These parameters are under the control of several brainstem nuclei that, in turn, are modulated by the central amygdala (CeA). The CeA expresses a large number of neuropeptide receptors and recently, we have shown how their activation can modulate these parameters in opposite way through a local inhibitory network. Clinical findings have shown that anxiety and fear responses in patients can be highly individual as they consist of a unique combination of changes in these physiological responses. We now hypothesize that these unique combinations result from endogenous differences in neuropeptidergic signaling at the level of the central amygdala. To test this, we are using a combined in vivo and in vitro approach on two rat strains with opposite anxiety phenotypes, the Roman High avoidance (RHA) and Roman Low Avoidance (RLA) rats. The in vivo part includes behavioral tests and online telemetry recordings of above mentioned parameters after neuropeptides injection in the CeA of freely moving rats. The in vitro part includes histological and electrophysiological techniques to study differences in receptor expression and neuropeptidergic modulation of cells in the CeA with brainstem projections identified by fluorescent retrograde tracing. The first electrophysiological results show an opposite modulation mediated by oxytocin and vasopressin on cells with identified projections to the periaqueductal grey, while other neuropeptides, such as CRF, galanin, DAGO, orexin and Neuropeptide S are currently being tested.

Effect of PPARs agonists in relation to oligodendrocyte maturation and during a demyelinating insult

Defaux, A., Zurich, M-G., Braissant, O., Honegger, P, Monnet-Tschudi, F.

Department of Physiology, University of Lausanne and Central Laboratory, CHUV, Lausanne.

Active demyelinating lesions in multiple sclerosis (MS) are surrounded by inflammatory foci. Physiological pathways have been discovered, which control the inflammatory process and are activated by an intense inflammatory response. The peroxisome proliferator-activated receptor (PPAR) transcription factors participate in these endogenous anti-inflammatory pathways. Besides their anti-inflammatory potential, PPARs are also involved in the maturation of oligodendrocytes, the myelin forming cells. These two properties suggest their usefulness for the protection against, or for a recovery from, a demyelinating event, such as observed in MS pathology. Among the three PPAR isoforms, PPAR- β is the most abundant in the brain. It was found in neurons and in astrocytes, and was reported to be strongly expressed in immature oligodendrocytes, and to play a role in their differentiation. The involvement of PPAR- β in oligodendrocyte maturation, its anti-inflammatory potential during antibody-mediated demyelination, and its supposed involvement in remyelination were studied in aggregating brain cell cultures, by the administration of a specific agonist of PPAR- β , GW501516. Based on measurements of 2',3'-cyclic nucleotide 3'-phosphohydrolase activity, it was found that GW 501516 applied at different maturational stages was toxic for immature oligodendrocytes and to some extent also for late differentiated oligodendrocytes, while it transiently stimulated myelinating oligodendrocytes. In order to test the role of PPAR- β in remyelination, GW501516 was applied 48h after antibody-mediated demyelination for one week. No effect on remyelination was found, but negative side effects on neurons, particularly on GABAergic neurons, were detected. To test the potential anti-inflammatory effect of the PPAR- β agonist, GW 501516 was applied either before or during the demyelinating treatment. No protective effect was found for oligodendrocytes 48 h after initiation of the demyelination, but again toxic effects on GABAergic neurons. Pioglitazone, an agonist of PPAR- γ , proved to be protective against demyelination when applied simultaneously with the demyelinating insult. Rosiglitazone, an agonist of the same family, but with a higher affinity for PPAR- γ than pioglitazone, did not confer protection against demyelination, but, it decreased the demyelination-induced upregulation of GFAP m-RNA, a marker of glial reactivity and indirect marker of brain inflammation.

These results show that the PPAR- β agonist promoted oligodendrocyte maturation transiently and during a narrow window of differentiation, while causing negative side effects on neurons which could interfere with myelination and/or remyelination. The distinct effects of the two PPAR- γ agonists suggest that they activate different molecular pathways, both in agreement with the presumed anti-inflammatory potential of these compounds.

MCV
Métabolisme et
Cardiovasculaire

Muscarinic Receptors Are Key Determinants in Developmental Origins of Pulmonary Endothelial Dysfunction

¹Peyter A., ¹Marino M., ¹Diaceri G., ²Moessinger A., ¹Muehlethaler V., ¹Tolsa J.,

Laboratoire de recherche en Néonatalogie¹, Pédiatrie/Division de Néonatalogie²,

Background: Perinatal adverse events are associated with the occurrence of chronic diseases in adulthood, such as cardiovascular diseases or diabetes. These diseases are characterized by a certain degree of endothelial dysfunction. Chronic pulmonary vascular diseases and abnormal pulmonary vasoreactivity in adulthood could be associated with a perinatal hypoxic insult. The muscarinic receptors to acetylcholine (ACh), an endothelium-dependent relaxing agent, and the endothelial nitric oxide synthase (eNOS) are determinants of the effects of ACh on vascular tone. In pulmonary arteries (PAs), the muscarinic receptor isoform M1 (M1AChR) is implicated in the vasoconstrictive effect of ACh, whereas the vasodilator effect of ACh is mediated by the muscarinic receptor isoform M3 (M3AChR).

Objectives: To determine long-lasting effects of perinatal hypoxia on the lung circulation, and to investigate mechanisms implicated in abnormal pulmonary vasoreactivity in adults born in hypoxia, with particular attention to endothelium-dependent and endothelium-independent relaxation.

Methods: Mice were exposed to hypoxia during the last 5 days of gestation and the first 5 days of life, and then bred in normoxia until adulthood. Adult mice were anesthetized, and closed chest measurements of Right Ventricular Pressure (RVP) were obtained. Isolated pulmonary artery reactivity, biochemical and molecular assays related to the nitric oxide/cyclic guanosine monophosphate (NO/cGMP) pathway were tested at adulthood.

Results: RVP measured in normoxia (21% O₂) was significantly higher in adult mice born in hypoxia (26.11 ± 0.19 mmHg) as compared to controls (24.95 ± 0.08 mmHg). Exposure to acute hypoxia (12% O₂) during hemodynamic measurements resulted in a significant increase of RVP in both groups, which was even significantly higher in animals born in hypoxia (29.58 ± 0.19 mmHg) than in controls (26.58 ± 0.08 mmHg). The maximal relaxation (E_{max}) induced by ACh in PAs of mice born in hypoxia was significantly decreased by about 25% as compared to controls (57.61 ± 4.74 % and 75.52 ± 4.67 %, respectively). In contrast, endothelium-independent relaxation induced by NO was similar in the perinatal hypoxia and control groups. ACh-induced relaxation was completely inhibited in the presence of 4-DAMP, a selective antagonist of the M3AChR or in the presence of nitro-L-arginine, an inhibitor of NOS. Pirenzepine, a preferential inhibitor of M1AChR, abolished the effects of perinatal hypoxia on ACh-induced relaxation, and M1AChR mRNA expression was increased in lungs and PAs of adult mice born in hypoxia as compared to controls (56.45 ± 14.61 % and 23.49 ± 4.73 %, respectively).

Summary: Transient perinatal hypoxic insult results in altered pulmonary circulation and permanent modifications of the NO/cGMP signaling pathway in the pulmonary vasculature, which could influence adult pulmonary vasoreactivity. The major alterations are found in the endothelium, with a predominant role for the M1AChR. This suggests that muscarinic receptors could be key determinants of "perinatal imprinting".

Lipid Rafts Play a Central Role in Regulating Leukocyte Rolling Under Flow Conditions.

¹ABBAL C., Lambelet M., Gerbex C., Bertaggia D., Martinez M., Arcaro A., Schapira M., Spertini O.,

*LCH*¹,

Selectins and their ligand P-selectin glycoprotein ligand-1 (PSGL-1) mediate leukocyte rolling along inflamed vessels. Cell rolling is modulated by selectin interactions with their ligands and by topographic requirements including L-selectin and PSGL-1 clustering on tips of leukocyte microvilli. Herein, we examined the involvement of membrane lipid rafts, which assemble signalling complexes, in regulating leukocyte rolling. Disruption of lipid rafts with cholesterol chelating agents depleted raft-associated PSGL-1 and L-selectin and strongly reduced leukocyte rolling on L-, P- and E-selectin. Cholesterol repletion reversed the inhibition of cell rolling. Importantly, leukocyte rolling on P-selectin induced the recruitment of the PSGL-1 associated src kinase Syk in lipid rafts. The inhibition of Syk activity or synthesis strongly inhibited leukocyte rolling on P-selectin whereas rolling on E-selectin or PSGL-1 was not affected. These observations indicate that leukocyte rolling on selectins is dependent on lipid raft integrity and that Syk critically participates to the regulation of leukocyte rolling.

Peroxynitrite inhibits the activity of the transcription factor GATA-4 in cardiomyocytes

^{1,2}LIAUDET L., ²Cardelli D., ³Levrant S., ⁴Waeber B., ⁴Feihl F.,

Soins intensifs de médecine¹, Division des soins intensifs de médecine², Division des soins intensifs de médecine et division de physiopathologie clinique³, Division de physiopathologie clinique⁴,

Introduction. Peroxynitrite (PN) is a potent oxidant proposed as a direct effector of myocardial damage in numerous cardiac pathologies, but its mechanisms of action remain only partly defined. GATA-4 is a transcription factor expressed in cardiomyocytes, which plays an important role as an anti-apoptotic factor in cardiomyocytes. We therefore investigated whether peroxynitrite might exert its toxicity by affecting the activity of this crucial survival factor in cardiomyocytes. **Methods and results.** The rat cardiomyocyte H9C2 cell line was used in this study. H9C2 cells were briefly (20 min) exposed to PN (50-250 μ M) and were then returned in culture medium. GATA-4 activity was determined 1-4 hours after PN stimulation by evaluating the level of phosphorylated (active) GATA-4 by western blotting. We also evaluated the transcriptional activity of GATA-4 by a luciferase gene reporter assay, using a vector containing the Bcl-XL promoter sequence harboring GATA-4 binding elements fused to a firefly luciferase reporter gene. **Results.** A strong basal activity of GATA-4 (high level of phosphorylated-GATA-4 and of GATA-4-dependent-luciferase activity) is present in unstimulated H9C2 cells. Treatment with PN (50-250 μ M) markedly reduces the level of phosphorylated GATA-4 after 1 to 4 hours. Furthermore, peroxynitrite (250 μ M) significantly reduces GATA-4 transcriptional activity evaluated at 4h after PN stimulation.

Conclusions. Peroxynitrite blocks GATA-4 phosphorylation and reduces GATA-4 transcriptional activity in cultured cardiomyocytes. This novel finding may represent a previously unidentified mechanism of peroxynitrite-dependent cytotoxicity in the heart.

The flagellin/toll-like receptor 5 (TLR5) pathway is a potent inducer of pro-inflammatory signaling in cardiomyocytes

¹LIAUDET L., ²ROLLI J., ³LEVRAND S., ⁴WAEBER B., ⁴FEIHL F., ²LIAUDET L.,

Soins intensifs de médecine¹, Division des soins intensifs de médecine², Division des soins intensifs de médecine et division de physiopathologie³, Division de physiopathologie⁴,

Background and aim of study. Gram-negative sepsis is frequently associated with the development of myocardial failure, which results from the release of circulating mediators by microorganisms, leading to myocardial cytotoxicity and inflammation. Flagellin is the major structure protein of the flagella from Gram-negative bacteria, which induces pro-inflammatory responses in several eukaryotic cell types via the activation of the Toll-like receptor 5 (TLR5). In this study, we investigated whether the flagellin/TLR5 signaling pathway might induce pro-inflammatory responses in cardiomyocytes, and thus represent a potential mechanism of myocardial failure during gram-negative sepsis. Methods.

The rat cardiomyocyte H9C2 cell line was used in this study. We first evaluated the expression of TLR5 by H9C2 cells, using RT-PCR (TLR5 mRNA), Western-blot and immunofluorescence (TLR5 protein). We then assessed the ability of recombinant flagellin (50 ng/ml, from Salmonella muenchen) to induce a pro-inflammatory response in H9C2 cells, evaluated by the activation state of NF-kappa B (NFKB), a crucial pro-inflammatory transcription factor, and the expression of pro-inflammatory genes. NFKB activation was monitored by the phosphorylation and degradation of its cytoplasmic inhibitor I kappa B (western blotting), the nuclear translocation of the p65 subunit of NFKB (western), the DNA binding activity of NFKB (electromobility shift) and the transcription of a transfected reporter gene (NFKB-luciferase gene reporter assay). The expression level of TNF alpha and MIP-2 mRNA, two endogenous genes transcriptionally regulated by NFKB, was assessed by RT-PCR, and MIP-2 protein was also detected by ELISA in the culture medium. Results. TLR5 mRNA and protein were both constitutively expressed at a high level in H9C2 cells. Exposure of H9C2 to 50 ng/ml flagellin resulted in a robust activation of NFKB in a time-dependent manner. Dose-response experiments indicated that flagellin at 1 ng/ml already significantly induced NFKB transcriptional activity. In accordance with NFKB activation, flagellin markedly stimulated the transcription of both TNF alpha and MIP-2. Conclusion. Flagellin from gram-negative bacteria is a potent activator of pro-inflammatory signaling in cardiomyocytes and may thus represent a previously unrecognized mediator of myocardial failure during gram-negative sepsis.

Therapy Modifications in Response to Poorly Controlled Hypertension, Dyslipidemia, and Diabetes Mellitus

¹RODONDI N., ²Peng T., ²Karter A., ³Bauer D., ⁴Kerr E., ²Selby J.,

*Médecine et Santé Communautaire*¹, Kaiser Permanente, CA², Internal Medicine, CA³, Ann Arbor, Michigan⁴,

BACKGROUND: Recent reports continue to show relatively poor levels of control for blood pressure in hypertension, LDL-cholesterol levels in patients with dyslipidemia, and hemoglobin A1c in diabetes. Evaluating whether physicians respond appropriately to poor risk factor control may better reflect quality of care than measuring proportions in control.

METHODS: We identified 253,238 adult patients from Kaiser Permanente Northern California with poor control of diabetes, hypertension or dyslipidemia. Poor control was defined as HbA1c values ³ 8.0%; BP levels of ³160/100 mm Hg) (³140/90 in persons with diabetes or prior target organ disease); and LDL-c ³5.0 mmol/L (or risk-specific definitions if high cardiovascular risk). During an 18-month period, we assessed the proportions of patients in poor control who experienced a change in pharmacotherapy within 6 months and defined “appropriate care” as a therapy modification or return to control without modification within 6 months. We assessed patient factors associated with “appropriate care” using multivariate logistic regression.

RESULTS: 64% of patients experienced modifications in therapy for poorly controlled systolic blood pressure, 71% for diastolic blood pressure, 56% for low-density lipoprotein cholesterol, and 66% for hemoglobin A1c within 6 months. Most frequent modifications were increases in number of drug classes (70-84%) and increased dosage (15-40%). An additional 7-11% of those with poorly controlled blood pressure, but only 3-4% of those with elevated low-density lipoprotein cholesterol or hemoglobin A1c, returned to control without therapy modification. Patients with co-occurrence of the conditions, higher baseline values, and target organ damage were more likely to receive “appropriate care”. In general, non-white patients (African-American, Asian, Latino) were significantly more likely to have appropriate physician actions for BP control, but significantly less likely than whites to have appropriate actions for HbA1c control. Latino and Asian patients, but not African Americans were more likely than whites to have appropriate responses for LDL-C control.

CONCLUSIONS: Physicians respond more quickly to poor risk factor control in the presence of higher cardiovascular disease risk. Room for improvement remains in rates of appropriate physician action to high risk levels. Evaluating quality by examining appropriateness of clinical actions represents an additional opportunity for improving decreasing cardiovascular risk.

Dr. Rodondi was supported by a grant from the Swiss National Foundation (PBLAB-102353).

A Re-Appraisal Of Stroke Risk In Fabry Disease

¹BRAKCH N., ³Barbey F., ⁴Linhart A., ¹Hayoz D.,

Angiologie, CHUV¹, Néphrologie, CHUV³, Internal Medicine, Prague⁴,

Background: Fabry disease (FD) is a life-threatening lysosomal storage disorder affecting both genders, and is characterized by progressive small vessel disease involving the heart, brain (TIA or stroke), and kidneys.

Objectives: We have investigated possible common causes of cerebrovascular and cardiac lesions in FD by studying carotid artery wall thickness, left ventricular (LV) mass, and by performing in vitro cellular proliferation studies.

Results: Radial artery wall thickness (high-resolution Doppler-echo) was increased in 16/17 FD patients (10M/6F, $P < 0.001$) as compared to controls. In a larger cohort of FD patients (24M/29F), mean (SD) common carotid artery intima-media thickness (CCA IMT) was increased; M: 706 ± 211 μ m, F: 749 ± 395 μ m; controls: 614 ± 113 μ m.

Thickening was homogenous and circumferential did not correlate with blood pressure. FD patients (M: 45 ± 1.7 years; and 55 ± 2.2 years) had no atherosclerotic lesions but carotid plaques were present in 44% of the controls (M: $n = 83$, 49 ± 1.7 years; F: $n = 37$, 52 ± 1.5 years). LV hypertrophy was found in 60% of men and 39% of women with FD. There was a strong positive correlation between LV mass and CCA IMT ($r^2 = 0.27$; $P < 0.0001$). In vitro vascular smooth muscle cell and neonatal cardiomyocytes proliferative response (plasma from 27 untreated FD patients and 30 controls) correlated with CCA IMT ($r^2 = 0.48$; $p < 0.01$) and LV mass index ($r^2 = 0.19$; $p = 0.028$), respectively.

Conclusions: Most FD patients showed arterial wall thickening without hypertension or atherosclerotic lesions. As correlations were found between LV mass, CCA IMT and proliferative response, the cardiac and cerebrovascular FD lesions may have a common cause (e.g. growth-promoting agents) other than pathologic substrate accumulation in vascular endothelial cells. The use of CCA IMT as a biomarker for cardiac involvement in FD has to be studied further. Cardiac complications such as atrial fibrillation and sustained arrhythmias add to the increased risk of stroke in FD. Correction of cardiovascular abnormalities by Fabrazyme® at 1 mg/kg every other week, as well as by drugs acting on classical stroke risk factors, may reduce the incidence of cerebrovascular events in FD.

Analyzes of expression of Sterol regulatory element binding proteins in developing peripheral nerve and evaluation of their implication in diabetic peripheral neuropathy.

¹DE PREUX A., ²Verheijen M., ³Rungger-Brändle E., ⁴Zhang W., ⁴Sima A.,
⁵Chrast R.,

Département de Génétique Médicale¹, Department of Molecular and Cellular Neurobiology, Vrije Universiteit, Amsterdam, The Netherlands.², Laboratoire de Biologie cellulaire, Clinique d'Ophthalmologie, HUG, Geneva, Switzerland³, Departments of Pathology and Neurology and The Morris Hood Comprehensive Diabetes Center, Wayne State University, Detroit, MI, USA.⁴, Department of Medical Genetics, University of Lausanne, Switzerland⁵,

Diabetic peripheral neuropathies (DPN) are a common chronic complication of both type I and II diabetes mellitus. Even though functional changes, including decreased nerve conduction velocity, and progressive neuroanatomical changes affecting neuronal structures are relatively well described, molecular mechanisms underlying DPN remain poorly understood.

Our previous gene expression profiling of peripheral nerve development has shown that a large cluster of genes implicated in lipid metabolism, including key transcription factors regulating expression of these genes such as Sterol regulatory element binding proteins (Srebp-s), were expressed in the endoneurium, presumably by Schwann cells. Previous in vitro and in vivo studies have shown that Srebp1c is implicated in fatty acid metabolism, Srebp2 in cholesterol synthesis and that Srebp1a activates both pathways. In order to test which of these isoforms play a role in peripheral nerve function we have performed Q-PCR analysis of Srebp expression in endoneurium of developing peripheral nerves. This analysis shows that expression of Srebp2 follows production of myelin (peaking around P10-P28), expression of Srebp1a is not changing and the expression of Srebp1c is upregulated in adult endoneurium only after myelination has been completed.

Srebp1c expression is under the control of insulin and glucose in several tissues, such as liver or kidney, in which it is implicated in complications due to diabetes mellitus. Misregulation of Srebp1c activity in Schwann cells in diabetic conditions could therefore result in defects in lipid biosynthesis and/or energy metabolism affecting the normal nerve function. To test this hypothesis we are analyzing Srebp1c expression both in STZ and BB/wor rats, 2 animal models of type I diabetes mellitus developing functional and structural changes similar to those observed in human DPN. This data should provide more insight into the potential role of Srebp transcription factors in normal peripheral nerve function and in the nerve affected by diabetic neuropathy.

Is Connexin 40 implicated in the pulmonary transmigration of neutrophil polymorphonuclear leucocytes ?

¹RIGNAULT S., ²Haefliger J., ¹Waeber B., ³Liaudet L., ¹Feihl F.,

Division de physiopathologie clinique¹, Service de médecine interne², Soins intensifs de médecine³,

The transmigration of neutrophil polymorphonuclear leucocytes through the microvascular endothelium is a cardinal event of acute inflammation. In vitro, gap junctional intercellular communication can restrict transendothelial neutrophil migration, but whether it also occurs in vivo is unknown. Connexin 40 (Cx40) is a gap junctional protein abundantly present in the lung, notably in vascular endothelium. Our in vivo experiments indicated that acute lung inflammation progressively and markedly reduced the pulmonary expression of Cx40, while not affecting the levels of other connexins. Therefore, we hypothesized that acute lung inflammation would be aggravated in knockout mice genetically deficient in Cx40. This hypothesis was tested in two different models: 1) pulmonary inflammation as a distant consequence of an abdominal infection caused by cecal ligation and perforation (CLP), and 2) airway instillation of lipopolysaccharide (LPS). Mice were sacrificed after 8 (CLP) or 6 hours (LPS). Broncho alveolar lavage (BAL) was carried out for the counting of airspace neutrophils. Lungs were then perfused in situ and harvested for the assay of myeloperoxidase (MPO) activity, a common index of tissue neutrophil infiltration. Neutrophil chemotaxis was assessed by measuring concentration of chemokines KC and MIP-2 in BAL fluid. Tissue infiltration by neutrophils was present in both models, while neutrophil migration to the airspaces occurred only with LPS instillation. In either model, the development of lung inflammation did not differ between wild type and Cx40-deficient mice. Conclusion: neutrophil transmigration in the lung appears not to be affected by the genetic deletion of Cx40, despite the drastic progressive downregulation of Cx40 expression in the lungs of wild type animals by acute inflammation.

AMP activated protein kinase activation decreases the expression of the gap junctional protein connexin36 in insulin-producing cell.

¹ALLAGNAT F., ²Martin D., ²Haefliger J., ²Waeber G.,

*Medecine Interne*¹, *medecine interne*²,

Control of insulin secretion is critical for the maintenance of normal levels of circulating glucose. In beta cell, the gap junction connexin36 (Cx36) is required to maintain the functional state of beta cells.

We have recently demonstrated that glucose represses the expression of Cx36 through the PKA-dependant activation of the repressor CREM, suggesting that Cx36 could be implicated in the development of the glucotoxicity phenomenon.

In this study, we tested the role of the AMP activated protein kinase (AMPK) on Cx36 expression in insulin-secreting cells. The AMPK is a metabolic stress-sensing protein kinase responsible for coordinating metabolism and energy demand. Forced activation of the AMPK using metformin or 5-aminoimidazole-4-Carboxamide-1-beta-4-Ribofuranoside (AICAR) induced a significant reduction of Cx36 levels in insulin-secreting cell lines and isolated pancreatic mouse islets. Both mRNA and protein levels of Cx36 were decreased in a dose- and time-dependent manner and actinomycin D experiments demonstrated that the effect of AICAR is transcriptional. The metformin and AICAR effects were blunted by the specific inhibitor of AMPK compound C, confirming the involvement of the AMPK in the control of Cx36 expression.

Transient transfection experiments revealed that the AMPK effect requires the presence of a sterol response element (SRE) located in the Cx36 promoter. AMPK is known to inhibit SREBP1c (SRE binding protein) in insulin-secreting cells and additional studies will be performed to assess the specific role of SREBP1c in the regulation of the Cx36 expression levels.

Considering the essential role of Cx36 in maintaining normal insulin secretion, these results suggest that Cx36 could be implicated in the alteration of insulin-secretion observed under stress conditions leading to AMPK activation.

Increased Connexin43 Expression in Human Saphenous Veins in Culture is Associated with Intimal Hyperplasia

¹HAEFLIGER J., ²Déglise S., ³Martin D., ²Probst H., ²Corpataux J.,

*Médecine Interne*¹, *Thoracic and Vascular Surgery*², *Département de Médecine Interne*³,

Intimal hyperplasia (IH) is a vascular remodelling process following a vascular injury. The mechanisms involved in IH consist of proliferation, dedifferentiation, as well as migration of medial smooth muscle cells (SMCs) towards the subintimal space. We postulated that gap junctions, which coordinate physiological processes such as cell growth and differentiation, might participate in the development of IH. Connexin43 (Cx43) expression levels may be altered in IH and we therefore evaluated the regulated expression of Cx43 in human saphenous veins in culture in presence or not of fluvastatin, an inhibitor of HMG CoA reductase activity. Segments of harvested human saphenous veins, obtained at the time of bypass graft, were opened longitudinally with luminal surface uppermost and maintained in culture for 14 days. We chose to focus on Cx43 and Cx40 out of the four connexins (Cx37, 40, 43 and 45) which we found by RT-PCR to be expressed in the saphenous vein, since Cx43 and Cx40 are the predominant connexins expressed by SMCs and endothelial cells. After 14 days of culture, histomorphometrical analysis showed a significant increase in the intimal thickness as observed during the process of IH. A time-course analysis revealed a progressive upregulation of Cx43 to reach a maximal increase of 6- to 8-fold at both transcript and protein levels after 14 days in culture. In contrast, the expression of Cx40, abundantly expressed in the endothelial cells, was not altered. Immunofluorescence showed a large increase in Cx43 within SMCs membranes of the media layer. The development of intimal hyperplasia in vitro was decreased in presence of fluvastatin, and was associated with reduced Cx43 expression. Conclusions: These data show that Cx43 is increased in vitro during the process of IH and that fluvastatin could prevent this induction, supporting a critical role for Cx43-mediated gap junctional communication in human vein during the development of IH.

Connexin43-dependent mechanism modulates renin secretion and hypertension

¹HAEFLIGER J., ²Krattinger N., ²Martin D., ²Pedrazzini T., ³Meda P.,

*Médecine Interne*¹, *Département de Médecine Interne*², *Département de Physiologie et Métabolisme*³,

To investigate the function of Cx43 during hypertension, we studied the mouse line Cx43KI32 (KI32), in which the coding region of Cx32 replaces that of Cx43. Within the kidneys of homozygous KI32 mice, Cx32 was expressed in cortical and medullary tubules, as well as in some extra- and intra-glomerular vessels, i.e. at sites where Cx32 and Cx43 are found in wild type (WT) mice. Under such conditions, renin expression was much reduced compared to that observed in the kidneys of WT and heterozygous KI32 littermates. After exposure to a high salt diet, all mice retained a normal blood pressure. However, whereas the levels of renin were significantly reduced in the kidneys of WT and heterozygous KI32, reaching levels comparable to those observed in homozygous littermates, they were not further affected in the latter animals. Four weeks after the clipping of a renal artery (2K1C model), 2K1C WT and heterozygous mice showed an increase in blood pressure and in the circulating levels of renin, whereas 2K1C homozygous littermates remained normotensive and showed unchanged plasma renin activity. Hypertensive, but not normotensive mice also developed cardiac hypertrophy. The data indicate that replacement of Cx43 by Cx32 is associated with decreased expression and secretion of renin, thus preventing the renin-dependent hypertension which is normally induced in the 2K1C model.

Microalbuminuria but not cystatin C is associated with carotid atherosclerosis in middle-aged adults

¹RODONDI N., ²Yerly P., ³Gabriel A., ⁴Burnier M., ⁵Paccaud F., ⁵Bovet P.,

*Médecine et Santé Communautaire*¹, *Division of Cardiology*², *Ministry of Health, Republic of Seychelles*³, *Division of Nephrology*⁴, *Community Medicine and Public Health*⁵,

Background: Cystatin C serum concentration, a measure of renal function, has recently been shown to be an independent predictor of cardiovascular events in adults aged 65 years and older. Microalbuminuria has also been suggested as a risk factor for cardiovascular events. However, the predictive role of these two markers have not been compared in a same population.

Methods: We studied the relationship between cystatin C (divided into tertiles), microalbuminuria (present or absent) and carotid atherosclerosis -a vascular disease outcome- in a cross-sectional, population-based random sample of 544 adults aged 35-64 from the Seychelles population (Indian Ocean). Intima-media thickness (IMT) and the presence of carotid plaques (any focal IMT thickening of ≥ 1.2 mm) were assessed with B-mode ultrasound (GE LogiBooq, 6-10 MHz transducer) and semiautomatic software (Metris, Paris).

Results: Cystatin C was associated with carotid plaques (p for trend <0.001), but this relationship disappeared after adjustment for age and traditional cardiovascular risk factors (p for trend = 0.61). In multivariate analysis, cystatin C was not associated with IMT (p for trend = 0.27). Microalbuminuria was associated with carotid plaques (OR: 2.19, 95%CI: 1.29-3.71) and with IMT (805 vs. 732 μ m, p <0.001). After adjustment for age and traditional risk factors, the association between microalbuminuria and IMT remained (p = 0.04) while the association with carotid plaques was reduced (OR: 1.74, 95%CI: 0.97-3.13, p = 0.06).

Conclusion: Microalbuminuria, but not cystatin C, is associated with carotid atherosclerosis beyond traditional cardiovascular risk factors among middle-aged adults. The predictive role of emerging cardiovascular risk factors might differ between middle-aged and older adults.

Pharmacogenetic analysis of the cardiovascular response in mice

¹BERTHONNECHE C., ²Pedrazzini T., ³Abriel H., ⁴Beckmann J., ⁵Maurer F.,

Department of Medical Genetics, UNIL¹, Department of Medicine, CHUV and UNIL², Department of Pharmacology and Service of Cardiology, CHUV and UNIL³, Department of Medical Genetics, UNIL and Service of Medical Genetics, CHUV⁴, Service of Medical Genetics, CHUV⁵,

Response variability to many common drugs may impose important clinical constraints, either leading to unwanted side-effects or showing at best little relief. Amid critical factors that may contribute to such drawbacks, common genetic variants may modulate not only disease but also drug action and response. The identification of pharmacogenetic determinants in humans is complicated by limitations (genetic heterogeneity, sample size, compliance to drug prescription, poly-medication, or placebo effect) that can be more easily addressed in controlled animal models. To date, most murine cardiovascular-associated quantitative trait loci (QTL) map concordant human QTLs. Furthermore, genetic determinants for both mono- and multigenic traits have been successfully characterised in such models. Thus, we reasoned that identifying pharmacogenetic variants in mice may advantageously contribute to the understanding of drug response variability in humans. Interestingly, as most inbred laboratory mice descend from a very limited number of progenitors, each strain can be considered as an individual member of a rather close family of mice. Furthermore, the elucidation of the mouse genome sequence, together with the availability of ever denser SNP maps for diverse inbred strains provide major tools to enhance and accelerate the mapping of mouse genetic traits by correlating in vivo phenotypes with SNP alleles. In order to develop a model of systemic and unbiased genome-wide screening for cardiovascular pharmacogenetic variants, we have started to phenotype age- and sex-matched inbred mice for parameters like blood pressure, heart rate and electrocardiogram, under basal conditions or in response to isoproterenol (a β -adrenergic agonist) or atenolol (a β -adrenergic antagonist). Preliminary data obtained in five strains show excellent reproducibility of intra-strain measurements. Furthermore, significant inter-strain differences were observed for all parameters recorded. These results, together with future data collected in additional strains, will be compared to the corresponding SNP maps by computational association methods. Ultimately, these association studies are anticipated to allow the mapping of relevant cardiovascular pharmacogenetic loci

Label retaining cells in the adult mouse heart

¹MEINHARDT A., ¹Grisel P., ²Bernasconi E., ¹Bougorski R., ¹Vassalli G.,

Service de Cardiologie¹, Service de Gastroenterologie²,

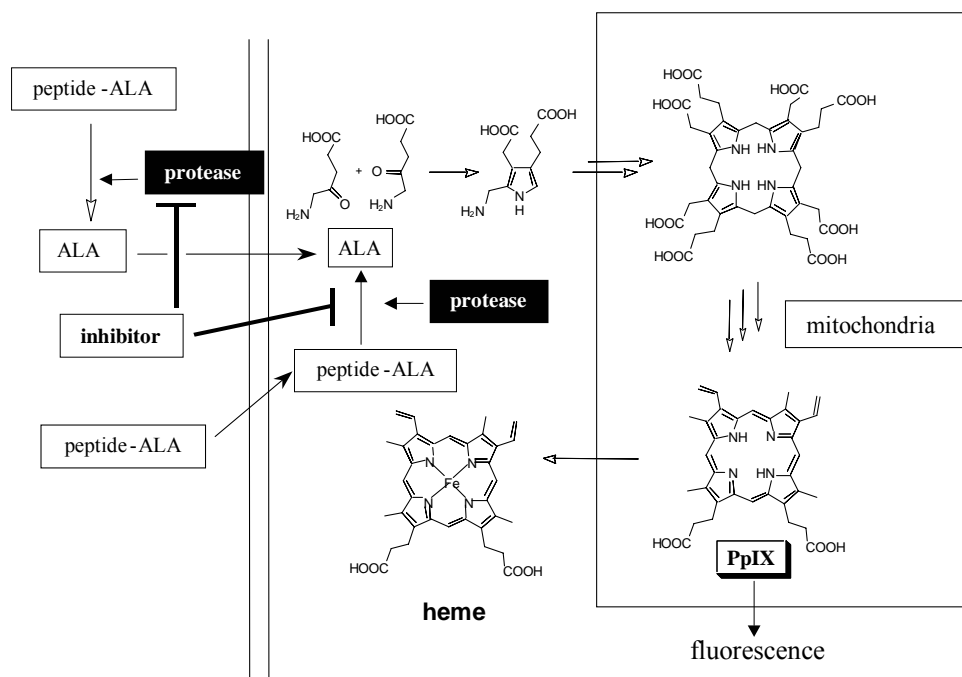
Recent reports have provided increasing evidence for the existence of one or more populations of resident stem or progenitor cells in adult hearts. Bromodeoxyuridine (BrdU)-label retention has been used to identify stem cells based on their characteristic of being slow cycling in various tissues such as skin and colon, but not in the heart. We investigated whether adult mouse hearts contain BrdU label-retaining cells (LRC). Using a BrdU pulse and chase-protocol, adult mouse hearts were analyzed immunohistochemically at different time points of chase (0-12 months). The number of LRC decreased from 12% at baseline (i.e., immediately after the BrdU pulse) to ~0,25% at 4 months of chase, but then remained stable (plateau) for up to 12 months. LRC were widely distributed across the heart; however, they showed a predominant localization at the ventricular tip and in the atria. LRC were mostly negative for differentiation markers of cardiac cell (myocytes, endothelial and smooth muscle cells, fibroblasts). A FACS-based method was set up to sort viable LRC that are currently kept in cell culture to investigate their in vitro proliferation and differentiation potential. Cardiac cells expressing stem cell antigen-1 (Sca-1), which accounted for 9,2±4,5% of non-myocytic cells in adult mouse hearts, showed a 2.5-fold enrichment in LRC, as compared to Sca-1-negative cells. In conclusion, the adult mouse heart contains LRC that retain the BrdU label for more than 1 year, a typical feature of stem cells. Enrichment of Sca-1-positive cardiac cells for the LRC subset also support the hypothesis that LRC are candidate cardiac-resident stem cells. This remains to be established by clonogenic analysis of the LRCs.

Determination of intracellular prolyl-specific proteases in intact living cells using protoporphyrin IX as a reporter system.

SCHMITT f., Berger Y., Chapuis C., Neier R., Juillerat L.,

*Pathology*²,

The determination of enzyme activity or inhibition in intact living cells is a problem in the development of inhibitors for intracellular proteases. The production of fluorescent protoporphyrin IX (PpIX) from the non-fluorescent *N*-Gly-Pro-5-aminolevulinic acid (ALA) substrates was used to evaluate the prolyl-specific dipeptidylpeptidase IV (DPP IV)-like and prolyl oligopeptidase (POP)-like activities of human cells.



Cellular Production of PpIX from Peptides-ALA

The results demonstrated that whereas POP-like activity was exclusively intracellular and could be attributed to the actual POP, the DPP IV-like activity could be related to cell-membrane DPP IV only in HT29 colon cell line. In the other breast and colon cell lines DPP IV-like activity was intracellular and displayed by other prolyl-specific dipeptidases. Gel filtration experiments demonstrated that different proteases hydrolyzed these ALA-derivatives. These observations have important consequences for the development and evaluation of selective inhibitors for these enzymes.

Use of isotope ratio mass spectrometry to detect doping with oral testosterone undecanoate: Inter-individual variability of $^{13}\text{C}/^{12}\text{C}$ ratio.

¹BAUME N., ²Saudan C., ²Desmarchelier A., ²Strahm E., ²Sottas P., ³Bagutti C., ⁴Cauderay M., ⁵Schumacher Y., ²Mangin P., ²Saugy M.,

Laboratoire Suisse d'Analyse du Dopage¹, LAD, Lausanne, Suisse², VidyMed, Lausanne, Suisse³, Hôpital du Samaritain, Vevey, Suisse⁴, Abtlg. Sportmedizin, Freiburg, Germany⁵,

The metabolic effect of multiple oral testosterone undecanoate (TU) doses over 4 weeks was assessed in 7 voluntary men. The protocol was designed to detect accumulation of the substance by choosing the appropriate spot urines collections time and to study the urinary clearance of the substance after weeks of treatment. Urines were analysed by a new GC/C/IRMS method to establish the $\delta^{13}\text{C}$ -values of testosterone metabolites (androsterone and etiocholanolone) together with an endogenous reference compound (16(5 α)-androstene-3 α -ol). The significant differences in inter-individual metabolism following TU intake was illustrated by large variations in $\delta^{13}\text{C}$ -values of both T metabolites (max $\Delta \delta^{13}\text{C}$ -values = 5.5 ‰), as well as by very stable longitudinal T/E profiles and carbon isotopic ratios in the first hours following administration. According to T/E ratios and $\delta^{13}\text{C}$ -values, the washout period after 80 mg TU intake was less than 48 hours for all subjects and no accumulation phenomenon was observed upon chronic oral administration.

Role of the alpha subunit second extracellular loop in the accessibility of K⁺ ions to their binding site in Na,K-TPase.

¹CAPENDEGUY O., ¹Horisberger J.,

*Pharmacologie et Toxicologie*¹,

The Na,K-ATPase is a transmembrane protein, necessary for maintaining the membrane potential, by transporting 3Na⁺ out the cell, and 2K⁺ into the cell, using the energy providing from one ATP molecule hydrolysis. There are some evidence that disorders of this protein is related to hypertension.

The aim of this study is to understand the mechanism of transport of the Na,K-ATPase and more precisely, the control of the extracellular K⁺ accessibility to their binding sites. The structure of the Na,K-ATPase is not known while the Ca-ATPase (SERCA) has been crystallised with a high resolution. By homology with the structure of the SERCA and supported by experimental studies, Na⁺ and K⁺ binding sites, implicating the 4th, 5th and 6th helices have been proposed for the Na⁺,K⁺-ATPase. To gain into understanding of access control of K⁺ binding sites from the extracellular side, we have targeted this study on the 2nd extracellular loop linking the TMS 3 and 4, because it closed of the cation pathway.

To this end we have mutated into cysteine the residues E314 to G326 of this loop and we have measured the functional activity by electrophysiological techniques. An accessibility study by a thiol reagent indicated a movement of the 2nd extracellular loop during the conformational changes. Then, we showed that some mutations or a thiol reagent binding could induce a large increase in apparent extracellular K⁺ affinity. These results showed that this loop was very important to permit the conformation change from E2P to E1 because introduction of one cysteine mutation was sufficient to affect the conformational equilibrium. These results combined with those of a precedent study (Capendeguy and Horisberger. 2004. J. of Physiology) on the 3rd extracellular loop (between the TMS 5 and 6) show that these 2 loops have a complementary function and could control by the K⁺ accessibility to their binding site from the extracellular side.

Augmentation de la résistance des cellules beta pancréatiques par les HDL: identification des voies de signalisation induites par les HDL par analyse transcriptomique (Affymetrix Gene Chip array)

¹BUTTY A., ³Au K., ³Mooser V., ²Waeber G., ⁴Widmann C.,

IBCM¹, CHUV², GlaxoSmithKline (USA)³, UNIL⁴,

Titre : Augmentation de la résistance des cellules beta pancréatiques par les HDL: identification des voies de signalisation induites par les HDL par analyse transcriptomique (Affymetrix Gene Chip array).

Objectifs : La dyslipidémie observée dans le diabète de type 2 (DT2) se caractérise par une augmentation des acides gras non estérifiés circulants et un changement de profile des lipoprotéines. La réduction des taux circulants de HDL-cholestérol est un facteur de risque indépendant pour le développement du DT2. Considérant que les HDL protègent les cellules beta de l'apoptose induite par les cytokines ou la privation de facteurs trophiques, des stratégies thérapeutiques visant à augmenter les HDL pourraient représenter une solution thérapeutique dans la prévention du développement du diabète. Afin d'identifier les voies de signalisation impliquées dans la protection induite par les HDL, les modifications d'expression génique induites par les HDL ont été investiguées par analyse transcriptomique.

Méthodes : Les HDL ont été isolées à partir de plasma humain. Des cellules beta-TC3 ont été cultivées 2 jours dans du milieu complet, puis incubées en présence ou en absence de 1 mM HDL-cholestérol dans des conditions trophiques normales ou en absence de sérum. L'ARN total a été préparé après 6 h. La puce Affymetrix gene chip mouse 430 version 2 et les programmes d'analyse bioinformatique associés à la technologie Affymetrix ont été utilisés pour l'analyse de l'expression des gènes.

Résultats : Les résultats préliminaires montrent que les cellules beta se protègent de l'apoptose en réprimant des gènes codant pour des cibles connues pour leur effet proapoptotiques dans d'autres systèmes cellulaires.

Conclusion : Les HDL protègent les cellules beta de l'apoptose induite par les cytokines et la privation de facteur trophiques. Notre étude permettant de mieux comprendre les voies de signalisation induites par les HDL pourrait faire émerger de nouvelles stratégies thérapeutiques dans la prévention du développement du DT2.

Stimulation of neuropeptide Y gene expression by hypoglycemia in primary cultures of hypothalamic neurons: the role of AMP kinase

¹Gamba M., ¹Chau Van C., ¹Gaillard R., ¹Pralong F.,

Service d'Endocrinologie, Diabétologie et Métabolisme¹,

Neuropeptide Y (NPY) is the most abundant peptide in the mammalian hypothalamus, and one of the most potent orexigenic factors known to date. Neurons expressing NPY in the hypothalamic arcuate nucleus are modulated by peripheral metabolic signals such as insulin and leptin, and the cytoplasmic enzyme AMP-activated kinase (AMPK) has recently been implicated in these effects.

In the present study, we used primary cultures of rat hypothalamic neurons (Bergonzelli et al) to further study the modulation of NPY neurons by metabolic stimuli. First, neurons in culture were exposed for 24 hours to extracellular glucose concentrations of 1 mM (low), 5.5 mM (normal) or 20 mM (high), and the levels of NPY mRNA measured by real time RT-PCR (LightCycler® technology). Whereas high glucose had no effect on basal NPY expression (measured at 5.5 mM glucose), low glucose induced an almost three-fold increase in NPY mRNA levels ($p < 0.01$). The potential role of AMPK in this effect was then evaluated in two ways. The phosphorylation of AMPK was studied by Western blot in low, normal or high glucose conditions, and the effects of AICAR, a stimulator of AMPK phosphorylation, on NPY gene expression were also evaluated. We found that in low glucose conditions, the phosphorylation of AMPK is indeed stimulated in our in vitro model. We also observed a nearly 6-fold stimulation of NPY gene expression by AICAR ($p < 0.01$). Studies are currently being performed with an enzyme inhibitor of AMPK to confirm the central role of this enzyme in the modulation of the activity of NPY-expressing neurons in response to variations in the extracellular glucose concentration.

Interestingly, metformin is a widely used oral antidiabetic agent acting at least partially via a modulation of AMPK activity. Since metformin administration in rodents is associated with a decrease in food intake, these results prompted us to test the effects of this drug on both AMPK phosphorylation and NPY gene expression in our culture model. We could show that metformin reduces significantly the expression NPY induced by low glucose, but surprisingly, we did not observe any effect of metformine on AMPK in this in vitro model. Therefore, our preliminary results suggest that anorexigenic effects of metformin may be at least partially mediated at the level of hypothalamic NPY neurons, but via mechanisms independent of AMPK.

Bergonzelli et al, Diabetes 50:2666, 2001

LH pulsatility during hyperinsulinemic euglycemic clamp studies: acceleration in normal female volunteers and no effect in PCOS patients

¹PRALONG F., ¹Moret M., ²Stettler R., ³Wirthner D., ¹Gaillard R., ²Tappy L.,

Service d'Endocrinologie, Diabétologie et Métabolisme¹, Département de Physiologie², Unité de Médecine de la Reproduction³,

Polycystic ovary syndrome (PCOS) is the most frequent endocrine disorder of women of reproductive age. This syndrome associates reproductive endocrine abnormalities with a metabolic dysfunction characterized by a tendency to overweight or frank obesity. A neuroendocrine hallmark of the gonadotrope axis of patients diagnosed with polycystic ovary syndrome (PCOS) is an accelerated frequency of LH pulses. Since elevated circulating levels of insulin are found in a majority of patients with PCOS, it has been postulated that insulin resistance participates to the etiopathogeny of the syndrome.

The present study was designed to assess the potential role played by elevated insulin levels in the accelerated pulsatility of LH. To this aim, we studied 6 normal female volunteers and 6 patients diagnosed with PCOS, aged between 16 and 32 years old. Mean BMI of controls was 21.1 kg/m², and mean BMI of PCOS patients was 25.7 kg/m² (a single patient being >30 kg/m²). All subjects were admitted on two separate occasions to the CRC of the Lausanne University Hospital for 12 hours of frequent (q 10 minutes) blood sampling studies of LH secretion. One of these admissions was the baseline study. During the other admission, a hyperinsulinemic, euglycemic clamp study was performed over the first 6 hours. Normal volunteers were studied in the follicular phase, between day 5 and day 11 of their cycle, and a serum progesterone level was obtained prior to the admission in all PCOS patients to avoid studying them after a spontaneous ovulation. The respective order of the baseline and the clamp study was determined randomly. Plasma LH levels were measured in all samples, and pulsatility analysed with the Pulse XP running on a PC.

The mean fasting baseline levels of insulin in PCOS patients were 10.58 IU/L, compared to the same values in normal controls of 7.55 IU/L. As anticipated, we found that PCOS patients at baseline exhibit an accelerated frequency of LH pulses compared to normal controls (11.0±0.6 vs 7.8±1.0 pulses per 12 hours, p=0.02, Chi square test), as well as higher mean LH levels (12.6±0.5 vs 6.7±2.2 IU/L, p=0.02, ANOVA).

Hyperinsulinemia had no effect on these parameters of LH secretion in PCOS patients, whereas we found that it induced a significant increase in the LH pulse frequency of the normal volunteers (from 7.8±1.0 IU/L to 10.2±1.25 IU/L, p=0.02, Chi square test). This increase in frequency was accompanied by a decrease in the LH pulse amplitude (from 2.7±0.21 IU/L to 1.9±0.15 IU/L, p=0.02, Chi square test). These results demonstrate for the first time in the human an effect of changes in peripheral insulin levels on LH secretion. Since pituitary LH secretion represent an indirect measure of hypothalamic GnRH secretion, our results demonstrate that like in rodents (Burcelin et al), insulin participates in the modulation of the activity of GnRH neurons in the human. We speculate that the neuroendocrine abnormalities of PCOS could at least partially result from endogenously elevated levels of circulating insulin.

Burcelin R et al, Endocrinology 144:4484, 2003.

SODIUM SELF-INHIBITION OF THE EPITHELIAL SODIUM CHANNEL: PROPERTIES OF THE EXTRACELLULAR SODIUM SENSING SITE.

¹BIZE V., ¹Horisberger J.,

Dpt de pharmacologie et toxicologie¹,

The epithelial sodium channel (ENaC) is a key component of the transepithelial Na⁺ transport, responsible for the maintenance of the sodium balance (that controls extracellular fluid volume and arterial blood pressure) and for the regulation of the surface fluid layer in airway epithelia. The open probability of ENaC is highly variable and seems to be dependent on the membrane potential and on the extracellular Na⁺ concentration, a phenomenon called "Na⁺ self inhibition": extracellular Na⁺ induces a decrease of the open probability of the channel and thus affects the rate of transepithelial Na⁺ transport with a fast time course (~1-2 s). The aim of our study is the determination of the properties of the extracellular Na⁺ sensing site (ionic selectivity and affinity). The approach we use is to measure amiloride-sensitive Na⁺ currents in *Xenopus laevis* oocytes expressing human or *Xenopus* ENaC, and loaded with Na⁺ (an intracellular concentration of about 50 to 80 mM). The effects of test solutions containing different cations were measured for potentials between -100 and +50 mV. Outward amiloride-sensitive currents recorded at +50 mV were inhibited by Na⁺ or Li⁺ (a 4-fold decrease for hENaC at 100 mM Na⁺ or Li⁺) compared to NMDG or a cation free solution (saccharose 180 mM). K⁺ also produced a small, ~15% inhibition of human ENaC at 100 mM. For Na⁺ and Li⁺, this "self inhibition" appeared to involve a binding site with an apparent affinity of ~100 mM. Moreover we observed that proteases treatments (trypsin or the Channel Activating Protease-1) abolish this inhibitory phenomenon, what matches with published results.

Structural basis for a novel SH3 domain function: Intrinsic dimerization of the IB1 scaffold protein

Guenat S., Kristensen O., Dar I., Kastrup J., Roduit R., Maurer F., Allaman-Pillet N., Beckmann J., Gajhede M., Bonny C.,

The mammalian scaffold protein islet-brain 1 (IB1) interacts with components of the c-Jun N-terminal kinase (JNK) signal-transduction pathway and has a central role in coordinating the advance of apoptotic events, mainly in neurons and pancreatic beta cells. IB1 is a multi domain protein known to mediate protein-protein interactions that contains a SH3 domain with a hitherto unknown function. Up to now, SH3 domains have been reported to be engaged in PXXP-dependent or independent protein-protein interactions. Here, we have characterized the function of IB1 SH3 domain in molecular detail using pull-down assays, mutagenesis studies and X-ray crystallography (pdb entries 1QZI, 1XB5 and 1XBQ). We show that the SH3 domain of IB1, is able to homodimerize. Surprisingly, the predominantly hydrophobic (70 % of the aa) and very tight binding interface does not involve any canonical PXXP motif but is formed by 10 direct hydrogen bonds and one salt bridge Arg13-Asp34 (R506 and D519 in rat IB1 sequence) and contains 10 bridging water molecules. These crystallographic data prompted us to evaluate the role of selected residues in dimerization by in vitro binding assays using SH3 mutants. Two mutants (R13A and R13E) failed to bind to wild type SH3 while mutations at other positions did not affect the process, highlighting the major role of Arg 13 in homodimerization. Additional data tend to favor a role for IB1 dimerization in controlling JNK signalling and call for a reassessment of the interactions between IB1 and its binding partners.

Rosiglitazone increases PPARg2 and 11bHSD1 gene expression in human adipose tissue

¹LEYVRAZ c., ²Suter M., ²Calmes J., ³Verdumo C., ³Gaillard R., ³Pralong F., ³Giusti V.,

*Endocrinologie, Diabétologie and Métabolisme*¹, *Chirurgie*², *Endocrinologie, Diabétologie et Métabolisme*³,

The synthetic thiazolidinedione agent rosiglitazone (RTZ) is a PPARg (peroxisome proliferator and activated receptors g) agonist that has attracted great attention thanks to its insulin sensitizing and anti-inflammatory properties. Activation of PPARg isoforms via RTZ treatment enhances insulin sensitivity without affecting insulin secretion, while negatively acting on glucose levels in the blood. These improvements are accompanied by a remodelling of the adipose tissue and, paradoxically, by an increase in fat storage, subcutaneous rather than visceral, and in some weight gain. We hypothesized that RTZ acts via specific modulation of both PPARg2, the most abundant isoform of PPARg in subcutaneous adipose tissue, and 11bHSD1 (11b-hydroxysteroid dehydrogenase type 1), a well recognized key enzyme involved in adipose tissue differentiation and obesity development.

In the work presented, we examined the effects of RTZ on PPARg2 and 11bHSD1 expression levels by real-time RT-PCR (LightCycler® technology). Measurements were made on two different models: first the human immortalized preadipocyte cell line (Chub-S7) and second, primary preadipocytes of visceral and subcutaneous adipose tissue obtained from obese women.

In the Chub-S7 cell line, a 17 days-treatment of RTZ induces a significant increase of PPARg2 and 11bHSD1 expression concomitantly with the differentiation of preadipocytes into mature adipocytes. Furthermore, 11bHSD1 expression decreases when RTZ is stopped, while PPARg2 expression stops increasing without decline. Data obtained from human primary adipocytes confirm the augmentation of PPARg2 induced by RTZ, that is even higher in subcutaneous than in visceral cells. In addition, RTZ significantly increases 11bHSD1 transcripts in visceral, but not in subcutaneous adipocytes. Taken together, these data suggest that RTZ stimulates directly 11bHSD1 expression in visceral areas that successively modulates PPARg2 expression in subcutaneous regions to promote the storage of free fatty acids.

In conclusion, these results allow for better delineating the mechanisms involved in directing lipids away from visceral areas towards subcutaneous depots. They also give new insights in the understanding of how treatment of patients with PPARg agonists like RTZ leads to fat accumulation in subcutaneous adipose tissue.

The Transcription Factor REST Impairs Insulin Secretion through Repression of Proteins of the Exocytotic Machinery

¹MARTIN D., ¹Allagnat F., ¹Regazzi R., ²Maechler P., ¹Haefliger J.,

*DMI*¹, *DCPM*²,

The transcriptional repressor Restrictive Element-1 Silencer Transcription factor (REST) restricts some neuronal traits to neurons by repressing neuronal genes expression in other cell types. Insulin producing beta cells share these common traits with neurons as REST is not expressed in both cell types. To evaluate the effect of REST expression over insulin secretion, we used adenoviral gene transfer in beta cell lines as well as in murine islets. As a consequence of REST expression, the capacity to secrete insulin was impaired in response to glucose, KCl, Leucine or to its non metabolized analogue 2-aminobicyclo-[2,2,1] heptane-2-carboxylic acid (BCH). We next dissociated first and second phase of regulated insulin secretion using diazoxide and KCl-induced depolarization and showed that REST affected both glucose-induced triggering and amplifying pathways. Monitoring of INS-1E membrane potentials with rhodamine 123 and bis-oxonol indicated that REST influenced neither mitochondrial membrane hyperpolarization nor plasma membrane depolarization capacities respectively. In order to identify REST target genes responsible for the alteration of insulin secretion, we evaluated the expression of proteins involved in the machinery of exocytosis. Several genes contained the REST recognition element and among them SNAP-25, Synaptotagmin (Syt) 4, 5, 7, and Complexin2 showed decreased mRNA levels after ectopic REST expression in beta cell lines. In INS-1E, a small interfering-RNA strategy directed against Syt 4 and Syt 7 further demonstrated their implication in glucose-induced insulin secretion. These data indicate that REST alters the secretory function of pancreatic beta cells by inhibiting the expression of key components of the terminal machinery of exocytosis.

Effect of Fructose Overfeeding and Fish Oil Administration on Hepatic De Novo Lipogenesis and Insulin Sensitivity in Healthy Men

¹FAEH D., ²Minehira K., ³Schwarz J., ⁴Periasami R., ⁵Tappy L.,

Université de Lausanne: département de physiologie et IUMSP¹, département de physiologie *Department of Physiology, University of Lausanne, Lausanne, Switzerland², Department of Medicine, University of California at San Francisco, San Francisco, California³, Basic Science, Touro University, Mareland, California⁴, Department of Physiology, University of Lausanne, Lausanne, Switzerland⁶,*

High-fructose diet stimulates hepatic de novo lipogenesis (DNL) and causes hypertriglyceridemia and insulin resistance in rodents. Fructose-induced insulin resistance may be secondary to alterations of lipid metabolism. In contrast, fish oil supplementation decreases triglycerides and may improve insulin resistance. Therefore, we studied the effect of high-fructose diet and fish oil on DNL and VLDL triglycerides and their impact on insulin resistance. Seven normal men were studied on four occasions: after fish oil (7.2 g/day) for 28 days; a 6-day high-fructose diet (corresponding to an extra 25% of total calories); fish oil plus high-fructose diet; and control conditions. Following each condition, fasting fractional DNL and endogenous glucose production (EGP) were evaluated using [1-¹³C]sodium acetate and 6,6-²H₂ glucose and a two-step hyperinsulinemic-euglycemic clamp was performed to assess insulin sensitivity. High-fructose diet significantly increased fasting glycemia ($7 \pm 2\%$), triglycerides ($79 \pm 22\%$), fractional DNL (sixfold), and EGP ($14 \pm 3\%$, all $P < 0.05$). It also impaired insulin-induced suppression of adipose tissue lipolysis and EGP ($P < 0.05$) but had no effect on wholebody insulin-mediated glucose disposal. Fish oil significantly decreased triglycerides (37%, $P < 0.05$) after high-fructose diet compared with high-fructose diet without fish oil and tended to reduce DNL but had no other significant effect. In conclusion, high-fructose diet induced dyslipidemia and hepatic and adipose tissue insulin resistance. Fish oil reversed dyslipidemia but not insulin resistance.

Increasing prevalence of diabetes mellitus and impaired fasting glucose in the Seychelles, a rapidly developing country

¹FAEH D., ²Gabriel A., ³Tappy L., ⁴Ravussin E., ⁵Bovet P.,

Université de Lausanne: département de physiologie et IUMSP¹, Ministry of Health, Victoria, Seychelles², Department of Physiology, University of Lausanne, Lausanne, Switzerland³, Pennington Biomedical Research Center, Baton Rouge, LA, U.S.A⁴, University Institute for Social and Preventive Medicine, Lausanne, Switzerland⁵,

Aims: To compare the prevalence of diabetes mellitus (DM) and impaired fasting glucose (IFG) in 1989 and 2004 in the population of the Seychelles, a rapidly developing country.

Methods: Population-based surveys were attended by 1081 persons aged 25-64 in 1989 (86.4% participation rate) and 1255 in 2004 (80.2%). Fasting blood glucose (FBG) was determined in both surveys. In 2004, an oral glucose tolerance test was performed if FBG was ≥ 5.6 mmol/l and diabetes not previously diagnosed (n=330).

Results: In 2004, the age-standardized prevalence of DM (under treatment, FBG ≥ 7.0 or 2h-BG ≥ 11.1) was 11.6% (95%CI: 8.9-14.2) in men and 11.8% (9.3-14.2) in women aged 25-64. The prevalence of impaired glucose tolerance (IGT, 2h-BG: 7.8-11.0) was 11.2% in men and 9.7% in women. The prevalence of IFG (FBG: 5.6-7.0) was 30.3% in men and 18.0% in women. DM, IGT and IFG were strongly associated with overweight and waist circumference. Based on FBG only, the prevalence of DM increased from 6.2% in 1989 to 9.6% in 2004, with 31% and 56% of them being aware of having DM, respectively. In the same 15-year period, mean body mass index and blood insulin concentration increased largely.

Conclusion: The prevalence of diabetes increased markedly during the past 15 years, which paralleled a sharp increase in the prevalence of overweight. High prevalences of IFG and/or IGT suggest that DM prevalence could further increase in the near future.

Smoking, alcohol drinking and cannabis use in adolescents in Seychelles (Indian Ocean), a country in rapid transition

¹FAEH D., ²Bovet P., ³Viswanathan B., ²Chiolero A., ⁴Warren W.,

Université de Lausanne: département de physiologie et IUMSP¹, University Institute for Social and Preventive Medicine, Lausanne, Switzerland², Ministry of Health, Victoria, Seychelles³, Centers for Disease Control and Prevention, Atlanta, USA⁴,

Objective: Risk behaviors tend to cluster among adolescents in most developed countries. This study aims at examining the prevalence of smoking, alcohol drinking and cannabis use in secondary school students in the Seychelles islands, a rapidly developing island state in the Indian Ocean.

Methods: Survey in a representative sample of all secondary school students in the Seychelles using an anonymous self-administered questionnaire (Global Youth Tobacco Survey). Smoking cigarettes on ≥ 1 day in the past 30 days; drinking any alcohol beverage on ≥ 1 day in the past 30 days and having used cannabis at least once in the past 12 months were considered.

Results: 1'321 (92%) of 1'442 eligible students aged 11 to 16 years completed the questionnaire. In boys and girls, respectively, the prevalence (95% CI) was 30% (26-34) / 21% (18-25) for smoking, 49% (45-54) / 48% (43-52) for drinking, and 17% (15-20) / 8% (6-10) for cannabis use. The prevalence of smoking, drinking and cannabis use increased with age. Smokers were two times more likely than non-smokers to drink and nine times more likely to use cannabis. Drinkers were three times more likely than non-drinkers to smoke or to use cannabis. All three risk behaviors were found in 9% of boys and 4% of girls.

Conclusion: Smoking, drinking and cannabis use were common and tended to cluster among secondary students. This stresses the need for early and integrated prevention programs.

FISH OIL EFFECTS ON ENERGY AND SUBSTRATE METABOLISM DURING EXERCISE IN HEALTHY MEN

¹BORTOLOTTI M., ²Tappy L., ²Schneiter P.,

Département de Physiologie¹, Physiologie²,

Objectives Fish oil consumption is thought to have cardioprotective effects through multiple mechanisms, including modulation of metabolic pathways. In this regard, FO supplementation prevents the development of diet-induced obesity and insulin resistance in rodents, and upregulate the expression of UCP3 in skeletal muscle. Thus it may be hypothesized that FO alters energy efficiency and/or lipid oxidation.

Methods 8 healthy male volunteers were studied with and without FO supplementation. Energy efficiency was assessed during 30 min of cycling exercise at 50% VO₂max performed 2h30 after a standardized breakfast. To be sure that postprandial state does not alter results, 4 of the 8 volunteers were asked to perform exercise in fasting state. Glycaemia, insulinemia, NEFAs concentrations, substrate oxidation, energy expenditure were not modified by fish oil supplementation.

Results Basal metabolic rate of fat oxidation and respiratory quotient were affected by FO, $P < 0.05$. Substrates concentrations, muscle efficiency (PPS, $P = 0.30$; FS, $P = 0.60$) and energy expenditure (PPS, $P = 0.94$; FS $P = 0.83$) were not modified between and no variation in cortisol was observed in fourth conditions.

Conclusion At rest, after an overnight fast, two weeks of FO supplementation was sufficient to alter lipid balance by increasing basal fat oxidation. However in our conditions, independently of the nutritional status, FO supplementation did not alter resting energy expenditure, energy efficiency, or the nature of fuel mix oxidized in healthy individual. It appears therefore unlikely that FO significantly contribute to weight maintenance by increasing energy expenditure during exercise in humans.

Insulin (Ins) vs. insulin-like growth factor type 1 (IGF-1) induction of sodium transport in the mCCDcl1 cells: evidence for the physiological role of IGF-1

¹GONZALEZ RODRIGUEZ E., ¹Gaeggeler H., ¹Rossier B.,

Département de Pharmacologie et Toxicologie¹,

Ins and IGF-1 have been shown to induce sodium transport (Isc) in the toad urinary bladder (Blazer-Yost *et al.* AJP 257 C612, 1989). In this amphibian model of the mammalian distal nephron, Ins and IGF-1 were equipotent, with similar threshold (0,1 nM), half-maximal (1 nM) and maximal (10 nM) stimulating concentrations. At high ligand concentrations, considerable crossover of Ins and IGF-1 binding to their cognate receptors may occur despite of a ≈ 100 fold difference in affinity. In addition, the two receptors activate common intracellular pathways, phosphorylating insulin receptor substrate (IRS) proteins on the same tyrosine residues and activating the same downstream signalling cascades. In order to determine the potential physiological relevance of the Ins vs IGF-1 signaling cascade in the distal nephron, we have took advantage of a new renal cell line derived from mouse cortical collecting duct (mCCD_{cl1}) by measuring the dose-dependency of the insulin- and IGF-1-stimulated Isc and its epithelial polarity. Both Ins and IGF-1 rapidly increased Isc (peaking at 1 h) in a dose-dependent manner when the hormones were applied on the basolateral side, but not on the apical side. IGF-1 is 50 fold more potent than to insulin ($K_{1/2}=0,41\pm 0,07$ nM vs. $20,88\pm 2,98$ nM) with similar maximal effect ($9,1\pm 0,3$ $\mu\text{A}/\text{cm}^2$ vs. $9,8\pm 0,3$ $\mu\text{A}/\text{cm}^2$). The responses were sustained for at least 6 hours. The initial response was insensitive to Actinomycin D (1 μM) whereas the sustained response was blocked. When applied at the same time as aldosterone both hormones were synergistic and were blocked by 50 μM LY294002. We conclude that: 1) Ins and IGF-1 increase Isc in the mCCD_{cl1} cells by occupancy of a basolateral receptor; 2) IGF-1 Isc response is observed at physiological concentrations presumably by activating its cognate receptor (IGF-1R). 3) Ins Isc response is observed at supra physiological concentrations presumably by "illicit" occupancy of IGF-1R; 4) the sustained response to insulin and IGF-1 is a transcriptionally mediated process, while the initial response is not; 4) both the aldosterone and IGF-1 responses are mediated by the PI3-K pathway. Our results may be relevant to understand the interaction between aldosterone and IGF-1 pathways during the circadian cycle and to explain the high prevalence of hypertension in acromegalic patients.

Effect of age and menopausal status on indices of coronary vasomotion in women without coronary risk factor

¹PRIOR J., ²Facta A., ²Schindler T., ²Oxilia-Estigarribia M., ²Hernandez-Pampaloni M., ²Campisi R., ²Zhang X., ¹Bischof Delaloye A., ²Nathan L., ²Schelbert H.,

Service de Médecine nucléaire¹, David Geffen School of Medicine, UCLA²,

Aim: The effect of menopause on coronary vasomotion indices has not been characterized in healthy women, and may help to understand the controversial cardiovascular effects of hormone replacement therapy (HRT). This study investigated whether aging and menopause would influence myocardial blood flow (MBF) responses to cold pressor testing (CPT; mainly endothelium-dependent, a marker of future atherosclerotic events) and pharmacologic vasodilation (STR; mainly vascular smooth-muscle-dependent) as measured by PET and ¹³N-ammonia.

Methods: Thirty women without coronary risk factor or HRT were subdivided according to menopausal status: Group 1 (n=14 premenopausal women; aged 32±6y [24-43y]) and Group 2 (n=16 postmenopausal women [menses cessation ≥1y]; aged 55±6y [46-67y]). MBF was measured at rest, during CPT (ice water) and STR (dipyridamole/adenosine). Wilcoxon ranksum tests and Spearman correlations were considered significant for p≤0.05.

Results: All laboratory and clinical variables were within normal range, but postmenopausal women presented higher total cholesterol (204±22 vs. 166±33mg/dl), LDL (124±19 vs. 102±30mg/dl), fasting glucose (87±9 vs. 78±8mg/dl) and mean arterial pressure (MAP; 89±10 vs. 74±6mmHg). During CPT, MAP and rate-pressure product (RPP; cardiac work index) were higher in Group 2, but the change in RPP from rest was similar across groups; during STR, heart rate (HR) was lower in Group 2. There was no intergroup difference in MBF at rest or in response to CPT and STR. Moreover, although some hemodynamic variables were correlated with age (MAP-RST, MAP-CPT, MAP-STR, RPP-RST, HR-STR), none of the MBFs was associated with age (all p>0.47).

Conclusions: Menopause and aging did not worsen the endothelium-dependent and -independent indices of coronary vasomotion in women with presumably healthy vasculature. Thus, in this population with low risk of cardiovascular events and normal coronary vasomotion, HRT might bring limited cardioprotective benefit.

MBF (ml/min/g)	Group 1	Group 2	P-Value
Rest	0.62±0.10	0.67±0.16	0.59
CPT	0.84±0.09*	0.91±0.20*	0.23
ΔCPT from Rest	0.22±0.09	0.23±0.10	0.53
STR	2.08±0.34*	2.12±0.63*	0.97

*p≤0.001 vs. Rest.

Should coronary circulatory dysfunction be part of the definition of the metabolic syndrome? A factor analysis using PET-measured myocardial blood flows with N-13-ammonia in nondiabetic individuals

¹PRIOR J., ²Schindler T., ²Hernandez-Pampaloni M., ²Facta A., ²Zhang X.,
¹Bischof Delaloye A., ²Hsueh W., ²Quiñones M., ²Schelbert H.,

Service de Médecine nucléaire¹, David Geffen School of Medicine at UCLA²,

AIM: Considerable controversies exist about the exact abnormalities that are part of the metabolic syndrome (MetS), which is a number of metabolic or physiologic abnormalities occurring together more often than by chance alone. Coronary circulatory dysfunction has been associated with individual abnormalities seen in conjunction with MetS. The aim of our study was to examine the interrelations of MetS criteria and coronary circulatory dysfunction.

METHODS: In 78 nondiabetic individuals (64% women, aged 33±6y) with various criteria of the MetS (overall prevalence 26%, defined according to ATPIII), we characterized coronary circulatory function with myocardial blood flow (MBF) measurements with PET and N-13-ammonia, at rest and during cold pressor testing (CPT= MBF difference from rest to a 2-min hand immersion in ice water, reflecting the mostly endothelium-dependent vasomotion) and dipyridamole (DIP, 4-min infusion, reflecting the total integrated vasodilator capacity). Principal component factor analysis was performed to define the factors composed of variables most often associated with MetS (BMI, triglycerides [TG], HDL, blood pressure [SBP/DBP], fasting glucose [GLUC]) and CPT and DIP responses, retaining only eigenvalues ≥ 1 , using Varimax rotation and considering only orthogonal factor loadings ≥ 0.4 .

RESULTS: The analysis suggested that at least 3 components were needed to explain the majority of the total variance (60%) in our set of 8 variables. The first component was constituted of 5 variables (BMI, TG, HDL, GLUC and CPT) explaining 31% of the variance, which is consistent with CPT response being associated with a metabolic component. The second component was related to blood pressure (SBP/DBP) with 15% of the variance explained. The last component was associated DIP response with HDL (14% of the variance).

CONCLUSIONS: Indices of coronary circulatory function, the endothelium-dependent vasomotion to sympathetic stimulation with cold and the total integrated vasodilator capacity, were among the variables often associated with MetS. This suggests that endothelial dysfunction could be considered as belonging to the core abnormalities of MetS. Thus, it may be advantageous to consider including abnormal coronary circulatory function in future definitions of this syndrome.

How close is the agreement between the guidelines for the primary prevention of cardiovascular diseases?

¹PRIOR J., ²Darioli R., ³Perdrix J., ⁴Kappenberger L.,

Service de Médecine nucléaire¹, PMU Lausanne, Department of Cardiology, CHUV², PMU Lausanne³, Department of Cardiology⁴,

How close is the agreement between the guidelines for the primary prevention of cardiovascular diseases?

Roger Darioli^{o*}, Jean Perdrix^{*}, Lukas Kappenberger^o, John Prior⁺

Department of Cardiology^o, Medical Policlinic^{*}, Department of Nuclear Medicine⁺, University Hospital, CH-1005 Lausanne, Switzerland

Background: Current guidelines for the primary prevention of cardiovascular disease (CVD) in clinical practice have emphasized the need to base intervention on assessment of individual global risk rather than on the level of any particular risk factor (RF). In contrast to NCEP/ATP-III guidelines, 3JE-ESC as well as IAS harmonized guidelines (IAS-HG) have included adjustment for European countries at low risk for CVD, such as Switzerland.

Objective: the objective of this study was to compare the risk stratification and the eligibility for lipid-lowering drug therapy when using these three most recommended guidelines.

Patients and method: 8829 individuals (F=41%), aged from 20-80yr, (mean = 45±12 yr) recruited in the "Lausanne Health Promotion Program" during 2001-2004 were analysed to assess their 10-year CV-risk and their eligibility for lipid-lowering drug therapy (LLD), using the three different guidelines mentioned above. Individuals with history of CVD and/or diabetes mellitus were excluded of this study. The determination of CV-RF was performed by standardized methods.

Results : the prevalence of CV-RF among the participants was the following: current smoking = 26%, hypertension = 27%, hypercholesterolemia = 18% and obesity = 12%. Comparative results for percentages of CV-high risk patients and LLD eligibility are presented in the next table:

Categories	3JE-ESC	IAS-HG	NCEP/ATP-III
High-risk (%)	1.4	0	4
Moderate-risk	--	29	26
Low-risk	98.6	71	70
Eligibility to LLD (%)	2.3	11.0	15.8
- agreement (%)	reference	90	86
- kappa value	"	0.22 (p< 0.001)	0.20 (p< 0.001)

The agreement between IAS-HG and NCEP-ATP-III guidelines achieves 99% with a higher kappa value (0.79, p< 0.001).

Conclusion: Our analysis demonstrated pronounced differences between guidelines, with marked clinical and economical implications. These resultants suggest the need to evaluate the additional predictive value of new techniques of atherosclerosis imaging to improve the identification of patients requiring more intensive therapy.

PREVALENCE AND CHARACTERISTICS OF METABOLIC SYNDROME: THE NEED OF A NEW STRATEGY OF PREVENTION

¹Darioli R., ²Perdrix J., ²Cornuz J., ³Masson J., ⁴Prior J.,

Department of Cardiology, CHUV¹, PMU Lausanne², Federation of Health Leagues, Lausanne³, Nuclear Medicine Department⁴,

Background: Primary prevention of cardiovascular diseases (CVD) is based on early identification of high-risk (HR) patients requiring more aggressive therapy. US and European guidelines have included Metabolic Syndrome (MS) as a key factor associated with HR for CVD. The purpose of this study was to evaluate the prevalence of MS among the participants to the "Lausanne Health Promotion Program", which was based on a traditional approach to prevent CVD.

Patients and Methods: This prospective study was carried out in Western part of Switzerland. From January 2001 to June 2004, using a mobile unit, 9'222 free-living participants (P) aged 18-80y were screened with standardized methods for CVD risk factors (RF), lifestyle habits, current drugs history. MS was defined according to ATP-III criteria (JAMA 1999; 285:486).

Results: Among 3,774 females (F) and 5,448 males (M), aged from 18 to 80y, 9.6% of F and 15.7% of M achieved > 3 criteria for MS and the prevalence of MS increased with age (decade) from 2% to 29% in F and from 6% to 26% in M. Among P with MS, hypercholesterolemia and hypertension were treated in 8% and 12%, respectively. Current smoking and lack of regular physical activity were observed in 27% and 45% of these P. Furthermore, the awareness of P for the MS was about zero.

Conclusions: In regard to the high prevalence of MS among our population, new strategies are urgently requested to identify this epidemic and to provide appropriate recommendations in the whole population in order to prevent further morbidity and mortality owing to diabetes and CVD.

Hypertension in the Seychelles population: Trends in prevalence, awareness, treatment and control, 1989-2004

¹DANON N., ¹Chiolerio A., ²Fostel J., ³Burnier M., ¹Paccaud F., ²Bovet P

¹University Institute of Social and Preventive Medicine, Lausanne, Switzerland

²Ministry of Health, Victoria, Seychelles

³Néphrologie, CHUV³,

Objective: To assess trends in blood pressure (BP) levels and control indicators in the Seychelles (Indian Ocean), a rapidly developing middle-income country, from 1989 to 2004.

Design and method: Independent population surveys were carried out in 1989 and 2004 using random age- and sex-stratified samples of the populations aged 25-64. Participation was 86% in 1989 and 80% in 2004.

Main outcome measures: The mean of the last two of three BP readings (mercury sphygmomanometer) was used. Body-mass index (BMI) was calculated. Results are standardized for age.

Results

	Men		Women	
	1989 (N = 513)	2004 (N = 568)	1989 (N = 568)	2004 (N = 687)
Mean				
Systolic BP (mmHg)	132.7	131.1	127.3	124.4*
Diastolic BP (mmHg)	87.1	85.5	82.5	81.3
BMI (kg/m ²)	23.3	25.5*	25.9	28.3*
Prevalence (%)				
BP ≥140/90	44.5	38.4*	32.8	24.8*
BP ≥140/90 or treatment (=HBP)	45.3	43.6	34.5	35.6
Among subjects with HBP:				
Aware	36.1	54.6*	49.1	75.1*
Treated	15.1	49.1*	30.8	72.1*
Controlled (<140/90)	1.7	11.9*	4.9	30.2*
Overweight (BMI ≥25kg/m ²)	27.9	51.9*	51.2	68.3*

*p<0.05, 1989 versus 2004

Mean systolic and diastolic BP decreased slightly from 1989 to 2004, while mean BMI increased sharply. Prevalence of hypertension remained stable. A marked improvement in awareness, treatment and control of hypertension is observed. Despite their lower BP values and prevalence of hypertension, women were more frequently aware, treated, and had a better control of hypertension.

Conclusion: The management of hypertension has been markedly improved in the Seychelles. However, this improvement is reflected essentially in a slight decrease in mean BP. This mitigated result is probably explained by the strong increase of BMI.

Human oxidized low-density lipoprotein-particles reduce the production and glucose-induced secretion of insulin: Implication of JNK signalling pathway.

¹ABDERRAHMANI A., ²Niederhauser G., ²Ferdaoussi M., ²Lenain v., ³Regazzi R., ²Waeber G.,

*Médecine Interne*¹, *Internal Medicine*², *Department of Cell Biology and Morphology*³,

Low Density Lipoprotein (LDL)-particles and oxidized-LDL (ox-LDL) concentrations are often increased in patients with Type 2 Diabetes (T2D) and metabolic syndrome. In this report, we investigated the effects of human LDL-particles in insulin expression and secretion in beta-cells. Two different insulin-secreting cell lines (INS-1 and MIN6) were incubated in the presence of different concentrations of LDL and ox-LDL (0.5 and 1 mM cholesterol). Compared to native human LDL-particles, ox-LDL-particles induced a drastic reduction in insulin expression and content. Glucose, leucine or KCl-induced insulin secretion was also impaired by ox-LDL compared to that with native LDL-particles. To identify the mechanism by which ox-LDL exerts its effect on insulin production, the rat insulin promoter construct linked to a luciferase gene reporter (RIPluc) was transiently transfected in the presence of LDL or ox-LDL. In the presence of ox-LDL particles, the luciferase activity of RIPluc was reduced by 75% compared to native LDL, indicating a loss of the transcriptional activity of insulin gene by ox-LDL. We next investigated whether the oxidative stress induced by ox-LDL particles might activate a MAPK signalling cascade. Ox-LDL particles reduced the expression of Islet-Brain 1/JNK-Interacting protein-1, resulting in the activation of JNK. Inhibition of JNK pathway by using JNK inhibitors peptides (JNKi) prevented the loss of insulin expression induced by ox-LDL. In conclusion, human ox-LDL particles have several deleterious effects on beta-cell function including a reduction in insulin gene transcription, insulin content and secretion. These effects are mediated, in part, by the activation of JNK and blocked by the use of JNKi.

Effects of a 4-week high fructose diet on insulin sensitivity and ectopic lipids

Kim-Anne Lê¹, David Faeh^{1,2}, Rodrigue Stettler¹, Michael Ith³, Roland Kreis³, Peter Vermathen³, Chris Boesch³, Eric Ravussin⁴, LucTappy^{1,5}

¹Department of Physiology, University of Lausanne, 1005 Lausanne, Switzerland

²University Institute of Social and Preventive Medicine, 1005 Lausanne, Switzerland

³Department of Clinical Research, MR Spectroscopy and Methodology, University of Bern, Switzerland

⁴Pennington Biomedical Research Center, Baton Rouge, LA, U.S.A.

⁵Division of Diabetes, Endocrinology and Metabolism, Lausanne University Hospital, 1011 Lausanne, Switzerland

Rodents fed a high fructose diet develop dyslipidemia and insulin resistance. It is however not known whether similar effects are observed in humans. We therefore assessed the impact of a 4-week high fructose diet (HFr) on insulin sensitivity (IS), ectopic lipids, glucose and lipid homeostasis.

Seven healthy men (24.7 ± 1.3 y; 17 ± 0.7 % body fat; Mean \pm SEM) underwent a 4-week HFr with 1.5 g fructose/kg/d supplementation. Fasting blood samples were collected weekly; IS, intrahepatocellular (IHCL) and intramyocellular (IMCL) lipids contents were measured before and after 1 and 4 weeks of HFr. Hepatic IS was assessed by the measures of hepatic glucose production (HGP by 6,6-²H₂ glucose) and its suppression by insulin whereas muscle IS was measured by whole body glucose disposal rate (GDR) during a 2-step hyperinsulinemic euglycemic clamp (0.3 and 1 mU/kg/min, 90 min each). Adipose tissue IS was estimated by measuring the decrease in systemic nonesterified fatty acids (NEFA) during the low dose insulin infusion. IHCL and IMCL were measured by ¹H magnetic resonance spectroscopy.

Within 4 weeks, HFr caused significant ($P < 0.05$) increases in fasting plasma concentrations of TG (+47%), very low density lipoprotein-TG (VLDL-TG) (+72%), lactate (+49%), glucose (+5.5%) and leptin (+48%) but did not change body weight, IMCL, IHCL and IS. IHCL correlated negatively with fasting TG after 4 weeks Hfr ($p < 0.05$). A similar trend was found at baseline and after one week, but did not reach significance. HFr shifted the relationship with fasting TG to the night.

These results indicate that short term high fructose diet increases hepatic triglyceride production in healthy subjects. However, it did not cause ectopic lipid deposition or insulin resistance, suggesting that hepatic triglyceride secretion and extrahepatic lipid disposal were stimulated appropriately to match hepatic lipid synthesis.

The N-terminal caspase-generated fragment of RasGAP (fragment N) negatively regulates Akt-mediated NFκB activation.

¹LOUKILI N., ¹Loukili N., Widmann C.,

DBCM¹, CHUV Lausanne

RasGAP is an unconventional caspase-3 substrate as it inhibits, rather than favors, apoptosis once partially cleaved into an N-terminal fragment named fragment N. This fragment protects cells by activating the Ras-PI3K-Akt pathway. Interestingly, fragment N blocks the ability of the activated Akt to stimulate NFκB. It has been shown that Akt/PKB stimulates NFκB by activating the Cot/Tpl2 kinase (a serine/threonine kinase, member of the mitogen-activated protein kinase kinase kinase (MAP3K)), which in turn phosphorylates and activates the IKKs and consequently NFκB. Here we show that the ability of fragment N to block Akt-induced activation is mediated by the capacity of fragment N to compete with Cot for binding to Akt. This might be crucial for fragment N to protect cells that are sensitive to NFκB-induced death such as pancreatic α cells.

GEN
Gènes et Environnement

Glutathione related genes and the risk of schizophrenia

¹TOSIC M., ²Ott J., ²Baral S., ¹Bovet P., ¹Deppen P., ¹Gheorghita F., ¹Matthey M., ³Parnas J., ¹Preisig M., ¹Saraga M., ¹Solida A., ⁴Timm S., ⁵Wang A., ⁶Werge T., ¹Cuenod M., ¹Do K.,

DUPA¹, Laboratory of Statistical Genetics, Rockefeller University, New York², University Department of Psychiatry, H:S Hvidovre Hospital, Denmark³, University Department of Psychiatry, H:S Frederiksberg, Denmark⁴, University Department of Psychiatry, H:S Amager Hospital, Denmark⁵, Copenhagen University, Denmark⁶,

Schizophrenia is a complex multi-factorial psychiatric disease with a strong genetic component. Previous studies showed decreased level of glutathione (GSH), the principal non-enzymatic antioxidant and redox regulator, both in cerebrospinal fluid and in prefrontal cortex. Expression study of 12 glutathione related genes in fibroblast cultured from skin biopsy showed significantly lower mRNA levels in patients for two genes: glutathione synthetase (GSS), and glutamate-cysteine ligase M (GCLM), modifier subunit of glutamate-cysteine ligase. These enzymes are directly involved in GSH synthesis and their expression is correlated.

To identify possible genetic causation to the diminished GSH levels, abnormal GSS and GCLM mRNA levels and eventually genetic factors involved in schizophrenia, we studied association of the SNP variants for GCLM and GSS genes and schizophrenia patients in two independent populations. Case-control association study in Lausanne sample (40 patients/31 controls) of 8 GCLM and 9 GSS SNP markers showed that the most common GCLM variants have significant joint effects on the risk of disease ($p=0.0009$). Genotype frequency analysis in a much bigger sample from Danish population (349/348) confirms a very strong association of GCLM SNP rs2301022 localized in the intron1. Nine patterns of CNP-588, rs2301022 and rs718875 in the 3,000 bp region that includes GCLM exon 1 showed different frequencies between patients and healthy controls, with Chi square value of 30.39 and $P=0.00375$. Linkage between schizophrenia and the GCLM SNPs was confirmed in independent set of family data (NIMH Genetics Initiative for Schizophrenia). These results suggest that particular alleles of GCLM and possibly GSS are vulnerability factors for schizophrenia and could be used as prediction tools.

Patterns in Retrovirus-Primate Host Co-evolution.

¹Ortiz M., ¹Bleiber G., ¹Martinez R., ²Kaessmann H., ¹Telenti A.,

Institut microbiologie¹, Centre intégratif de génomique²,

Background:

The current distribution of retroviruses among human and non-human primate species reflects substantial co-evolution between the host and the infectious agent. Adaptation of the virus to pressure exerted by the immune system and other host cell barriers (such as innate cellular defenses), will affect the evolution of both host and viral genomes. Evolutionary analysis may serve as a useful tool to identify the host and viral proteins involved in genetic conflicts. The present study assesses global adaptation between primates and SIVs, and uses four model host proteins to better define patterns of adaptive evolution.

Methods:

Congruence of host and virus phylogeny was tested as follows. First a phylogenetic tree was reconstructed based on all available full-length genomes from SIV isolates using MEGA3.1. These were then matched to the phylogenetic tree of human and non-human primates. Patterns of substitutional evolution were assessed for TRIM5, TRIM19/PML, PPIA, and APOBEC3G using DNA from human, great apes, gibbons, Old World and New World monkeys. All selection analyses, including the analysis of positive selection in the cellular defense genes were performed by the PAML (Phylogenetic Analysis by Maximum Likelihood) program package.

Results:

Matching of primate and SIV/HIV phylogenetic trees indicate that host-virus co-evolution precisely predicts the phylogeny of SIV isolates. Detailed analysis of the four model proteins confirmed the previously described pattern of (i) strong positive selection on TRIM5 and multiple regions of conflict, and identified (ii) strong positive selection on APOBEC3G with better defined regions of host gene-virus co-evolution than previously reported, (iii) strong purifying selection for TRIM19/PML with absence of residues under positive selection, and (iv) full conservation of PPIA among primates.

Conclusions:

Comparative phylogenetic analysis underscores the extent of co-evolution of the primate hosts and their SIV species. In contrast to TRIM5 and APOBEC3G, evolutionary analysis at the protein level suggests that PPIA (incorporated into HIV-1) is not under differential pressure in primates. The strong conservation of the TRIM19/PML protein sequences among primates suggests that this gene does not play a role in antiretroviral defense.

Variation in the Antiretroviral Protein TRIM5alpha in Humans

¹Goldschmidt V., ¹Ortiz M., May M., ¹Martinez R., ²Kaessmann H., ¹Bleiber G.,
¹Telenti A.,

Institut de microbiologie¹, Centre intégratif de génomique²,

Background:

The host protein TRIM5a is a key mediator of restriction to foreign viruses. Although TRIM5 of Old World monkeys shows high sequence similarity to human TRIM5, HIV encounters a block after entry into these primate cells. We seek to identify differences in TRIM5 sequences in humans, to determine sequence conservation in monkeys and to assess their influence on HIV-1 progression in vitro and in vivo.

Methods:

SNP discovery used a panel of DNA from 128 healthy Swiss Caucasian blood donors. DNA was investigated by single strand conformation polymorphism and sequencing using primers targeting exons, intron/exon boundaries and promoter. For evolutionary analysis, DNA of apes, Old and New World monkeys (n=15) was amplified with the same primers and subjected to sequence alignment with the human reference.

SNPs were assessed in vitro by measuring HIV-1 replication in CD4+ T-cells of healthy blood donors, and in vivo by analysing square root transformed CD4 T cell counts - modeled as a linear function of time since estimated date of seroconversion - in participants of the Swiss HIV Cohort Study (n=851).

Results:

Of 5970 bp analysed in human TRIM5, 21 polymorphisms were identified: 16 are in the non-coding region, 5 are coding, of which 4 change the amino acid: H43Y (ring domain), R136Q (coiled-coil domain), G249D, H419Y (SPRY domain). Comparative sequence analysis with non-human primates revealed sequence conservation for amino acids except for R136. Surprisingly, the human variant glutamine at this position (allele frequency of 35%), is present in all apes and monkeys except for chimpanzee.

No influence on HIV-1 replication in vitro was observed for the SNPs. In vivo, the low frequency haplotype (0.6%) comprising 746A (249D) and 1255T (419Y) associated with CD4+ cell improvement (gradient offset: 0.94, SE: 0.73).

Conclusion:

Human TRIM5 shows a high sequence variability in a DNA collection of healthy blood donors, with an unusual high number of non-synonymous amino acid substitutions. They occur mainly at evolutionary conserved sites and therefore deserve further analysis. Our in vivo data may reveal protective effects for two variant alleles – trends that may be confirmed in a bigger dataset.

Keywords: TRIM5a, SNP, HIV-1

Novel dystrophin mutation revealed by systematic analysis of muscle dystrophin mRNA in a BMD family

¹KUNTZER T., ²Dunand M., Leturcq F., ²Kuntzer T.,

Neurologie Bh07/306¹, neurologie chuv²,

Introduction: Duchenne's (DMD) and Becker's (BMD) muscular dystrophies are allelic X linked neuromuscular disorders. They are due to mutations in the dystrophin gene. Large deletions of this gene are the cause of most (@65%) cases of DMD/BMD. The remaining cases are mainly due to point mutation which until recently were underdiagnosed. This can lead to difficulties assessing the diagnosis and giving accurate genetic counseling.

Objective : To highlight difficulties in assessing the diagnosis in point mutation of the dystrophin gene resulting in alteration of RNA splicing in one Becker patient. To make a phenotype-genotype correlation in a novel point mutation of the dystrophin gene.

Material and method : This 42-year-old father of 3 girls, was investigated since his last teens for a progressive limb-girdle weakness. At age 4 his calves were hypertrophic and he had a tendency to walk on hills. By age 10, he was complaining of calves cramps and by age 20, climbing stairs became difficult. Since 30-year old, he fell occasionally, but is still ambulant. Exertional myoglobinuria happened twice. One out of his 3 brothers is known to have the same clinical pattern. On examination calves are hypertrophic, he has mild proximal muscle weakness of the upper extremities and severe proximal muscle weakness on lower limbs. Walking unaid is hardly achieved. Serum creatine kinase levels have always been elevated 5-10 folds. Three muscle biopsy have revealed a dystrophic pattern. Western-blot analysis showed reduction of normal size dystrophin. Heart evaluations were normal. A diagnosis of BMD has been suspected since 1989. After gross gene defect was excluded by PCR multiplex and Southern blot, complete muscle dystrophin mRNA was analyzed by RT-PCR amplification and sequenced. Point mutation was confirmed by sequencing genomic DNA.

Results: A point mutation (IVS 43 + 5 del G) was found, resulting in alternative splicing of mRNA.

Conclusion: The BMD phenotype without cardiomyopathy of our patient is explained by the presence of an alternative splicing of mRNA leading to a normal but diminished dystrophin.

Genetic Variability of CYP2B6 in Individuals with Extremely High Efavirenz Plasma Concentrations

¹ROTGER M., ³Colombo S., ³Cavassini M., ⁴Furrer H., ⁵Elzi L., ⁶Günthard H.,
³Décosterd L., ¹Telenti A.,

Institute de Microbiologie¹, University Hospital, Lausanne³, University Hospital, Bern⁴, University Hospital, Basel⁵, University Hospital, Zurich⁶,

Background: Plasma concentrations of efavirenz (EFV) are known for a high degree of inter-individual variability. EFV is mainly metabolized by CYP2B6. We looked for genetic polymorphisms in the CYP2B6 gene in individuals with extremely high EFV plasma levels in order to identify genetic polymorphisms that could explain the extremely elevated drug concentrations.

Methods: Genomic DNA was obtained from 5 individuals with repeatedly high plasma concentrations in the range of 9165 to 59400 ng/ml (therapeutic range, 1000 to 4000 ng/ml). All presented neuropsychological toxicity that resolved after treatment discontinuation or dose reduction. Promoter region (3051bp) including the phenobarbital-responsive enhancer module (PBREM) and the xenobiotic responsive enhancer module (XREM), and the nine exons together with the exon-intron boundaries (3917bp) of CYP2B6 were screened by direct sequencing.

Results: All individuals carried two copies of known or probable SNPs associated with loss of function. Two individuals were CYP2B6*6D (Q172H, K262R) homozygous (one native of Switzerland and the other of Thailand). A third individual (native of Thailand) carried one CYP2B6*6E allele (also characterized by Q172H, K262R) and one *6D copy. The fourth individual (native of Congo) carried the recently reported CYP2B6*18 (I328T) and one *6D copy. The last patient (native from Ivory Coast) carried a possible new allele which would include new exonic nonsynonymous SNPs in exon 6 (T306S) and in exon 7 that introduces a stop codon (R378stop) and one *6D copy. Previously reported SNPs were identified in the promoter region; none were localized in the PBREM or in the XREM modules.

Conclusions: Independently of the diverse ethnicities, these individuals consistently presented two copies of CYP2B6 loss-of function alleles. Other predisposing

Transcriptional profiling of homogenous pools of dorsal root ganglia neurons for the study of neuropathic pain mechanisms

¹BERTA T., ²Perrin F., ³Pertin M., ⁴Descombes P., ³Gilliard N., ³Spahn D., ⁵Kato A., ³Décosterd I.,

*Anesthésiologie*¹, *CMU, Genève*², *Anesthésiologie, Lausanne*³, *NCCR "Frontiers in Genetics", Genève*⁴, *CMU, Genève*⁵,

Peripheral neuropathic pain (NP) is a chronic and intractable type of pain related to peripheral nerve damage or dysfunction. NP is the result of changes in injured and in adjacent non-injured neurons by which of particular concern are transcriptional modifications in non-injured nociceptors. By combining laser capture microdissection (LCM) and microarray technologies, our aim is to identify a specific transcriptional profile due to peripheral nerve injury in the population of nociceptors, while injured nociceptors, other dorsal root ganglia (DRG) neurons and satellite cells are excluded of the analysis. In the spared nerve injury (SNI) rat model, injections of retrograde fluorescent tracer in specific nerve territories were applied to distinguish injured and non-injured neurons in DRG. One week after SNI, DRG were collected and handled in RNase free conditions. Collection by LCM of neuron of interest was established by the presence of fluorescence and cell size. RNA quality was assessed by electrophoresis and linearly amplified. Cell capture accuracy was verified with real-time RT-PCR by the absence/presence of specific cell-type markers. Electropherograms and GeneChip Test3 (Affymetrix) demonstrated a high quality of our RNA issue from pools of 2500-3000 captured cells. GFAP (satellite cell marker) and NF-200 (large cell marker) transcripts are absent from samples of nociceptors and presence of ATF3 (marker of cell injury) is present only in injured nociceptor samples. Accurate results obtained after analysis by Affymetrix GeneChip shows the feasibility of our procedure. We successfully implement a large-scale approach using LCM and microarray technology for analyzing thousand of genes in specific neuronal populations. This approach will be essential for dissecting out molecular mechanisms of neuropathic pain disease. This study is supported by Swiss national science foundation and Mercier foundation for science.

DESCRIBING PATHOGENICITY ISLAND TRANSFERS USING BIOINFORMATICS.

¹COLLYN f., ²Guy L., ²Roten C.,

Dpt de Microbiologie Fondamentale¹, DMF²,

YAPI is a pathogenicity island (PAI) shared by both enteropathogenic bacteria *Yersinia pseudotuberculosis* and *Y. enterocolitica*. Thirty-two of their coding sequences were found to be related with those of SPI-7 and 1 W14, two PAIs respectively encoded by *Salmonella enterica* serovar Typhi and *Photobacterium luminescens*. Their gene organization is highly conserved, suggesting they derived from a unique genetic element transmitted to the four recipient species. This common PAI module also bears a pil operon responsible for type IV pili biogenesis similar to those encoded by the R64 conjugative plasmids family. We hypothesize that the latter plasmid family was the genetic source of this shared PAIs module.

horizontal PAI transfers are individually rare, they were seldom reproduced successfully in controlled experiments. We consequently chose bioinformatics for validating our proposal. Theoretically, conjugative plasmids could have been integrated in the chromosome of each bacterial species, leading to independent generations of similar islands. However, when comparing the frequency and gene order conservation of all orthologs shared by each PAI/plasmid, the results clearly indicate that one unique ancestral PAI emerged from the conjugative plasmid and next disseminated to the three other bacterial species by PAI transfer.

conjugative plasmid was described in *Salmonella*, and never isolated from *Photobacterium* or *Yersinia*. So, considering the most parsimonious scenario, the ancestral transmitted PAI module would have appeared in *Salmonella*. To confirm this hypothesis, we compared R64 dinucleotide usage biases to those of orthologs set of each related PAI. SPI-7 was the only one displaying dinucleotide signature close to R64-plasmid family. This is consistent with the most parsimonious scenario implying a PAI generation in *Salmonella* chromosome. Consequently, the genetic transfer occurred from *Salmonella* to *Yersinia* and *Photobacterium*: for the first time, we oriented an ancient PAI transfer using comparative PAI genomics.

Inducible nitric oxide synthase in epithelial cells of small intestine: role in innate immunity

¹SAYAR S., ¹Hausel P., ²Sirard J., ¹Felley-Bosco E.,

*Pharmacology and Toxicology*¹, *Institut de Biologie, Lille*²,

Inducible nitric oxide synthase (iNOS) is expressed in intestinal epithelial cells but its function in these cells is not clear. The aim of our study is to investigate the potential role of epithelial iNOS in innate immunity against *Salmonella typhimurium*. Indeed, although *Salmonella typhimurium* must penetrate the intestinal epithelial barrier prior to the initiation of the disease, most previous studies aimed at clarifying the role of iNOS in immunity were performed after either iv or ip administration of the bacteria. Therefore the role of epithelial iNOS is remained unanswered.

Overnight starved iNOS deficient and C57BL/6 mice receiving L-arginine, the substrate of iNOS, in drinking water were administered p.o. a *Salmonella* strain containing a transposon encoding for kanamycin resistance. 3h after gavage animals were sacrificed and small intestine was collected to analyze either iNOS expression or bacterial content. For control, spleens were also processed. The load of *Salmonella* was higher in iNOS deficient. To investigate more specifically epithelial cells, the latter were isolated from lamina propria using continuous ethylenediaminetetra-acetic acid washing of ileum. Villi fraction was collected as tissue recovered by filtering through a cell sieve. Crypts were recovered in the filtrate. To quantitatively determine villi and crypt enrichment, RNA was extracted from both fractions and cryptidin-5 (crypt marker) and aminopeptidase-N (villi marker) were measured by quantitative RT-PCR. iNOS protein and activity was determined in villi, crypt and lamina propria fractions. Expression of iNOS was detected only the villi fraction of wt mice. Villi fraction was selected to investigate the interaction of *Salmonella typhimurium* with epithelial cell using the invasion assay. During invasion assay *Salmonella typhimurium* induced iNOS expression in ileal villi of wt mice. The load of *Salmonella* was higher in villi from iNOS deficient mice.

These in vivo and ex vivo results suggest that iNOS may play role in *Salmonella typhimurium* invasion of ileal villi of wt mice.

Acknowledgments:

This work was supported by the Swiss National Science Foundation (SNSF 3100A0-103928) and EC grant QLRT2001-02357.

Characterization of the effector recognition domain of the HbpR transcription activator of *Pseudomonas azelaica*

¹VOGNE C., ¹Beggah S., ¹van der Meer J.,

Département de microbiologie fondamentale UNIL LAUSANNE¹,

Pseudomonas azelaica HBP1 is able to grow on biaromatic compounds, such as 2-hydroxybiphenyl (2-HBP), as sole carbon and energy sources. The first steps of 2-HBP metabolism depend on three enzymes encoded by the *hbp* genes: *hbpCA* and *hbpD*. Detection of 2-HBP by *P. azelaica* is achieved by a transcriptional regulatory protein, called HbpR. The gene encoding the HbpR protein is located just upstream of the *hbpCD* operon. This protein, which belongs to the XylR/DmpR-type family of transcription regulators, activates transcription from two promoters, PhbpC and PhbpD, in the presence of 2-HBP. HbpR has a modular structure consisting of an amino-terminal signal-perception A-domain linked by a short B-domain to a central activator C-domain and a carboxy-terminal D-domain containing the HTH DNA binding motif. The interaction between the A-domain and 2-HBP is supposed to cause a conformational change in the HbpR protein, which thereby becomes competent as a transcriptional activator through the C-domain localised ATPase activity. The aim of this study is to modify the effector binding domain in the regulatory protein HbpR to obtain different mutants endowed with a new effector-binding site and a wide range of substrate specificities. Firstly, the A-domain was modeled in its tertiary structure by a bioinformatics approach. Specific mutations in the A-domain gene region corresponding to two identified putative binding pockets for 2-HBP were created by site directed mutagenesis. After the introduction of all mutated sequences in a plasmid containing an HbpR-regulated promoter driving the expression of the GFP, mutants were tested for their inducibility to different biaromatic pollutants. The position of the mutants was related to the bioinformatic-derived structure. Secondly, the HbpR protein was purified as an N-terminal HIS-tag fusion protein and subjected to cryoelectron microscopy in the presence or absence of the DNA bound by the protein.

Fine mapping of genes influencing lentiviral susceptibility

¹LOEUILLET C., ²Deutsch S., ³Munoz M., ⁴Wyniger J., ²Antonarakis S.,
⁵Beckmann J., ³Telenti A.,

*IMUL CHUV¹, Genetic Medecine and development, Geneva², Institute of Microbiology, Lausanne³,
Institute of Microbiology, Lausanne⁴, Division of medical genetic, Lausanne⁵,*

Background: Susceptibility to infectious diseases is a complex trait determined by several to many host genetic factors. Unique to infectious diseases is the possibility to establish ex vivo models of cellular susceptibility to a pathogen thereby facilitating its genetic analysis.

Material and methods: We used lymphoblastoid cell lines from multigeneration families (Centre d'Etude du Polymorphisme Humain, CEPH) to assess genetic factors influencing processes of immortalization by Epstein Barr virus (EBV), infection by HIV-1-derived lentiviral vectors, and expression of cellular proteins.

Results: The approach proved best at measuring heritability of the ex vivo trait of lentiviral transduction (23 to 54%), EBV LMP1 expression (49 to 73%), and expression of various selected cellular genes (average 14 to 100%). Linkage analysis using 200 individuals from 15 CEPH families identified a chromosomal locus on chromosome 8 for lentiviral susceptibility (LOD=2.89, $p=2E-04$, genomewide significance threshold=2.83), and on chromosome 10 for the cellular gene CD39 (LOD=8.02, $p=0$, genomewide significance threshold=7.75), indicating a cis-regulation of its expression. No eQTL was found for EBV LMP1 expression. For both traits, association analyses and fine mapping using the HapMap have confirmed these chromosomal phenotype-linked regions. For lentiviral susceptibility, analysis identified one SNP and 5 genes positional candidate genes. Three SNPs, representing two putative mechanisms of cis control were associated with the CD39 phenotype: one marker closely to the CD39 gene itself, the 2 others SNPs in incomplete linkage disequilibrium, map to a neighboring gene.

Conclusion: This approach should allow the standardized measurement of hereditary control for a wide number of infectious pathogens in a standardized ex vivo model system.

Autosomal dominant nemaline myopathy: Search for a candidate gene in a large family.

¹JEANNET P., ²Mittaz-Crettol L., ²Pittet V., ³Dunand M., ⁴Lobrinus A., ³Kuntzer T., ²Bonafe L.,

*Neuropédiatrie*¹, *Division Pédiatrie Moléculaire*², *Service de Neurologie*³, *Département de Pathologie*⁴,

Nemaline myopathy (NEM) is a rare form of congenital myopathy whose phenotype varies from severe fatal neonatal forms to milder adult onset forms. Weakness is often prominent in the face, neck and proximal limb muscles. The presence of rod-like (nemaline) structures in muscle fibers on muscle biopsy is diagnostic. Mutations in a number of different genes are known to cause this disorder. All encode components of skeletal muscle sarcomeric thin filaments (α -tropomyosin, nebulin, α -actin, skeletal, β -tropomyosin, and slow troponin T). Autosomal recessive and autosomal dominant (AD) forms exist.

We present a large AD family with an unusual, mild phenotype and an unknown genetic cause at this point.

The proband is a three year old girl who presented with neonatal hypotonia, she walked at 18 months, but still can't run at 3 years. On examination she is hypotonic, she has proximal limbs weakness and deep tendon reflexes are weak. Serum CK are normal.

Two affected first cousins walked around 24 months and can't run at three and five years. All other affected family members are adults with difficulties running, and mild axial and proximal weakness. They have no marked limitations in their daily activities. Many have been hiking in the Alps for many years as a hobby, men did their military service.

All performed biopsies showed a predominance of type I fibers, which were of smaller size (typical in many congenital myopathies). Nemaline rods were observed in only a few fibers, and seemed to increase in number with age.

Genetic linkage analysis was performed for 5 of the 6 previously described loci for NEM (NEM1 : 1q21-23, NEM3: 1q42.1, NEM4: 9p13.2-13.1, NEM5: 19q13.4 NEM6: 15q) and all were excluded in this family. The linkage analysis for the last locus is in progress as well as genome-wide analysis.

Amplification of the c-myc gene in acute myeloid leukemia harboring double minute chromosomes

D. Mühlematter¹, V. Parlier¹, S. Bougeon¹, V. Beyer¹, D. Ahmad¹, S. Arcioni¹, O. Bruzzese¹, L. Etter¹, M.-C. Ruchet¹, S. von der Aa¹, M. Duchosal², U. Hess³, S. Meyer-Monard⁴, A. Tichelli⁴, U. Schanz⁵, E. Jacky⁶, M. Jotterand¹

¹*Service de génétique médicale, Unité de cytogénétique du cancer,* ²*Service d'hématologie, CHUV, Lausanne;* ³*Fachbereich Onkologie/Hämatologie, Kantonsspital St-Gallen;* ⁴*Hämatologielabor, Universitätsspital Basel;* ⁵*Abteilung für Hämatologie, Universitätsspital Zürich,* ⁶*Abteilung für Onkologie, Universitätsspital Zürich*

Double minute chromosomes (dmin) are small extrachromosomal elements resulting from gene amplification. Dmin are rare in hematological malignancies (about 1 % of cytogenetically abnormal cases) and mainly occur in acute myeloid leukemia (AML) and myelodysplastic syndromes, often associated with trisomy 4. The prognosis associated with dmin, considered as poor, seems to be improved in the presence of an otherwise normal karyotype or a single chromosome abnormality. In hematological malignancies, while most dmin contain amplified sequences of the c-myc gene located in 8q24, the amplification of c-myc does not seem to be associated with its overexpression.

We report on 5 cases of dmin-containing AML (3M, 2F, age : 37 to 69) with amplification of the c-myc gene detected by fluorescence in situ hybridization (FISH) using 5'-and 3'-labelled dual color c-myc probes. Depending on patients studied, the total number of dmin per cell varied between 14 and 46. Three patients showed a complex karyotype including trisomy 4 in one of them and del(9)(q13q22) in 2. The 2 others patients showed either an otherwise normal karyotype or Y loss. In 2 out of the 3 cases with apparently normal chromosomes 8 and in one case with t(3;8)(p13;q24.1), the probe hybridized only to one of the 2 homologues or to the normal chromosome 8 respectively. These findings confirm previous observations and bring further support to the mechanism of deletion-episome formation-amplification for dmin generation. In the last case, a monosomy 8 detected by conventional cytogenetics was confirmed by FISH with a centromeric probe, but hybridization with c-myc probes showed 2 signals on a marker chromosome, i.e. one fusion signal and one signal corresponding to the 5' part of the gene, suggesting the presence of a c-myc rearrangement. Despite the small number of patients, our findings do not confirm the previously reported association of dmin with female sex and advanced age.

Variation in the Antiretroviral Protein TRIM5 α in Humans

Valérie Goldschmidt^{1*}, Millan Ortiz¹, Margaret May², Raquel Martinez¹, Henrik Kaessmann³, Gabriela Bleiber¹, Amalio Telenti^{1,4} and the Swiss HIV Cohort Study

Institute of Microbiology, University of Lausanne, Switzerland¹, Department of Social Medicine, University of Bristol, U.K.², Center for integrative genomics, University of Lausanne, Switzerland³, Swiss HIV Cohort Study⁴

Keywords: TRIM5 α , SNP, HIV-1

Background:

The host protein TRIM5 α is a key mediator of restriction to foreign viruses. Although *TRIM5* of Old World monkeys shows high sequence similarity to human *TRIM5*, HIV encounters a block after entry into these primate cells. We seek to identify differences in *TRIM5* sequences in humans, to determine sequence conservation in monkeys and to assess their influence on HIV-1 progression *in vitro* and *in vivo*.

Methods:

SNP discovery used a panel of DNA from 128 healthy Swiss Caucasian blood donors. DNA was investigated by single strand conformation polymorphism and sequencing using primers targeting exons, intron/exon boundaries and promoter. For evolutionary analysis, DNA of apes, Old and New World monkeys (n=15) was amplified with the same primers and subjected to sequence alignment with the human reference.

SNPs were assessed *in vitro* by measuring HIV-1 replication in CD4+ T-cells of healthy blood donors, and *in vivo* by analysing square root transformed CD4 T cell counts - modeled as a linear function of time since estimated date of seroconversion - in participants of the Swiss HIV Cohort Study (n=851).

Results:

Of 5970 bp analysed in human *TRIM5*, 21 polymorphisms were identified: 16 are in the non-coding region, 5 are coding, of which 4 change the amino acid: H43Y (ring domain), R136Q (coiled-coil domain), G249D, H419Y (SPRY domain). Comparative sequence analysis with non-human primates revealed sequence conservation for amino acids except for R136. Surprisingly, the human variant glutamine at this position (allele frequency of 35%), is present in all apes and monkeys except for chimpanzee.

No influence on HIV-1 replication *in vitro* was observed for the SNPs. *In vivo*, the low frequency haplotype (0.6%) comprising 746A (249D) and 1255T (419Y) associated with CD4+ cell improvement (gradient offset: 0.94, SE: 0.73).

Conclusion:

Human *TRIM5* shows a high sequence variability in a DNA collection of healthy blood donors, with an unusual high number of non-synonymous amino acid substitutions. They occur mainly at evolutionary conserved sites and therefore deserve further analysis. Our *in vivo* data may reveal protective effects for two variant alleles – trends that may be confirmed in a bigger dataset.

EHU
Environnement humain

Fracture Index validation in a population-based sample of Swiss elderly women using a QUS device.

¹LAMY O., Krieg M.,

*Médecine interne*¹,

Background : Due to the magnitude of osteoporosis and its related morbidity and mortality, the identification of high risk individuals for fracture is essential. The Fracture Index (6 questions), an assessment tool with or without DEXA measurement, was shown to be predictive of hip fracture, as well as vertebral and nonvertebral fractures in postmenopausal women (D. Black et al. Osteoporosis Int 2001). The Swiss Evaluation of the Methods of Measurement of Osteoporotic Fracture Risk (SEMOM) study is a prospective multicenter study which compares 3 QUS devices for the assessment of fracture risk in a population-based sample of Swiss elderly women. The aim of the study was to validate the Fracture Index in the SEMOM study, including QUS in place of DEXA measurement.

Method : Among the 7062 women age 70 years or older (75.2 ± 3.1), 607 clinical fractures were reported. According to the Fracture Index scoring, women were divided in quintiles. A linear increase of fracture risk was assumed during the follow-up (conservative approach). The follow-up duration varied from 953 to 1121 days, according to the quintile group and the type of fracture.

Results : 495, 1679, 1264, 2276, and 1348 women were included respectively in quintile one to five. The total number of clinical fractures was 21, 88, 85, 205 and 208, respectively. The annualised incidence of clinical fracture per 1000 women increased from 14.1, 18.3, 23.7, 32.8, to 59.1 with the quintile one to five. The total number of hip fracture was 0, 9, 13, 25 and 43 corresponding to an annualised incidence per 1000 women of 0.0, 1.8, 0.8, 3.8, and 11.4.

Conclusion : The Fracture Index is a very simple tool that identified women at high risk for fracture, and may defined a threshold for treatment. The use of QUS device in place of DEXA seem very attractive. The risk of fracture observed in our Swiss cohort was lower than in the SOF or EPIDOS studies. It may be in part explained by the shorter follow-up period or by the younger age of women. Another explanation may be the difference of fracture risk related to different population or country.

L'ostéoporose reste largement sous-diagnostiquée et sous-traitée : exemple des patients hospitalisés pour une fracture ostéoporotique.

¹LAMY O., Simard N., Borens O., Krieg M.,

*Médecine interne*¹,

Introduction : La fracture ostéoporotique est la première cause d'hospitalisation en Suisse, et une source majeure de morbidité / mortalité. Les traitements à disposition permettent de diminuer de 30 à 50% le risque fracturaire. De nombreux travaux montrent que l'ostéoporose reste largement sous-diagnostiquée et sous-traitée. Nous avons voulu connaître quelle prise en charge pour l'ostéoporose avait été prodiguée à des patients admis à l'hôpital pour une fracture a priori liée à l'ostéoporose.

Méthode : Analyse des dossiers de tous les patients adultes admis consécutivement au CHUV du 1er octobre 2004 au 1er avril 2005 pour une fracture (diagnostic primaire). Un entretien d'information a eu lieu avec tous les patients (et/ou leur proche) de 50 ans et plus chez qui la fracture était a priori en relation avec une ostéoporose. L'entretien a porté notamment sur la réalisation d'une densitométrie osseuse et sur la prescription d'un traitement contre l'ostéoporose.

Résultats : 339 patients > 50 ans ont été admis aux urgences pour une fracture. La moyenne d'âge était de 73 ans chez les femmes et 76 ans chez les hommes, 238 (70%) étaient des femmes. Les principales fractures étaient : hanche 120, jambe et cheville 60, poignet 57, humérus 51, vertèbre 23. Deux cent septante-deux patients (81%) ont été hospitalisés en milieu aigu pour 11±6 jours, 162 (60%) ont été transférés pour réhabilitation. Cent huitante-deux patients (54%) avaient des antécédents fracturaires à l'âge adulte. Vingt-huit patients (8%) avaient eu une densitométrie osseuse au préalable, 74 (22%) recevaient du calcium et de la vitamine D, et 18 (3%) un traitement spécifique pour l'ostéoporose.

Conclusion : Comme l'attestent ces chiffres lausannois, la fracture ostéoporotique est un problème majeur de santé publique. Cependant, nombre de ces fractures auraient pu être prévenues par une prise en charge et un traitement appropriés. Il importe donc d'offrir un bilan et un traitement adéquats aux patients ayant des antécédents de fracture, et de développer des outils simples pour identifier les patients à haut risque de fracture.

A sociolinguistic study of intercultural medical-preventive discourse: Evaluation and potential improvements of Aids prevention addressed to French-sp

SINGY P., Guex P., Weber O., Sulstarova B., Schaffter M.

Service de Psychiatrie de liaison, Lausanne

Sub-Saharan migrants represent a segment of the population in Switzerland, particularly threatened by HIV infection. This population shows a rather low level of awareness of the virus, its transmission and the resulting disease. Consequently, there is a dramatic need for expanded and improved prevention activities, most of which will rely on linguistic communication. In language matters, the current official strategy recommends a maximal use of original African languages in prevention. Yet, some preexisting research results suggest that this opinion might not be shared by the target population of the examined prevention.

To address this situation, a qualitative sociolinguistic research program is currently attempting to understand the linguistic stakes of the preventive activity among the francophone Sub-Saharan minority group in French-speaking Switzerland. This program tries, amongst other things, to enhance knowledge as to the nature of the impact the different languages can have in the varying contexts of prevention. This knowledge should help inform decision makers' choices as to the language(s) that would best serve prevention.

To reach its goals, the team of sociolinguists involved in the study opted for an action-research program. The method consists of an investigation of the linguistic and social imaginaries, emerging from the content analyses of semi-directive interviews conducted with privileged witnesses of the investigated prevention (exploratory phase), as well as with members of the target population (main phase).

The analysis of the exploratory phase interviews reveals that the privileged witnesses of prevention challenge the dominant prevention strategy, in that it appears that the use of French cannot be bypassed, even in situations where the addressor and the addressee of prevention share a common African language. More specifically, the interviewees view code-switching practices between African languages and French as more economic than African language only preventive interactions. They also underline that the use of French may facilitate discussions on taboo subjects like Aids and/or sexuality whereas other sensitive topics such as witchcraft might in fact more easily emerge in conversations led in African languages.

Le sens des mots de la prévention VIH/sida en Suisse Romande : présentation des premiers résultats d'une enquête liant sciences médicales et sciences de la communication

¹Singy P., ¹Schaffter M., ²Bourquin C., ²Prikhodkine A., ³Spencer B., Guex P.,

DUPA/Service de psychiatrie de liaison¹, UNIL/Section de linguistique², UEPP/IUMSP³,

Nous présentons ici une enquête menée entre 2004 et 2006 en Suisse romande sous l'égide du CHUV et de la Faculté des Lettres de l'Université de Lausanne. Partant du constat que le langage reste un instrument fondamental dans la lutte contre la propagation du sida, la recherche SEMSIDA vise à déterminer dans quelle mesure les mots de la prévention sont compris de manière homogène au sein de la population générale et des émetteurs de messages préventifs.

Au plan méthodologique, la recherche procède en 4 phases. Par une analyse des messages de prévention diffusés en Suisse Romande depuis 1996, nous avons identifié 61 mots et expressions fréquents et centraux. Une série d'entretiens auprès de 30 acteurs de prévention vise à déterminer le sens qu'ils accordent aux items en question. Quant à la population générale, elle est approchée qualitativement au niveau vaudois (60 entretiens semi-directifs avec questionnaires) ainsi que par une phase d'enquête téléphonique sur un échantillon représentatif à l'échelle de la Suisse romande (N=500).

Parvenus à mi-chemin du plan procédural, nous proposons l'exposé de résultats préliminaires issus des questionnaires soumis à l'échantillon indicatif (N=60) mentionné plus haut. Les réponses à ce questionnaire révèlent le degré de compréhension des membres de l'échantillon à l'égard d'une liste de 40 mots et expressions de la prévention. L'analyse de ces données vise en particulier à déterminer dans quelle mesure les mots déclarés méconnus par les personnes interrogées varient selon les critères sociologiques structurant l'échantillon (âge, sexe, niveau de formation, rural/citadin).

Une application importante de ces résultats est de permettre aux intervenants de la santé d'adapter au mieux leur langage à celui de leurs interlocuteurs. Notons enfin que l'enquête SEMSIDA vise à fournir dès septembre 2006 une description détaillée de la variation des significations attachées aux termes et expressions de la prévention VIH/sida.

HUMAN MERCURY EXPOSURE ASSOCIATED WITH ARTISANAL GOLD MINING IN BURKINA FASO

¹BERODE M., ²BELEM T., ²KARFO K., ¹SOTTAS P., ¹DROZ P.,

DUMSC/IST¹, Office de Santé des Travailleurs OST, Ouagadougou, Burkina Faso²,

Introduction

Artisanal gold-mining activities are in full rise in Burkina Faso with about 200 active sites spread in the entire country. The mining process involves the extraction of gold from the ore by mercury amalgamation, followed by roasting the resulting product to vaporize mercury out of the amalgam. A health survey was conducted among the working population of several sites by the OST. As part of this survey, biomonitoring was used to assess mercury exposure associated with the various activities. The results obtained are reported and discussed here.

Objective

This part of the study was undertaken to assess mercury exposure in the various mining sites, and associated with the different jobs carried out. Mercury excretion in urine was used as indicator of current exposure.

Methods

Ninety-three subjects associated with gold mining activities in 8 sites participated in this pilot study. Biomonitoring was performed by mercury determination in spot urine samples collected before shift in a metal-free polystyrene flask. Samples were refrigerated the same day, then frozen and delivered to the IST laboratory in Switzerland. Analysis was carried out by cold vapor atomic absorption spectrometry for mercury, and colorimetry for creatinine. Occupational history was assessed by local medical personnel using a standard questionnaire.

Results

From the 91 urine samples collected, 52 came from "unrefined gold" dealers (group A) who are also doing amalgam roasting, 33 from workers involved in ore washing and the amalgamation process (group B), and 6 from workers concerned with mining, crushing, grinding stages (group C). Urinary mercury excretion ranged from 4 to 1707 mg/g creatinine with a global average of 194 mg/g. Seventy percent of the urinary results are above the BEI of 35 mg/g creatinine recommended by ACGIH. Mean urinary concentrations were respectively for each group A, B, and C of 299, 73 and 17 mg/g, indicating a very high exposure for "unrefined gold" dealers due to their roasting activity. Analysis of the results by sites, occupations and work processes shows a very high variability in mercury exposure.

Results obtained can be used to target prevention programs and activities in order to reduce mercury exposure in the concerned population.

Key words: gold mining, mercury, amalgamation, biomonitoring, prevention program

Effects of bioaerosol exposure on work-related symptoms among Swiss sawmill workers

¹OPPLIGER A., ²Rusca S., ¹Charrière N.,

IST¹, CIMO, Monthey²,

Exposure to bioaerosol in the occupational environment of sawmill could be associated to a wide range of health effects, in particular respiratory impairment, allergy and organic dust toxic syndrome. Twelve sawmills in the French part of Switzerland were investigated and the relationship between levels of bioaerosols (organic dust, airborne bacteria and airborne fungi) and medical symptoms including lung function decline was explored. Health questionnaire was administrated to 111 sawmill workers. Results showed that in every sawmills concentration of airborne fungi exceeded the limit recommended by the Swiss National Insurance (SUVA). This elevated fungi level significantly influenced the occurrence of bronchial syndrome (defined by cough and expectorations). No other health effects could be associated to the measured exposures. However, we observed a significant effect of seniority on irritation syndrome (defined by itching/running nose, snoring and itching/red eyes) as the junior workers showed an increased risk of suffering of irritation. Lung functions tests were not influenced by bioaerosol or dust exposure levels.

Relationships between musical structure and psychophysiological measures of emotion

¹GOMEZ P., ¹Danuser B.,

Institut de Santé au Travail¹,

We explored the relationships between eleven structural features of 16 musical excerpts and both self-reports of valence and arousal and different physiological measures (respiration, skin conductance, heart rate) in 31 subjects. The structural features were judged by musical experts. The relationships between musical features and experienced emotions corresponded well with those known between musical structure and perceived emotions. Tempo, accentuation and rhythmic articulation were the features that best discriminated high arousal from low arousal whereas mode, harmonic complexity and rhythmic articulation were those that best differentiated between negative and positive valence. Tempo, accentuation and rhythmic articulation linearly correlated with inspiratory time, expiratory time, minute ventilation and skin conductance. Other musical features showed quadratic relationships. Breathing was faster for fast, accentuated, staccato pieces with simple harmony. Minute ventilation was highest for fast, accentuated, staccato excerpts in major mode with outstanding rhythms and complex and dissonant harmonies. Skin conductance was highest for fast, accentuated, staccato, loud selections with vague rhythms and low pitch. Heart rate was higher for fast pieces than slow pieces. It is suggested that the musical features analyzed played a primary role in the induction of both the subjective and physiological responses to the music.

BLOOD PRESSURE IN CHILDREN AND ADOLESCENTS, AND ASSOCIATION WITH BODY SIZE, IN THE SEYCHELLES, A RAPIDLY DEVELOPING COUNTRY

¹CHIOLERO A., ¹Paccaud F., ¹Bovet P.,

Institut universitaire de médecine sociale et préventive (IUMSP)¹,

BACKGROUND. The prevalence of overweight in youth has sharply increased over the past two decades in western countries and in many developing countries. There is concern that this could lead to an increase in the prevalence of high blood pressure (BP).

OBJECTIVES. To assess the prevalence of elevated BP in children and adolescents aged 5-16 in the Seychelles, a rapidly developing middle-income country, and the relationship between BP and body size.

METHODS. Survey of weight, height and BP in all students of four school grades (age 5-6, 9-10, 12-13 and 15-16, respectively). We used American CDC criteria to define BMI categories and elevated BP.

RESULTS. From 18'177 eligible children, weight, height and BP were measured in 15'670 (86%). The prevalence of elevated systolic or diastolic BP (\geq 95th percentile for age, sex and height) was 9.2% (standard error: 0.3) in boys and 10.1% (0.3) in girls. The prevalence of overweight (BMI \geq 95th percentile for age and sex) was 7.5% (0.3) in boys and 7.8% (0.3) in girls. Among overweight boys, 15.2% (0.1) had elevated systolic BP and 13.6% (0.1) had elevated diastolic BP, compared to 5.0% (0.3) and 4.2% (0.2) in boys with normal weight (BMI <85th percentile), respectively. These figures were 18.9% (0.2) and 20.0% (0.2) in overweight girls compared to 4.4% (0.3) and 5.0% (0.3) in girls with normal weight, respectively (all comparisons: $P < 0.001$).

CONCLUSION. Age and sex adjusted BP was strongly associated with BMI and the prevalence of elevated BP was 3-4 times higher in overweight than lean children. Although experimental data are needed, these observational data suggest that weight control is a key component for BP control programs in children.

Attachement mère-enfant, alliance familiale et développement de la théorie de l'esprit

¹CUENNET M., ²Cuennet M., ²Favez N.,

DUPA / IUP / UR-CEF¹, DUPA / IUP / Unité de Recherche du Centre d'Etude de la Famille²,

The question of the influence of family and caregiver environment on the cognitive and relational abilities of children, and youngsters is currently the object of much debate.

This study is part of a longitudinal research on the development of three-way affective communication (Father-Mother-Child), and on the affective, cognitive and social development of the child within the family. The theoretical background and our hypothesis refer to the theory of mind, to the theory of attachment, and to the research on family context. What we are especially interested in investigating is the influence that both the child-mother attachment, and the family alliance have on the children's performances at the theory of mind tasks at age 5. The family alliance is the capacity for members of a family to accomplish a task in a coordinated manner, and to share affective pleasure during that activity. Theory of mind is the ability for someone to imagine another person's perception of a given situation, and the thoughts and emotions that go along with that perception. This theory describes the ability to attribute mental states (beliefs, desires, knowledge) to others. This ability emerges between the ages of 4 and 6, and is crucial for the child's development, as it is involved in initiating and maintaining social relationships, and in learning abilities. Therefore, identifying the factors that influence the acquisition of theory of mind is relevant.

Several studies have pointed the link between mother-child attachment and acquisition of theory of mind abilities (Fernyhough, 1994, Meins et al. 1998, Arranz et al. 2002, Douglas et al. 2000). Others results suggest a link between family context (e.g. daily family rules) and theory of mind (Pears & Moses 2003, George & Solomon 1996). Our aim is to compare the predictive value of attachment and family alliance on theory of mind acquisition, and to test their interplay.

Our sample consists in 20 non-referred volunteers families with their first-born child. The families are seen three times, when their first-born child is 3, 9 and 18 months, to assess the family alliance using the Lausanne Trilogue Play (LTP), a semi-standardised situation. These three points of measure give an evolution pattern of family alliance. At 17 months, the toddler's pattern of attachment is assessed using the Strange Situation paradigm. At 4;9 years the child's cognitive and theory of mind abilities are evaluated using the unexpected transfer task (Wimmer & Perner, 1983) and the false belief and emotion task (Harris et al., 1989) for the theory of mind. Child cognitive and language development is controlled with the WPPSI-R.

On the one hand preliminary results (linear stepwise regression) showed no significant link between mother-child attachment and theory of mind scores. On the other hand, we found an important link between family alliance and theory of mind abilities at age 5.

Display conditions and desktop videoconferencing: advances in collaborative ergonomics

¹ARIAL M., ¹Francioli D., ¹Danuser B.,

IST¹,

The development of videoconferencing technologies is not a new topic. History of videoconferencing is characterized by a succession of technical improvement and commercial disappointment. This has led to questioning and renewing some conceptual aspects in telecommunications in order to better understand, improve, and implement such solutions. We identified three different perspectives that contributed to shape and orient the research and development of videoconferencing technologies: improving image and sound, replicating face-to-face conditions; and supporting collaboration. Each of these perspectives appears relevant in order to implement videoconferencing in cooperative technologies.

Implementing videoconferencing in cooperative technologies raises many questions. First, diverging results were identified in the scientific literature concerning the importance of seeing the other collaborators while performing cooperative tasks. The relevance as well as the benefits of the visual contact in cooperation was first addressed. The first conclusion from our literature review as well as from a qualitative study is that videoconferencing is relevant in distributed cooperation.

The question of display characteristics for the person view in distributed cooperative application was also measured in the frame of an empirical experiment. We performed a 2X2 factorial experiment measuring cooperative performance, satisfaction and social presence experienced by collaborators performing a distributed cooperative task for two levels of display (factor 1) and two levels of task characteristics (factor 2). No main effect of factor 1 or factor 2 was identified. However, for the subjects having dual display, score for social presence indicator was significantly higher in the group of subjects receiving complementary information than in the group having the same information. No such difference was observed in the group of participants using only one display. These findings suggest the need to consider the task characteristics in defining the type of display condition to implement for videoconferencing in cooperative application.

POPULATION-BASED REGISTRATION OF PHENOTYPIC, ANATOMIC AND FAMILIAL DATA FOR MELANOMA: RESULTS FROM A SWISS MULTICENTRIC STUDY

¹BULLIARD J., ²De Weck D., ³Fisch T., ⁴Bordoni A., ⁵Levi F.,

IUMSP, DUMSC¹, Wallis Cancer Registry, Sion, Switzerland², Cancer Registry of Sankt-Gallen and Appenzell, Sankt-Gallen, Switzerland³, Ticino Cancer Registry, Locarno, Switzerland⁴, Vaud Cancer Registry, Lausanne, Switzerland, Neuchâtel Cancer Registry, Neuchâtel, Switzerland⁵,

CONTEXT AND OBJECTIVES:

A multicentric study was set up to assess the feasibility for Swiss cancer registries of actively retrieving 3 additional variables of epidemiological and aetiological relevance for melanoma, and of potential use for the evaluation of prevention campaigns.

MATERIAL AND METHODS:

The skin type, family history of melanoma and precise anatomical site were retrieved for melanoma cases registered in 5 Swiss cantons (Neuchâtel, St-Gall and Appenzell, Vaud and Wallis) over 3 to 6 consecutive years (1995-2002). Data were obtained via a short questionnaire administered by the physicians – mostly dermatologists – who originally excised the lesions. As the detailed body site was routinely collected in Ticino, data from this Cancer Registry were included in the body site analysis. Relative melanoma density (RMD) was computed by the ratio of observed to expected numbers of melanomas allowing for body site surface areas, and further adjusted for site-specific melanocyte density.

RESULTS:

Of the 1,645 questionnaires sent, 1,420 (86.3%) were returned. The detailed cutaneous site and skin type were reliably obtained for 84.7% and 78.7% of questionnaires, and family history was known in 76% of instances. Prevalence of sun-sensitive subjects and patients with melanoma affected first-degree relatives, two target groups for early detection and surveillance campaigns, were 54.1% and 3.4%, respectively.

After translation into the 4th digit of the International Classification of Diseases for Oncology, the anatomical site codes from printed (original information) and pictorial support (body chart from the questionnaire) concurred for 94.6% of lesions. Discrepancies occurred mostly for lesions on the upper, outer part of the shoulder for which the clinician's textual description was "shoulder blade". This differential misclassification suggests an under-estimation by about 10% of melanomas of the upper limbs and an over-estimation of 5% for truncal melanomas.

Sites of highest melanoma risk were the face, the shoulder and the upper arm for both sexes, the back for men and the leg for women. Three major features of this series were: (1) an unexpectedly high RMD for the face in women (6.2 vs 4.2 in men), (2) the absence of a male predominance for melanomas on the ears, and (3) for the upper limbs, a steady gradient of increasing melanoma density with increasing proximity to the trunk, regardless of sex.

DISCUSSION AND CONCLUSION:

The feasibility of retrieving the skin type, the precise anatomical location and family history of melanoma in a reliable manner was demonstrated thanks to the collaboration of Swiss dermatologists. Use of a schematic body drawing improves the quality of the anatomical site data and facilitates the reporting task of doctors.

Age and sex patterns of RMD paralleled general indicators of sun exposure and behaviour, except for the hand (RMD=0.2). These Swiss results support some site or sun exposure specificity in the aetiology of melanoma.

Shielding considerations in helical tomotherapy

¹BAECHLER S., ¹Gardon M., ¹Sans-Merce M., ¹Moeckli R.,

DUMSC/IRA¹,

Helical tomotherapy is a new slice by slice intensity-modulated radiation therapy (IMRT) treatment. Due to the increased beam-on time to deliver a given target dose, room shielding considerations have to be reassessed for a tomotherapy facility. Indeed, the weekly workload is typically one order of magnitude higher than for conventional radiation therapy. To resolve these problems, a conservative method for calculating required thickness of shielding is proposed in this work.

Generally, linear accelerators must be shielded for primary, leakage and scatter photon radiation. For tomotherapy, primary radiation is no more the main room-shielding issue since a beam stop is mounted on the gantry directly opposite to the source. On the other hand, due to the longer irradiation time, the accelerator head leakage becomes a major concern. A model has been developed to determine leakage radiation levels throughout the room for continuous gantry rotation. Compared to leakage radiation, scatter radiation is a minor contribution. Tomotherapy machines operate at a nominal energy of 6 MV, and therefore neutron production is negligible.

Longitudinal profiling of urinary steroids by gas chromatography/combustion/isotope ratio mass spectrometry: diet change may result in carbon isotopic variations

¹Saudan C., ²Kamber M., ³Barbati G., ¹Robinson N., ¹Desmarchelier A., ¹Mangin P., ¹Saugy M.,

LAD - IUML - CHUV¹, Swiss Federal Office of Sport², Ospedale Fatebenefratelli - Rome - Italie³,

Abstract

Longitudinal profiling of urinary steroids was investigated by using a gas chromatography/combustion/isotope ratio mass spectrometry (GC/C/IRMS) method. The carbon isotope ratio of three urinary testosterone (T) metabolites: androsterone, etiocholanolone, 5 β -androstane-3 α ,17 β -diol (5 β -androstenediol) together with 16(5 α)-androstene-3 α -ol (androstenol) and 5 β -pregnane-3 α ,20 α -diol (5 β -pregnanediol) were measured in urine samples collected from three top-level athletes over two years. Throughout the study, the subjects were living in Switzerland and were residing every year for a month or two in an African country. ¹³C-enrichment larger than 2.5 ‰ was observed for one subject after a two-month stay in Africa. Our findings reveal that ¹³C-enrichment caused by a diet change might be reduced if the stay in Africa was shorter or if the urine sample was not collected within the days after return to Switzerland. The steroids of interest in each sample did not show significant isotopic fractionation that could lead to false positive results in anti-doping testing. In contrast to the results obtained with the carbon isotopic ratio, profiling of urinary testosterone/epitestosterone (T/E) ratios was found to be unaffected by a diet change.

Etude de l'éblouissement au moyen d'un photoluminancemètre numérique

¹FRANCIOLI D., ¹Arial M.,

IURST¹,

Dans le cadre de notre recherche visant à l'étude du confort visuel en terme d'éblouissement et de performance visuelle, nous avons développé une méthode de mesure photométrique du champ visuel au moyen d'un appareil de photographie numérique muni d'un objectif fish-eye. Etant donné qu' UGR est l'indice d'éblouissement officiel CIE, nous voulions pouvoir le comparer avec nos indices.

L'expérience en laboratoire comportait deux étapes. Dans un premier temps l'appareil photonumérique a été calibré, et dans un deuxième temps 20 sujets ont été soumis à 16 distributions lumineuses impliquant des degrés divers d'éblouissement (avec sources étendues). Ces sujets devaient répondre à une série de questions permettant de cerner leur sensation d'éblouissement lors d'une tâche de lecture sur un écran de pc.

La calibration a permis de montrer qu'avec l'aide de seulement 7 photographies, (7 réglages de vitesse d'obturation et d'ouverture), il était possible d'estimer les luminances du champ visuel avec une erreur suffisamment faible (<10%) pour l'étude du confort visuel.

Cette étude a montré que l'indice UGR ne caractérisait pas assez bien l'éblouissement, du fait de la présence de sources lumineuses étendues (mal représentées par cet indice).

Ce résultat nous a conduit à élaborer un nouvel indice d'éblouissement. Non seulement il inclut des paramètres photométriques et physiologiques simples caractérisant mieux le phénomène, mais il présente un certain nombre d'autres avantages par rapport à l'indice UGR:

Ø l'effet des sources étendues (ex: fenêtres) est mieux caractérisé.

Ø l'éblouissement se définit par rapport à une tâche et à un individu (son profil visuel).

Ø n'est plus nécessaire de distinguer les sources de lumière.

The narrative LTP (Lausanne Trilogic Play)

¹ABBET E., ¹Favez N.,

DUPA/IUP/Unité de recherche du Centre d'Etude de la Famille (CEF)¹

The scenario in four parts of the classic LTP is also taken up in the Narrative LTP. The main difference lies in the fact that the parents are invited to help the child to tell a story, with little dolls, about a child left in two persons' care for a week-end during which his parents take time together.

Assessment of the Narrative LTP is done with a new grid of coding called Narrative Evaluation's Scales (NES). The NES is mainly based on different theoretical currents, as the systemic influence and the basis framework of the "classic" LTP, the literature about narratives, and finally the scales of Fiese et al. (1999), Oppenheim & Renouf (1991) and Peterson & McCabe (according to the theory of Labov & Waltezky, 1967).

The NES contains 22 Likert scales (in 5 points) like the organization of the family, the co-parental relationship, the involvement of the child in the task, the capacity of verbalization of positive or negative affects and the general atmosphere of the situation. These scales are merged in three groups, in order to evaluate (i) the family play in terms of "trilogue" or family functioning when parents and child co-constructing a story, (i) the "form" of the narration and (i) the "content" of the co-constructed stories. So the narratives are not analyzed in a psycholinguistic perspective.

Thanks to the NES, our results using the statistics show the link between the family alliance over the first two years and the narratives of an emotional event at 5 : the families in difficulty during the first two years of the life of the child (pattern 3) have as well difficulties in the organisation of the story. The contents of their stories show that they are less able to integrate positive or negative affects and to mention psychological states in their narrations than the two other categories of family (pattern 1 and 2) (Favez et al.).

Helicobacter pylori and Campylobacter sp: a source of occupational risk in sewage workers?

¹RINSOZ T., ¹Oppliger A., ²Hilfiker S.,

Institut de santé au travail (IST)¹, Abteilung für Arbeits- und Umweltmedizin (Institut für Sozial- und Präventivmedizin und medizinische Poliklinik)²,

Contaminated water is recognised as an important vehicle for the transmission of several viral and bacterial diseases. The kind and quantity of microorganisms present in sewage reflects both clinical and sub-clinical infections prevalent in the community. *Helicobacter pylori* is the causative agent of gastritis and duodenal ulcer and plays a role in the development of gastric cancer. It is considered a class I carcinogen by the International Agency for research on cancer. The transmission of *H.pylori* remains unclear, but the ability to culture *H. pylori* from stools suggests that it is viable in sewage systems. *Campylobacter sp.* is widespread in the environment and causes enteritis. Results from several countries have shown that these bacteria are ubiquitous in sewage and that human and animal waste from abattoirs and animal livestock are the major sources. *H. pylori* and *Campylobacter sp.* are nutritionally fastidious bacteria cultured in complex media with additional growth supplements and need to be cultured in a microaerophilic atmosphere. Moreover, after several days of growth in vitro, or when present in water, they undergo a morphological change and lose their culturability (viable but non-culturable form). To overcome this problem, molecular techniques can be used to detect those bacteria in the environment.

The aim of this study was to develop a reliable quantitative PCR-based method to detect and quantify those two bacteria in aerosols and water of sewage treatment plants. The presence of *Campylobacters sp.* and *Helicobacter pylori* was estimated by real-time PCR on raw sewage water and treated water of nine sewage treatment. *Campylobacters sp.* DNA was detected in raw sewage water and in some treated water.

ENA
Environnement Naturel

Evalutation de l'exposition professionnelle aux ultraviolets chez les travailleurs du bâtiment de la région valaisanne

¹MILON a., ¹Vernez D., ²Bulliard J.,

Institut de Santé au Travail¹, Institut universitaire de médecine sociale et préventive²,

Une exposition excessive, intermittente ou chronique, au rayonnement ultraviolet solaire est à l'origine de la majorité des cancers de la peau chez l'homme. L'augmentation de l'irradiation solaire au sol en raison de la pollution anthropique, l'élévation du niveau de vie (vacances dans des régions de forte irradiation) et le développement des activités de plein air contribuent à une augmentation de l'exposition. Ce n'est donc pas un hasard si, de tous les cancers, ce sont les cancers de la peau qui connaissent le plus fort taux de croissance (en terme de cas diagnostiqués). La Suisse est parmi les pays d'Europe les plus touchés par ce phénomène.

L'objectif de ce projet a été d'évaluer l'exposition individuelle aux ultraviolets chez les travailleurs en extérieur ainsi que de caractériser l'influence des facteurs individuels (posture, orientation par rapport au soleil) sur l'exposition effective.

Des mesures d'exposition individuelle aux UV ont été effectués chez des travailleurs du bâtiment à trois groupes d'altitudes dans le canton du Valais. L'exposition effective a été mesurée au moyen de dosimètres à film de spores (BioSense) positionnés sur 5 parties du corps: le nuque, l'épaule gauche, l'épaule droite, le bas du dos et le front. L'irradiation ambiante a été mesurée en poste fixe à proximité immédiate des travailleurs exposés au moyen d'un dosimètre à film de spore et d'un dosimètre numérique (modèle X2000, Gigahertz-Optik GmbH). L'activité posturale et les conditions d'exposition durant les périodes de mesure ont par ailleurs été relevées à l'aide de techniques d'observations similaires à celles utilisées en ergonomie. Le canevas d'observation utilisé comprenait 5 postures (assis, à genoux, debout penché, debout bras en bas, debout bras levés) ainsi que 4 orientations par rapport au soleil (soleil derrière, à droite, à gauche, en face).

<i>Altitude:</i>	<i>Valeur moyenne</i>	<i>Ecart type</i>
	<i>[MED]</i>	<i>[MED]</i>
500-600m	4.7	2.8
1400-1500m	8.6	4.1
2000-2500m	11.4	9.9

Exposition individuelle journalière moyenne en fonction de l'altitude (Norme SUVA = 0.12 MED)

L'exposition mesurée lors de journées ensoleillées est importante. La dose journalière obtenue dépasse largement les limites d'exposition recommandées pour des peaux non protégées, justifiant pleinement l'emploi systématique de mesures préventives. Une importante variabilité de la dose journalière et de l'exposition relative a par ailleurs été observée, suggérant une forte influence de facteurs individuels ainsi que des épisodes d'expositions subaiguës. Il est reconnu que ce type d'exposition, difficilement maîtrisable, joue un rôle important dans l'occurrence du cancer basocellulaire et du mélanome

Pour ces raisons, des campagnes ciblées, par le canal professionnel, chez les populations de travailleurs à risque sont recommandées. De plus, en raison d'un risque d'exposition subaiguë apparemment accru, les travailleurs de haute altitude devraient bénéficier d'un examen médical préventif. Sur le plan de la recherche, le développement de cadastres posturaux par professions et de modèles d'exposition prédictifs permettrait de mieux caractériser le risque.

Monitoring phenanthrene bioavailability in soil: emerging outlooks from bacterial biosensor technology

¹TECON R., ¹van der Meer J.,

Département de Microbiologie Fondamentale¹,

Among the large variety of organic pollutants, the environmental fate of polycyclic aromatic hydrocarbons (PAHs) deserves special interest due to their toxic and sometimes carcinogenic properties. In soil and sediments, the biodegradation of PAHs is strongly reduced by their low availability for indigenous micro-organisms, thus restricting the efficiency of bioremediation strategies for the clean-up of contaminated sites. To better understand the key processes involved in PAH availability, it would be nice to have more efficient monitoring tools. For this purpose, we developed a bacterial biosensor to detect phenanthrene – a model PAH of low molecular weight – using the phenanthrene-degrading strain *Burkholderia* sp. RP007 carrying a *gfp*-based plasmid reporter system. In shaken liquid cultures, the bacterial biosensor produced measurable GFP fluorescence in the presence of phenanthrene crystals. Interestingly, the induction of GFP fluorescence was not determined by phenanthrene concentration in the medium, but was dependent of the flux of compound towards the bacterial cells. Besides, preliminary results showed that the bacterial biosensor was able to detect phenanthrene in an artificially contaminated soil, therefore demonstrating its use for future in situ assessments of PAH bioavailability.

IMI
Immunité et Infection

Ritonavir boosted atazanavir-lopinavir combination : a pharmacokinetic interaction study of total, unbound plasma and cellular exposure

¹Cavassini M., ²Colombo S., ²Buclin T., ³Telenti A.,

MIN¹, pharmacologie clinique², institut de microbiologie³,

Objectives: To assess potential pharmacokinetic (PK) interactions between atazanavir (ATV, 300 mg QD) and lopinavir (LPV, 400 mg BID), both boosted by ritonavir (RTV, 100 mg).

Design: Two-parallel groups, addition of LPV in patients receiving ATV (n=6), and of ATV in patients receiving LPV (n=7), with before-after comparisons.

Methods: Each group had two complete PK profiles before and 2 weeks after the addition of the second protease inhibitor (PI). Total plasma concentrations (C_{tot}) were analysed by HPLC-UV, unbound plasma concentrations (C_u) and cellular concentrations (C_{cell}) by LC-MS/MS. Plasma and cellular PK parameters were calculated. Unbound and cellular fractions were expressed as C_u/C_{tot} and C_{cell}/C_{tot} ratio. Data were analysed by paired Student t-test on log values; correlations between C_{cell}, C_u and C_{tot} were explored by log-log linear regression.

Results: Adding LPV to ATV did not influence the plasma and cellular PK parameters of ATV. Adding ATV to LPV was associated with a decrease in LPV concentrations (by 16% for AUC, C_{max} and C_{trough}, NS; and by 35% for C_{min}, p=0.04). The RTV PK parameters remained unmodified. The C_{cell}/C_{tot} and C_u/C_{tot} ratio was unaffected by the addition of the second PI and remained stable throughout dosing interval. Good correlations were observed between C_{cell}, C_u and C_{tot} for each drug. No relevant toxicity was observed.

Conclusions: Adding LPV to ATV did not influence the plasma and cellular PK parameters of ATV. Adding ATV to LPV caused a limited decrease in LPV concentrations. The clinical significance of this reduction is unknown and warrants further investigation to determine the need for LPV dosage individualization in selected cases.

Set-up of a HIV-adherence clinic in a University outpatient clinic and pharmacy

¹SCHNEIDER M., ²Cavassini M., ¹Krummenacher I., ¹Bugnon O.,

Pharmacie, Policlinique Médicale Universitaire¹, Maladies Infectieuses²,

Background and Objective: To ensure successful treatment, HIV patients must maintain a very high degree of adherence over time. However, many patients encounter barriers to adherence and need support. Patients experiencing problems with their highly active antiretroviral treatment (HAART) are referred to a pharmacist team who works as consultants in adherence. We describe here the first 15 patients having entered the programme.

Design: Patients are seen by the same pharmacist as often as necessary (each 3-6 weeks). The pharmacist organizes individualized semi-structured interviews based on cognitive, emotional, behavioural, social and motivational issues. The HAART is dispensed in electronic pill-containers (that record date and time of openings). Before each medical visit, the patient is provided with an adherence report (compilation of electronic adherence data and results of the adherence consultation) that is brought to the physician.

Setting: University HIV outpatient clinic and pharmacy.

Main Outcome Measures: Adherence to treatment (days with correct dosing, %) and persistence on treatment (duration before change of HAART because of viral failure, in days).

Results: The HIV adherence programme has started in August 2004 and 15 patients have been included so far (9 males; median age 37; 6 African; 4 patients taking a first, 6 a second and 5 a third line of treatment). Reasons for inclusion were: known non-adherence in 10 patients, detectable viral load in 3, and prevention of non-adherence because of unstable social/psychological issues in 2 patients. In the on-going programme, 8 patients have been followed up so far for > 6 months, 4 for > 2 months and 3 for less than 2 months. Among the 13 patients followed up for at least 1 month, 11 have a continuous adherence > 90%. None of the patients so far had a change in their HAART. Main problems discussed are acceptance of disease/treatment, previous experiences with HAART, cultural issues, memory impairment, ways to integrate HAART in daily life, prevention and management of side effects, prevention if schedule is disrupted. Support is very well accepted because it is non-judgemental and addresses patients issues.

Conclusions: The set-up of the programme is successful and a prospective trial is now being organized to assess the cost-effectiveness of the programme in comparison to standard of care.

Selective leukocytapheresis and inflammatory bowel diseases (IBD)

¹Felley C., ²Latado H., ³Majcherczyk P., ¹Michetti P., ²Felley-Bosco E.

Department of Gastroenterology & Hepatology, CHUV Lausanne, Switzerland¹, Department of Pharmacology & Toxicology, University of Lausanne, Switzerland², Institute of Fundamental Microbiology, University of Lausanne, Switzerland³,

Background: Ulcerative colitis (UC) is thought to result from persistent recruitment of inflammatory cells into the gut. $\alpha 4$ -integrins are present on activated leukocytes and play a central role in this recruitment. Recently, an antibody directed against the $\alpha 4\beta 7$ -integrin complex showed efficacy in UC, suggesting a general benefit of preventing intestinal immune cell recruitment in IBD. The Adacolumn leukocytapheresis is a device designed for selective depletion of activated granulocytes and monocytes

Aim: To investigate the mechanism of action of apheresis-induced clinical improvement in UC.

Methods: the profile of selected genes was analyzed by quantitative PCR in leukocytes removed from the patients during the first or fifth apheresis. Analyzed genes included immunoglobulin receptors CD16A and B (Fc- γ receptor 3A and B), integrins $\alpha 4$ and $\beta 7$, Toll-like receptors 2 and 4 (TLR2, TLR4), cannabinoid receptor 2 (CNR2), chemokine (C-X-C motif) receptor 3 and inducible nitric oxide synthase (iNOS). Cells remaining in the apheresis column were sampled as follows: fraction eluting spontaneously and fraction resistant to wash of the beads with phosphate buffered saline (PBS). The fraction eluting spontaneously was also tested functionally for TNF α release after stimulation with lipopolysaccharide (LPS), Pam3Cys, *Bacillus subtilis* or *Staphylococcus aureus* peptidoglycan (PGN).

Results: At the first apheresis, the most abundant genes in both spontaneously eluted fraction and attached cells were CD16A and B. The expression of the other genes was: TLR4 and TLR2 > integrins $\alpha 4$ and $\beta 7$ > CNR2 and CXCR3 > iNOS. In cells attached to the beads collected at the fifth apheresis a significant ($p < 0.05$, paired t-test) 47% decrease of integrin $\alpha 4$ expression was observed compared to spontaneously eluted cells. The same significant decrease was observed when comparing attached cell fraction at the first or at the fifth apheresis within the same patient. This was accompanied by a significant decrease in CD16A expression. In spontaneously eluted leukocytes a significant 48% decrease in CXCR3 was observed. In this fraction functional tests demonstrated an equivalent response to LPS or Pam3Cys but a hundred fold highest sensitivity to *Bacillus subtilis* PGN compared to *Staphylococcus aureus* PGN.

Conclusion: The decrease of $\alpha 4$ -integrin, which has been used as a target for IBD therapy, suggests that one potential mechanism involved in the Adacolumn apheresis is treatment-induced release of factors modulating integrin $\alpha 4$ expression. These factors may be the same that decrease the expression of CD16A in bead-attached or CXCR3 in spontaneously eluted leukocytes.

Validation and improvement of an automated surveillance system (ASS) for nosocomial bacteremia

¹BELLINI C., ²Petignat C., ²Francioli P., ³Wenger A., ³Bille J., ⁴Klopotov A.,
⁵Vallet Y., ⁴Patthey R., ²Zanetti G.,

*DAMPH/MIN*¹, *DAMPH*², *IMU*³, *INH*⁴, *DAMPH/INH*⁵,

Objectives: We developed a computerized ASS for bacteremia in a 850-bed university hospital. The aims of this study were to validate ASS-generated results and to identify possible improvements.

Methods: The ASS was based on a computerized data warehouse that included laboratory data (date of all blood and catheter cultures, and species identification and antibiotic susceptibility testing in positive cultures) and demographic data (patients' ID, ward, and date of admission). Algorithms distinguished true bacteremia from contamination (culture of a possible contaminant in one of several blood samples), nosocomial bacteremia (positive culture of blood drawn > 48 hours after admission), and catheter-related bacteremia among the latter (same bacteria with the same antibiotic susceptibility in blood and on IV catheter cultured simultaneously +/- 6 days). Bacteremias that occurred more than 3 days apart were considered distinct episodes.

We reviewed all positive blood cultures classified by the ASS as nosocomial bacteremia not related to a catheter in adult patients admitted over 2 years on the following wards: surgery, medicine, and medical and surgical ICUs. The gold standard for validation of classification by the ASS was a manual review of patients' charts using the CDC criteria for nosocomial infections.

Results: The ASS identified 154 nosocomial bacteremia not related to a catheter. 106/154 (69%) were confirmed by chart review (77% in medicine, 60% in surgery, and 73% in ICU). There were 3 reasons for misclassification by the ASS: a late documentation of community-acquired bacteremias in 3/154 (2%) cases; the absence of catheter culture in 25 (16%) cases of bacteremia clinically attributed to catheter infection; and duplication of bacteremia sustained over >3 days in 20 (13%) cases (13 of which being fungemia in surgical patients). We explored 2 alternative uses of available data to improve ASS performance: 1) attributing all coagulase-negative bacteremias to catheter infections led to correct classification of 8/154 (5%) more cases at the price of 2 additional misclassifications; 2) extending the time interval to 10 days for definition of duplicates in case of fungemia allowed correct classification of 11/154 (7%) cases at no cost. The ASS accurately classified nosocomial bacteremia not related to catheter in 78% of the cases by implementing both strategies.

Conclusion: ASS is a promising alternative to manual surveillance of nosocomial bacteremia

Parasite-mediated NFkB activation protects Plasmodium berghei-infected hepatocytes from Fas(CD95/Apo-1)-induced apoptosis via upregulation of inducible nitric oxide synthase

¹TORGLER R., Bongfen S., Romero J., Thome-Miazza M., Corradin G.,

Department of Biochemistry, University of Lausanne¹,

As Plasmodium parasites are obligate intracellular parasites, they have to perform essential adaptations to ensure development, replication and survival within a host cell. As shown for various bacteria, viruses and parasites, pathogen-derived adaptations often implicate the activation of the host cell transcription factor NFkB. Host cell death, being a cardinal problem of an intracellular pathogen can be inhibited by NFkB. Different anti-apoptotic molecules are regulated by NFkB and block apoptosis at various stages of the apoptotic machinery. Therefore, inhibition of NFkB in infected cells can result in impaired development of intracellular pathogens due to enhanced apoptosis of their host cell.

In this study we have investigated whether NFkB is activated in hepatocytes by Plasmodium berghei sporozoites after infection, and if so, whether NFkB is crucially involved in Plasmodium liver-stage development.

Our experiments show, that Plasmodium sporozoites activate NFkB in hepatocytes. Shortly after infection, Ikb β N, the natural inhibitor of NFkB is phosphorylated which leads to its ubiquitin-dependent proteosomal degradation. Surprisingly, sporozoite-induced NFkB abolishes the number of infected cells in a time-dependent manner. The number of infected hepatocytes is significantly higher in cells pretreated with the specific NFkB inhibitor BAY11-7082 compared to untreated or control treated cells. However, when Fas(CD95/Apo-1)-mediated apoptosis is induced, the infected cells seem to be resistant, unlike infected hepatocytes in which NFkB has been blocked by BAY11-7082. We provide further evidence that sporozoite-mediated NFkB activation induces iNOS (inducible nitric oxide synthase) expression in hepatocytes. In addition, we demonstrate that sporozoite-induced iNOS expression is responsible for the decrease of Plasmodium-infected hepatocytes. Simultaneously, NFkB-mediated iNOS expression contributes to the protection of infected cells from Fas(CD95/Apo-1)-induced apoptosis. Infected hepatocytes treated with the specific iNOS inhibitor SMT (S-Methylisothiourea Sulfate) were more susceptible to apoptosis compared to control cells. In conclusion, our data underline the importance for Plasmodium sporozoites to activate NFkB to be protected against a distinct form of apoptosis. Furthermore, with regard to inhibition of apoptosis, iNOS expression can have also an advantageous effect on Plasmodium hepatocyte infection.

Preexisting Inflammation in Combination with High-Tidal Volume Ventilation (HTVV) Potentiates Proinflammatory Cytokine Expression in Newborn Rats

¹ROTH-KLEINER M., ¹Roth-Kleiner M., ²Ridsdale R., ²Cao L., ²Kuliszewski M., ²Tseu I., ²McKerlie C., ²Post M.,

CHUV/ DMCP/ Division de Néonatalogie¹, Lung Biology Program, Hospital for Sick Children, Toronto²,

Background: High levels of proinflammatory cytokines are associated with increased risk of chronic lung disease (CLD) in premature infants. Chorioamnionitis as well as mechanical ventilation have both been shown to increase cytokine expression in lung tissue and blood. Little is known about their combined effect.

Objective: To test the hypothesis that low-dose lipopolysaccharide (LPS) exposure would modify the cytokine response to HTVV in newborn rats.

Methods: Newborn Wistar rats (3-6 days) were randomly assigned to four groups (I-IV: 11–13 animals/group). The animals of group III and IV were injected 24h prior ventilation with 3 mg LPS /kg body weight, while I and II received saline. Group II and IV were subjected to HTVV (25ml/kg) for 3h. Lung IL-6, MIP-2, IL-1 β and TNF- α mRNA were determined by realtime RT-PCR. Cytokine protein content was measured in bronchoalveolar lavage fluid (BALF). Statistical analysis: one-way ANOVA and t-test (significance: $p < 0.05$).

Results: LPS injection reduced weight gain within the 24h following injection from 17.9% (saline) to 11.4% ($p < 0.05$). Pre-treatment with LPS did neither affect lung compliance nor blood gas values. LPS alone did not change cytokine expression. In contrast, HTVV alone increased mRNA expression of IL-6 by 7.2 fold, MIP-2 by 7.3 fold and IL-1 β by 1.8 fold ($p < 0.05$). The combination of HTVV and LPS further increased the expression of IL-6 (II vs IV; 10.5 fold) and IL-1 β (II vs IV; 2.5 fold). IL-6 protein content in BALF increased with HTVV and LPS+HTVV treatments (I 19.4, II 34.0, III 17.5, IV 43.7 pg/ml).

Conclusions: Whereas low grade systemic inflammation alone does not change the innate immune response, its combination with HTVV potentiates the proinflammatory cytokine expression in the immature lung. Therefore, we speculate that premature infants born in a context of chorioamnionitis are at higher risk to develop ventilator associated lung injury and CLD than those without preexisting inflammation.

Silencing of both b-TrCP1 and HOS (b-TrCP2) is required to suppress HIV-1 Vpu-mediated CD4 down-modulation

¹BUTTICAZ C., Wyniger J., Muñoz M., Michielin O., Telenti A., Rothenberger S.,

Institut de Microbiologie¹,

Background : HIV-1 interacts with CD4 within the endoplasmic reticulum of infected cells, where it targets CD4 for degradation through the interaction b-TrCP1. This F-box protein functions as the substrate recognition subunit of the SCF b-TrCP E3 ubiquitin ligase. Humans possess a homologue of b-TrCP1, HOS, also named b-TrCP2. Here, we assess whether b-TrCP2 shares with its homologue structural and functional properties that would allow it to bind Vpu, modulate CD4 expression, and thus participate in HIV-1 pathogenesis.

Methods: We modeled the structure of b-TrCP2 to analyse the similarities with its homologue. Interaction between Vpu, b-TrCP1 and b-TrCP2 were assessed in co-immunoprecipitation experiments. Expression vectors for b-TrCP1, b-TrCP2 and a chimeric Vpu-GFP were transfected into HeLa CD4+ cells. Protein expression was verified 24 hours post-transfection by western blot, and CD4 cell surface levels were determined by FACS. Silencing of endogenous b-TrCP1 and/or b-TrCP2 used synthetic siRNAs, prior to transfection. The role of b-TrCP1 and b-TrCP2 in HIV-1 the life cycle was assessed using silencing prior to viral infection .

Results: Modeling of the ligand-binding domain of b-TrCP1 and b-TrCP2 showed striking surface similarities between both proteins. Both homologues were able to bind Vpu. Expression of Vpu-GFP induced a 50% decrease of cell surface CD4 mean fluorescence intensity. Co-expression of b-TrCP1 resulted in an additional 15% decrease. Similar results are obtained when b-TrCP2 was co-expressed. Single silencing of b-TrCP1 or b-TrCP2 minimally reversed CD4 down-modulation. Effective reversal required both genes to be silenced simultaneously. We measured virus replication in HeLa CD4+ cells after RNAi of b-TrCP1 and/or b-TrCP2, and found a maximal inhibition when both genes were jointly silenced.

Conclusions: b-TrCP2 shares with b-TrCP1 the capacity to bind Vpu. Silencing of both genes is required to suppress HIV-1 Vpu-mediated CD4 down-modulation, and to maximally limit the role of b-TrCP in the HIV-1 cycle.

Macrophage Migration Inhibitory Factor (MIF) Plays an Important Role in the Host Innate Immune Defenses against *Candida* infection

¹NICOLO C., ¹Le Roy D., ¹Knaup Reymond M., ¹Roger T., ¹Calandra T.,
*Maladies Infectieuses*¹,

Background: Invasive candidiasis has emerged worldwide as an increasingly frequent cause of infections in critically ill patients and are associated with high morbidity and mortality. The balance between pro-inflammatory (IL-12, IFN γ) and anti-inflammatory (IL-10) cytokines is a key determinant of the outcome of fungal infections. MIF, a pro-inflammatory cytokine, is an important effector molecule of innate immunity and has been shown to play a central role in the pathogenesis of bacterial sepsis. In the present study, we examined the role of MIF in the pathogenesis of invasive candidiasis.

Methods: BALB/c mice injected with anti-MIF or control IgG or IgG antibodies (2 mg i.p) 30 minutes before an i.v. injection of $3.5\text{-}5 \times 10^5$ CFU of a clinical isolate of *C. albicans*. MIF, IL-10, IL-12 and IFN γ levels and fungal loads were measured in blood, spleen and kidney 1, 2, 3, 5 and 10 days post-infection. Body weight and survival were followed daily.

Results: Following an intravenous injection, *C. albicans* was rapidly cleared from the circulation and preferentially colonized the kidney. Development of renal candidiasis was accompanied by a substantial decrease of MIF concentrations in the kidney (from 37.5 ± 4.2 at day 0 to 19 ± 4.65 $\mu\text{g/g}$ at day 10, $P=0.002$). Neutralization of MIF activity with anti-MIF IgG decreased the pro-inflammatory response in the kidney, as shown by a reduction of IL-12/IL-10 ($P=0.002$) and of IFN γ /IL-10 ($P=0.001$) ratios. Moreover, treatment of mice with anti-MIF IgG markedly increased mortality of invasive candidiasis (from 40% in control IgG treated mice to 73% in anti-MIF IgG treated mice, $P=0.02$).

Conclusion: Neutralizing MIF activity impairs the host pro-inflammatory response and augment lethality of invasive candidiasis. Thus, these data identify MIF as an important effector molecule of the host innate immune defenses against *Candida* infection.

Altered Expression of Penicillin-Binding Proteins (PBPs) in Penicillin-Treated *Streptococcus gordonii*

¹HAENNI M., ¹Moreillon P.,

Département de Microbiologie Fondamentale¹, UNIL Lausanne

Background: *S. gordonii* carries 5 PBPs which share homology with those of *S. pneumoniae* (PBP1A, 1B, 2A, 2B, and 2X). In penicillin-resistant isolates, consecutive PBP mutations result in lower penicillin-affinity of PBP2X, 2B and 1A, respectively. However, whether this results in altered expression of PBP genes is unknown.

Methods: Transcriptional fusions of PBPs with the luciferase reporter gene were constructed in the susceptible parent (penicillin MIC = 0.008 mg/l), in a penicillin-resistant mutant presenting point mutations in PBP2X and 2B (penicillin MIC = 2 mg/l), and in three deletion mutants in PBP1A, 2A and 2B. Luciferase activity was determined in the presence or not of penicillin.

Results: Expression of PBPs increased proportionally to bacterial growth, but with a hierarchy of PBP2X>1A=2B>2A. The expression hierarchy was similar in the parent and the resistant mutant, but expression was 2-fold greater in the resistant isolate. Subinhibitory concentrations of penicillin resulted in a specific increase in PBP2A in the resistant mutant, while other PBPs levelled off. PBP-deletions did not yield clear expression patterns, except for deletion of PBP2B, which decreased the expression of other PBPs globally.

Conclusion: (i) The conserved expression patterns, but different expression levels, in the parent and resistant mutant indicate the existence of resistance-linked alterations that are not related to specific PBPs. Whether this increased expression participates to penicillin-resistance remains to be determined. (ii) The increase in PBP2A by subinhibitory concentrations of penicillin indicates penicillin-related induction of a gene, which could be involved in peptidoglycan repair. (iii) The absence of clear expression patterns after PBP deletion indicates that regulation of PBP genes is not PBP interdependent. Hence, PBP are regulated both globally and individually.

Macrophage Migration Inhibitory Factor (MIF) Gene Polymorphisms and Tuberculosis

¹RENNER P., Roger T., Anderson S., Chanson A., Bochud M., Bochud P., Levin M., Calandra T.,

*Infectious diseases*¹

Background: The pro-inflammatory cytokine MIF is an important effector molecule of innate immunity and inflammation. Two functional polymorphisms of the MIF promoter, a 5 to 8 CATT tetranucleotide repeat at -794 (-794 CATT₅₋₈) and a G/C single nucleotide polymorphism at -173 (-173*G/C SNP), have been associated with susceptibility to and/or severity of rheumatoid arthritis, atopy and ulcerative colitis.

Objective: To study whether *MIF* gene polymorphisms were associated with either susceptibility to or severity of tuberculosis (TB) and to analyze the functional and biological effects of *MIF* polymorphisms *in vitro*.

Methods: Case control study including healthy Mantoux positive adults, healthy Mantoux positive and negative children and children with active TB from 2 groups: the Xhosa ethnicity (black) and the Cape coloured (descendants from a mixed population of imported slaves). -794 CATT₅₋₈ microsatellite and -173*G/C SNP were detected by high-resolution gel-electrophoresis and TaqMan[®] SNP Genotyping Assay, respectively. *MIF* promoter alleles (-1073/+129) were cloned into a luciferase reporter construct and tested in THP-1 human monocytic cells.

Results: A novel microsatellite composed of 3 CATT repeats at position -794 was identified in Xhosa and Cape colored. The overall frequencies of CATT₃₋₈ and -173*G/C alleles were:

allele:	CATT ₃	CATT ₅	CATT ₆	CATT ₇	-173*C	-173*G
Xhosa	1.7%	39.8%	41.5%	17%	53.5%	46.5%
Cape colored	0.5%	31.1%	50.2%	18.2%	37.5%	62.5%
Caucasian	0%	27.5%	61.8%	10.4%	17.8%	82.2%

In contrast to what has been observed in Caucasians, there was no linkage disequilibrium between the -173*G/C SNP and -794 CATT₃₋₈ microsatellite in Xhosa.

The frequencies of both -173*G/C and -794 CATT₃₋₈ polymorphisms were similar in patients and controls. However, in the Cape colored cohort, the frequency of the -794 CATT₆₋₆ genotype was found to be significantly decreased in cases with extrapulmonary TB when compared to controls (3.4% vs. 33.3% [mantoux (mx) neg. children], 43.8% [mx pos children] and 32.6% [mx pos adults]; p=0.004, p=0.044 and p=0.012, respectively). Interestingly, transient transfection of *MIF* promoter constructs in THP-1 monocytes showed that the transcriptional activity of the *MIF* promoter increased with the number of CATT repeats, suggesting an increased MIF protein production for carriers of the CATT₆ allele.

Conclusions: Taken together with our previous results in Caucasians, these results show that genotype and allele frequencies of -173*G/C SNP and -794 CATT MIF-promoter polymorphisms vary substantially between different ethnic groups, underlining the vital importance of ethnic stratification of genetic association studies.

The negative association between the -794 CATT₆₋₆ genotype and extrapulmonary TB in the Cape colored cohort suggests that this genotype confers an improved ability to contain *mycobacterium tuberculosis* in the lung, depending on the ethnic background. This could be due to an increased expression of MIF protein, as indicated by the increased transcriptional activity of the 6-CATT-reporter construct *in vitro*.

Identification of Genomic Determinants Acting on the Efficiency of Internal Ribosome Entry Site Elements of Viral and Cellular Origin

¹KAZADI K., ¹Loeuillet C., ²Beckmann J., ³Moradpour D., ¹Telenti A.,

Microbiology institut, CHUV¹, Division of Medical Genetic, CHUV², Division of Gastroenterology and Hepatology, CHUV³,

Background: Internal ribosome entry sites (IRESs) are used in eukaryotic cells to control mRNA translation under cellular stress (apoptosis, heat shock) or during the G2 phase of the cell cycle. IRESs are also used by viruses as a strategy to bypass inhibition of cap-dependent translation that commonly results from viral infection. We aimed at identifying genomic determinants of differences in cellular control of IRES-mediated translation.

Methods: We investigated two viral IRESs (Encephalomyocarditis virus (EMCV) and Hepatitis C virus (HCV)), and two cellular IRESs (the inhibitor of apoptosis XIAP and the oncogene c-myc). We used EBV-immortalized B lymphoblastoid cells from the Centre d'Etude du Polymorphisme Humain (CEPH) representing an in vitro approach to family structures allowing genome scan analyses. In addition, 293T, Hela, Huh-7, BHK-21, CHO, Raji and Jurkat cell lines were used to establish the methods. Bicistronic lentiviral constructs included: mRFP (red) under the control of CMV- or EF1a-promoters, followed by eGFP (green) after an IRES element. After lentivirus transduction, the relative expression of the two markers was assessed by FACS.

Results: Both HCV and EMCV IRES exhibited cell-dependent translational activity. Relative HCV IRES activity (green/red) ranged from 0.3 (293T) to 3.1 (Raji), and EMCV IRES from 1.2 (293T) to 2.7 (Huh-7). Analysis of CEPH B lymphoblastoid cell lines from different individuals using an HCV IRES (n=16) or an EMCV IRES (n=3) identified interindividual differences of 2.8-fold and 1.07-fold, respectively. Testing of cellular IRESs is ongoing.

Conclusion: We hypothesize that IRES efficiency depends on different cellular transcriptional and translational factors. Optimization of CEPH transduction with bicistronic constructs will allow us to evaluate heritability and to perform genome scan analyses with the aim to identify chromosomal associations with the control of IRES activity.

GENE EXPRESSION ANALYSIS OF THE CLC GENOMIC ISLAND OF PSEUDOMONAS SP. STRAIN B13

¹GAILLARD M., Ajil-Zaraa I., Lacour S., ¹van der Meer J.,

Département de microbiologie fondamentale, UNIL Lausanne

The *clc* element is a mobile DNA element from the group of genomic islands. It was originally identified in *Pseudomonas* sp. strain B13 which is able to metabolize 3-chlorobenzoate (3-CBA). The ability to degrade 3-CBA originates from the *clcABDE* genes, which are located on the *clc* element. The *clc* element can excise and transfer from strain B13 to other bacteria. Critical to the excision process is a phage-like integrase gene encoded on the *clc* element itself. The transfer process itself is not known. Interestingly, the DNA sequence of a large region of the *clc* element is conserved between various genomic islands suggesting a central common function for this region in the behaviour of the islands, such as conjugation. Analysis of the complete *clc* element sequence also revealed the presence of other metabolic genes, like those for 2-aminophenol degradation. In addition, genes with high similarity to a multicomponent aromatic ring dioxygenase were detected, which may be responsible for the first step in 3-chlorobenzoate degradation, a step which is still undescribed. In this study we analyzed the expression of several genes on the *clc* element, including catabolic and conserved hypothetical genes, by RNA hybridization. Among the analyzed genes, we found a putative helicase that was only expressed in stationary phase and in presence of 3-CBA. The expression of an helicase under conditions favourising the mobility supports the idea of a conjugative system encoded by the *clc* element. We are currently looking for other genes implicated in bacterial conjugation. Concerning the catabolic genes, we found that the 2-aminophenol dioxygenase is only expressed in strain B13 cultivated in presence of 2-aminophenol. This result suggests that the 2-aminophenol pathway could be functional and leading to new adaptive properties for the bacterium.

Lack of Correlation between In Vitro Biofilm Formation and In Vivo Virulence of *Streptococcus gordonii* in Experimental Endocarditis

¹BIZZINI A., ¹Entenza J., ¹Beggah S., ¹Giddey M., ¹Vouillamoz J., ¹Moreillon P.,

Département de microbiologie fondamentale, UNIL Lausanne

BACKGROUND

The ability to form a biofilm (BFM) is a pathogenic factor in many bacteria. However, the correlation between *in vitro* BFM formation and *in vivo* virulence in infective endocarditis is not clear. *S. gordonii* can cause infective endocarditis. Here, we generated BFM-deficient mutants of *S. gordonii* by targeting various pathways reported to alter BFM (quorum sensing, fructose metabolism, cell wall formation) and assessed their virulence in a rat model of experimental endocarditis (EE).

METHODS

Deletion mutants of the wild type (WT) were constructed by PCR ligation mutagenesis. BFM was quantified using a microtiter plate assay, and its structure assessed by confocal microscopy. Strains were tested for adherence to platelet-fibrin clots (PFC) and for their ability to produce EE in rats with catheter-induced aortic vegetations. Animals were inoculated with 10^6 CFU, sacrificed 3 days later and quantitative cultures of vegetations performed.

RESULTS

Strains	BFM		Relative PFC Adherence	Infected vegetations/total (\log_{10} CFU/g)
	Quantification	Layer structure		
WT	100 %	Confluent	100 %	9/9 (8.5)
WT Δ <i>comD</i>	29 %	Loose	120 %	8/8 (7.5)
WT Δ <i>fruK</i>	42 %	Loose	144 %	9/9 (7.9)
WT Δ <i>pbp2b</i>	38 %	Patchy	124 %	8/8 (8.8)

CONCLUSION

BFM mutants were altered in BFM formation and structure *in vitro*, and were slightly more adherent to PFC. However, an impaired BFM production did not influence the *in vivo* ability of *S. gordonii* to colonize vegetations and multiply locally. Thus, although other pathways allowing the bacteria to form a BFM *in vivo* cannot be excluded, our results show that the lack of BFM formation *in vitro* does not correlate with a decreased virulence in *S. gordonii* EE.

The *Bacillus subtilis* *pgcA* gene encodes alpha-phosphoglucomutase involved in biofilm formation

¹LAZAREVIC V., Soldo B., Noël M., Harold P., Dimitri K., ¹Vladimir L.,

Département de Microbiologie Fondamentale¹, UNIL Lausanne

Mutations associated with a phosphoglucomutase (PGM) deficiency were mapped to *pgcA*, a 1698-bp ORF located at 86° on the *Bacillus subtilis* chromosome. To confirm that the identified mutations are indeed responsible for the mutant phenotype, they were back crossed into the wild type strain. Mutation transfer was accompanied by altered colony aspect, altered cell morphology and formation of aggregated cell masses when grown in liquid medium, resistance to phages phi-29 and rho-11, an impaired PGM activity in the soluble cell extract fraction and deficiency in biofilm formation which could be due to reduced intracellular pool of UDP-glucose. The role of UDP-glucose in the synthesis of cell wall polymers that might influence biofilm formation on an abiotic (PVC) surface is discussed.

IDENTIFICATION OF AN EXPANDED POPULATION OF ACTIVATED CD4+ T CELLS IN LIVER TRANSPLANT RECIPIENTS DEFINED BY CD25+CD45RO+IL7R+ PHENOTYPE

¹CODARRI L., ²Ciuffreda D., ³Vallotton L., ⁴Pascual M., ³Giuseppe P.,

*Collaborated equally to this work

Immunology and Allergy/LIPS¹, Immunology/LIPS², Immunology/LIPS³, Transplantation⁴,

Aim of the study: To analyze the different cell populations of activated CD4+CD25+ T cells in different cohorts of liver transplant recipients.

Background: CD25 is the alpha chain of the IL-2 receptor and it is expressed either constitutively by CD4+CD25+ T regulatory cells (T regs) or by antigen-specific activated CD4+ T cells. T regs mediate suppressor function and have been proposed to control effector

responses to alloantigens in transplantation.

Methods: A total of 36 liver transplant recipients were studied: 17 HCV-infected and 19 HCV negative (transplanted for alcoholic liver cirrhosis) and 25 healthy individuals as controls. In order to characterize the different cell populations of CD4+CD25+ cells, we performed phenotypic and functional analyses and evaluated the expression of Foxp-3, a molecular marker of Tregs. The phenotypic analysis included the evaluation of CD45RO and IL-7R while the functional analysis the ability to suppress anti-CD3 plus anti-CD28 or mixed lymphocyte reaction mediated proliferation.

Results: The flow cytometry analysis allowed to identify two populations of CD4 T cells based on the expression of CD45RO and IL-7R, CD45RO+IL7R+ and CD45RO+IL7R-. Of interest, the CD45RO+IL-7R+ cells were significantly expanded (21%+/-7%, mean+/-SD, of CD4+CD25+ cells) in the HCV negative transplant recipients compared to HCV positive transplant recipients (9%+/-5% of CD4+CD25+ cells) and to healthy individuals (5%+/-3% of CD4+CD25+ cells) (P<0.05).

The CD45RO+IL7-R- cells expressed Foxp-3 and mediated suppressor function thus indicating that these cells were typical T regs while the CD45RO+IL-7R+ cells did not expressed Foxp-3 and lacked suppressor function. Therefore, CD45RO+IL-7R+ cells are likely typical activated antigen-specific CD4+CD25+ T cells.

Eight out 17 HCV positive transplant recipients were treated with PEG-IFN and ribavirin. In patients with viral clearance (HCV RNA below the limit of detection in a qualitative PCR assay) on treatment, we observed an expansion of CD45RO+IL7R+ cells (11%+/-4% before versus 26%+/-12% after treatment and suppression of virus replication).

In the HCV-infected transplant recipients who did not respond to antiviral therapy the percentage of this population remained unchanged overtime (10%+/-4% before and on treatment).

Conclusions: A population of activated CD4 T cells defined by the expression of CD25, CD45RO and IL-7R is expanded in liver transplant recipients. The expansion of this population appears to be negatively modulated by HCV replication.

Studies are ongoing to determine the antigen specificity of the CD4+CD25+CD45RO+IL-7R+ cells and in particular whether these cells are alloreactive CD4 T cells.

Regulation of Human Macrophage Migration Inhibitory Factor (MIF) Gene Expression : Sp1 and CREB Mediate Basal MIF Promoter activity, whereas MIF mRNA Stability Confers Cell-Specific Expression

¹ROGER T., ²Ding X., ²Chanson A., ²Renner P., ²Calandra T.,

Infectious Diseases, BH19-111, CHUV¹, Infectious Diseases²,

Background : The cytokine macrophage migration inhibitory factor (MIF) is an important regulator of innate immunity, inflammation and oncogenesis. Although MIF was discovered nearly 40 years ago, the molecular mechanisms regulating the expression of the *MIF* gene still remain largely unknown. Our previous analysis of MIF promoter activity in THP-1 monocytic cells identified two proximal Sp1 and CRE DNA-binding sites as critical positive regulatory elements of *MIF* transcription.

Objective : To study the transcriptional and post-transcriptional regulation of *MIF* in human cells.

Methods : Experiments were performed with human THP-1 monocytic cells, HeLa cervix epithelial cells, A549 airway epithelial cells, HaCat keratinocytes and peripheral blood mononuclear cells, murine bone-marrow derived macrophages and Sf9 insect cells. MIF mRNA, protein and full-length, truncated or mutated promoter activities were assessed by Northern blotting, Western blotting and luciferase reporter assay, respectively. Transcription factor binding activity was assessed by electrophoretic mobility shift assay, supershift and chromatin immunoprecipitation. Genomic DNA methylation was assessed by sodium bisulfite sequencing.

Results : Electrophoretic mobility shift assays, supershifts and chromatin immunoprecipitation analyses showed that the transcription factors Sp1 and CREB bound to the proximal Sp1 and CRE sites of the MIF promoter *in vivo*. Mithramycin A, a competitive inhibitor of Sp1 binding to DNA, strongly reduced MIF promoter activity and mRNA levels in THP-1 cells, whereas expression of Sp1 in Sp1-deficient Sf9 insect cells increased MIF promoter activity. The Sp1 and CRE sites also regulated *MIF* expression in HeLa and A549 epithelial cells and in HaCat keratinocytes. Albeit located in a CpG island, *MIF* expression was not modulated by DNA methylation of its CpG sites. Steady state MIF mRNA levels correlated with mRNA half-lives in HeLa, A549, HaCat and THP-1 cells suggesting that mRNA stability is a key determinant of cell-specific post-transcriptional control of MIF expression.

Conclusions : The present findings provide evidence implicating Sp1 and CREB and mRNA stability in transcriptional and post-transcriptional regulation of human *MIF* gene expression. The identification of the factors involved in the regulation of the constitutive *MIF* gene expression may provide important insights into the molecular mechanisms leading to increased MIF expression in cancer and in inflammatory and auto-immune diseases.

Mechanism of Membrane Association of the Hepatitis C Virus NS3-4A Complex

¹BERKE J., ²Brass V., ²Blum H., ³Penin F., ⁴Moradpour D.,

*Gastroentérologie et Hépatologie*¹, *2Department of Medicine II, University of Freiburg, D-79106 Freiburg*², *Institut de Biologie et Chimie des Protéines, CNRS-UMR 5086, F-69367 Lyon*³, *1Division of Gastroenterology and Hepatology, Centre Hospitalier Universitaire Vaudois, CH-1011 Lausanne*⁴,

Background and aim: Hepatitis C virus (HCV), a member of the Flaviviridae family of positive-strand RNA viruses, is a major cause of chronic hepatitis, liver cirrhosis and hepatocellular carcinoma worldwide. HCV nonstructural proteins form a membrane-associated replication complex together with replicating viral RNA and altered host cell membranes. NS3-4A, a multifunctional protein harboring serine protease and RNA helicase activities, is an essential component of this complex and a prime target for antiviral intervention. We previously demonstrated that NS3 is targeted to membranes via interaction with its cofactor NS4A. The aim of this project was to further characterize the mechanism of membrane association of the HCV NS3-4A complex.

Methodology: The minimal domain responsible for membrane association of NS4A was investigated by fluorescence microscopy and membrane flotation analyses. The membrane topology of NS4A was investigated by fusion of artificial glycosylation acceptor sites. The mechanism of membrane association was investigated further using in vitro transcription-translation assays. Conserved amino acid residues within the membrane segment of NS4A were mutated and the effect of these mutations on HCV RNA replication was investigated in the replicon system.

Results: The N-terminal 21 amino acids are required for membrane association of HCV NS4A and traverse the phospholipid bilayer as a transmembrane segment. Processing between NS3 and NS4A was required for integral membrane association of NS3-4A. Consistent with these results, membrane association occurred by a posttranslational mechanism. Certain amino acid substitutions in the membrane segment of NS4A abolished HCV RNA replication without interfering with membrane association of NS3-4A.

Conclusions: HCV NS3-4A is targeted to membranes by a posttranslational mechanism, resulting in translocation of the N-terminal 21 amino acids of NS4A across the membrane and integral membrane association. The discordance between preserved membrane association and defective HCV RNA replication of certain mutants indicates that the membrane segment of NS4A may have additional functions beyond serving as a membrane anchor and may be involved in critical protein-protein interactions essential for the assembly of a replication complex. Such interactions are currently being investigated by fluorescence resonance energy transfer (FRET) analyses. These studies should contribute to our understanding of the functional architecture of the HCV replication complex and may allow to define novel targets for antiviral intervention.

The Histone Deacetylase (HDAC) Inhibitor Trichostatin A (TSA) Inhibits Innate Immune Responses

¹ROGER T., ²Ding X., ²Le Roy D., ²Knaup Reymond M., ²Chanson A., ²Calandra T.,

Infectious Diseases, BH19-111, CHUV¹, Infectious Diseases²,

Background: HDAC inhibitors (HDIs), among which trichostatin A (TSA), are anti-cancer agents that have shown beneficial effects for the treatment of various solid or haematological malignancies in phase I-II clinical trials. In recent years, HDIs have emerged as potent anti-inflammatory drugs in models of chronic/auto-immune inflammatory diseases such as asthma, colitis, rheumatoid arthritis, hepatitis and lupus erythematosus. Our objective was to study the effect of TSA on innate immune responses.

Methods: Mouse RAW 264.7, thioglycollate-elicited and bone marrow-derived macrophages, mouse splenocytes and human whole blood were pre-incubated 1 h with TSA (0-0.1 μ M) before stimulation for 15 min-18 h (macrophages and whole blood) or 48 h (splenocytes) with ultra-pure LPS (100 ng/ml), Pam₃CSK₄ (10 μ g/ml), peptidoglycan (10 μ g/ml), CpG oligonucleotide (2 μ M) or heat-killed ($5 \cdot 10^7$ CFU/ml) *E. coli*, *S. aureus*, *S. pneumoniae* and *C. albicans*.

Results: TSA dose-dependently inhibited (up-to 100% at 0.1 μ M TSA) stimulus-induced TNF and IL-6 release by murine macrophages and dendritic cells and by human whole blood. The inhibition of cytokine release by TSA-treated RAW 264.7 macrophages was associated with a diminished nuclear translocation of NF- κ B (assessed by band shifts) and a strong inhibition of NF- κ B-mediated transcriptional activity (measured in cells transiently with an NF- κ B luciferase reporter vector) and cytokine mRNA expression. TSA also fully abrogated splenocyte proliferation in response to microbial stimuli.

Conclusions: TSA inhibits *in vitro* innate immune responses to microbial products. HDI treatment may therefore weaken the innate immune status of cancer patients with these drugs. On the other hand, HDIs may represent a new class of agents that may be used to dampen the overwhelming inflammatory response in septic patients. These two hypothesis are currently tested in pre-clinical models.

Inhibition of Histone Deacetylase Down-regulates Macrophage Migration Inhibitory Factor (MIF) Expression by Deacetylating the MIF Promoter and Impairing MIF Gene Transcription

¹ROGER T., ²Ding X., ²Roger T., ²Le Roy D., ²Chanson A., ²Calandra T.,

Infectious Diseases, BH19-111, CHUV¹, Infectious Diseases²,

Background : Histone deacetylase inhibitors (HDI) were originally developed as anti-cancer agents with the ability to induce the differentiation or the apoptosis of tumor cells. In phase I-II clinical trials, HDI have shown beneficial effects for the treatment of various solid tumors or haematological malignancies. Yet, the molecular basis of the anti-tumoral effects of HDI is not fully understood. Macrophage migration inhibitory factor (MIF), a pro-inflammatory cytokine, has recently been implicated in cell proliferation, angiogenesis and oncogenesis and may therefore represent a novel target of HDI action.

Objective: To study whether HDI modify the expression of MIF in human cells.

Methods : Human whole blood, HeLa cervix epithelial cells, HaCat keratinocytes and U-937, KG1a and HL-60 leukemic cell lines were exposed to trichostatin A (TSA), a prototypical HDI. *MIF* gene transcription, mRNA, protein and full-length, truncated or mutated promoter activities were assessed by nuclear run on, Northern blotting, Western blotting and luciferase reporter assay, respectively. Transcription factor binding activity was assessed by electrophoretic mobility shift assay and chromatin immunoprecipitation. HDAC activity was measured using a HDAC assay kit. Acid soluble histones were extracted and analyzed for acetylation by Western blotting.

Results : MIF expression was strongly down-regulated by TSA in all cell types. Nuclear run on analyses showed that TSA reduced *MIF* gene transcription. Yet, TSA did not affect MIF promoter activity (as measured by transient transfection). It also did not reduce the nuclear content of Sp1 and CREB, two transcription factors previously shown to be necessary for *MIF* gene expression. Surprisingly, even though global histone acetylation was strongly increased by TSA, by contrast, TSA deacetylated the histones associated with the MIF promoter as assessed by chromatin immunoprecipitation. This effect required protein synthesis and was coupled with a decreased recruitment of Sp1 and CREB to the bona fide MIF promoter.

Conclusions : TSA down-regulates MIF expression by a novel molecular mechanism involving local deacetylation of histones and reduced transcription of the *MIF* gene. Considering that MIF is over-expressed in human neoplasia and required for tumor associated angiogenesis, our findings suggest that the anti-tumoral effects of HDI may be mediated by a down-regulation of MIF expression.

Development of a Model System to Study Hepatitis B and C Virus Coinfection

¹GOUTTENOIRE J., ²Gajer M., ²Brass V., ²Sun D., ²Blum H., ²Nassal M.,
³Moradpour D.,

*Gastroentérologie et Hépatologie*¹, Department of Medicine II, University of Freiburg, D-79106 Freiburg², Division of Gastroenterology and Hepatology, Centre Hospitalier Universitaire Vaudois, CH-1011 Lausanne³,

Background and aim: Hepatitis B virus (HBV) and hepatitis C virus (HCV) share similar routes of transmission. By consequence, coinfection with both viruses is frequent. Coinfection has been associated with more severe liver disease and frequent progression to liver cirrhosis and hepatocellular carcinoma (HCC). On the other hand, clinical evidence suggests reciprocal replicative suppression of the two viruses ('viral interference'). Due to the lack of appropriate model systems, however, virtually nothing is known about molecular interactions between HBV and HCV. The aim of this study was to develop a model system to study HBV and HCV coinfection.

Methods: A tetracycline-regulated gene expression system and subgenomic HCV replicons were used to generate Huh-7 human HCC cell lines replicating both HBV and HCV. Protein expression was studied by conventional SDS-PAGE and native agarose gel immunoblot assays. HBV and HCV replication were investigated by Southern and Northern blot, respectively. The subcellular localization of viral proteins was studied by immunofluorescence and confocal laser scanning microscopy.

Results: Three successive transfection and selection steps allowed the establishment of Huh-7 cells inducibly replicating HBV and constitutively replicating a subgenomic HCV RNA. Thus, HBV replication could be switched on and off in the same cell while HCV RNA replication occurred continuously. HBV and HCV replication could be inhibited specifically using adefovir and interferon-alpha, respectively. HBV protein expression and replication slightly reduced HCV RNA and protein levels. HBV core protein was found not to colocalize with HCV nonstructural proteins. Studies on the subcellular localization of the other viral proteins are in progress. Interferon-alpha inhibited HCV RNA replication in a dose-dependent manner regardless of the presence or absence of HBV replication. Thus, replicating HBV did not affect the direct antiviral effect of interferon-alpha on HCV replication.

Conclusions: We describe a novel model system allowing the study of interactions between HBV and HCV. Understanding such interactions at the molecular level should yield new insights into the pathogenesis and clinical management of HBV-HCV coinfection. Ongoing efforts are aimed at extending this system to the in vitro production of infectious HBV and HCV.

Functional and phenotypic characterization of HCV-specific T cells in chronic HCV mono- and HIV/HCV co-infection.

¹DUTOIT V., ¹Comte D., ¹Pantaleo G.,

*IAL*¹,

Background: Phenotypic and functional characterization of several virus-specific T cell responses including CMV, EBV and HIV-1 have been performed in the last years. However, these parameters have only sporadically been assessed for HCV-specific T cell responses. The influence of HIV-1 co-infection on the function of HCV-specific T cells has also rarely been addressed. We therefore aimed to investigate and compare these issues in the context of HCV mono-infection and HIV/HCV co-infection.

Methods: HCV-specific CD4+ and CD8+ T cells from chronically HCV mono-infected (n = 10) and HIV/HCV co-infected (n = 8) individuals were tested for proliferation using the CFSE dye assay after stimulation with the cognate peptide. In addition, profiles of IFN-g and IL-2 secretion and of differentiation markers (CD45RA and CCR7) expression by specific T cells were analyzed by multi-color flow cytometry. Finally, ability of HCV-specific CD8+ T cells to lyse autologous peptide-pulsed EBV-transformed B cell lines was investigated.

Results: Both CD4+ and CD8+ HCV-specific T cells from HCV mono-infected individuals were clearly able to proliferate after 5 to 7 days stimulation with the corresponding HCV-derived peptide in absence of exogenous help such as IL-2. Most interestingly, HCV-specific T cells from HIV/HCV co-infected individuals exerted a similar proliferation potential. In addition, in contrast to what has been observed for HIV-1-specific CD4+ and CD8+ T cells which are composed exclusively of IFN-g-secreting cells in the untreated chronic phase of infection, HCV-specific T cells displayed a poly-functional profile of cytokine secretion, with CD4+ T being composed of single IL-2, double IFN-g/IL-2 and single IFN-g-secreting cells and CD8+ T cells of double IFN-g/IL-2 and single IFN-g-secreting cells. This profile was observed for both HCV mono-infected and HIV/HCV co-infected patients. Finally, HCV-specific CD4+ and CD8+ T cells were found predominantly in the CD45RA- CCR7- effector memory subset but were also observed in the CD45RA-CCR7+ central memory subset. Finally, HCV-specific CD8+ T cells were able to lyse autologous EBV-transformed B cell lines pulsed with the cognate HCV peptide, both in HCV mono- and HIV/HCV co-infection.

Conclusions: The presence of polyfunctional HCV-specific T cells indicates a preservation of immune functions in HCV infection and it may be consistent with a slower progression of HCV compared to HIV infection.

Identification and characterization of an expanded CD4+ CD25+ T cell population with putative allospecific properties in a kidney transplant recipient with chronic humoral rejection.

Vallotton Laure¹, Codarri Laura¹, Ciuffreda Donatella¹, Harari Alexandre¹, Venetz Jean-Pierre², Pascual Manuel², Pantaleo Giuseppe¹

¹ Labo. d'immunopathologie du SIDA, Service d'Immunologie et d'Allergie, CHUV

² Centre de Transplantation d'Organes, CHUV

Background: CD4+ CD25+ T cells can belong to 2 different groups of T lymphocytes: activated T cells or regulatory T cells. We have recently identified CD127 (IL-7 receptor) as a useful marker to distinguish these 2 populations; regulatory T cells (defined by a high expression of the transcription factor FoxP3) are mainly CD45RO+ CD127- whereas activated T cells (which are FoxP3 negative) mainly CD45RO+ CD127+. In liver transplant recipients, we found that the CD45RO+ CD127+ population was significantly expanded (21±7%) in HCV negative patients compared to HCV positive patients (9±5%) and to healthy subjects (5±3%)(see poster of Laura Codarri et al.). To further analyse the phenotype and function of this CD4+25+45RO+127+ population, we chose to test kidney transplant recipients, because in the case of a living donor transplantation we have access to peripheral blood mononuclear cells (PBMC) from the donor, which are essential for in vitro experiments that mimic the transplantation status.

Aim of the study: Phenotypic and functional characterization of a subset of CD4+ CD25+ T cells in a kidney transplant recipient with biopsy-proven chronic rejection.

Methods: We performed phenotypic (expression of CD4, CD25, CD45RO and CD127, FoxP3) and functional (MLR assay, production of IL-2 and IFN γ) analyses on the PBMC of a 27 years old female who received a kidney from a living related donor in 1997. Despite an immunosuppressive therapy composed of tacrolimus and prednisone, she was diagnosed of chronic humoral rejection with anti-donor HLA antibodies (anti-DR15).

Results: The CD4+ CD25+ T cell population was only slightly increased in this patient compared to healthy control subjects (3.58% versus 2.51±0.12%). In contrast, the CD4+25+45RO+127+ population was found to be highly expanded (42.70% of CD4+25+ T cells versus 5±3% in healthy control subjects and 19.18±6.43% in two kidney transplanted patients without rejection) and was FoxP3 negative. In MLR assays, we tested the proliferative capacity of this population: we observed a five-fold stronger proliferation when stimulated by irradiated donor PBMC compared to a stimulation by irradiated 3rd party PBMC. The CD4+25-45RO+127+ and CD4+25-45RO-127+ populations, used as controls, showed a two-fold, respectively three-fold, stronger proliferation compared to a stimulation by a 3rd party. We then assessed the production of cytokines (IL-2 and IFN γ) by the CD4 T cells when co-cultured overnight with irradiated donor PBMC: the CD4+25+45RO+127+ population had the highest frequency of cytokine secreting T cells (single IL-2 11.91%, dual IL-2/ IFN γ 5.95%, single IFN γ 6.75%); by contrast, the overnight stimulation of two other subjects with irradiated 3rd party PBMC did not induce any cytokine production.

Conclusion: In a kidney transplant recipient with chronic humoral rejection we have found an expanded CD4+ CD25+ population characterized by the expression of CD45RO and CD127, which was able to proliferate and secrete cytokines quickly when stimulated by donor-specific PBMC. This finding suggests that the expanded CD4+25+45RO+127+ population constitutes a memory pool of alloreactive CD4 T cells directed towards donor-specific antigens. Work is ongoing to determine if this T cell population may identify transplant recipients with chronic rejection versus stable patients or "tolerant" patients.

Index des auteurs

Remarque: Auteur principal en gras

ABAZA AOUATEF **NEU-56**/
ABBAL CLAIRE **MCV-5**/
ABBET ELODIE **EHU-35**/
ABDERRAHMANI AMAR **MCV-39**/
ABRIEL HUGUES MCV-17/
AHMAD D GEN-23
AJIL-ZARAA IMÈNE IMI-14/
ALLAGNAT FLORENT **MCV-13**/MCV-28/
ALLAMAN IGOR NEU-36/
ALLAMAN-PILLET NATHALIE MCV-26/
ALLAOUA MOHAMED **NEU-22**/
ALTWEGG M. THE-31/
AMINIAN KAMIAR THE-34/THE-35/
ANDERSON SUZANNE IMI-11/
ANNONI JEAN-MARIE NEU-3/
ANTONARAKIS STYLIANOS GEN-20/
ARCARO ALEXANDRE MCV-5/
ARCIONI S GEN-23
ARIAL MARC **EHU-25**/EHU-30/
ARNOLD PIERRE **THE-40**/
ASAHI N ODE-16/
ASAL SASCHA THE-40/
AU KARIN MCV-22/
AUBRY DOMINIQUE ODE-4/
AUDERSET KATYA ODE-11/ODE-6/ODE-18
AUFÈRE LAURENCE THE-40/
AUGSBURGER MARC NEU-54/
AVENATI T THE-18
AVOIS LIDIA **THE-32**/
BACCAGLIONI EMANUELA **NEU-13**/
BACHMANN CLAUDE NEU-7/NEU-8/
BADAUT JEROME NEU-15/
BAECHLER SÉBASTIEN **EHU-27**/
BAGUTTI CARLO MCV-20/
BALMAS BOURLOUD KATIA ODE-11/ODE-6/ODE-18
BARAKAT-WALTER IBTISSAM NEU-29/NEU-30/
BARAL SANDRA GEN-1/
BARBATI GIULIA EHU-28/
BARBEY FRÉDÉRIC MCV-9/
BAUER DOUGLAS MCV-8/
BAUMANN PIERRE NEU-23/
BAUME NORBERT **MCV-20**/
BAÏSSE-AGUSHI BÉNÉDICTE **MCV-4**/
BECK POPOVIC MAJA ODE-11/
BECKMANN JACQUES IMI-12/GEN-20/MCV-17/MCV-26/
BEGGAH SIHAM GEN-17/IMI-15/
BELEM TOUNABA EHU-7/

BELLINI CRISTINA **IMI-4**/
BENHATTAR JEAN ODE-15/ODE-17/
BENKELFAT CHAWKI NEU-18/
BERGER YANN MCV-19/
BERKE JAN MARTIN **IMI-19**/
BERNARDINELLI YANN **NEU-33**/
BERNASCONI ERIC MCV-18/
BERNEY ALEXANDRE **NEU-18/NEU-19**/
BERODE MICHÈLE **EHU-7**/
BERTA TEMUGIN **GEN-7**/NEU-12/
BERTAGGIA DEBORA MCV-5/
BERTHONNECHE CORINNE MCV-17/
BESSON JACQUES NEU-23/THE-40/
BEYER V GEN-23
BIGLIARDI PAUL **NEU-4**/
BIGLIARDI-QI MEI NEU-4/
BILLE JACQUES GEN-13/ODE-2/IMI-4/THE-31
BIOLEY GILLES ODE-8/
BISCHOF DELALOYE ANGELIKA NEU-22/ MCV-34/MCV-35/
BIZE VINCENT **MCV-25**/
BIZZINI ALAIN **IMI-15**/
BLEIBER GABRIELA GEN-2/GEN-3/GEN-24
BLOCH JOCELYNE THE-2/
BLUM HUBERT E IMI-19/IMI-22
BOCHUD FRANÇOIS O. ODE-3/
BOCHUD MURIELLE IMI-11/
BOCHUD PIERRE-YVES IMI-11/
BOGOUSSLAVSKY JULIEN NEU-14/NEU-15/NEU-19/NEU-3/NEU-54/NEU-55/THE-
23/THE-24/ NEU-22/
BOLAY SASKIA THE-39/
BOLOGNINI MONIQUE NEU-40/
BONAFE LUISA GEN-21/
BONDALLAZ PERCY **NEU-30**/
BONGFEN SILAYUV IMI-5/
BONNY CHRISTOPHE MCV-26/
BONVALLAT SÉVERINE NEU-16/
BORDONI A EHU-26/
BORENS OLIVIER EHU-2/
BORGOÑO CARLA A. ODE-5/
BORRUAT FRANÇOIS-XAVIER NEU-55/THE-22/
BORSELLO TIZIANA NEU-50/
BORTOLOTTI MURIELLE **MCV-32**/
BOSMAN FRED T ODE-17/
BOTEZ STEPHAN THE-22/
BOUGEL STÉPHANIE **ODE-15**/
BOUGEON S GEN-23
BOUGORSKI ROUSLAN MCV-18/
BOURQUIN CÉLINE EHU-5/
BOUTREL BENJAMIN **NEU-3**/
BOVET P NEU-58/
BOVET PASCAL EHU-16/MCV-16/MCV-30/MCV-31/MCV-38/
BOVET PIERRE GEN-1/NEU-23/NEU-6/

BRAISSANT OLIVIER **NEU-7**/NEU-8/NEU-61
BRAKCH NOUREDDINE **MCV-9**/
BRAMBILLA LILIANA NEU-13/
BRASS VOLKER IMI-19/IMI-22/
BRAWAND MARLYSE NEU-23/
BRIOSCHI ANDREA **NEU-55**/
BROCARD MURIELLE NEU-23/
BRUGGIMANN LAURE NEU-3/
BRUNET JEAN-FRANÇOIS **THE-2**/
BRUZZESE O GEN-23
BUCLIN THIERRY IMI-1
BUGNON OLIVIER IMI-2/ THE-18/ THE-19
BULLIARD JEAN-LUC **EHU-26**/ENA-1/
BURGAT LAURENCE **NEU-35**/
BURKHALTER JULIA NEU-20/
BURKHARD PIERRE NEU-19/
BURNAND BERNARD THE-2/THE-8/THE-9/
BURNIER MICHEL MCV-16/MCV-38/ THE-18
BUTTET SOVILLA JOCELYNE NEU-35/
BUTTICAZ CHRISTOPHE **IMI-8**/
BUTTY ANNE-CHRISTINE **MCV-22**/
BÜRGI RALPH NEU-56/
CABUNGCAL JAN HARRY **NEU-11/NEU-38**/ NEU-23/
CAGNON LAURÈNE NEU-7/**NEU-8**/
CALANDRA THIERRY IMI-18/IMI-20/IMI-21/IMI-11/IMI-9/ODE-16/ODE-2/
CALMES JEAN-MARIE MCV-27/
CAMEN CHRISTIAN NEU-6/
CAMMOUN LEILA **NEU-58**/
CAMPISI R MCV-34/
CAO LEI THE-33/
CAPENDEGUY OIHANA **MCV-21**/
CARDELLI DAVID **MCV-6**/
CARDINAUX JEAN-RENÉ NEU-53/
CARNAL BÉATRICE NEU-51/
CAROTA ANTONIO NEU-55/
CARRERA EMMANUEL **THE-23**/
CASTELLA CYRIL **ODE-3**/
CAUDERAY MICHEL MCV-20/
CAVASSINI MATTHIAS GEN-6/IMI-1/THE-13/THE-14/IMI-2/
CEROTTINI JEAN-CHARLES ODE-8/
CESSON VALERIE **ODE-9**/ODE-13
CHAGAS JAIR R. ODE-5/
CHALARD ROMILDA NEU-39/**NEU-53**/
CHANSON ANNE-LAURE IMI-18/IMI-20/IMI-21/IMI-11/
CHAPPUIS CÉLINE NEU-23/**NEU-32**/
CHAPUIS CATHERINE MCV-19/
CHARRIÈRE NICOLE EHU-8/
CHATTON JEAN-YVES NEU-33/
CHAU VAN CATHERINE MCV-23/
CHIOLERO ARNAUD **EHU-16**/MCV-31/MCV-38/
CHRAST ROMAN MCV-11/
CIARDO D. THE-31/

CIUFFREDA DONATELLA IMI-17/IMI-24
CLARKE PETER G.H. NEU-50/NEU-52/NEU-41
CLARKE STEPHANIE NEU-1/NEU-25/NEU-35/NEU-6/NEU-28
CLOUTIER SYLVAIN M. ODE-5/
COCCHI LUCA **NEU-14**/
COCHARD NATHALIE NEU-23/
CODARRI LAURA **EHU-5/IMI-17/IMI-24**
COLLYN FRANÇOIS **GEN-10/GEN-13**/
COLOMBO SARA GEN-6/**IMI-1**
COMTE DENIS IMI-23/
CONUS PHILIPPE NEU-23/
CORNUZ J MCV-37/
CORPATAUX JEAN-MARC MCV-14/
CORRADIN GIAMPIETRO ODE-13/ODE-9/IMI-5/
CORREA RAFAEL EHU-5/
COSTE ALIX GEN-13/
CRETOL SÉVERINE **NEU-23**/
CROQUETTE-KROKKAR MARINA NEU-23/
CUENNET MYRIAM **EHU-17**/
CUÉNOD MICHEL NEU-11/NEU-21/NEU-23/NEU-38/NEU-45/NEU-46/NEU-58/GEN-1
DANIEL ROY THOMAS THE-26/THE-27/
DANON NADIA **MCV-38**/
DANUSER BRIGITTA EHU-16/EHU-25/EHU-9/
DAR IMRAN MCV-26/
DARIOLI R **MCV-36/MCV-37**/
DE CASTRO RIBEIRO MARLISE **NEU-15**/
DE PREUX ANNE-SOPHIE **MCV-11**/
DE SANTIS LAURA **NEU-28**/
DE SMEDT MAGDA EHU-5/
DE WECK D EHU-26/
DEBATISSE DAMIEN NEU-30/NEU-59/THE-23/**THE-26/THE-27**/
DEBONNEL GUY NEU-18/
DECOSTERD ISABELLE NEU-12/
DEFAUX A NEU-61
DEHDASHTI AMIR THE-26/
DEMIERRE MICHEL THE-37/
DEPERTHES DAVID ODE-5/
DEPPEN P NEU-58/
DEPPEN PATRICIA GEN-1/NEU-23/NEU-32/NEU-45/
DERIAZ OLIVIER THE-40/
DESCOMBES FRANÇOIS ODE-3/
DESCOMBES PATRICK GEN-7/
DESMARCHELIER AURÉLIEN EHU-28/MCV-20/
DESPLAND PAUL-ANDRÉ THE-23/
DEUTSCH SAMUEL GEN-20/
DEVAUD JEAN-CHRISTOPHE THE-13/
DEVUYST GERALD THE-23/
DIACERI GIACOMO MCV-4/
DIAMANDIS ELEFTHERIOS P. ODE-5/
DIKSIC MIRKO NEU-18/
DIMITRI KARAMATA IMI-16/
DIMITROVA NEVENA **THE-17**/

DING XAVIER IMI-18/IMI-20/IMI-21/
DO KIM GEN-1/NEU-11/NEU-14/NEU-38/NEU-58/NEU-21/**NEU-23**/NEU-32/NEU-45/NEU-46/
DOMENIGHETTI ANDREA MCV-4/
DONDA ALENA ODE-13/ODE-9/
DROZ PIERRE-OLIVIER EHU-7/
DU PASQUIER RENAUD NEU-14/
DUBOCHET JACQUES NEU-5/
DUCHOSAL MICHEL A ODE-19/ODE-4/GEN-23
DUNAND MURIELLE GEN-21/**GEN-5/THE-22**/
DUPUIS MARC ODE-19/ODE-4/
DUTOIT VALÉRIE **IMI-23**/
DUVOISIN BERTRAND ODE-16/ODE-2/
DÉCOSTERD ISABELLE GEN-7/
DÉCOSTERD LAURENT GEN-6/
DÉGLISE SÉBASTIEN **MCV-14**/
DÉGLON JEAN-JACQUES NEU-23/
EAP CHIN B. NEU-23/
ECKSTEIN MIGUEL P. ODE-3/
ELZI LUIGIA GEN-6/
ENTENZA JOSÉ IMI-15/
ETEMAD-SAJADI ALI **THE-36**/
ETTER L GEN-23
FACTA A MCV-34/MCV-35/
FAEH DAVID **MCV-29/MCV-30/MCV-31**/ MCV-40
FATTET S ODE-18/
FAVEZ NICOLAS EHU-17/EHU-35/
FAVRAT BERNARD THE-2/THE-8/THE-9/
FAVRE DIMITRI **ODE-7**/
FAVRE M THE-18
FEIHL FRANÇOIS MCV-12/MCV-6/MCV-7/THE-17
FELBER LOYSE **ODE-5**/
FELLEY CHRISTIAN **IMI-3**/
FELLEY-BOSCO EMANUELA GEN-13/ IMI-3
FERDAOUSSI MOURAD MCV-39/
FIGUEIREDO HUGO **THE-18**/
FIRSOV DMITRI GEN-13/
FISCH T EHU-26/
FLAHAUT MARJORIE ODE-11/ODE-6/ODE-18
FORNARI ELEONORA **NEU-31**/
FOSTEL JULITA MCV-38/
FRANCIOLI DAVID EHU-25/EHU-30/
FRANCIOLI PATRICK IMI-4/
FRASCAROLO FRANCE THE-17/
FRITSCHY JEAN-MARC NEU-1/
FUA PASCAL THE-35/
FURRER HANSJAKOB GEN-6/
GABRIEL ANNE MCV-16/MCV-30/
GAEGGELER HANS-PETER MCV-33/
GAILLARD MURIEL **IMI-14**/
GAILLARD ROLF MCV-23/MCV-24/MCV-4/MCV-27
GAJER MARKUS **IMI-22**/

GAJHEDE MICHAEL MCV-26/
GALISSON FRÉDÉRIQUE MCV-4/
GAMBA MARCELLA **MCV-23**/
GANTELET EMILIEN **NEU-29**/NEU-30/
GARCIA MIGUEL EHU-5/
GARDAZ JEAN-PATRICE THE-41/
GARDON MANUEL EHU-27/
GAVILLET MATHILDE **NEU-36**/
GENOUD CHRISTEL **NEU-45**/
GERBEX CAROLE MCV-5/
GERTSCH AURÉLIE NEU-54/
GHEORGHITA FULVIA GEN-1/
GHIKA JOSEPH NEU-22/NEU-54/NEU-55/THE-23/THE-24/NEU-19
GIDDEY MARLYSE IMI-15/
GILLIARD NICOLAS GEN-7/NEU-12/
GINET VANESSA **NEU-52**/
GIRAUD SYLVAIN MCV-4/
GIROUD CHRISTIAN **NEU-54**/
GIULIANI FABIENNE NEU-39/
GIUSEPPE PANTALEO IMI-17/
GIUSTI VITTORIO MCV-27/
GIVEL JEAN-CLAUDE THE-37/THE-41/
GIÉ OLIVIER **THE-41**/
GOBBI GABRIELLA NEU-18/
GOBELET CHARLES THE-40/
GOLDSCHMIDT VALERIE **GEN-3/GEN-24**
GOMEZ PATRICK **EHU-9**/
GONZALEZ ANDINO SARA NEU-10/NEU-6/
GONZALEZ RODRIGUEZ ELENA **MCV-33**/
GOTHUEY ISABELLE NEU-23/
GOURDON GENEVIÈVE NEU-29/
GOUTTENOIRE JÉRÔME IMI-22/
GRANDCHAMP NICOLAS NEU-43/
GRAVE DE PERALTA MENENDEZ ROLANDO NEU-10/
GREANEY PETER ODE-19/ODE-4/
GREINER RA THE-5/
GRENINGLOH GABRIELE NEU-30/
GRISEL PHILIPPE MCV-18/
GRONCHI ALINE NEU-19/
GROSS NICOLE ODE-11/**ODE-18**/ODE-6/
GUDINCHET FRANÇOIS THE-3/
GUENAT SYLVIE **MCV-26**/
GUEX PATRICE EHU-5/NEU-19/ EHU-4
GUIDI RAFFAELLA NEU-21/
GUIGNARD E THE-19
GUIGNARD LAURENCE NEU-14/
GUTIERREZ DANIEL THE-3/
GUTTORMSEN SISSEL EHU-16/
GUY LIONEL GEN-10/**GEN-13**/
GYGI CHRISTIAN M. ODE-5/
GYSIN RENÉ NEU-23/**NEU-45**/
GÜNTHARD HULDRYCH GEN-6/

HAEFLIGER JACQUES-ANTOINE MCV-12/MCV-13/MCV-14/**MCV-15**/MCV-28/
HAENNI MARISA **IMI-10**/
HAGMANN P NEU-58/
HALFON OLIVIER NEU-3/NEU-34/NEU-40/NEU-53/
HARARI ALEXANDRE EHU-5/IMI-24
HAROLD POOLEY IMI-16/
HARRIS MICHAEL GEN-13/
HAUSEL PIERRETTE GEN-13/
HAUSER P.M. **THE-31**/
HAYOZ DANIEL MCV-9/
HEN RENÉ NEU-56/
HENRY HUGUES NEU-7/
HERNANDEZ-PAMPALONI M MCV-34/MCV-35/
HERRMANN FRANÇOIS NEU-54/
HERZIG LILLY THE-2/**THE-8**/THE-9/
HERZOG MICHAEL NEU-34/
HESS U GEN-23
HILFIKER SILVIA EHU-38/
HINRIKSON H.P. THE-31/
HIROZ PHILIPPE **THE-37**/THE-41/
HIRT LORENZ NEU-15/
HOLZER LAURENT **NEU-34**/
HONEGGER PAUL NEU-7/NEU-8/NEU-61
HORISBERGER JEAN-DANIEL MCV-21/MCV-25/
HORNUNG JEAN-PIERRE NEU-11/NEU-23/NEU-56/NEU-57/
HSUEH WA MCV-35/
HYJAZI ALEXANDRE THE-14/
HÄMMING ROBERT NEU-23/
HÜTTEMANN HARDY NEU-23/
ISCHER FRANCOISE GEN-13/
ISEL FRÉDÉRIC NEU-35/
ISOM LORI NEU-12/
ITH M MCV-40
JACKY E GEN-23
JANDUS CAMILLA **ODE-8**/
JATON K. THE-31/
JAUGEY LAURE NEU-34/
JEANNET PIERRE-YVES GEN-21/
JI RU RONG NEU-12/
JICHLINSKI PATRICE ODE-5/THE-15/
JILEK SAMANTHA **NEU-14**/
JOLLES BRIGITTE **THE-34**/**THE-35**/
JORAY SABINE NEU-22/**NEU-54**/NEU-55/THE-24/
JOSEPH JEAN-MARC ODE-11/ODE-6/ODE-18
JOTTERAND M GEN-23
JUBIN ALEXANDRA NEU-40/
JUILLERAT ANNE-CLAUDE NEU-54/
JUILLERAT LUCIENNE MCV-19/
JUNOD MICHEL **THE-2**/
KAESER MÉLANIE THE-2/
KAESSMANN HENRIK GEN-2/GEN-3/GEN-24
KAMBER MATTHIAS EHU-28/

KAPPENBERGER L MCV-36/
KARFO K EHU-7/
KARTER ANDREW MCV-8/
KASTRUP JETTE S. MCV-26/
KATO ANN GEN-7/
KAZADI KAYOLE IMI-12/
KERR EVE MCV-8/
KINKEL KAREN ODE-3/
KLAUSER PAUL NEU-5/
KLILA HEDI THE-40/
KLOPOTOPV ADRIANA IMI-4/
KNAUP MARLYS ODE-16/ODE-2/
KNAUP REYMOND MARLIES IMI-20/IMI-9/
KNOTT GRAHAM WILLIAM NEU-45/
KNYAZEVA MARIA NEU-31/
KOVÁCS KRISZTIAN A. **NEU-53**/
KRAFTSIK RUDOLF NEU-11/NEU-29/NEU-51/
KRATTINGER NATHALIE MCV-15/
KREIS R MCV-40
KRIEG MARC-ANTOINE EHU-1/EHU-2/THE-5/
KRISTENSEN OLE MCV-26/
KRUMMENACHER ISABELLE IMI-2/
KUCERA PAVEL THE-37/THE-41/
KULISZEWSKI MAJEK IMI-7/
KUNTZER THIERRY GEN-21/GEN-5/NEU-29/THE-22/THE-40/
KÜNDIG CHRISTOPH ODE-5/
LACOUR STÉPHAN IMI-14/
LAGOPOULOS LUCIENNE **ODE-19**/ODE-4/
LAMBELET MARTINE MCV-5/
LAMY OLIVIER EHU-1/EHU-2/THE-5/
LATADO HÉLIA IMI-3/
LAVOIE SUZIE NEU-21/**NEU-46**/
LAZAREVIC VLADIMIR IMI-16/
LÊ K.A.**MCV-40**
LE GOFF GÉRALDINE NEU-14/
LE ROY DIDIER IMI-20/IMI-21/IMI-9/
LEISINGER HANS-JÜRGE ODE-5/
LENAIN VINCENT MCV-39/
LEPORE MARIO MCV-4/
LEPORI DOMENICO THE-3/
LETURCQ FRANCE GEN-5/
LEUBA GENEVIÈVE **NEU-51**/NEU-39
LEVI F EHU-26/
LEVIN MIKE IMI-11/
LEVRAND SANDRA MCV-6/MCV-7/
LEYVRAZ CÉLINE **MCV-27**/
LEYVRAZ PIERRE-FRANÇOIS THE-35/
LIAUDET LUCAS MCV-12/MCV-4/MCV-6/MCV-7/THE-17
LIEBY PATRICIA EHU-5/
LINHART ALES MCV-9/
LOBRINUS ALEXANDRE GEN-21/
LOEUILLET CORINNE IMI-12/**GEN-20**/

LOUKILI NOUREDDINE **MCV-41**/
LUESCHER IMMANUEL ODE-9/
LUTHI FRANCOIS THE-34/
MACH JEAN-PIERRE ODE-13/ODE-9/
MAEHLER PIERRE MCV-28/
MAEDER PHILIPPE NEU-10/NEU-31/
MAEDER-INGVAR MALIN THE-23/
MAGARA FULVIO NEU-13/NEU-30/**NEU-48/NEU-54**/
MAGISTRETTI PIERRE NEU-13/NEU-3/NEU-36/NEU-59/NEU-48/NEU-547NEU-53
MAGNIN GUYLÈNE NEU-52/
MAJCHERCZYK PAUL ANTHONY IMI-3/**ODE-12**
MANGIN PATRICE EHU-28/MCV-20/NEU-54/THE-32/
MARCHETTI OSCAR ODE-16/ODE-2/THE-39/
MARCON CLARA C NEU-48/NEU-54/
MARINO MATHIEU MCV-4/
MARTI MAUDE NEU-36/
MARTIN DAVID MCV-13/MCV-14/MCV-15/**MCV-28**/
MARTIN JEAN-LUC **NEU-20**/
MARTIN-SÖLCH CHANTALE THE-40/
MARTINET D ODE-18/
MARTINEZ MANUEL MCV-5/
MARTINEZ RAQUEL GEN-2/GEN-3/GEN-24
MARTUZZI ROBERTO **NEU-10**/
MASSON JC MCV-37/
MATSUURA S ODE-16/
MATTHEY MARIE-LOUISE GEN-1/
MAURER FABIENNE **MCV-17**/MCV-26/
MAY MARGARET GEN-3/GEN-24
MCKENNA THERESE ODE-12/
MCKERLIE COLIN IMI-7/
MCMANUS JOHN THE-37/
MEDA PAOLO MCV-15/
MEIER ROLAND ODE-11/ODE-6/ODE-18
MEINHARDT ANDREA **MCV-18**/
MEULI RETO NEU-10/NEU-31/THE-24/
MEYER-MONARD S GEN-23
MEYLAN RAPHAËL NEU-28/
MICHEL CHRISTOPH NEU-10/NEU-28/
MICHEL PATRIK THE-23/
MICHETTI PIERRE IMI-3/
MICHIELIN OLIVIER IMI-8/
MICHOD DAVID **ODE-2**/
MILON ANTOINE **ENA-1**/
MINEHIRA KAORI MCV-29/
MITTAZ-CRETTOL LAURÉANE **GEN-21**/
MOECKLI RAPHAËL EHU-27/
MOESSINGER ADRIEN MCV-4/
MONACHON CEDRICK NEU-57/
MONNAT MARTINE NEU-23/
MONNET-TSCHUDI F **NEU-61**
MOOSER VINCENT MCV-22/
MORADPOUR DARIUS IMI-19/IMI-22/IMI-12/

MOREILLON PHILIPPE IMI-10/IMI-15/ODE-12/
MORET MALLORY MCV-24/
MOTTIER VINCENT NEU-41/
MUEHLEMATTER D **GEN-23**
MUEHLETHALER VINCENT **MCV-4**/
MULLER DOMINIQUE NEU-5/
MUNOZ MIGUEL GEN-20/
MURRAY MICAH NEU-10/NEU-25/NEU-28/**NEU-6**/NEU-28/NEU-35
MUÑOZ MIGUEL IMI-8/
MÜHLEMANN NICOLE THE-8/
MÜHLETHALER-MOTTET A ODE-18/ODE-6/**ODE-11**
MÜHLETHALER-MOTTET ANNICK ODE-6/
NAHIMANA AIMABLE ODE-19/**ODE-4**/
NASSAL MICHAEL IMI-22/
NATHAN L MCV-34/
NEIER REINHARD MCV-19/
NICOLAS DOMINIQUE NEU-11/NEU-57/
NICOLO CATHERINE **IMI-9**/
NIEDERHAUSER GUY MCV-39/
NIKONENKO IRINA NEU-5/
NIQUILLE ANNE **THE-19**/
NISHIKAWA MASAMI NEU-18/
NOËL MÉDICO IMI-16/
ODDO MAURO MCV-4/**THE-17**/
OGAY SANDY MCV-4/
OPPLIGER ANNE EHU-38/EHU-8/
ORTIZ MILLÁN **GEN-2**/GEN-3/GEN-24
OTT JURG GEN-1/
OXILIA-ESTIGARRIBIA MA MCV-34/
PACCAUD FRED EHU-16/MCV-16/MCV-38/
PANIZZON RENATO NEU-4/
PANNATIER ANDRÉ THE-13/
PANTALEO GIUSEPPE IMI-23/EHU-5/NEU-14/IMI-24
PARLIER V GEN-23
PARNAS JOSEF GEN-1/
PASCUAL ANDRES **THE-39**/
PASCUAL MANUEL IMI-17/IMI-24
PATTHEY RENÉ IMI-4/
PEDRAZZINI THIERRY MCV-15/MCV-17/MCV-4/
PELLERIN LUC NEU-13/
PENG TIFFANY MCV-8/
PENIN FRANÇOIS IMI-19/
PERDRIX J MCV-36/MCV-37/
PERIASAMI RAJ MCV-29/
PERRET SOPHIE **MCV-4**/
PERRIN FLORENCE GEN-7/
PERTIN MARIE GEN-7/**NEU-12**/
PETCHANIKOW CYRIL NEU-57/
PETIGNAT CHRISTIANE IMI-4/
PETIT JEAN-MARIE NEU-54/
PEYTER ANNE-CHRISTINE MCV-4/
PICHON FABIEN **NEU-37**/

PICKENHAGEN ANOUCHKA NEU-59/
PINGET CHRISTOPHE THE-15/
PITTET VALÉRIE GEN-21/
PLANCHEREL BERNARD NEU-40/
PLUM JEAN EHU-5/
POISBEAU PIERRICK NEU-60/
POLLO CLAUDIO NEU-19/NEU-30/
POST MARTIN IMI-7/
POWELL ANDREW NEU-12/
PRALONG ETIENNE **NEU-30**/NEU-59/THE-26/THE-27/
PRALONG FRANCOIS MCV-23/MCV-24/MCV-27
PREISIG MARTIN GEN-1/NEU-23/
PREISSMANN DELPHINE NEU-14/**NEU-43**/
PRIKHODKINE ALEXEI EHU-5/
PRIOR JOHN **MCV-34/MCV-35**/MCV-36/NEU-22/MCV-37
PROBST ALPHONSE NEU-1/
PROBST HERVÉ MCV-14/
PUYAL JULIEN **NEU-41**/NEU-50/
QUIÑONES MJ MCV-35/
RAVUSSIN ERIC MCV-30/ MCV-40
REGAZZI ROMANO MCV-28/MCV-39/
REGLI LUCA NEU-15/THE-26/
RENNER PASCAL IMI-18/**IMI-11**/
RIBORDY V THE-17
RIDSDALE ROSS IMI-7/
RIEDERER BEAT **NEU-16**/NEU-51
RIEDERER IRÈNE NEU-16/
RIGNAULT STÉPHANIE **MCV-12**/
RIHS-MIDDEL MARGRET THE-40/
RINSOZ THOMAS **EHU-38**/
ROBERT BRUNO ODE-9/
ROBINSON J OWEN ODE-2/ODE-16
ROBINSON NEIL EHU-28/
RODONDI NICOLAS **MCV-16/MCV-8**/
RODUIT RAPHAEL MCV-26
ROGER THIERRY **IMI-18/IMI-20/IMI-21**/IMI-11/IMI-9/
ROLLI JOËLLE **MCV-7**/
ROMAILLER MATHIAS NEU-40/
ROMERO JACKELINE IMI-5/
ROMERO PEDRO ODE-8/
ROS JACQUELINE NEU-13/
ROSENBLATT-VELIN NATHALIE MCV-4/
ROSSIER BERNARD GEN-13/MCV-33/
ROSSIER YANN THE-40/
ROTEN CLAUDE-ALAIN GEN-10/GEN-13/
ROTGER MARGALIDA GEN-6/
ROTH-KLEINER MATTHIAS **IMI-7**/
ROTHEN STÉPHANE **THE-11**/
ROTHENBERGER SYLVIA IMI-8/
ROUILLER ERIC THE-2/
ROULET ELIANE THE-27/
RUCHET M.C GEN-23

RUFFIEUX CHRISTIANE NEU-3/THE-23/
RUIZ JUAN MCV-4/
RUIZ VIVIANE NEU-23/
RUNGGER-BRÄNDLE ELISABETH MCV-11/
RUSCA SOPHIE **EHU-8**/
SACCO CAROLYN **NEU-1**/
SANGLARD DOMINIQUE GEN-13/
SANS-MERCE MARTA EHU-27/
SARAGA MICHAEL GEN-1/NEU-19/
SATOMURA S ODE-16/
SAUDAN CHRISTOPHE **EHU-28**/MCV-20/
SAUGY MARTIAL EHU-28/MCV-20/THE-32/
SAUTTER CHIARA **NEU-26**/
SAYAR SALIHA BEYZA **GEN-13**/
SCHAFFTER MANUEL EHU-5/ EUH-4
SCHALLER MARIE-DENISE MCV-4/THE-17
SCHANZ U GEN-23
SCHAPIRA MARC MCV-4/MCV-5/
SCHELBERT HR MCV-34/MCV-35/
SCHENK FRANÇOISE NEU-14/NEU-23/NEU-26/NEU-39/NEU-43/NEU-53/NEU-38
SCHINDLER TH MCV-34/MCV-35/
SCHLAGETER VINCENT THE-37/THE-41/
SCHLUEP MYRIAM NEU-14/NEU-3/
SCHMIDT SABINE ODE-16/ODE-2/
SCHMITT FRÉDÉRIC **MCV-19**/
SCHNEIDER MARIE PAULE **IMI-2**/ THE-18/ THE-19
SCHNEITER PHILIPPE MCV-32/
SCHNIDER ARMIN NEU-28/
SCHUMACHER YORCK OLAF MCV-20/
SCHWARZ JEAN-MARC MCV-29/
SEELENTAG WALTER ODE-17/
SELBY JOE MCV-8/
SENN LAURENCE **ODE-16/ODE-2**/
SHAFY SAMIHA EHU-16/
SIEGRIST OLIVIER THE-34/
SIMA ANDERS MCV-11/
SIMARD NATHALIE EHU-2/
SIMIONI SAMANTA **NEU-3**/
SIMON OLIVIER THE-40/
SINGY PASCAL **EHU-4/EHU-5**/
SIRARD JEAN-CLAUDE GEN-13/
SOLDO BLAZENKA IMI-16/
SOLIDA ALESSANDRA GEN-1/NEU-23/
SOTTAS PIERRE-EDOUARD EHU-7/MCV-20/ODE-3/
SOUZA LIMA FABIANA NEU-3/
SPAHN DONAT GEN-7/NEU-12/
SPEISER DANIEL ODE-8/
SPENCER BRENDA EHU-5/
SPERDIN HOLGER NEU-25/
SPERTINI OLIVIER MCV-4/MCV-5/
SPIERER LUCAS **NEU-25**/
SPORKERT FRANK NEU-54/

STEIMER THIERRY NEU-48/
STETTLER RODRIGUE MCV-24/ MCV-40
STEULLET PASCAL **NEU-21**/NEU-23/NEU-46/
STIRNEMANN KATHRIN **ODE-13**/ODE-9/
STOOP RON NEU-59/NEU-60/
STRAHM EMMANUEL MCV-20/
STÉPHAN PHILIPPE **NEU-40**/
SULSTAROVA BRIKELA EHU-4
SUN DIANXING IMI-22/
SUTER MAYA NEU-40/
SUTER MICHEL MCV-27/
TAPPY LUC MCV-24/MCV-29/MCV-30/MCV-32/MCV-40
TARDIF ERIC NEU-1/NEU-25/NEU-28/
TASINATO ANDREA ODE-5/
TATE SIMON NEU-12/
TECON ROBIN **ENA-2**/
TELENTI AMALIO IMI-12/GEN-2/GEN-20/GEN-3/IMI-8/GEN-6/IMI-1/THE-14/GEN-24
THIRAN JEAN-PHILIPPE NEU-10/NEU-58
THOME-MIAZZA MARGOT IMI-5/
TICHELLI A GEN-23
TIMM SALLY GEN-1/
TOLNAY MARCUS NEU-1/
TOLSA JEAN-FRANÇOIS MCV-4/
TORGLER RALPH **IMI-5**/
TOSIC MIRJANA **GEN-1**/NEU-23/NEU-45/
TRUTTMANN ANITA NEU-52/
TSEU IRENE IMI-7/
TURNER VINCENT GEN-13/
VALLET YANNICK IMI-4/
VALLOTTON LAURE IMI-17/ **IMI-24**
VAN DER LINDEN MARTIAL NEU-54/
VAN DER MEER JAN ROELOF ENA-2/GEN-17/IMI-14/
VASLIN ANNE NEU-41/**NEU-50**/
VASSALLI GIUSEPPE MCV-18/
VAUDAUX PIERRE ODE-12/
VENETZ JEAN-PIERRE IMI-24
VERDON FRANÇOIS THE-2/THE-8/**THE-9**/
VERDUMO CHANTAL MCV-27/
VERDUN FRANCIS R. ODE-3/**THE-3**/
VERHEIJEN MARK H.G. MCV-11/
VERMATHEN P MCV-40
VERNAY ANDRÉ NEU-51/
VERNEZ DAVID ENA-1/
VIANIN PASCAL NEU-14/NEU-32/
VILLEMURE JEAN-GUY NEU-19/NEU-30/NEU-59/THE-2/THE-26/THE-27/
VINGERHOETS FRANÇOIS NEU-19/
VISWANATHAN BHARATHI MCV-31/
VIVIANI DANIELE **NEU-60**/
VLADIMIR LAZAREVIC **IMI-16**/
VOGNE CHRISTELLE GEN-17/
VOIROL PIERRE **THE-13**/
VOLTERRA ANDREA NEU-13/

VON DER AA S GEN-23
VOUILLAMOZ JACQUES IMI-15/
VUADENS PHILIPPE THE-40/
VUAGNIAUX GREGOIRE GEN-13/
WAEBER BERNARD MCV-12/MCV-6/MCV-7/
WAEBER GÉRARD MCV-13/MCV-39/MCV-4/MCV-22
WAECHTER VANESSA NEU-41/
WALICKI JOËL **ODE-10**/ODE-7/
WANG AUGUST GEN-1/
WANKMUELLER NOEMIE **THE-40**/
WANNIER THIERRY THE-2/
WARREN WICK MCV-31/
WASSERFALLEN JEAN-BLAISE THE-14/THE-15/THE-5/
WEBER OREST EHU-4
WEINGUNI PASCAL NEU-40/
WELKER EGBERT NEU-37/NEU-45/
WENGER ALINE IMI-4/
WERGE THOMAS GEN-1/
WIDER CHRISTIAN NEU-19/
WIDMANN CHRISTIAN MCV-22/ODE-10/ODE-2/ODE-7/THE-6/
WIRTHNER DANIEL MCV-24/
WOOLF CLIFFORD NEU-12/
WYNIGER JOSIANE IMI-8/
WYNIGER JOSIANNE GEN-20/
YAN PU **ODE-17**/
YANG JIANG-YAN ODE-10/
YERLY PATRICK MCV-16/
ZALILA HABIB **NEU-57**/
ZANETTI GIORGIO IMI-4/
ZHANG WEIXIAN MCV-11/
ZHANG X MCV-34/MCV-35/
ZIMMERMANN PHILIPPE EHU-16/
ZUBER BENOÎT **NEU-5**/
ZURICH M-G NEU-61